THE ROLES OF PROGRANULIN AND TMEM106B IN LYSOSOMAL PHYSIOLOGY AND NEURODEGENERATIVE DISEASE

A Dissertation

Presented to the Faculty of the Graduate School

of Cornell University

In Partial Fulfillment of the Requirements for the Degree of

Doctor of Philosophy

by

Daniel Harris Paushter

May 2018

© 2018 Daniel Harris Paushter

THE ROLES OF PROGRANULIN AND TMEM106B IN LYSOSOMAL PHYSIOLOGY AND NEURODEGENERATIVE DISEASE

Daniel Harris Paushter, Ph.D.

Cornell University 2018

Frontotemporal lobar degeneration (FTLD) is a devastating, clinically heterogeneous neurodegenerative disease that results in the progressive atrophy of the frontal and temporal lobes of the brain. Most often presenting with drastic alterations in personality and behavior, as well as a gradual decline in language capabilities, FTLD is the second leading cause of early-onset dementia only after Alzheimer's disease. One of the major causes of familial FTLD is haploinsufficiency of the protein, progranulin (PGRN), resulting from mutation in the granulin (*GRN*) gene. Interestingly, PGRN shows a dosage-dependent disease correlation, and *GRN* mutation resulting in complete loss of PGRN causes the lysosomal storage disease (LSD), neuronal ceroid lipofuscinosis (NCL). In this text, my co-workers and I demonstrate that PGRN is proteolytically processed in the lysosome into discrete granulin peptides, which may possess distinct functions. We have independently found interactions between PGRN or granulin peptides and three lysosomal hydrolases: Cathepsin D (CTSD), glucocerebrosidase (GBA), and α-N-acetylgalactosaminidase (NAGA). The activity of each of these enzymes was found to be reduced in $Grn^{-/-}$ mice, indicating that a potential mechanism of PGRN-related disease may be dysfunction of multiple lysosomal

hydrolases. In addition to possessing an indeterminate lysosomal function, PGRN has also been shown to be a neurotrophic factor. Completion of a high-throughput screen searching for the receptor that mediates this function identified cluster of differentiation 68 (CD68) and neuropilin 2 (NRP2) as putative PGRN receptors.

A second protein that has become of interest to the study of FTLD is TMEM106B. Variants of *TMEM106B* have been associated with an increased risk of developing FTLD, especially in cases of *GRN* mutation (FTLD-*GRN*). Although TMEM106B is known to be an endolysosomal transmembrane protein that regulates lysosomal morphology and degradative capacity, its exact function is unclear. Our current findings suggest that TMEM106B may regulate cellular levels of the phosphoinositide, $PI(3,5)P_2$. In summary, our work supports a lysosomal role of the FTLD- and NCL-related protein, PGRN, and identifies a novel function of the FTLD risk factor, TMEM106B.

BIOGRAPHICAL SKETCH

Growing up, Daniel Paushter was always most passionate about two things: animals and science. While studying at the University of Illinois at Urbana-Champaign, Daniel interned over the course of several summers in the Department of Clinical Affairs at Northfield Laboratories, a company which developed a novel blood substitute for use in emergency medicine. Upon graduating, he chose to pursue biomedical research and joined the Chicago Diabetes Project at the University of Illinois at Chicago. There, he participated in translational research as part of a Phase III clinical trial investigating islet transplantation as a treatment for type 1 diabetes. While he was involved in several projects, he primarily studied the use of alginate microencapsulation of islets to mitigate immune reactivity with the goals of reducing immunosuppressant requirements and extending graft survival. It was through his extensive work with non-human primates that he was motivated to pursue a career in veterinary medicine.

Daniel joined the College of Veterinary Medicine at Cornell University in 2013, and while he thoroughly enjoyed the veterinary curriculum, he realized that he wanted to continue with research as well. He completed laboratory rotations and applied to the Combined DVM-PhD Program, to which he was accepted. For his graduate work, Daniel joined the laboratory of Dr. Fenghua Hu, where he explored the relationships of the proteins, progranulin (PGRN) and TMEM106B, to the neurodegenerative diseases, frontotemporal lobar degeneration (FTLD) and neuronal ceroid lipofuscinosis (NCL). After finishing his PhD, Daniel will complete the remaining two years of veterinary school. He then hopes to work in a field where he can combine his interests in veterinary medicine and research.

Dedicated to:

Bernice and Joseph Wallace

Anne and Matthew Paushter

Haruye and Hiram “Skinny” Hagiwara

ACKNOWLEDGEMENTS

Foremost, I would like to thank my advisor, Dr. Fenghua Hu, for her years of mentorship that have been instrumental in allowing me to advance as a researcher. The time and instruction she has provided, as well as the trust that she has placed in me as a member of her lab have been paramount. I would also like to thank Dr. Xiaolai Zhou, with whom I collaborated on several projects, for his incredible work ethic, precision, and guidance. I would like to thank my committee members, Dr. Margaret Bynoe, Dr. Sergiy Libert, and Dr. David Lin for their feedback and advice throughout my studies, and for joining in the major milestones along the way. I would also like to thank Dr. Hélène Marquis, the chair of the Combined DVM-PhD Program, for being truly invested in the quality and advancement of the program.

From Northfield Laboratories, I extend my sincerest thanks to George Allen Hides. His enthusiasm, dedication to his work, knowledge, and devotion to teaching and mentoring were foundational in directing me toward a career in research.

There are several people from the University of Illinois at Chicago whom I must acknowledge as well. I would like to thank Dr. José Oberholzer for accepting me into his laboratory and providing me with the chance to learn from a team of highly experienced doctors and scientists. I would like to express my gratitude to Dr. Meirigeng Qi for his endless patience and positivity, and for sharing his expansive knowledge of medicine and surgery. I especially owe a great debt to Dr. Barbara Barbaro for truly guiding the earliest years of my research career. Any meticulousness, ability to coordinate experiments, or basic laboratory skills that I developed prior to beginning my PhD are credited to her.

From my personal life, I would like to thank every member of my family. I owe everything to my parents, Ellen and David, who have always fostered my interests in animals and science, even when that meant a house full of reptiles, amphibians, and small mammals. They have always unconditionally supported me, and I would not be receiving this degree if it were not for them. Thanks to my brother, Aaron, and my sister, Rebecca, for their encouragement and moral support. Thank you to Alison Smith and Jeri and Neal Hagiwara for always cheering me on and backing my endeavors. A special thank you to Dr. Steven Gould, who has been a strong advocate for me and has continually encouraged my academic and professional goals. Finally, I would like to thank my wife, Tuesday, for her endless patience and understanding during these hectic years. I have countlessly relied on her for reassurance and support, and could not have asked for a better person with whom to have shared this experience.

TABLE OF CONTENTS

CHAPTER 1

PROGRANULIN, THE LYSOSOME, AND NEURODEGENERATION

Published as Paushter DH, Du H, Feng T, Hu F. The lysosomal function of progranulin, a guardian against neurodegeneration. Acta Neuropathol. 2018 May 9. doi: 10.1007/s00401-018-1861-8. [Epub ahead of print] Review.

1.1 Abstract

Progranulin (PGRN), encoded by the *GRN* gene in humans, is a secreted growth factor implicated in a multitude of processes ranging from regulation of inflammation to wound healing and tumorigenesis. The clinical importance of PGRN became especially evident in 2006, when heterozygous mutation in the *GRN* gene, resulting in haploinsuffiency, was found to be one of the main causes of frontotemporal lobar degeneration (FTLD). FTLD is a clinically heterogeneous disease that results in the progressive atrophy of the frontal and temporal lobes of the brain. Despite significant research, the exact function of PGRN and its mechanistic relationship to FTLD remain unclear. However, growing evidence suggests a role for PGRN in the lysosome – most striking being that homozygous *GRN* mutation leads to neuronal ceroid lipofuscinosis (NCL), a lysosomal storage disease (LSD). Since this discovery, several links between PGRN and the lysosome have been established, including the existence of two independent lysosomal trafficking pathways, intralysosomal processing of PGRN into discrete functional peptides, and direct and indirect regulation of lysosomal hydrolases.

Here, we summarize the cellular functions of PGRN, its roles in the nervous system, and its link to multiple neurodegenerative diseases, with a particular focus dedicated to recent lysosome-related mechanistic developments.

1.2 Introduction

1.2.1 *GRN* mutation causes frontotemporal lobar degeneration and neuronal ceroid lipofuscinosis

The clinical importance of progranulin (PGRN; also known as acrogranin; granulin-epithelin precursor (GEP); GP88; PC cell-derived growth factor (PCDGF); and proepithelin (PEPI)) became evident in 2006, when heterozygous mutations in the *GRN* gene, resulting in haploinsuffiency, were found to cause frontotemporal lobar degeneration (FTLD) [8, 27, 35, 70, 79, 115]. FTLD is a clinically heterogeneous, incurable neurodegenerative disease resulting in frontotemporal dementia (FTD), most often presenting with drastic alterations in behavior and personality, including social disinhibition as well as gradual decline in language capabilities [82]. Although the exact mechanism is unknown, the disease is characterized by progressive atrophy of the frontal and temporal lobes of the brain. FTLD is the second leading cause of early-onset dementia after Alzheimer's disease (AD), and is the third most common cause of cortical dementia [82, 99]. FTD can clinically be divided into distinct subtypes based upon earliest primary signs of disease. Behavioral-variant FTD is associated with sometimes severe alterations in personality and behavior, while primary progressive aphasia (PPA), which can be subdivided into semantic dementia (SD) and progressive nonfluent aphasia (PNFA), is associated with marked dysfunction in language

processing and production. Interestingly, there is also overlap between the development of FTLD and the motor neuron disease, amyotrophic lateral sclerosis (ALS), with many FTLD patients developing motor neuron disease and many ALS patients showing cognitive decline [67]. In addition to classification by clinical presentation, FTLD can also be grouped by common histopathological features. Chief findings include inclusion bodies positive for tau protein (FTLD-Tau), ubiquitinated TAR DNA-binding protein 43 (TDP-43) (FTLD-TDP), or fused in sarcoma protein (FTLD-FUS) [71]. Although not all cases have a clear genetic component, there are several gene mutations known to result in FTLD, with major contributors including *GRN*, microtubule-associated protein tau (*MAPT*) and chromosome 9 open reading frame 72 (*C9orf72*) [97]. Since it was first associated with FTLD, more than 60 disease-causing *GRN* mutations have been identified [97]. Accounting for ~20-25% of familial FTLD cases and ~10% of all FTLD cases, with the majority producing truncated transcripts that are degraded by nonsense-mediated mRNA decay, *GRN* mutation is primarily associated with the FTLD-TDP subtype and shows minimal connection with ALS [108].

Perhaps the most important finding leading to a hypothetical lysosomal function of PGRN was the 2012 discovery of a pair of siblings with adult-onset neuronal ceroid lipofuscinosis (NCL), with exome sequencing pointing to a homozygous variant in *GRN* resulting in a premature stop [114]. Like FTLD, NCLs are a family of neurodegenerative diseases that are symptomatically and pathologically diverse [60, 76, 86]. Clinical presentations encompass cognitive and motor deterioration, epilepsy, and retinopathy, with pathology including lysosomal accumulation of lipofuscin, an autofluorescent lipid and protein aggregate. NCLs were previously classified by age of

onset, but with progressing molecular technologies, are now classified by genetic cause, of which 13 specific genes *(CLN1-13)*, including *GRN (CLN11)*, have been identified [26, 86]. Since the first cases of *GRN*-related NCL came to prominence, a second family has been identified wherein both parents developed FTLD and were found to be *GRN* mutant carriers, while their daughter who received two copies of the mutant allele developed adult-onset NCL, confirming the dosage effects of PGRN in disease manifestation [3]. More importantly, NCL-related phenotypes are reported in FTLD patients with *GRN* mutation [39, 131, 139], supporting the theory that lysosomal dysfunction might serve as a common mechanism of these two diseases.

1.2.2 GRN mutation is associated with AD

In addition to *GRN* mutation directly causing FTLD and NCL, PGRN has been linked to the pathophysiology of AD, although the exact nature of the relationship is less well-defined. AD is the most common senile dementia, characterized by the accumulation of insoluble amyloid-β (Aβ) plaques, neurofibrillary tangles of hyperphosphorylated tau, and gradual memory impairment. A number of groups have found that the T-allele of a *GRN* single nucleotide polymorphism (SNP), rs5848, in the 3'-untranslated region (3'-UTR), is associated with an increased risk of AD, which has been further supported by meta-analytic studies [55, 66, 111, 142]. The risk of AD development is inversely proportional to serum PGRN levels, as AD patients carrying homozygous T alleles have lower serum PGRN [49], possibly due to translational inhibition consequent to increased miRNA binding [98].

In AD mouse models, PGRN expression is dramatically upregulated in microglia [92] and in axons [40] around Aβ plaques. However, conflicting results have been obtained regarding the effect of PGRN in AD. PGRN has been demonstrated to attenuate pathological phenotypes, including Aβ plaque burden, neuroinflammatory markers, and memory impairment in AD mouse models in some studies [74, 134]. Other studies, however, have demonstrated that some AD phenotypes are *improved* by PGRN deficiency [47, 119]. The root of this discrepancy is currently unclear, but it has been proposed to be due to variations in mouse strains used or age of animals assessed. Despite this, it is clear from human studies that PGRN is an important marker and modulator of disease susceptibility in AD.

1.2.3 PGRN is a conserved, multifunctional pro-protein with unique structure

Structurally, PGRN is a 593 amino acid, 88 kDa protein that is highly glycosylated (~65 kDa without glycosylation) with 4 confirmed, and 1 putative, N-linked glycosylation sites [116]. It is comprised of seven full (domains A-G) and one half (domain p or "paragranulin") conserved granulin domains connected by short linker regions [127]. The general structure of the granulin domains is unique, with each full domain consisting of approximately 55 residues, with 2 (granulin G) or 4 (other granulins) double cysteine motifs and 4 single cysteine motifs. Structural studies of human granulin A and a granulin derived from carp revealed stacks of β-hairpins held together tightly by six disulfide bonds [48, 128, 137]. Despite this bonding, there appears to be great variability in the rigidity and flexibility of each mammalian granulin [127]. Notably, PGRN can be proteolytically processed to release individual granulin peptides,

which are evidenced to possess functions independent of, and sometimes in contrast to, the full-length precursor. These granulin peptides were, in fact, discovered a few years before PGRN, having been isolated from epidermal carcinoma, rat kidney, and inflammatory exudates [10, 15, 112]. PGRN/granulin homologs are found across taxa, ranging from plants to invertebrates, such as sponges, worms, and insects, to vertebrates, including fish and mammals [90]. Transcriptionally, the *GRN* gene is expressed to varying degrees across a wide range of tissues and cell types, including a variety of neurons, immune cells, and epithelial cells [28]. While the exact function of PGRN remains elusive, it has been found to be involved in numerous normal physiologic and pathologic processes.

1.2.4 PGRN is a growth factor involved in inflammation, wound healing, and tumorigenesis

When granulin peptides were first discovered in 1990, their primary role was attributed to the modulation of cell growth [42]. Originally termed "epithelins", the first two peptides to be isolated were shown to have opposing effects on the *in vitro* growth of a murine keratinocyte cell line [96, 112]. As with its derivative peptides, full-length PGRN can function as a growth factor. Recombinant PGRN supplied in the culture media of two epithelial cell lines showed stimulation of proliferation [28]. Similarly, PGRN has been demonstrated to stimulate endothelial cell migration and vessel growth *in vitro* and *in vivo* [44, 125]. Multiple studies have shown that PGRN is able to modulate MAPK/ERK, PI3K/Akt, and FAK signaling pathways, despite the lack of a previously identified PGRN signaling receptor [43, 68, 151]. A recent study, however,

indicates that PGRN binds to the receptor tyrosine kinase, EPH receptor A2 (EphA2) and, through this binding, is able to activate MAPK and Akt signaling pathways **(Fig. 1.1) (Table 1.1)** [83].

Owing at least in part to its mitogenic and angiogenic effects, PGRN expression has been linked to several cancers, generally with direct correlation between increasing PGRN expression and cancer severity [1, 31, 109, 123, 124]. PGRN may also be a useful biomarker in a number of cancers, such as ovarian epithelial cancer and malignant lymphoma, where elevated serum PGRN levels can be indicative of disease and prognostic of lower survival [6, 147].

In addition to the roles PGRN plays in cell proliferation, wound healing, and tumorigenesis, it is a well-established modulator of immune function [20, 51, 57, 121, 126]. In *C. elegans*, a PGRN homolog was reported to slow clearance of apoptotic cells [56]. Microglia, the resident immune cells in the brain, especially those which have become reactive following insult or trauma, produce and secrete especially high levels of PGRN [50, 75, 81, 94, 158], and PGRN has been shown to regulate microglial activation, migration, phagocytosis, and synapse pruning [69, 72, 95, 132, 149]. Thus, one role of PGRN in neurodegenerative diseases appears to be regulating microglia-mediated inflammatory responses. Interestingly, PGRN and granulin peptides have been found to possess opposing inflammatory functions, with PGRN generally being anti-inflammatory and granulin peptides pro-inflammatory [61, 160]. Studies in *C. elegans* have even suggested that granulin peptides might be toxic [104], although this has yet to be reported in mammalian systems. Because of the stark contrast in inflammatory effects, extracellular processing of PGRN into granulin peptides may be

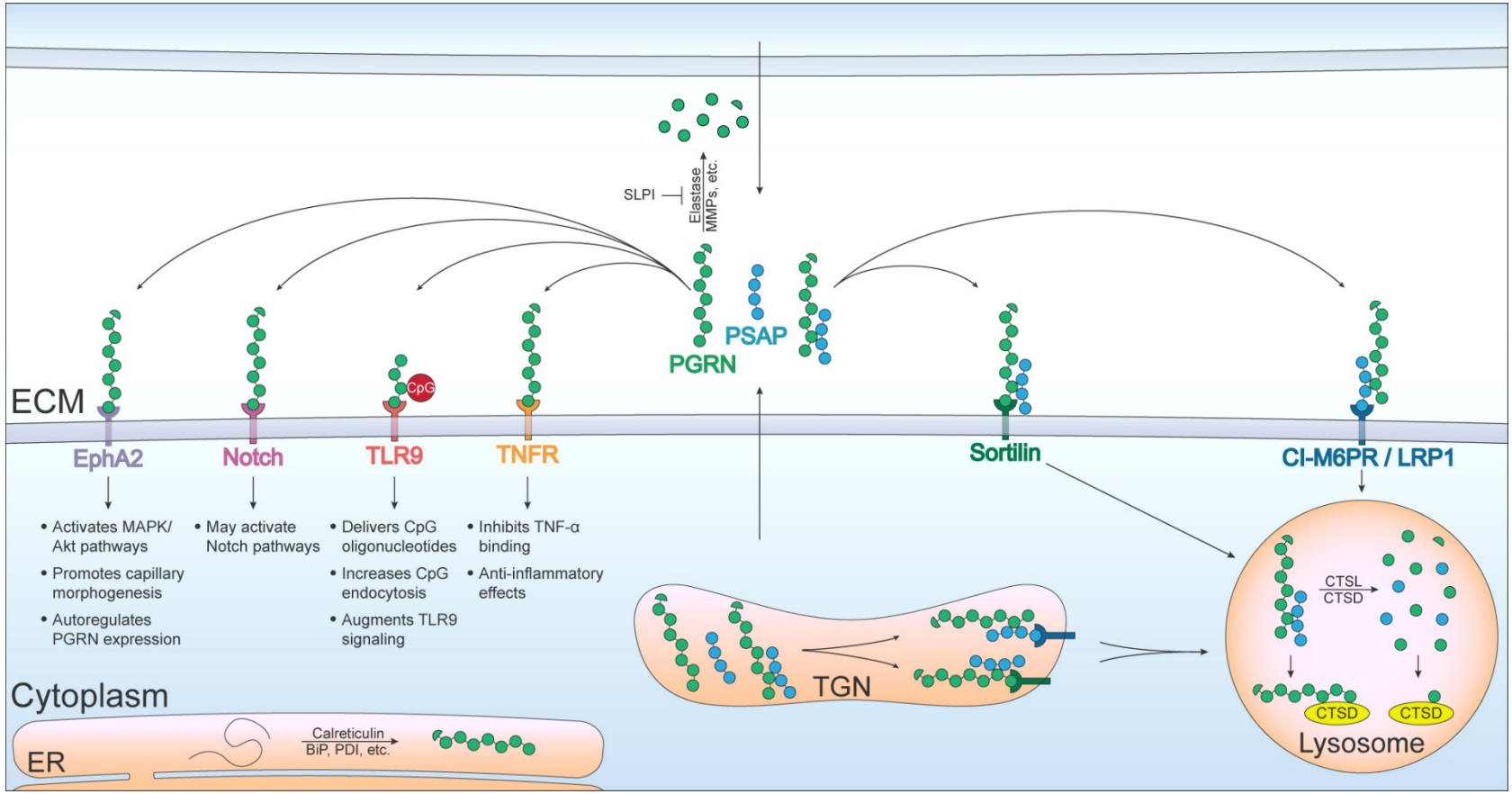
SLPI
Elastase
MMPs, etc.
PSAP
PGRN
ECM
CpG
EphA2
Notch
TLR9
TNFR
Sortilin
CI-M6PR / LRP1
• Activates MAPK/ Akt pathways
• Promotes capillary morphogenesis
• Autoregulates PGRN expression
• May activate Notch pathways
• Delivers CpG oligonucleotides
• Increases CpG endocytosis
• Augments TLR9 signaling
• Inhibits TNF-α binding
• Anti-inflammatory effects
TGN
CTSL
CTSD
CTSD
CTSD
Lysosome
Cytoplasm
ER
Calreticulin
BiP, PDI, etc.

Figure 1.1. PGRN interactions, trafficking, and proteolysis. Several PGRN receptors have been identified, including EphA2, Notch, TLR9, and TNFR. Chaperones, such as BiP and PDI ensure proper folding of PGRN in the ER. Mature PGRN can be delivered to the lysosome from the TGN or extracellular space by two independent pathways. 1) PGRN binds directly to the trafficking receptor, sortilin, which delivers it to the lysosome. 2) PGRN binds to the soluble lysosomal protein, PSAP, which then binds to either of its own trafficking receptors, the CI-M6PR or LRP1, and carries PGRN with it to the lysosome. The complementary relationship also exists, wherein PGRN transports PSAP to the lysosome via sortilin. Upon reaching the lysosome, PGRN can be cleaved by CTSL into individual granulin peptides and PSAP cleaved by CTSD into individual saposins. PGRN/granulin E can then bind to CTSD to help stabilize it and/or augment its activity.

Table 1.1. Known PGRN Protein Interactors

Class	Protein	Description	Functional Significance	Ref.
ECM/Serum Proteins	COMP	Cartilage-related protein	Enhances PGRN proliferative effect on chondrocytes	[143]
	HDL/apo A-I	Lipoprotein/HDL protein	May limit PGRN processing to suppress inflammation	[89]
	Perlecan	Proteoglycan	Diminishes mitogenic effects of PGRN	[37]
Secreted Proteins	ADAMTS-7	Protease, digests COMP	Processes PGRN into granulin peptides	[7]
	MMP-9[a]/12/14	Endopeptidase	Processes PGRN into granulin peptides	[18, 118, 141]
	NE	Serine protease	Processes PGRN into granulin peptides	[160]
	PR3	Serine protease	Processes PGRN into granulin peptides	[58]
	SLPI	Inhibitor of NE	Sequesters PGRN, inhibits processing by NE	[160]
Membrane Proteins	Dlk1[b]	EGF-like homeotic protein	Unknown function	[9]
	EphA2	Receptor tyrosine kinase	Upregulates PGRN, activates MAPK/Akt pathways	[83]
	Notch 1-4	Growth signaling receptors	May promote peripheral nerve regeneration	[5]
	Sortilin	Endocytic/signaling receptor	Traffics PGRN to the lysosome	[50]
	TLR9	Immune receptor	PGRN products aid CpG oligonucleotide delivery	[91]
	TNFR1/2	Inflammatory signaling	PGRN may competitively inhibit TNFR	[122]
Lysosomal Proteins	CTSD	Aspartyl protease	PGRN stabilizes and activates	[11, 131, 154]
	CTSL	Cysteine protease	Processes PGRN into granulin peptides	[46, 65, 155]
	GBA	Glucocerebrosidase	PGRN acts as co-chaperone with Hsp70	[52, 53]
	PSAP	Precursor to saposins	Lysosomal trafficking and level regulation	[156-158]
ER Proteins	BiP	Chaperone	Likely aids in PGRN folding and secretion	[4]
	Calreticulin	Chaperone	Likely aids in PGRN folding and secretion	[4]
	ERp5/57/72	Disulfide bond regulation	Likely aids in PGRN folding and secretion	[4]
	GRP94	HSP/chaperone	Likely aids in PGRN folding and secretion	[4]
	Hsp70	HSP/chaperone	PGRN/Hsp70 act as co-chaperones for GBA/LIMP-2	[4, 52]
	PDI	Disulfide bond regulation	Likely aids in PGRN folding and secretion	[4, 157]

[a]PGRN in media was increased in MMP-9 knockdown cells, but binding and cleavage were not shown, [b]yeast two-hybrid

Abbreviations: ADAMTS-7, a disintegrin and metalloproteinase with thrombospondin motifs 7; BiP, binding immunoglobulin protein; COMP, cartilage oligomeric matrix protein; CTSD, cathepsin D; CTSL, cathepsin L; Dlk1; delta-like protein 1; EGF, epidermal growth factor; EphA2, ephrin type-A receptor 2; ERp, endoplasmic reticulum protein; GBA, glucocerebrosidase; GRP94, heat shock protein Hsp90 family protein; HDL/apo A-I, high-density lipoprotein/apolipoprotein A1; Hsp70, heat shock protein 70; PSAP, prosaposin; MMP, matrix metalloproteinase; NE, neutrophil elastase; PDI, protein disulfide isomerase; PR3, proteinase 3; SLPI, secretory leukocyte protease inhibitor; TLR9, toll-like receptor 9; TNFR, tumor necrosis factor receptor.

tightly regulated, and PGRN can be cleaved by multiple proteases, including neutrophil elastase, a disintegrin and metalloproteinase with thrombospondin motifs 7 (ADAMTS-7), proteinase 3, matrix metalloproteinase (MMP)-9, MMP-12, and MMP-14 **(Fig. 1.1)** [7, 18, 58, 118, 141, 160]. There is some evidence that PGRN may bind the tumor necrosis factor (TNF) receptors, with competitive inhibition of TNF-α providing a mechanism of action **(Fig. 1.1)** [122]. However, there has been dispute about the nature of this relationship and whether it is physiologically real [24].

Considering the relationship between PGRN and neurodegeneration and its described functions as a growth and survival factor, it is not surprising that PGRN and at least one granulin peptide can function as neurotrophic factors, promoting neuron survival and neurite outgrowth *in vitro* and *in vivo,* both in mammalian systems and in Zebrafish [25, 28, 29, 34, 36, 62, 103, 132, 138]. A proteomic screen with gene ontology enrichment analysis has revealed an association between PGRN and Notch receptor signaling, with reported binding between PGRN and Notch1, 2, 3, and 4 **(Fig. 1.1)** [5]. However, it is not known whether this interaction mediates the neurotrophic effects of PGRN.

While loss of a direct neurotrophic or inflammation regulatory effect of PGRN could contribute to neurodegeneration in FTLD, the genetic link between PGRN and NCL strongly supports a lysosomal function of PGRN, as all the NCL genes discovered so far play a direct or indirect role in regulating lysosomal function [26]. With this understanding, there has been a new focus on identifying this potential function.

1.3 PGRN and the Lysosome

1.3.1 Lysosomal dysfunction in models of PGRN deficiency

Several groups have utilized mouse and cellular models of PGRN deficiency to try to recapitulate the disease processes of *GRN*-related FTLD and NCL. Although pathology in $Grn^{-/-}$ mouse models tends to be more moderate than in human cases, a number of phenotypes have been reported, including exaggerated inflammatory responses, microgliosis, astrogliosis, and behavioral dysfunction such as OCD-like and disinhibition-like behavior [69, 72, 101, 149, 150]. In addition to these broad observations, signs of lysosomal dysfunction have also been reported. Aged $Grn^{-/-}$ mice develop lipofuscin deposits and enlarged lysosomes, signatures of NCL **(Fig. 1.2a, 1.2b)** [2, 93, 140]. As occurs with FTLD with *GRN* mutations (FTLD-*GRN*), at least one group has observed phosphorylated TDP-43 accumulation in $Grn^{-/-}$ mice [150]. Additional links to the endolysosomal system include diffuse or granular cytosolic ubiquitin deposits [2, 140, 150] and aggregation of the autophagy-related protein, ubiquitin-binding protein p62 [120]. Reduced autophagic flux and autophagy-dependent clearance have also been reported in PGRN-deficient mice [21]. Human FTLD-*GRN* patient-derived primary fibroblasts showed decreased lysosomal protease activity, and lymphoblasts contained NCL-like storage material [139]. Similarly, FTLD-*GRN* patient induced pluripotent stem cell (iPSC)-derived cortical neurons have been shown to develop NCL- and FTLD-like pathologies, such as enlarged vesicles, lipofuscin accumulation, and a specific lysosomal cathepsin deficiency [131]. These models provide strong evidence for lysosomal dysfunction in cases of PGRN deficiency.

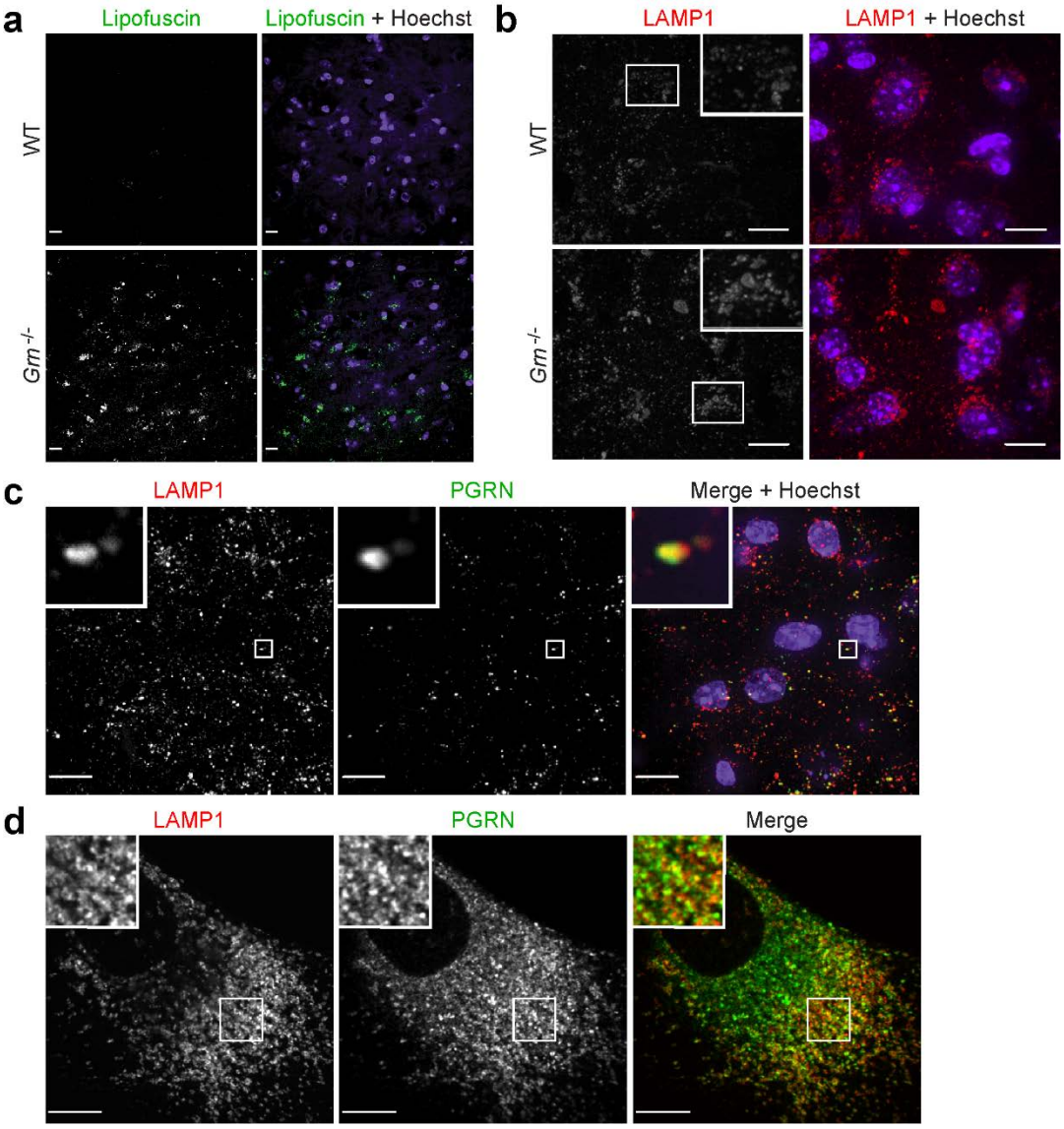
a
Lipofuscin
Lipofuscin + Hoechst
WT
Gm-/-
b
LAMP1
LAMP1 + Hoechst
WT
Gm-/-
c
LAMP1
PGRN
Merge + Hoechst
d
LAMP1
PGRN
Merge

Figure 1.2. PGRN is a lysosome-resident protein important for lysosome function. **a)** Increased lipofuscin accumulation in *Grn*$^{-/-}$ mice. Brain sections from 4-month-old WT and *Grn*$^{-/-}$ mice were imaged at 488 nm to detect auto-fluorescence (green). Hoechst 33342 was used as a nuclear marker. Scale bar = 10 μm. **b)** Lysosome enlargement in *Grn*$^{-/-}$ mice. Brain sections from 10-month-old WT and *Grn*$^{-/-}$ mice were immunostained with rat anti-mouse LAMP1 antibodies. Hoescht 33342 was used as a nuclear marker. Scale bar = 10 μm. **c)** PGRN co-localizes with the lysosome marker, LAMP1, in mouse brain. A brain section from a 1-month-old WT mouse was immunostained with sheep anti-mouse PGRN and rat anti-mouse LAMP1 antibodies. Hoechst 33342 was used as a nuclear marker. Scale bar = 10 μm. **d)** PGRN co-localizes with the lysosome marker, LAMP1 in human fibroblasts. Primary human fibroblasts were immunostained with goat anti-human PGRN and rabbit anti-human LAMP1 antibodies. Scale bar = 10 μm. a, b contributed by H.D. c contributed by T.F.

Importantly, there is pathologic overlap between FTLD-*GRN* patients and cells derived [39, 131, 139].

1.3.2 *GRN* transcriptomics and lipidomics

Transcriptomic analyses have also provided novel insights into the relationship between PGRN and the lysosome. Transcription factor EB (TFEB) is known to regulate the expression of most lysosomal genes [105]. In deleterious situations where nutrients are scarce or lysosomal function is diminished, TFEB translocates to the nucleus and stimulates lysosomal biogenesis. Studies have found that the *GRN* gene is under the transcriptional control of TFEB, supporting a lysosomal association [12, 105].

Multiple transcriptomic studies have also confirmed a critical lysosomal role of PGRN and a transcriptional upregulation of many lysosomal genes in response to PGRN deficiency in mice [32, 59, 69, 119, 120]. A microglia-specific transcriptomic study revealed an age-dependent upregulation of many lysosomal genes and genes related to innate immunity, including *Cd68*, triggering receptor expressed on myeloid cells 2 (*Trem2*), and complement genes *C1qa*, *C1qb*, *C1qc* and *C3* in response to PGRN deficiency [69]. Lysosomal dysfunction has been previously linked to dysregulation of innate immunity [80], although the mechanistic connection between these two processes still needs to be worked out.

Using a model of primary human neural progenitor cells with shRNA *GRN* knockdown, upregulation of genes related to apoptotic regulation and Wnt signaling was detected with gene ontology analysis [102]. Additionally, enrichment in ontology categories related to ubiquitination was observed, with upregulation of associated genes

including ubiquitin-conjugating and -ligating enzymes. As ubiquitin-positive TDP-43 inclusions are a hallmark of FTLD-*GRN* and lysosomal degradation is one of the primary mechanisms of processing ubiquitinated proteins, this is further evidence of an association between loss of PGRN and lysosomal dysfunction.

Based upon previous findings demonstrating altered lysosome homeostasis in association with *GRN* loss, one group hypothesized that PGRN might help regulate lysosomal lipid metabolism [32]. Lipidomic analysis demonstrated dosage-dependent differences in brain lipids in both humans and mice with PGRN insufficiency, mainly found to be related to triacylglyceride, diacylglyceride, phosphatidylethanolamine, and phosphatidylserine subspecies. Transcriptomic analysis of $Grn^{+/-}$ and $Grn^{-/-}$ mouse brains showed a number of differentially expressed transcripts involved in lipid metabolism, including lipid hydrolases that could potentially explain lipodomic changes observed.

1.3.3 Lysosomal trafficking of PGRN

Among the earliest findings linking PGRN to the lysosome was the discovery that PGRN is lysosomally localized **(Fig. 1.2c, 1.2d)** [50, 81]. The endocytic receptor, sortilin, was identified as a high-affinity binding partner of PGRN and shown to mediate its lysosomal trafficking **(Table 1.1)** [50]. This sortilin-mediated sorting is likely to occur both at the trans-Golgi network (TGN) in the biosynthetic pathway, and at plasma membrane in the endocytic pathway **(Fig. 1.1)**. In the brain, PGRN is expressed by microglia, neurons, astrocytes, endothelial cells, and oligodendrocyte precursor cells, with microglia having the highest expression levels [152]. Thus, the extracellular pool

of PGRN is likely derived from several sources. Sortilin is a VPS10 family member highly expressed in neurons, which is also known to bind the nerve growth factor precursor (proNGF) and neurotensin [23, 30, 73, 87]. The binding of PGRN to sortilin is dependent on the final 3 amino acids, QLL, and more specifically, the terminal carboxylate of PGRN [153], and loss of these completely abolishes the interaction. Consistent with the role of sortilin as a PGRN trafficking receptor, sortilin is not required for the neurotrophic function of PGRN in cell culture [29, 36]. However, a recent study demonstrated that the PGRN-sortilin interaction strengthens and maintains developing climbing fiber inputs, counteracting synapse elimination in the developing cerebellum [130]. It remains to be determined whether this is dependent on sortilin-mediated PGRN endocytosis or on active signaling at the plasma membrane.

Although genetic ablation of sortilin in mice leads to a fivefold increase in the levels of serum PGRN, it is still successfully delivered to neuronal lysosomes, suggesting the essential existence of an alternative trafficking pathway [50, 157]. Interestingly, this was shown to be mediated not by direct binding to another transmembrane trafficking receptor, but through an indirect mechanism whereby PGRN binds to the soluble lysosomal protein, prosaposin (PSAP) **(Table 1.1)**. When PSAP binds to either of its own trafficking receptors, the cation-independent mannose-6-phosphate receptor (CI-M6PR) or the low-density lipoprotein receptor-related protein 1 (LRP1), it carries PGRN along with it to the lysosome. Like sortilin, PSAP is able to traffic PGRN from the secretory pathway as well as from the extracellular space **(Fig. 1.1)**. The importance of this was underscored when loss of just one functional *Psap* allele was sufficient to significantly increase plasma PGRN levels in mice [157].

Additionally, the reciprocal trafficking, wherein PGRN transports PSAP to the lysosome via sortilin, has also been shown to occur **(Fig. 1.1)** [158].

PSAP is a proprotein composed of four homologous saposin domains (A, B, C, and D), and is known to be proteolytically processed in the lysosome into individual saposin peptides [88]. These peptides are responsible for activating different lysosomal sphingolipid-degrading enzymes and loss of PSAP function has been linked to lysosomal storage diseases (LSDs), including Gaucher disease (GD) and metachromatic leukodystrophy. The interaction between PGRN and PSAP is mediated by the linker region connecting saposins B and C and multiple granulin domains, with granulin D and E showing the most substantial binding [156].

The discoveries of independent PGRN trafficking pathways correlate nicely with studies searching for genetic determinants of plasma PGRN levels. Genome-wide association studies (GWAS) linked plasma PGRN levels to SNPs in both sortilin and PSAP, further confirming the importance of these two routes of trafficking [19, 84]. However, this does not preclude the possibility that additional pathways exist. In theory, PGRN might be carried to the lysosome by binding to other soluble lysosomal proteins, like PSAP, or by interacting with additional lysosomal trafficking receptors.

1.3.4 PGRN loss reduces lysosomal saposins

Ensuing research on the PGRN-PSAP relationship indicates that one of the mechanisms of pathology in cases of PGRN deficiency may be a reduction in neuronal lysosomal saposin levels due to a loss of indirect PSAP lysosomal trafficking via sortilin, which is highly expressed in neurons **(Fig. 1.1)** [158]. In support of the importance of this

trafficking pathway, immunofluorescence imaging of brain sections from either *Grn*$^{-/-}$ or *Sort*$^{-/-}$ mice showed a significant reduction in neuronal PSAP, and brain sections from FTLD-*GRN* patients showed a significant reduction in neuronal PSAP, saposin A, saposin B, and saposin C in the orbitofrontal cortex compared to healthy control or AD patient brain. Interestingly, saposin D, a known component of lipofuscin, accumulates in enlarged lysosomes of FTLD-*GRN* brain samples, which might reflect different biochemical properties and degradation routes of saposin peptides in the lysosome. Importantly, this reduction in saposin levels was specific to FTLD-*GRN,* but not FTLD-Tau patients, further implicating PGRN in this effect. Furthermore, loss of PSAP in mice was found to cause pathology and behavioral phenotypes reminiscent of FTLD. Therefore, by regulating PSAP trafficking, PGRN determines neuronal saposin levels and loss of neuronal saposins is likely to contribute to FTLD-like phenotypes.

1.3.5 PGRN is lysosomally processed into granulin peptides

With accumulating evidence that, in addition to being highly secreted, PGRN is localized to the lysosome and an understanding that it can be proteolytically processed into granulin peptides in the extracellular space, a natural corollary was that PGRN could be processed within the lysosome in a manner similar that of its binding partner, PSAP. One important implication is that, once liberated, granulin peptides could potentially each be involved in unique interactions, regulating different aspects of lysosomal physiology like the saposin peptides derived from PSAP. In fact, recent studies suggest that this may be the case **(Fig. 1.1)**.

Several laboratories have independently found that PGRN can be processed intracellularly in a lysosome-dependent manner [46, 155]. Granulin peptides were readily detected in lysates from several immortalized cell lines, and extracellular PGRN was efficiently endocytosed and processed into granulin peptides. While PGRN was detected in both the cell lysates and conditioned media collected from these cells, granulin peptides were almost undetectable in the media, indicating that, at least in these conditions, the peptides are not secreted nor produced extracellularly [46, 155]. This is also an assurance that the peptides detected internally were not endocytosed from the media.

Chemical inhibition of lysosomes was found to increase full-length PGRN, while decreasing granulin peptides, indicating that proper lysosome functioning is necessary for peptide generation [46, 155]. Perturbation of PGRN lysosomal trafficking also led to reduced production of granulin peptides [46, 155]. Additionally, cathepsin L (CTSL) was identified as a PGRN protease capable of efficiently cleaving PGRN into distinct peptides [46, 65, 155]. Liquid chromatography-mass spectrometry was used to identify the CTSL cleavage sites within PGRN, which were found to reside within its linker regions and were mostly distinct from those of neutrophil elastase [65].

These data are significant because, while it has been postulated that granulin peptides may exist in the lysosome, cumulatively, this is the first clear evidence of their lysosomal occurrence. These results support the hypothesis that granulin peptides may be functional units within the lysosome and relevant to the disease mechanisms of FTLD and NCL. Importantly, haploinsufficiency of full-length PGRN in FTLD leads to haploinsuffiency of granulin peptides [46]. While the functions of granulin peptides

remain to be fully elucidated, at the time of this writing, two different lysosomal enzymes have been shown to be positively regulated by PGRN or granulin peptides: cathepsin D (CTSD) and glucocerebrosidase (GBA).

1.3.6 PGRN regulates CTSD activity

The first evidence of a conceivable association between PGRN and lysosomal proteases comes from studies in *Arabidopsis* and several other plant species. Certain plant vacuolar cysteine proteases, such as the *Arabidopsis* protein, Responsive-to-Desiccation-21 (RD21), contain a granulin domain that is homologous to those found in mammalian PGRN [41, 129, 144]. The function of this domain is still unclear, but multiple studies have suggested that it is involved in the regulation, either positive or negative, of the maturation and enzymatic functioning of these proteases [144-146].

The existence of vacuolar combined granulin-proteases intimates the possibility of the existence of an analogous relationship in mammalian cells. Recently, three groups independently identified a functional relationship between PGRN, as well as select granulin peptides, and the lysosomal enzyme, CTSD [11, 131, 154]. CTSD is an aspartyl protease responsible for degrading proteins in the lysosome. Mutations in CTSD have been associated with AD and, as occurs with PGRN deficiency, CTSD loss in humans results in NCL [110, 136] and CTSD-deficient mice develop phosphorylated TDP-43 aggregates [39].

A correlation between PGRN deficiency and CTSD expression was previously established when *Grn*$^{-/-}$ mice were found to have an increase in both the immature and mature forms of CTSD, which rise up to 10x compared to WT mice by 20-24 months

of age [39]. In a model of facial crush injury, CTSD was the most highly transcriptionally upregulated gene in the facial motor nucleus of *Grn*$^{-/-}$ mice [11]. Likewise, human FTLD-*GRN* patient iPSC-derived cortical neurons showed an increase in mature CTSD [131].

While the upregulation of CTSD expression could be due to broader effects of PGRN loss, novel interactions between PGRN/granulin peptides and CTSD were established via overexpression and co-immunoprecipitation [154], as well as by pulldown of recombinant PGRN or granulin E added to mouse brain lysate [11]. Perhaps the most profound new findings are that CTSD activity is reduced in instances of PGRN deficiency, that PGRN stabilizes CTSD, and that PGRN and granulin E specifically modulate the activity of this protease. CTSD activity was significantly decreased across a range of tissue lysates from *Grn*$^{-/-}$ mice by as early as 2 months of age [154], and heterozygous *GRN* mutant iPSC-derived cortical neurons showed a significant decrease in CTSD activity, despite the above-mentioned increase in mature CTSD protein levels [131]. Remarkably, the reduction in CTSD activity in brain lysates of aged *Grn*$^{-/-}$ mice, normalized to mature CTSD, could be rescued by the addition of recombinant PGRN [11]. A direct augmentation of CTSD activity was demonstrated when recombinant PGRN or granulin E increased the activity of recombinant CTSD in a dose-dependent manner [11, 131]. Additionally, recombinant PGRN was found to increase the stability of CTSD at temperatures equal to or exceeding 37 °C, likely contributing to the observed enhancement of activity [11].

These new discoveries make CTSD a protein of great interest with respect to the role of PGRN in the development of FTLD and NCL. With the observed direct binding,

moderation of CTSD stability and activity, and overlap in disease and pathology, it is reasonable that CTSD deficiency subsequent to PGRN loss may be at least a partial mechanism of these two diseases. This also spurs the notion that PGRN/granulin peptides may directly stabilize or modulate the activity of other lysosomal enzymes, especially proteases similar to CTSD.

1.3.7 PGRN is a co-chaperone for GBA

A second lysosomal enzyme that has become of interest to PGRN-related pathologies is GBA, a β-glucosidase that cleaves glucocerebroside into glucose and ceramide [13]. Genetic mutation leading to GBA deficiency causes GD, the most common LSD [13, 14]. GBA mutation is also a recognized risk factor for Parkinson's disease (PD), with 5-10% of patients carrying a mutant gene [106].

An association between PGRN and GD was reported in 2016, when a significant decrease in serum PGRN levels was found in GD patients [53]. Likewise, under induced chronic inflammatory conditions, *Grn*$^{-/-}$ mice showed GD phenotypes, including hepatosplenomegaly, glycolipid accumulation in bone marrow, and appearance of Gaucher-like cells in multiple tissues, which could be rescued by supplementation with a human GBA analog [53]. Upon further investigation, PGRN, primarily through the C-terminal granulin E region, was shown to mediate an interaction between heat shock protein 70 (Hsp70) and GBA, as well as the GBA trafficking receptor, lysosome membrane protein 2 (LIMP-2) [52]. Endogenous GBA was found to be mislocalized and aggregated in the cytoplasm in *Grn*$^{-/-}$ mice under these inflammatory conditions.

However, GBA protein levels and enzymatic activity were not affected in *Grn*$^{-/-}$ mouse tissue lysates [53].

These studies identify PGRN as a functional co-chaperone of Hsp70, GBA, and LIMP-2 and suggest that in cases of PGRN deficiency, loss of Hsp70 chaperone function may result in mislocalization and loss of function of GBA. As with CTSD deficiency due to PGRN loss, GBA deficiency may be a mechanism of PGRN-related FTLD and NCL. Although these results need to be replicated, they open new avenues of research, as it is possible that PGRN, in conjunction with Hsp70 or possibly other heat shock proteins, acts as a co-chaperone for other lysosomal enzymes.

It is worth noting that PSAP is known to interact with CTSD [38, 45, 64], and saposin peptides with GBA [77, 78]. As PGRN can regulate CTSD activity and CTSD is the major contributor to PSAP processing to active saposins, it stands to reason that changes in PGRN levels may potentially alter PSAP processing. Likewise, GBA, an enzyme that is specifically activated by saposin C (and to a lesser extent, saposin A), could be impacted by this. Because of the complexity of these associations, more work is required to determine how PGRN loss affects these proteins and what the downstream consequences are.

1.3.8 TMEM106B is a risk factor for FTLD with *GRN* mutations

In 2010, a GWAS to detect gene loci imparting susceptibility to FTLD-TDP identified a then-uncharacterized transmembrane protein, TMEM106B, which showed risk vulnerability specific to *GRN* mutation carriers [133]. There are some indications that the pathologic connection to TMEM106B is related to increased levels of the protein.

First, elevated levels of TMEM106B have been found in the post-mortem brains of FTLD-TDP patients [22]. Second, a coding variant, p.T185S, was shown to be in linkage disequilibrium with a protective minor allele of the gene [33, 135]. One study suggested that the protective nature of this variant may be due to its more rapid degradation and subsequent lower levels [85]. Thus, it appears that elevated TMEM106B levels are associated with increased risk of FTLD with *GRN* mutations.

Early characterization of TMEM106B found it to be a glycosylated, type II transmembrane protein primarily localized to endosomes and lysosomes [16, 22, 63]. With the association between elevated TMEM106B levels and disease, significant effort has gone into examining the effects of TMEM106B overexpression. The most obvious phenotype associated with TMEM106B overexpression is lysosomal enlargement, which has been observed in multiple cell lines [16, 17, 22, 117]. Overexpression also results in a decreased capacity to degrade endocytic cargo [16], which could be due to inhibition of lysosomal acidification [22]. Likewise, it has been shown to increase intracellular PGRN levels [16, 22], which was recently demonstrated to likely be due to inhibition of processing into granulin peptides [46].

One study has identified an interaction between TMEM106B and microtubule-associated protein 6 (MAP6), and indicated a role for TMEM106B in dendritic trafficking of lysosomes [107]. An interaction between TMEM106B and the FTLD-related protein, charged multivesicular body protein 2B (CHMP2B), a component of endosomal sorting complexes required for transport-III (ESCRT-III), has also been reported [54]. Recently, Klein, et al. generated a *Tmem106b* knockout mouse model and found that loss of the protein resulted in a downregulation of several lysosomal

enzymes and vacuolar-ATPase AP1 and V0 domain subunits [59]. Similar to overexpression models, *Tmem106b*$^{-/-}$ primary cortical neurons showed a decrease in lysosomal acidification and, likely related to this, the authors found that TMEM106B interacts with the V-ATPase AP1 subunit in HEK293T cells.

Loss of TMEM106B was also found to ameliorate many of the pathological phenotypes associated with *Grn*$^{-/-}$ mice [59]. In double knockout animals, TMEM106B loss corrected retinal degeneration and rescued hyperactivity in *Grn*$^{-/-}$ mice. However, some detriments associated with PGRN deficiency, including lipofuscin accumulation and CD68 upregulation in microglia were not corrected [69, 119]. The authors argue that PGRN and TMEM106B regulate lysosomal biology in opposite directions.

To determine the *in vivo* effect of TMEM106B overexpression, a transgenic mouse line incorporating human TMEM106B under the neuron-specific CAMKII alpha promoter was created [159]. However, TMEM106B levels were found to be tightly regulated and were not elevated in the transgenic line compared to WT mice. Because TMEM106B is a risk factor for *GRN* mutant carriers, the authors wanted to see if PGRN regulates TMEM106B homeostasis. *Grn*$^{-/-}$ mice developed elevated levels of TMEM106B protein in the cortex with aging, which was further increased by the expression of the TMEM106B transgene. In the *Grn*$^{-/-}$ background, transgene expression was associated with greater lipofuscin accumulation and a higher percentage of neurons containing enlarged lysosomes, indicating greater lysosomal dysfunction. These results nicely recapitulate the genetic interaction between *GRN* and *TMEM106B* seen in human FTLD cases.

Intriguingly, a recent analysis identified a dominant D252N mutation in TMEM106B as a cause of hypomyelinating leukodystrophy [113, 148]. This disease is characterized by an intractable deficit in myelination leading to clinical signs, such as nystagmus, ataxia, and spasticity. It is not clear at the moment how TMEM106B mutation causes this disease, or whether this relates in any way to its relationship with PGRN and FTLD. In addition to this new disease association, a recent study identified *TMEM106B* and *GRN* as two main determinants of differential aging in the cerebral cortex with genome-wide significance [100].

It is still uncertain what the exact function of TMEM106B is or how it alters FTLD susceptibility. However, a great deal has been learned about the protein since it rose to prominence eight years ago. It is now understood that TMEM106B is an important regulator of lysosomal morphology and function, potentially through moderation of lysosomal acidification, and that an increase in TMEM106B levels produces grossly enlarged, poorly functioning lysosomes. This, alone or in combination with a reduction in PGRN processing, could potentially exacerbate lysosomal defects associated with PGRN haploinsufficiency in FTLD.

1.4 Discussion

The mechanistic link between PGRN and neurodegeneration has been elusive since its deficiency was first found to result in FTLD over a decade ago. Since that time, however, steady progress has been made in dissecting its function. Commonalities between PGRN-related FTLD and NCL pathology have been identified, PGRN has been shown to be trafficked to and processed in the lysosome, and direct mechanisms

of lysosomal dysfunction due to PGRN loss have been established. Taken together, these results strongly support that the loss of a necessary lysosomal function of PGRN likely contributes to neurodegeneration. However, it remains to be shown that findings, such as regulation of CTSD and GBA function by PGRN directly influence FTLD and NCL pathology. More so, these leaps in our understanding also raise new questions. Does PGRN modulate the activity of other lysosomal enzymes? Do other granulin peptides possess lysosomal functionality? Is there a greater significance to the overlap between binding partners and downstream functions of PGRN and PSAP? Notably, in addition to *GRN*, many other ALS/FTLD-associated genes, including *C9orf72*, valosin-containing protein (*VCP)/p97*, *CHMP2B*, sequestosome 1 (*SQSTM1)*, TANK-binding kinase 1 (*TBK1),* and optineurin (*OPTN),* are involved in endolysosome trafficking and the autophagy-lysosome pathway [97]. Therefore, lysosomal dysfunction may serve as a common mechanism of ALS/FTLD. As research pushes forward and we better understand the biological role of PGRN, we move closer to determining the mechanisms of related neurodegenerative diseases and developing new therapeutics to treat such conditions.

1.5 Acknowledgements

This work is supported by funding to F.H. from NINDS (R01NS088448, R01NS095954).

List of Abbreviations in Main Text

3'-UTR – 3'-untranslated region
Aβ – Amyloid-β
AD – Alzheimer's disease
ADAMTS-7 – A disintegrin and metalloproteinase with thrombospondin motifs 7
ALS – Amyotrophic lateral sclerosis
C9orf72 – Chromosome 9 open reading frame 72
CHMP2B – Charged multivesicular body protein 2B
CI-M6PR – Cation-independent mannose-6-phosphate receptor
CLN11 – Ceroid-lipofuscinosis, neuronal 11
CPPIC – Cysteine protease of protease-inhibitor complex
CTSD – Cathepsin D
CTSL – Cathepsin L
EphA2 – EPH receptor A2
ESCRT-III – Endosomal sorting complexes required for transport-III
FTD – Frontotemporal dementia
FTLD – Frontotemporal lobar degeneration
FTLD-FUS – FTLD with fused in sarcoma protein-positive inclusions
FTLD-*GRN* – FTLD with *GRN* mutation
FTLD-TAU – FTLD with tau-positive inclusions
FTLD-TDP – FTLD with TAR DNA-binding protein 43-positive inclusions
GBA – Glucocerebrosidase
GD – Gaucher disease
GEP – Granulin-epithelin precursor
GWAS – Genome-wide association study
Hsp70 – Heat shock protein 70
iPSC – Induced pluripotent stem cell
LIMP-2 – Lysosome membrane protein 2
LRP1 – Low-density lipoprotein receptor-related protein 1
LSD – Lysosomal storage disease
MAP6 – Microtubule-associated protein 6
MAPT – Microtubule-associated protein tau
NCL – Neuronal ceroid lipofuscinosis
OPTN – Optineurin
PCDGF – PC cell-derived growth factor
PD – Parkinson's disease
PEPI – Proepithelin
PGRN – Progranulin
PNFA – Progressive nonfluent aphasia
PPA – Primary progressive aphasia
proNGF – Nerve growth factor precursor
PSAP – Prosaposin
RD21 – Responsive-to-dessication-21
SD – Semantic dementia
SQSTM1 – Sequestosome 1

SNP – Single nucleotide polymorphism
TBK1 – TANK-binding kinase 1
TDP-43 – TAR DNA-binding protein 43
TFEB – Transcription factor EB
TGN – Trans-Golgi network
TNF – Tumor necrosis factor
Trem2 – Triggering receptor expressed on myeloid cells 2
VCP – Valosin-containing protein

REFERENCES

1. Abrhale T, Brodie A, Sabnis G, Macedo L, Tian C, Yue B, Serrero G (2011) GP88 (PC-Cell Derived Growth Factor, progranulin) stimulates proliferation and confers letrozole resistance to aromatase overexpressing breast cancer cells. BMC Cancer 11:231.

2. Ahmed Z, Sheng H, Xu YF, Lin WL, Innes AE, Gass J, Yu X et al. (2010) Accelerated lipofuscinosis and ubiquitination in granulin knockout mice suggest a role for progranulin in successful aging. Am J Pathol 177:311-324.

3. Almeida MR, Macario MC, Ramos L, Baldeiras I, Ribeiro MH, Santana I (2016) Portuguese family with the co-occurrence of frontotemporal lobar degeneration and neuronal ceroid lipofuscinosis phenotypes due to progranulin gene mutation. Neurobiol Aging 41:200 e201-205.

4. Almeida S, Zhou L, Gao FB (2011) Progranulin, a glycoprotein deficient in frontotemporal dementia, is a novel substrate of several protein disulfide isomerase family proteins. PLoS ONE 6:e26454.

5. Altmann C, Vasic V, Hardt S, Heidler J, Haussler A, Wittig I, Schmidt MH et al. (2016) Progranulin promotes peripheral nerve regeneration and reinnervation: role of notch signaling. Mol Neurodegener 11:69.

6. Arechavaleta-Velasco F, Perez-Juarez CE, Gerton GL, Diaz-Cueto L (2017) Progranulin and its biological effects in cancer. Med Oncol 34:194.

7. Bai XH, Wang DW, Kong L, Zhang Y, Luan Y, Kobayashi T, Kronenberg HM et al. (2009) ADAMTS-7, a direct target of PTHrP, adversely regulates endochondral bone growth by associating with and inactivating GEP growth factor. Mol Cell Biol 29:4201-4219.

8. Baker M, Mackenzie IR, Pickering-Brown SM, Gass J, Rademakers R, Lindholm C, Snowden J et al. (2006) Mutations in progranulin cause tau-negative frontotemporal dementia linked to chromosome 17. Nature 442:916-919.

9. Baladron V, Ruiz-Hidalgo MJ, Bonvini E, Gubina E, Notario V, Laborda J (2002) The EGF-like homeotic protein dlk affects cell growth and interacts with growth-modulating molecules in the yeast two-hybrid system. Biochem Biophys Res Commun 291:193-204.

10. Bateman A, Belcourt D, Bennett H, Lazure C, Solomon S (1990) Granulins, a novel class of peptide from leukocytes. Biochem Biophys Res Commun 173:1161-1168.

11. Beel S, Moisse M, Damme M, De Muynck L, Robberecht W, Van Den Bosch L, Saftig P et al. (2017) Progranulin functions as a cathepsin D chaperone to stimulate axonal outgrowth in vivo. Hum Mol Genet.

12. Belcastro V, Siciliano V, Gregoretti F, Mithbaokar P, Dharmalingam G, Berlingieri S, Iorio F et al. (2011) Transcriptional gene network inference from a massive dataset elucidates transcriptome organization and gene function. Nucleic Acids Res 39:8677-8688.

13. Beutler E, Demina A, Gelbart T (1994) Glucocerebrosidase mutations in Gaucher disease. Mol Med 1:82-92.

14. Beutler E, Grabowski G (1995) Guacher disease, vol 7th Ed. The Metabolic Basis of Inherited Disease. McGraw-Hill, New York

15. Bhandari V, Palfree RG, Bateman A (1992) Isolation and sequence of the granulin precursor cDNA from human bone marrow reveals tandem cysteine-rich granulin domains. Proc Natl Acad Sci U S A 89:1715-1719.

16. Brady OA, Zheng Y, Murphy K, Huang M, Hu F (2013) The frontotemporal lobar degeneration risk factor, TMEM106B, regulates lysosomal morphology and function. Hum Mol Genet 22:685-695.

17. Busch JI, Unger TL, Jain N, Tyler Skrinak R, Charan RA, Chen-Plotkin AS (2016) Increased expression of the frontotemporal dementia risk factor TMEM106B causes C9orf72-dependent alterations in lysosomes. Hum Mol Genet 25:2681-2697.

18. Butler GS, Dean RA, Tam EM, Overall CM (2008) Pharmacoproteomics of a metalloproteinase hydroxamate inhibitor in breast cancer cells: dynamics of membrane type 1 matrix metalloproteinase-mediated membrane protein shedding. Mol Cell Biol 28:4896-4914.

19. Carrasquillo MM, Nicholson AM, Finch N, Gibbs JR, Baker M, Rutherford NJ, Hunter TA et al. (2010) Genome-wide screen identifies rs646776 near sortilin as a regulator of progranulin levels in human plasma. Am J Hum Genet 87:890-897.

20. Cenik B, Sephton CF, Kutluk Cenik B, Herz J, Yu G (2012) Progranulin: a proteolytically processed protein at the crossroads of inflammation and neurodegeneration. J Biol Chem 287:32298-32306.

21. Chang MC, Srinivasan K, Friedman BA, Suto E, Modrusan Z, Lee WP, Kaminker JS et al. (2017) Progranulin deficiency causes impairment of autophagy and TDP-43 accumulation. J Exp Med 214:2611-2628.

22. Chen-Plotkin AS, Unger TL, Gallagher MD, Bill E, Kwong LK, Volpicelli-Daley L, Busch JI et al. (2012) TMEM106B, the Risk Gene for Frontotemporal Dementia, Is Regulated by the microRNA-132/212 Cluster and Affects Progranulin Pathways. J Neurosci 32:11213-11227.

23. Chen LW, Yung KK, Chan YS, Shum DK, Bolam JP (2008) The proNGF-p75NTR-sortilin signalling complex as new target for the therapeutic treatment of Parkinson's disease. CNS Neurol Disord Drug Targets 7:512-523.

24. Chen X, Chang J, Deng Q, Xu J, Nguyen TA, Martens LH, Cenik B et al. (2013) Progranulin does not bind tumor necrosis factor (TNF) receptors and is not a direct regulator of TNF-dependent signaling or bioactivity in immune or neuronal cells. J Neurosci 33:9202-9213.

25. Chitramuthu BP, Baranowski DC, Kay DG, Bateman A, Bennett HP (2010) Progranulin modulates zebrafish motoneuron development in vivo and rescues truncation defects associated with knockdown of Survival motor neuron 1. Mol Neurodegener 5:41.

26. Cotman SL, Karaa A, Staropoli JF, Sims KB (2013) Neuronal ceroid lipofuscinosis: impact of recent genetic advances and expansion of the clinicopathologic spectrum. Curr Neurol Neurosci Rep 13:366.

27. Cruts M, Gijselinck I, van der Zee J, Engelborghs S, Wils H, Pirici D, Rademakers R et al. (2006) Null mutations in progranulin cause ubiquitin-positive frontotemporal dementia linked to chromosome 17q21. Nature 442:920-924.

28. Daniel R, He Z, Carmichael KP, Halper J, Bateman A (2000) Cellular localization of gene expression for progranulin. J Histochem Cytochem 48:999-1009.

29. De Muynck L, Herdewyn S, Beel S, Scheveneels W, Van Den Bosch L, Robberecht W, Van Damme P (2013) The neurotrophic properties of progranulin depend on the granulin E domain but do not require sortilin binding. Neurobiol Aging 34:2541-2547.

30. Dicou E, Vincent JP, Mazella J (2004) Neurotensin receptor-3/sortilin mediates neurotensin-induced cytokine/chemokine expression in a murine microglial cell line. J Neurosci Res 78:92-99.

31. Edelman MJ, Feliciano J, Yue B, Bejarano P, Ioffe O, Reisman D, Hawkins D et al. (2014) GP88 (progranulin): a novel tissue and circulating biomarker for non-small cell lung carcinoma. Hum Pathol 45:1893-1899.

32. Evers BM, Rodriguez-Navas C, Tesla RJ, Prange-Kiel J, Wasser CR, Yoo KS, McDonald J et al. (2017) Lipidomic and Transcriptomic Basis of Lysosomal Dysfunction in Progranulin Deficiency. Cell Rep 20:2565-2574.

33. Finch N, Carrasquillo MM, Baker M, Rutherford NJ, Coppola G, Dejesus-Hernandez M, Crook R et al. (2011) TMEM106B regulates progranulin levels and the penetrance of FTLD in GRN mutation carriers. Neurology 76:467-474.

34. Gao X, Joselin AP, Wang L, Kar A, Ray P, Bateman A, Goate AM et al. (2010) Progranulin promotes neurite outgrowth and neuronal differentiation by regulating GSK-3beta. Protein Cell 1:552-562.

35. Gass J, Cannon A, Mackenzie IR, Boeve B, Baker M, Adamson J, Crook R et al. (2006) Mutations in progranulin are a major cause of ubiquitin-positive frontotemporal lobar degeneration. Hum Mol Genet 15:2988-3001.

36. Gass J, Lee WC, Cook C, Finch N, Stetler C, Jansen-West K, Lewis J et al. (2012) Progranulin regulates neuronal outgrowth independent of sortilin. Mol Neurodegener 7:33.

37. Gonzalez EM, Mongiat M, Slater SJ, Baffa R, Iozzo RV (2003) A novel interaction between perlecan protein core and progranulin: potential effects on tumor growth. J Biol Chem 278:38113-38116.

38. Gopalakrishnan MM, Grosch HW, Locatelli-Hoops S, Werth N, Smolenova E, Nettersheim M, Sandhoff K et al. (2004) Purified recombinant human prosaposin forms oligomers that bind procathepsin D and affect its autoactivation. Biochem J 383:507-515.

39. Gotzl JK, Mori K, Damme M, Fellerer K, Tahirovic S, Kleinberger G, Janssens J et al. (2014) Common pathobiochemical hallmarks of progranulin-associated frontotemporal lobar degeneration and neuronal ceroid lipofuscinosis. Acta Neuropathol 127:845-860.

40. Gowrishankar S, Yuan P, Wu Y, Schrag M, Paradise S, Grutzendler J, De Camilli P et al. (2015) Massive accumulation of luminal protease-deficient axonal lysosomes at Alzheimer's disease amyloid plaques. Proc Natl Acad Sci U S A 112:E3699-3708.

41. Gu C, Shabab M, Strasser R, Wolters PJ, Shindo T, Niemer M, Kaschani F et al. (2012) Post-translational regulation and trafficking of the granulin-containing protease RD21 of Arabidopsis thaliana. PLoS One 7:e32422.

42. He Z, Bateman A (2003) Progranulin (granulin-epithelin precursor, PC-cell-derived growth factor, acrogranin) mediates tissue repair and tumorigenesis. J Mol Med 81:600-612.

43. He Z, Ismail A, Kriazhev L, Sadvakassova G, Bateman A (2002) Progranulin (PC-cell-derived growth factor/acrogranin) regulates invasion and cell survival. Cancer Res 62:5590-5596.

44. He Z, Ong CH, Halper J, Bateman A (2003) Progranulin is a mediator of the wound response. Nat Med 9:225-229.

45. Hiraiwa M, Martin BM, Kishimoto Y, Conner GE, Tsuji S, O'Brien JS (1997) Lysosomal proteolysis of prosaposin, the precursor of saposins (sphingolipid activator proteins): its mechanism and inhibition by ganglioside. Arch Biochem Biophys 341:17-24.

46. Holler CJ, Taylor G, Deng Q, Kukar T (2017) Intracellular Proteolysis of Progranulin Generates Stable, Lysosomal Granulins that Are Haploinsufficient in Patients with Frontotemporal Dementia Caused by GRN Mutations. Eneuro 4.

47. Hosokawa M, Tanaka Y, Arai T, Kondo H, Akiyama H, Hasegawa M (2018) Progranulin haploinsufficiency reduces amyloid beta deposition in Alzheimer's disease model mice. Exp Anim 67:63-70.

48. Hrabal R, Chen Z, James S, Bennett HP, Ni F (1996) The hairpin stack fold, a novel protein architecture for a new family of protein growth factors. Nat Struct Biol 3:747-752.

49. Hsiung GY, Fok A, Feldman HH, Rademakers R, Mackenzie IR (2011) rs5848 polymorphism and serum progranulin level. J Neurol Sci 300:28-32.

50. Hu F, Padukkavidana T, Vaegter CB, Brady OA, Zheng Y, Mackenzie IR, Feldman HH et al. (2010) Sortilin-mediated endocytosis determines levels of the frontotemporal dementia protein, progranulin. Neuron 68:654-667.

51. Jian J, Konopka J, Liu C (2013) Insights into the role of progranulin in immunity, infection, and inflammation. J Leukoc Biol 93:199-208.

52. Jian J, Tian QY, Hettinghouse A, Zhao S, Liu H, Wei J, Grunig G et al. (2016) Progranulin Recruits HSP70 to beta-Glucocerebrosidase and Is Therapeutic Against Gaucher Disease. EBioMedicine 13:212-224.

53. Jian J, Zhao S, Tian QY, Liu H, Zhao Y, Chen WC, Grunig G et al. (2016) Association Between Progranulin and Gaucher Disease. EBioMedicine 11:127-137.

54. Jun MH, Han JH, Lee YK, Jang DJ, Kaang BK, Lee JA (2015) TMEM106B, a frontotemporal lobar dementia (FTLD) modifier, associates with FTD-3-linked CHMP2B, a complex of ESCRT-III. Mol Brain 8:85.

55. Kamalainen A, Viswanathan J, Natunen T, Helisalmi S, Kauppinen T, Pikkarainen M, Pursiheimo JP et al. (2013) GRN variant rs5848 reduces plasma and brain levels of granulin in Alzheimer's disease patients. J Alzheimers Dis 33:23-27.

56. Kao AW, Eisenhut RJ, Martens LH, Nakamura A, Huang A, Bagley JA, Zhou P et al. (2011) A neurodegenerative disease mutation that accelerates the clearance of apoptotic cells. Proceedings of the National Academy of Sciences of the United States of America 108:4441-4446.

57. Kao AW, McKay A, Singh PP, Brunet A, Huang EJ (2017) Progranulin, lysosomal regulation and neurodegenerative disease. Nature reviews Neuroscience 18:325-333.

58. Kessenbrock K, Frohlich L, Sixt M, Lammermann T, Pfister H, Bateman A, Belaaouaj A et al. (2008) Proteinase 3 and neutrophil elastase enhance inflammation in mice by inactivating antiinflammatory progranulin. J Clin Invest 118:2438-2447.

59. Klein ZA, Takahashi H, Ma M, Stagi M, Zhou M, Lam TT, Strittmatter SM (2017) Loss of TMEM106B Ameliorates Lysosomal and Frontotemporal Dementia-Related Phenotypes in Progranulin-Deficient Mice. Neuron 95:281-296 e286.

60. Kohlschutter A, Schulz A (2009) Towards understanding the neuronal ceroid lipofuscinoses. Brain Dev 31:499-502.

61. Kojima Y, Ono K, Inoue K, Takagi Y, Kikuta K, Nishimura M, Yoshida Y et al. (2009) Progranulin expression in advanced human atherosclerotic plaque. Atherosclerosis 206:102-108.

62. Laird AS, Van Hoecke A, De Muynck L, Timmers M, Van den Bosch L, Van Damme P, Robberecht W (2010) Progranulin is neurotrophic in vivo and protects against a mutant TDP-43 induced axonopathy. PLoS ONE 5:e13368.

63. Lang CM, Fellerer K, Schwenk BM, Kuhn PH, Kremmer E, Edbauer D, Capell A et al. (2012) Membrane orientation and subcellular localization of transmembrane protein 106B (TMEM106B), a major risk factor for frontotemporal lobar degeneration. J Biol Chem 287:19355-19365.

64. Laurent-Matha V, Lucas A, Huttler S, Sandhoff K, Garcia M, Rochefort H (2002) Procathepsin D interacts with prosaposin in cancer cells but its internalization is not mediated by LDL receptor-related protein. Exp Cell Res 277:210-219.

65. Lee CW, Stankowski JN, Chew J, Cook CN, Lam YW, Almeida S, Carlomagno Y et al. (2017) The lysosomal protein cathepsin L is a progranulin protease. Mol Neurodegener 12:55.

66. Lee MJ, Chen TF, Cheng TW, Chiu MJ (2011) rs5848 Variant of Progranulin Gene Is a Risk of Alzheimer's Disease in the Taiwanese Population. Neurodegener Dis 8:216-220.

67. Lomen-Hoerth C, Anderson T, Miller B (2002) The overlap of amyotrophic lateral sclerosis and frontotemporal dementia. Neurology 59:1077-1079.

68. Lu R, Serrero G (2001) Mediation of estrogen mitogenic effect in human breast cancer MCF-7 cells by PC-cell-derived growth factor (PCDGF/granulin precursor). Proc Natl Acad Sci U S A 98:142-147.

69. Lui H, Zhang J, Makinson SR, Cahill MK, Kelley KW, Huang HY, Shang Y et al. (2016) Progranulin Deficiency Promotes Circuit-Specific Synaptic Pruning by Microglia via Complement Activation. Cell.

70. Mackenzie IR, Baker M, Pickering-Brown S, Hsiung GY, Lindholm C, Dwosh E, Gass J et al. (2006) The neuropathology of frontotemporal lobar degeneration caused by mutations in the progranulin gene. Brain 129:3081-3090.

71. Mackenzie IR, Neumann M (2016) Molecular neuropathology of frontotemporal dementia: insights into disease mechanisms from postmortem studies. J Neurochem 138 Suppl 1:54-70.

72. Martens LH, Zhang J, Barmada SJ, Zhou P, Kamiya S, Sun B, Min SW et al. (2012) Progranulin deficiency promotes neuroinflammation and neuron loss following toxin-induced injury. J Clin Invest 122:3955-3959.

73. Mazella J, Zsurger N, Navarro V, Chabry J, Kaghad M, Caput D, Ferrara P et al. (1998) The 100-kDa neurotensin receptor is gp95/sortilin, a non-G-protein-coupled receptor. J Biol Chem 273:26273-26276.

74. Minami SS, Min SW, Krabbe G, Wang C, Zhou Y, Asgarov R, Li Y et al. (2014) Progranulin protects against amyloid beta deposition and toxicity in Alzheimer's disease mouse models. Nat Med 20:1157-1164.

75. Moisse K, Volkening K, Leystra-Lantz C, Welch I, Hill T, Strong MJ (2009) Divergent patterns of cytosolic TDP-43 and neuronal progranulin expression following axotomy: implications for TDP-43 in the physiological response to neuronal injury. Brain Res 1249:202-211.

76. Mole SE, Cotman SL (2015) Genetics of the neuronal ceroid lipofuscinoses (Batten disease). Biochim Biophys Acta 1852:2237-2241.

77. Morimoto S, Kishimoto Y, Tomich J, Weiler S, Ohashi T, Barranger JA, Kretz KA et al. (1990) Interaction of saposins, acidic lipids, and glucosylceramidase. J Biol Chem 265:1933-1937.

78. Morimoto S, Martin BM, Yamamoto Y, Kretz KA, O'Brien JS, Kishimoto Y (1989) Saposin A: second cerebrosidase activator protein. Proc Natl Acad Sci U S A 86:3389-3393.

79. Mukherjee O, Pastor P, Cairns NJ, Chakraverty S, Kauwe JS, Shears S, Behrens MI et al. (2006) HDDD2 is a familial frontotemporal lobar degeneration with ubiquitin-positive, tau-negative inclusions caused by a missense mutation in the signal peptide of progranulin. Ann Neurol 60:314-322.

80. Nabar NR, Kehrl JH (2017) The Transcription Factor EB Links Cellular Stress to the Immune Response. Yale J Biol Med 90:301-315.

81. Naphade SB, Kigerl KA, Jakeman LB, Kostyk SK, Popovich PG, Kuret J (2010) Progranulin expression is upregulated after spinal contusion in mice. Acta Neuropathol 119:123-133.

82. Neary D, Snowden JS, Gustafson L, Passant U, Stuss D, Black S, Freedman M et al. (1998) Frontotemporal lobar degeneration: a consensus on clinical diagnostic criteria. Neurology 51:1546-1554.

83. Neill T, Buraschi S, Goyal A, Sharpe C, Natkanski E, Schaefer L, Morrione A et al. (2016) EphA2 is a functional receptor for the growth factor progranulin. J Cell Biol 215:687-703.

84. Nicholson AM, Finch NA, Almeida M, Perkerson RB, van Blitterswijk M, Wojtas A, Cenik B et al. (2016) Prosaposin is a regulator of progranulin levels and oligomerization. Nat Commun 7:11992.

85. Nicholson AM, Finch NA, Wojtas A, Baker MC, Perkerson RB, 3rd, Castanedes-Casey M, Rousseau L et al. (2013) TMEM106B p.T185S regulates TMEM106B protein levels: implications for frontotemporal dementia. J Neurochem 126:781-791.

86. Nita DA, Mole SE, Minassian BA (2016) Neuronal ceroid lipofuscinoses. Epileptic Disord 18:73-88.

87. Nykjaer A, Lee R, Teng KK, Jansen P, Madsen P, Nielsen MS, Jacobsen C et al. (2004) Sortilin is essential for proNGF-induced neuronal cell death. Nature 427:843-848.

88. O'Brien JS, Kishimoto Y (1991) Saposin proteins: structure, function, and role in human lysosomal storage disorders. FASEB J 5:301-308.

89. Okura H, Yamashita S, Ohama T, Saga A, Yamamoto-Kakuta A, Hamada Y, Sougawa N et al. (2010) HDL/apolipoprotein A-I binds to macrophage-derived progranulin and suppresses its conversion into proinflammatory granulins. J Atheroscler Thromb 17:568-577.

90. Palfree RG, Bennett HP, Bateman A (2015) The Evolution of the Secreted Regulatory Protein Progranulin. PLoS ONE 10:e0133749.

91. Park B, Buti L, Lee S, Matsuwaki T, Spooner E, Brinkmann MM, Nishihara M et al. (2011) Granulin is a soluble cofactor for toll-like receptor 9 signaling. Immunity 34:505-513.

92. Pereson S, Wils H, Kleinberger G, McGowan E, Vandewoestyne M, Van Broeck B, Joris G et al. (2009) Progranulin expression correlates with dense-core amyloid plaque burden in Alzheimer disease mouse models. J Pathol 219:173-181.

93. Petkau TL, Neal SJ, Milnerwood A, Mew A, Hill AM, Orban P, Gregg J et al. (2012) Synaptic dysfunction in progranulin-deficient mice. Neurobiol Dis 45:711-722.

94. Philips T, De Muynck L, Thu HN, Weynants B, Vanacker P, Dhondt J, Sleegers K et al. (2010) Microglial upregulation of progranulin as a marker of motor neuron degeneration. J Neuropathol Exp Neurol 69:1191-1200.

95. Pickford F, Marcus J, Camargo LM, Xiao Q, Graham D, Mo JR, Burkhardt M et al. (2011) Progranulin is a chemoattractant for microglia and stimulates their endocytic activity. Am J Pathol 178:284-295.

96. Plowman GD, Green JM, Neubauer MG, Buckley SD, McDonald VL, Todaro GJ, Shoyab M (1992) The epithelin precursor encodes two proteins with opposing activities on epithelial cell growth. J Biol Chem 267:13073-13078.

97. Pottier C, Ravenscroft TA, Sanchez-Contreras M, Rademakers R (2016) Genetics of FTLD: overview and what else we can expect from genetic studies. J Neurochem 138 Suppl 1:32-53.

98. Rademakers R, Eriksen JL, Baker M, Robinson T, Ahmed Z, Lincoln SJ, Finch N et al. (2008) Common variation in the miR-659 binding-site of GRN is a major risk factor for TDP43-positive frontotemporal dementia. Hum Mol Genet 17:3631-3642.

99. Ratnavalli E, Brayne C, Dawson K, Hodges JR (2002) The prevalence of frontotemporal dementia. Neurology 58:1615-1621.

100. Rhinn H, Abeliovich A (2017) Differential Aging Analysis in Human Cerebral Cortex Identifies Variants in TMEM106B and GRN that Regulate Aging Phenotypes. Cell Syst 4:404-415 e405.

101. Roberson ED (2012) Mouse models of frontotemporal dementia. Ann Neurol 72:837-849.

102. Rosen EY, Wexler EM, Versano R, Coppola G, Gao F, Winden KD, Oldham MC et al. (2011) Functional genomic analyses identify pathways dysregulated by progranulin deficiency, implicating Wnt signaling. Neuron 71:1030-1042.

103. Ryan CL, Baranowski DC, Chitramuthu BP, Malik S, Li Z, Cao M, Minotti S et al. (2009) Progranulin is expressed within motor neurons and promotes neuronal cell survival. BMC Neurosci 10:130.

104. Salazar DA, Butler VJ, Argouarch AR, Hsu TY, Mason A, Nakamura A, McCurdy H et al. (2015) The Progranulin Cleavage Products, Granulins, Exacerbate TDP-43 Toxicity and Increase TDP-43 Levels. The Journal of neuroscience : the official journal of the Society for Neuroscience 35:9315-9328.

105. Sardiello M, Palmieri M, di Ronza A, Medina DL, Valenza M, Gennarino VA, Di Malta C et al. (2009) A gene network regulating lysosomal biogenesis and function. Science 325:473-477.

106. Schapira AH (2015) Glucocerebrosidase and Parkinson disease: Recent advances. Mol Cell Neurosci 66:37-42.

107. Schwenk BM, Lang CM, Hogl S, Tahirovic S, Orozco D, Rentzsch K, Lichtenthaler SF et al. (2014) The FTLD risk factor TMEM106B and MAP6 control dendritic trafficking of lysosomes. Embo J.

108. Schymick JC, Yang Y, Andersen PM, Vonsattel JP, Greenway M, Momeni P, Elder J et al. (2007) Progranulin mutations and amyotrophic lateral sclerosis or amyotrophic lateral sclerosis-frontotemporal dementia phenotypes. J Neurol Neurosurg Psychiatry 78:754-756.

109. Serrero G, Hawkins DM, Yue B, Ioffe O, Bejarano P, Phillips JT, Head JF et al. (2012) Progranulin (GP88) tumor tissue expression is associated with increased risk of recurrence in breast cancer patients diagnosed with estrogen receptor positive invasive ductal carcinoma. Breast Cancer Res 14:R26.

110. Shacka JJ, Roth KA (2007) Cathepsin D deficiency and NCL/Batten disease: there's more to death than apoptosis. Autophagy 3:474-476.

111. Sheng J, Su L, Xu Z, Chen G (2014) Progranulin polymorphism rs5848 is associated with increased risk of Alzheimer's disease. Gene 542:141-145.

112. Shoyab M, McDonald VL, Byles C, Todaro GJ, Plowman GD (1990) Epithelins 1 and 2: isolation and characterization of two cysteine-rich growth-modulating proteins. Proc Natl Acad Sci U S A 87:7912-7916.

113. Simons C, Dyment D, Bent SJ, Crawford J, D'Hooghe M, Kohlschutter A, Venkateswaran S et al. (2017) A recurrent de novo mutation in TMEM106B causes hypomyelinating leukodystrophy. Brain 140:3105-3111.

114. Smith KR, Damiano J, Franceschetti S, Carpenter S, Canafoglia L, Morbin M, Rossi G et al. (2012) Strikingly different clinicopathological phenotypes determined by progranulin-mutation dosage. Am J Hum Genet 90:1102-1107.

115. Snowden JS, Pickering-Brown SM, Mackenzie IR, Richardson AM, Varma A, Neary D, Mann DM (2006) Progranulin gene mutations associated with frontotemporal dementia and progressive non-fluent aphasia. Brain 129:3091-3102.

116. Songsrirote K, Li Z, Ashford D, Bateman A, Thomas-Oates J (2010) Development and application of mass spectrometric methods for the analysis of progranulin N-glycosylation. J Proteomics 73:1479-1490.

117. Stagi M, Klein ZA, Gould TJ, Bewersdorf J, Strittmatter SM (2014) Lysosome size, motility and stress response regulated by fronto-temporal dementia modifier TMEM106B. Mol Cell Neurosci 61:226-240.

118. Suh HS, Choi N, Tarassishin L, Lee SC (2012) Regulation of progranulin expression in human microglia and proteolysis of progranulin by matrix metalloproteinase-12 (MMP-12). PLoS ONE 7:e35115.

119. Takahashi H, Klein ZA, Bhagat SM, Kaufman AC, Kostylev MA, Ikezu T, Strittmatter SM (2017) Opposing effects of progranulin deficiency on amyloid and tau pathologies via microglial TYROBP network. Acta Neuropathol 133:785-807.

120. Tanaka Y, Chambers JK, Matsuwaki T, Yamanouchi K, Nishihara M (2014) Possible involvement of lysosomal dysfunction in pathological changes of the brain in aged progranulin-deficient mice. Acta Neuropathol Commun 2:78.

121. Tanaka Y, Matsuwaki T, Yamanouchi K, Nishihara M (2013) Exacerbated inflammatory responses related to activated microglia after traumatic brain injury in progranulin-deficient mice. Neuroscience 231:49-60.

122. Tang W, Lu Y, Tian QY, Zhang Y, Guo FJ, Liu GY, Syed NM et al. (2011) The growth factor progranulin binds to TNF receptors and is therapeutic against inflammatory arthritis in mice. Science 332:478-484.

123. Tangkeangsirisin W, Hayashi J, Serrero G (2004) PC cell-derived growth factor mediates tamoxifen resistance and promotes tumor growth of human breast cancer cells. Cancer Res 64:1737-1743.

124. Tangkeangsirisin W, Serrero G (2004) PC cell-derived growth factor (PCDGF/GP88, progranulin) stimulates migration, invasiveness and VEGF expression in breast cancer cells. Carcinogenesis 25:1587-1592.

125. Toh H, Cao M, Daniels E, Bateman A (2013) Expression of the growth factor progranulin in endothelial cells influences growth and development of blood vessels: a novel mouse model. PLoS ONE 8:e64989.

126. Toh H, Chitramuthu BP, Bennett HP, Bateman A (2011) Structure, function, and mechanism of progranulin; the brain and beyond. J Mol Neurosci 45:538-548.

127. Tolkatchev D, Malik S, Vinogradova A, Wang P, Chen Z, Xu P, Bennett HP et al. (2008) Structure dissection of human progranulin identifies well-folded granulin/epithelin modules with unique functional activities. Protein Sci 17:711-724.

128. Tolkatchev D, Ng A, Vranken W, Ni F (2000) Design and solution structure of a well-folded stack of two beta-hairpins based on the amino-terminal fragment of human granulin A. Biochemistry 39:2878-2886.

129. Tolkatchev D, Xu P, Ni F (2001) A peptide derived from the C-terminal part of a plant cysteine protease folds into a stack of two beta-hairpins, a scaffold present in the emerging family of granulin-like growth factors. J Pept Res 57:227-233.

130. Uesaka N, Abe M, Konno K, Yamazaki M, Sakoori K, Watanabe T, Kao TH et al. (2018) Retrograde Signaling from Progranulin to Sort1 Counteracts Synapse Elimination in the Developing Cerebellum. Neuron 97:796-805 e795.

131. Valdez C, Wong YC, Schwake M, Bu G, Wszolek ZK, Krainc D (2017) Progranulin-mediated deficiency of cathepsin D results in FTD and NCL-like phenotypes in neurons derived from FTD patients. Hum Mol Genet 26:4861-4872.

132. Van Damme P, Van Hoecke A, Lambrechts D, Vanacker P, Bogaert E, van Swieten J, Carmeliet P et al. (2008) Progranulin functions as a neurotrophic factor to regulate neurite outgrowth and enhance neuronal survival. J Cell Biol 181:37-41.

133. Van Deerlin VM, Sleiman PM, Martinez-Lage M, Chen-Plotkin A, Wang LS, Graff-Radford NR, Dickson DW et al. (2010) Common variants at 7p21 are associated with frontotemporal lobar degeneration with TDP-43 inclusions. Nat Genet 42:234-239.

134. Van Kampen JM, Kay DG (2017) Progranulin gene delivery reduces plaque burden and synaptic atrophy in a mouse model of Alzheimer's disease. PLoS One 12:e0182896.

135. Vass R, Ashbridge E, Geser F, Hu WT, Grossman M, Clay-Falcone D, Elman L et al. (2011) Risk genotypes at TMEM106B are associated with cognitive impairment in amyotrophic lateral sclerosis. Acta Neuropathol 121:373-380.

136. Vidoni C, Follo C, Savino M, Melone MA, Isidoro C (2016) The Role of Cathepsin D in the Pathogenesis of Human Neurodegenerative Disorders. Med Res Rev.

137. Vranken WF, Chen ZG, Xu P, James S, Bennett HP, Ni F (1999) A 30-residue fragment of the carp granulin-1 protein folds into a stack of two beta-hairpins similar to that found in the native protein. J Pept Res 53:590-597.

138. Wang J, Van Damme P, Cruchaga C, Gitcho MA, Vidal JM, Seijo-Martinez M, Wang L et al. (2010) Pathogenic cysteine mutations affect progranulin function and production of mature granulins. J Neurochem 112:1305-1315.

139. Ward ME, Chen R, Huang HY, Ludwig C, Telpoukhovskaia M, Taubes A, Boudin H et al. (2017) Individuals with progranulin haploinsufficiency exhibit features of neuronal ceroid lipofuscinosis. Sci Transl Med 9.

140. Wils H, Kleinberger G, Pereson S, Janssens J, Capell A, Van Dam D, Cuijt I et al. (2012) Cellular ageing, increased mortality and FTLD-TDP-associated neuropathology in progranulin knockout mice. J Pathol 228:67-76.

141. Xu D, Suenaga N, Edelmann MJ, Fridman R, Muschel RJ, Kessler BM (2008) Novel MMP-9 substrates in cancer cells revealed by a label-free quantitative proteomics approach. Mol Cell Proteomics.

142. Xu HM, Tan L, Wan Y, Tan MS, Zhang W, Zheng ZJ, Kong LL et al. (2017) PGRN Is Associated with Late-Onset Alzheimer's Disease: a Case-Control Replication Study and Meta-analysis. Mol Neurobiol 54:1187-1195.

143. Xu K, Zhang Y, Ilalov K, Carlson CS, Feng JQ, Di Cesare PE, Liu CJ (2007) Cartilage oligomeric matrix protein associates with granulin-epithelin precursor (GEP) and potentiates GEP-stimulated chondrocyte proliferation. J Biol Chem 282:11347-11355.

144. Yamada K, Matsushima R, Nishimura M, Hara-Nishimura I (2001) A slow maturation of a cysteine protease with a granulin domain in the vacuoles of senescing Arabidopsis leaves. Plant Physiol 127:1626-1634.

145. Yamada T, Kondo A, Ohta H, Masuda T, Shimada H, Takamiya K (2001) Isolation of the protease component of maize cysteine protease-cystatin

complex: release of cystatin is not crucial for the activation of the cysteine protease. Plant Cell Physiol 42:710-716.

146. Yamada T, Ohta H, Masuda T, Ikeda M, Tomita N, Ozawa A, Shioi Y et al. (1998) Purification of a novel type of SDS-dependent protease in maize using a monoclonal antibody. Plant Cell Physiol 39:106-114.

147. Yamamoto Y, Goto N, Takemura M, Yamasuge W, Yabe K, Takami T, Miyazaki T et al. (2017) Association between increased serum GP88 (progranulin) concentrations and prognosis in patients with malignant lymphomas. Clin Chim Acta 473:139-146.

148. Yan H, Kubisiak T, Ji H, Xiao J, Wang J, Burmeister M (2018) The recurrent mutation in TMEM106B also causes hypomyelinating leukodystrophy in China and is a CpG hot spot. Brain.

149. Yin F, Banerjee R, Thomas B, Zhou P, Qian L, Jia T, Ma X et al. (2010) Exaggerated inflammation, impaired host defense, and neuropathology in progranulin-deficient mice. J Exp Med 207:117-128.

150. Yin F, Dumont M, Banerjee R, Ma Y, Li H, Lin MT, Beal MF et al. (2010) Behavioral deficits and progressive neuropathology in progranulin-deficient mice: a mouse model of frontotemporal dementia. FASEB J 24:4639-4647.

151. Zanocco-Marani T, Bateman A, Romano G, Valentinis B, He ZH, Baserga R (1999) Biological activities and signaling pathways of the granulin/epithelin precursor. Cancer Res 59:5331-5340.

152. Zhang Y, Chen K, Sloan SA, Bennett ML, Scholze AR, O'Keeffe S, Phatnani HP et al. (2014) An RNA-sequencing transcriptome and splicing database of glia, neurons, and vascular cells of the cerebral cortex. The Journal of neuroscience : the official journal of the Society for Neuroscience 34:11929-11947.

153. Zheng Y, Brady OA, Meng PS, Mao Y, Hu F (2011) C-terminus of progranulin interacts with the beta-propeller region of sortilin to regulate progranulin trafficking. PLoS ONE 6:e21023.

154. Zhou X, Paushter DH, Feng T, Pardon CM, Mendoza CS, Hu F (2017) Regulation of cathepsin D activity by the FTLD protein progranulin. Acta Neuropathol 134:151-153.

155. Zhou X, Paushter DH, Feng T, Sun L, Reinheckel T, Hu F (2017) Lysosomal processing of progranulin. Mol Neurodegener 12:62.

156. Zhou X, Sullivan PM, Sun L, Hu F (2017) The interaction between progranulin and prosaposin is mediated by granulins and the linker region between saposin B and C. J Neurochem.

157. Zhou X, Sun L, Bastos de Oliveira F, Qi X, Brown WJ, Smolka MB, Sun Y et al. (2015) Prosaposin facilitates sortilin-independent lysosomal trafficking of progranulin. J Cell Biol 210:991-1002.

158. Zhou X, Sun L, Bracko O, Choi JW, Jia Y, Nana AL, Brady OA et al. (2017) Impaired prosaposin lysosomal trafficking in frontotemporal lobar degeneration due to progranulin mutations. Nat Commun 8:15277.

159. Zhou X, Sun L, Brady OA, Murphy KA, Hu F (2017) Elevated TMEM106B levels exaggerate lipofuscin accumulation and lysosomal dysfunction in aged mice with progranulin deficiency. Acta Neuropathol Commun 5:9.

160. Zhu J, Nathan C, Jin W, Sim D, Ashcroft GS, Wahl SM, Lacomis L et al. (2002) Conversion of proepithelin to epithelins: roles of SLPI and elastase in host defense and wound repair. Cell 111:867-878.

CHAPTER 2

LYSOSOMAL PROCESSING OF PROGRANULIN

Published as Zhou X*, Paushter DH*, Feng T, Sun L, Reinheckel T, Hu F. Lysosomal processing of progranulin. Mol Neurodegener. 2017 Aug 23;12(1):62. doi: 10.1186/s13024-017-0205-9. *Equal contributors.

2.1 Abstract

Background: Mutations resulting in progranulin (PGRN) haploinsufficiency cause frontotemporal lobar degeneration with TDP-43-positive inclusions (FTLD-TDP), a devastating neurodegenerative disease. PGRN is localized to the lysosome and important for proper lysosome function. However, the metabolism of PGRN in the lysosome is still unclear. **Results:** Here we report that PGRN is processed into ~10kDa peptides intracellularly in multiple cell types and tissues and this processing is dependent on lysosomal activities. PGRN endocytosed from the extracellular space is also processed in a similar manner. We further demonstrated that multiple cathepsins are involved in PGRN processing and cathepsin L cleaves PGRN *in vitro*. **Conclusions:** Our data support that PGRN is processed in the lysosome through the actions of cathepsins. **Keywords:** Progranulin (PGRN), cathepsin, lysosome, frontotemporal lobar degeneration (FTLD), neuronal ceroid lipofuscinosis (NCL).

2.2 Introduction

Progranulin (PGRN) is an evolutionarily conserved glycoprotein of 7.5 granulin repeats encoded by the granulin (*GRN*) gene in humans [1-4]. Mutations in the *GRN* gene are associated with several neurodegenerative diseases [1-4]. While PGRN haploinsufficiency is a leading cause of frontotemporal lobar degeneration (FTLD) [5], complete loss of PGRN is known to cause neuronal ceroid lipofuscinosis (NCL) [6, 7], a group of lysosomal storage diseases. Accumulating evidence suggests an important function of PGRN in the lysosome. Transcription of the *GRN* gene is regulated by the transcriptional factor, TFEB, together with a number of essential lysosomal genes [8] and PGRN is trafficked to lysosomes through two distinct pathways [9, 10]. However, the metabolism of PGRN in the lysosome remains to be determined. One interesting hypothesis is that PGRN is processed into granulin peptides in a similar manner to prosaposin (PSAP), the precursor of saposin peptides (A, B, C, D) that are essential for lysosomal glycosphingolipid metabolism [11-13], and that granulins function to regulate enzymatic activities in the lysosome [2].

2.3 Results

Intracellular processing of PGRN

To test the potential processing of PGRN, we immunoprecipitated PGRN and any potential PGRN-derived peptides from primary microglia grown in [^{35}S]-labeled methionine- and cysteine-containing medium using a homemade antibody previously characterized [10]. The immunoprecipitates were separated by Tricine-SDS polyacrylamide-gel-electrophoresis (PAGE) to resolve peptides below 10-15kDa and

were visualized using autoradiography. In addition to full-length PGRN, a band of approximately 10kDa, corresponding to the expected size of granulin peptides, was present in wild type (WT) mouse microglia but absent in *Grn*$^{-/-}$ microglia **(Fig. 2.1a)**, indicating that these were peptides derived from PGRN. Although PGRN has been shown to be cleaved by elastase and MMPs extracellularly [14, 15], we failed to detect any significant processed PGRN products in the secreted fraction **(Fig. 2.1a)**, suggesting that PGRN is primarily processed intracellularly in microglia.

Previously, we reported an interaction between PGRN and PSAP [10]. However, PGRN does not bind to processed saposin peptides [10, 16]. While, based on the autoradiography results alone, we can not rule out that there might be other peptides interacting with PGRN, most likely the peptides that we visualized are PGRN-derived. To confirm this, we attempted to detect these peptides via Western blotting. A clear 10kDa band was detected in lysates from the wild type mouse embryonic fibroblasts (MEFs) but was absent from *Grn*$^{-/-}$ fibroblasts using commercial polyclonal anti-mouse PGRN antibodies **(Fig. 2.1b)**. This band was also detected in the brain, liver, spleen, kidney, lung and heart lysates from wild type mice **(Fig. 2.1c, 2.1d)**, but was absent in lysates derived from *Grn*$^{-/-}$ tissues **(Fig. 2.1d)**. These data further support the existence of intracellular, PGRN-derived peptides in multiple cell and tissue types. Because PGRN haploinsufficiency causes FTLD, we also tested whether the rate of PGRN processing is altered in *Grn*$^{+/-}$ versus WT spleen. The amount of both PGRN and granulin peptides is reduced in *Grn*$^{+/-}$ samples and there is no statistically significant difference in PGRN processing between WT and *Grn*$^{+/-}$ **(Fig. 2.1e)**.

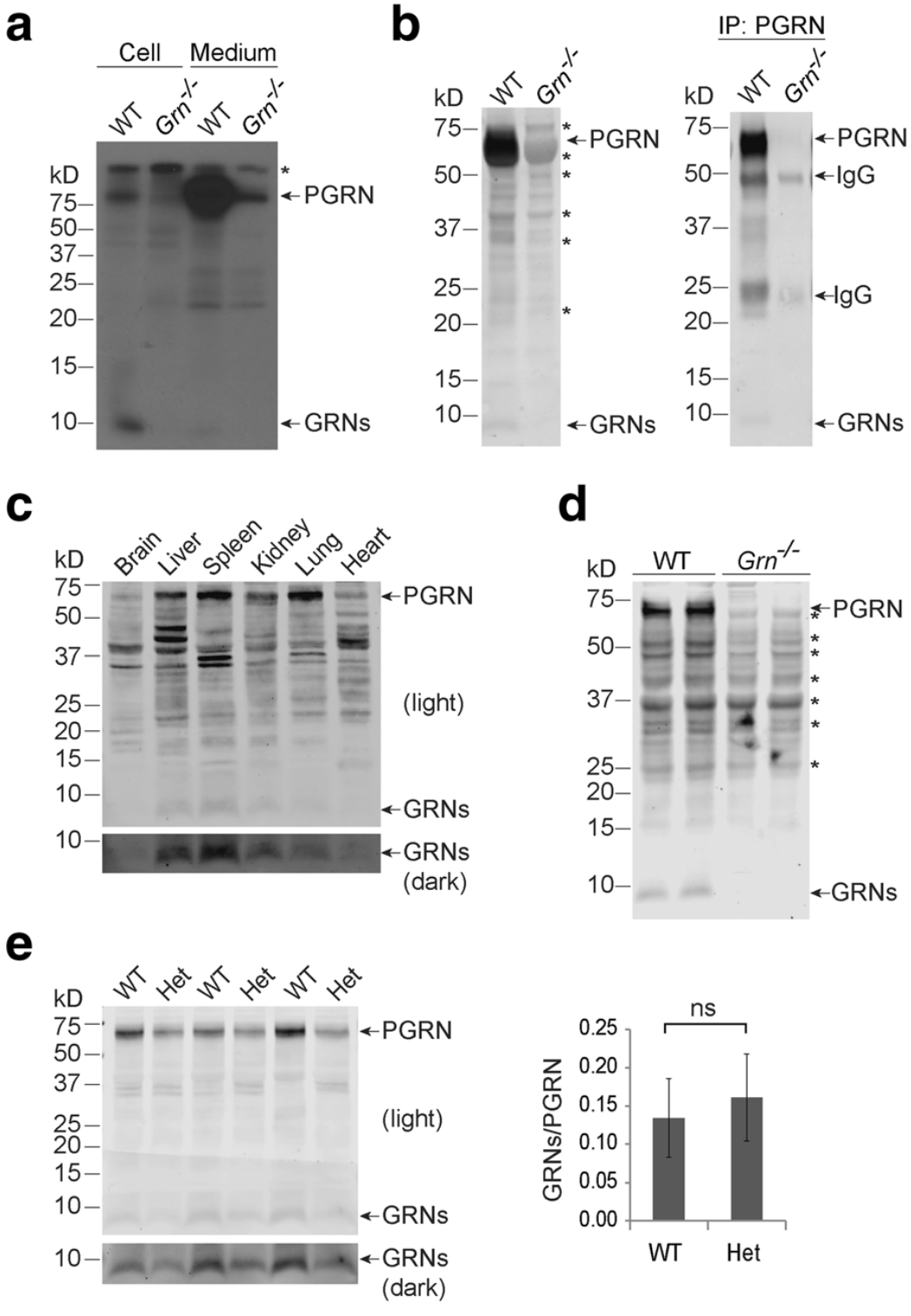
a
Cell
Medium
WT
Grn-/-
WT
Grn-/-
kD
75
50
37
25
20
15
10
PGRN
GRNs
b
kD
WT
Grn-/-
75
50
37
25
20
15
10
PGRN
GRNs
IP: PGRN
WT
Grn-/-
kD
75
50
37
25
20
15
10
PGRN
IgG
IgG
GRNs
c
kD
Brain
Liver
Spleen
Kidney
Lung
Heart
75
50
37
25
20
15
10
PGRN
(light)
GRNs
10
GRNs
(dark)
d
kD
WT
Grn-/-
75
50
37
25
20
15
10
PGRN
GRNs
e
kD
WT
Het
WT
Het
WT
Het
75
50
37
25
20
15
10
PGRN
(light)
GRNs
10
GRNs
(dark)
ns
GRNs/PGRN
0.25
0.20
0.15
0.10
0.05
0.00
WT
Het

Figure 2.1. Intracellular processing of PGRN. ***a***, Primary microglia from WT and *Grn*$^{-/-}$ mice were labeled with [^{35}S]methionine and [^{35}S]cysteine for 24 hours. Cell lysates and media were immunoprecipitated by homemade rabbit anti-PGRN antibodies and separated by 16% Tricine-SDS PAGE. The PGRN and PGRN-derived peptide (GRNs) signals were visualized by autoradiography. * indicates non-specific bands. Please note there is a weak non-specific band same size as full-length PGRN in both lysate and medium. ***b***, PGRN processing in MEF cells. Equal amounts of cell lysate from primary WT and *Grn*$^{-/-}$ MEF cells (left) and the rabbit anti-PGRN IP products from WT and *Grn*$^{-/-}$ MEF cells (right) were separated on 4-12% Bis-Tris gels and blotted with sheep anti-mouse PGRN antibodies (1:1000). * indicates non-specific bands. Please note that PGRN runs slightly differently on Tricine gel and Bis-Tris gel. ***c****,* PGRN processing in mouse tissues. Equal amounts of tissue lysates were separated on a 4-12% Bis-Tris gel and blotted with sheep anti-mouse PGRN antibodies (1:1000). ***d****,* Brain tissues from WT and *Grn*$^{-/-}$ adult mice were lysed with RIPA buffer at a ratio of 1:10 (g:mL) and an equal amount of protein was separated on a 4-12% Bis-Tris gel and immunoblotted with sheep anti-mouse PGRN antibodies (1:300). ***e****,* Spleen tissues from WT and *Grn*$^{+/-}$ (Het) adult mice were lysed with RIPA buffer at a ratio of 1:10 (g:mL) and an equal amount of protein was separated on a 4-12% Bis-Tris gel and immunoblotted with sheep anti-mouse PGRN antibodies (1:1000). The ratios between granulin peptides (GRNs) and PGRN were quantified. ns: not significant, student's T-test. a, b, d contributed by X.Z.

PGRN processing is lysosome-dependent

It was previously shown that PGRN is localized to lysosomes within the cell [9, 10]. Although sortilin is the canonical lysosomal trafficking receptor for PGRN, we have recently shown that PSAP, but not sortilin, is required for PGRN lysosomal trafficking in fibroblasts, which express only negligible levels of sortilin [10]. To determine whether lysosomal trafficking is required for PGRN processing, we assessed PGRN processing in WT and *Psap*$^{-/-}$ fibroblasts. PSAP ablation totally abolished PGRN processing, which could be rescued by expression of PSAP with a viral vector **(Fig. 2.2a)**. Furthermore, PGRN processing was normal in fibroblasts in which sortilin had been deleted [10] **(Fig. 2.2a)**. Taken together, these data suggest that lysosomal trafficking is required for PGRN processing.

Because PGRN can also be delivered to lysosomes from the extracellular space [9, 10], we wanted to determine whether extracellular-derived, endocytosed PGRN can also be processed. To assess this, we treated primary *Grn*$^{-/-}$ cortical neurons with purified recombinant human PGRN. A 10kDa band, corresponding to the size of granulin peptides, was detected when extracellular PGRN was added **(Fig. 2.2b)**. Furthermore, PGRN uptake and lysosomal delivery is known to be enhanced by PSAP [10]. Consistent with this, the presence of recombinant PSAP greatly facilitated neuronal uptake of full-length PGRN and also increased the levels of processed granulin peptides **(Fig. 2.2b)**.

To test the direct role of the lysosome in PGRN processing, we treated MEFs with lysosomal inhibitors known to interfere with lysosomal acidification. Either bafilomycin A1, alone, or chloroquine with ammonium chloride were used. Both

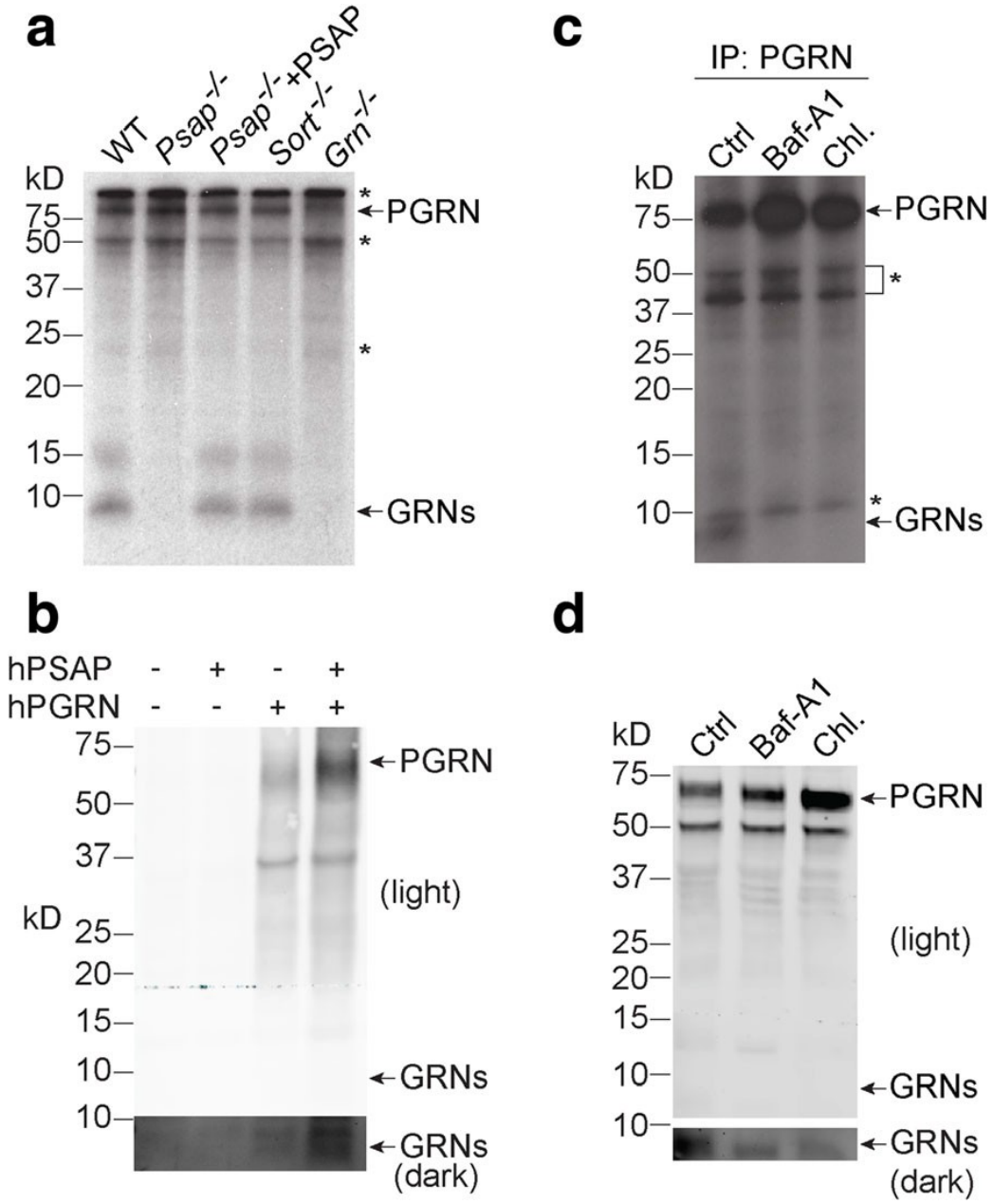
a
WT
Psap-/-
Psap-/- +PSAP
Sort-/-
Grn-/-
kD
75
50
37
25
20
15
10
PGRN
GRNs
b
hPSAP - + - +
hPGRN - - + +
kD
75
50
37
25
20
15
10
10
PGRN
(light)
GRNs
GRNs
(dark)
c
IP: PGRN
Ctrl
Baf-A1
Chl.
kD
75
50
37
25
20
15
10
PGRN
GRNs
d
kD
Ctrl
Baf-A1
Chl.
75
50
37
25
20
15
10
10
PGRN
(light)
GRNs
GRNs
(dark)

Figure 2.2. PGRN processing is lysosome-dependent. ***a***, Primary *Sort*$^{-/-}$, *Grn*$^{-/-}$, and *Psap*$^{-/-}$ MEF cells, and *Psap*$^{-/-}$ MEF cells infected with *PSAP* lentivirus were labeled with [^{35}S]-methionine and [^{35}S]-cysteine for 24 hours. Equal amounts of cell lysate were immunoprecipitated with a homemade rabbit anti-PGRN antibody and separated by 16% Tricine-SDS PAGE. The PGRN and PGRN-derived peptide (GRNs) signals were visualized by autoradiography. * indicates non-specific bands. ***b,*** PGRN delivered from the extracellular space is processed in primary cortical neurons (DIV12). Primary cortical neurons were treated with either human PGRN (hPGRN, 1 μg/mL) alone or together with recombinant human PSAP (hPSAP, 1 μg/mL) as indicated for 16 hours. The cells were harvested and proteins were separated on a 4-12% Bis-Tris gel, then blotted with goat anti-human PGRN antibodies. ***c,*** Intracellular processing of PGRN is dependent on lysosomal activity. Primary MEF cells were labeled with [^{35}S]-methionine and [^{35}S]-cysteine and treated with different lysosomal inhibitors: 50 nM bafilomycin or 15 mM ammonium chloride + 100 μM chloroquine for 16 hours. The cell lysates were immunoprecipitated with rabbit anti-PGRN antibodies and separated by 16% Tricine-SDS PAGE. PGRN and PGRN-derived peptides were visualized by autoradiography. * indicates non-specific bands. ***d,*** Primary MEF cells were treated with different lysosomal inhibitors, as above. The cell lysates were separated on a Bis-Tris gel, then blotted with sheep anti-mouse PGRN antibodies. a-c contributed by X.Z.

bafilomycin A1 and chloroquine/ammonium chloride treatment led to the reduction of the 10kDa granulin peptide bands and increased levels of full-length PGRN with both radiolabeling and Western blot analysis **(Fig. 2.2c, 2.2d)**, supporting that proper lysosomal function is required for intracellular PGRN processing.

PGRN processing is dependent on cathepsins

Because cathepsins are the main proteases in the lysosome [17, 18], we predicted that one or more could be involved in PGRN processing. To determine the role of several well-studied cathepsins in PGRN processing, we tested PGRN processing in fibroblasts deficient in either cathepsin B (Ctsb), cathepsin L (Ctsl), cathepsin D (Ctsd), cathepsin K (Ctsk), cathepsin Z (Ctsz), or deficient in both cathepsin B (Ctsb) and cathepsin L (Ctsl), which were derived from available knockout mice. Deletion of cathepsin L, K or Z had no effect on PGRN processing, while ablation of either cathepsin B or D resulted in ~50% reduction in the ratio of processed PGRN peptides versus full-length PGRN **(Fig. 2.3a, 2.3b)**. Interestingly, ablation of both cathepsin B and L resulted in a much greater decrease in PGRN processing than cathepsin B deletion alone **(Fig. 2.3a, 2.3b)**, suggesting that cathepsins B and L might play redundant roles in PGRN processing, which is consistent with reported redundancy between these enzymes [19]. To determine the direct roles of cathepsins B, D and L in PGRN processing, we tested the ability of recombinant cathepsins to cleave recombinant PGRN *in vitro*. While cathepsin B and D were capable of cleaving PGRN to a minor degree, incubation of recombinant PGRN with cathepsin L led to the generation of 10kDa bands, corresponding to the size of granulin peptides **(Fig. 2.3c, 2.3d)**. This is consistent with

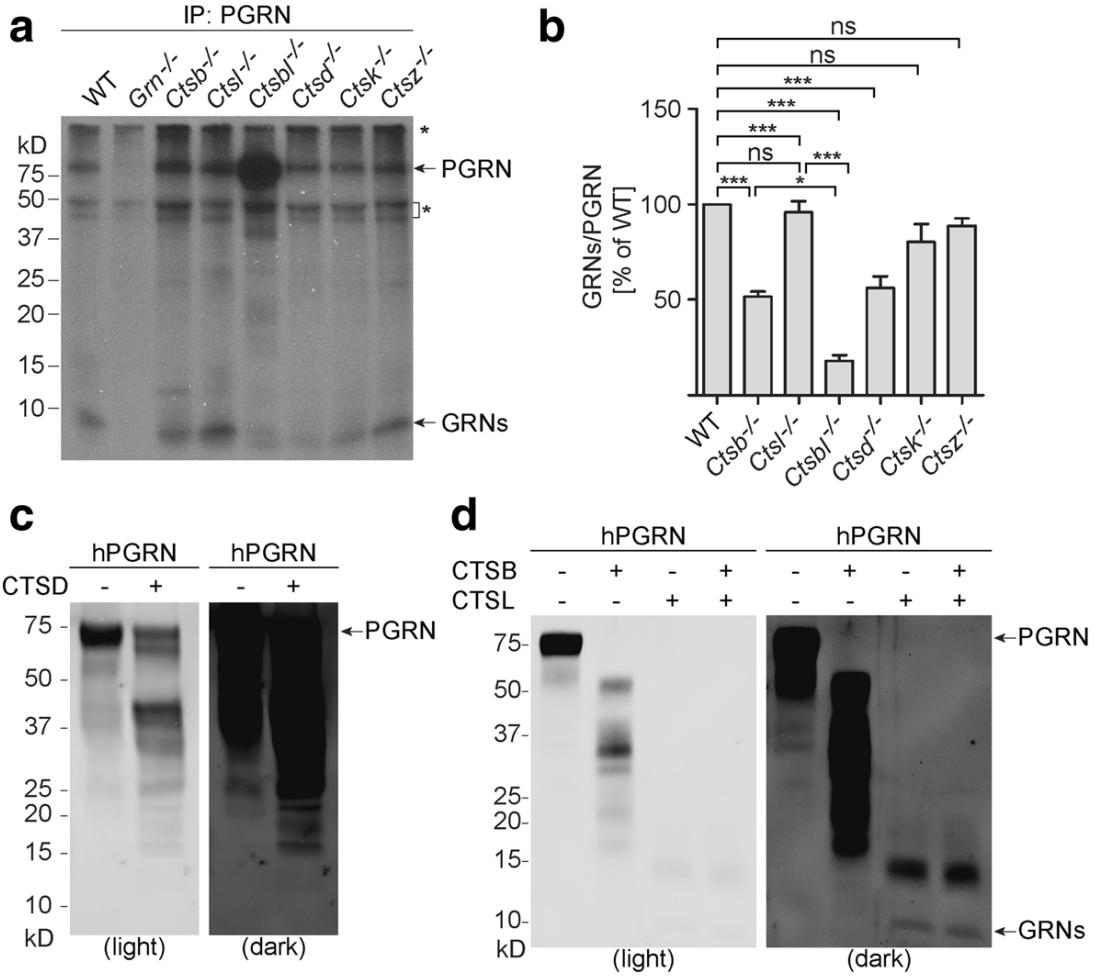
a
IP: PGRN
WT
Grn-/-
Ctsb-/-
Ctsl-/-
Ctsbl-/-
Ctsd-/-
Ctsk-/-
Ctsz-/-
kD
75
50
37
25
20
15
10
PGRN
GRNs
b
GRNs/PGRN [% of WT]
150
100
50
ns
ns
***
***
***
ns
***
*
WT
Ctsb-/-
Ctsl-/-
Ctsbl-/-
Ctsd-/-
Ctsk-/-
Ctsz-/-
c
hPGRN
hPGRN
CTSD
- + - +
75
50
37
25
20
15
10
kD
PGRN
(light)
(dark)
d
hPGRN
hPGRN
CTSB
CTSL
- + - + - + - +
- - + + - - + +
75
50
37
25
20
15
10
kD
PGRN
GRNs
(light)
(dark)

Figure 2.3. **PGRN processing by cathepsins.** ***a***, Cathepsin- and PGRN-deficient MEF cells were labeled with [^{35}S]-methionine and [^{35}S]-cysteine for 24 hours and the cell lysates were then immunoprecipitated with rabbit anti-PGRN antibodies and separated by 16% Tricine-SDS PAGE. PGRN and PGRN-derived peptides were visualized by autography. * indicates non-specific bands. ***b***, Quantification of PGRN and PGRN-derived peptides in (a). 10kDa PGRN-derived peptides were normalized with full-length PGRN signals in each group. Data are presented as means ± s.e.m. n=3, *P<0.05; ***P<0.001, ns, no significance, one-way ANOVA, Tukey's Multiple Comparison Test. ***c***, Recombinant cathepsin D was incubated with recombinant human PGRN in acidic buffer for 16 hours. Proteins were separated on a Bis-Tris gel and blotted with goat anti-human PGRN antibodies. ***d***, Recombinant cathepsin B and L were incubated with recombinant human PGRN as indicated in acidic buffer for 4 hours. Proteins were separated on a Bis-Tris gel and blotted with goat anti-human PGRN antibodies. a, b contributed by X.Z.

another study published while our manuscript was under revision [20], in which they confirmed that cathepsin L cleaves PGRN in the linker regions between granulin peptides using mass spectrometry. These data suggest that cathepsins are the key lysosomal enzymes involved in intracellular PGRN processing.

2.4 Discussion

Many lysosomal proteins are known to undergo processing in the acidic environment. One example is prosaposin (PSAP), which is known to be processed into saposin peptides (A, B, C, D) in the lysosome [11-13]. In this manuscript, we showed that PGRN, the precursor of granulin peptides, is processed intracellularly in a lysosome-dependent manner and that multiple cathepsins are likely to be involved in this processing. While our *in vitro* analysis demonstrated that cathepsin L is very potent in processing PGRN to granulin peptides **(Fig. 2.3d)**, cathepsin L deficient MEFs do not show obvious defects in PGRN processing **(Fig. 2.3a, 2.3b)**, suggesting there is another protease playing a role redundant to cathepsin L *in vivo*. MEFs deficient in both cathepsin B and L have minimal ability to process PGRN **(Fig. 2.3a, 2.3b)** despite cathepsin B being minorly active towards PGRN *in vitro* **(Fig. 2.3d)**, indicating that cathepsin B is not the enzyme directly processing PGRN in cathepsin L deficient MEFs. However, lysosomal enzymes are often activated by the action of other enzymes, especially in the case of cathepsins. Thus, it is possible that an unidentified protease that is activated by cathepsin B is responsible for processing PGRN in the absence of cathepsin L.

Our data also showed that PGRN is processed to the 10kDa peptides in multiple cell types and tissues and both mouse and human PGRN are processed in a similar manner, which suggests that lysosomal PGRN processing is general phenomena present in all cell types and conserved during evolution. While it is likely that these 10kDa peptides are a mixture of granulin peptides, the exact sequences of these peptides need to be further analyzed. Future studies using mass spectrometry and development of tools and reagents to characterize individual granulin peptides will allow a better understanding of PGRN processing.

Recently, PGRN was shown to physically interact with cathepsin D and regulate its activity [21, 22]. Multiple granulins are involved in this interaction [21, 22]. One intriguing possibility is that granulins modulate cathepsin activities in the lysosome. Different granulins might also interact with different proteins in the lysosome, in a manner similar to how saposins activate different enzymes in the glycosphingolipid degradation pathway. Future endeavors to identify lysosomal proteins interacting with these granulin peptides will help us to obtain a better understanding of their functions in the lysosome.

Conclusion

Our data support that PGRN is processed in a lysosome-dependent manner and cathepsin L cleaves PGRN *in vitro*. Further studies on the interacting partners of these processed peptides will provide a better understanding of PGRN function in the lysosome.

2.5 Materials and Methods

Pharmacological Reagents and Antibodies

The following antibodies were used in this study: goat anti-human PGRN (1:1000 for Western blot) and sheep anti-mouse PGRN (1:300 for brain lysate Western blot, 1:1000 for other Western blots,) from R&D systems. Recombinant cathepsin D and L proteins are from R&D systems. Bafilomycin A1, ammonium chloride and chloroquine were from Sigma.

Expression constructs

Human CTSB and CTSD cDNA in the pDONR223 vector were obtained from the ORFeome Collection (kind gifts from Dr. Haiyuan Yu). CTSB-myc-His and CTSD-myc-His constructs were generated using a gateway reaction with pDONR223-CTSB/CTSD and a modified pcDNA3.1/myc-His A vector (Invitrogen), engineered with a gateway cassette.

Cell culture, DNA transfection, protein purification, and PSAP lentivirus production and infection

HEK293T were maintained in Dulbecco's Modified Eagle's medium (Cellgro) supplemented with 10% fetal bovine serum (Gibco) and 1% Penicillin–Streptomycin (Invitrogen) in a humidified incubator at 37ºC and 5% CO_2. Cells were transiently transfected with polyethylenimine as described [23]. Conditioned medium from cells transfected with the Cathepsin B-myc-His construct was collected 4 days after transfection and incubated with cobalt beads. After extensive washing, recombinant Cathepsin B was eluted with imidazole and dialyzed to PBS buffer. Recombinant human PGRN was purified from the conditioned medium of FH14 cells [14] stably

expressing C-terminal FLAG-His-tagged human PGRN as above. Primary microglia, cortical neurons, and fibroblasts were cultured as described [10]. Primary cathepsin KO fibroblasts were derived from *ctsd-/-*[24], *ctsb-/-* [25], *ctsl-/-* [26], *ctsb-/- ctsl-/-* [19], *ctsk-/-* [27] and *ctsz-/-* [28] mice. PSAP lentiviruses were generated from HEK293T cells and then used to infect *Psap*$^{-/-}$ fibroblasts as described [10].

Metabolic labeling and PGRN processing assay

To obtain [^{35}S]-labeled PGRN, culture medium was replaced with methionine- and cysteine-free DMEM with 10% dialyzed FBS for 2 h before the addition of [^{35}S]-labeled methionine and cysteine. After 24 h incubation, cells were lysed with lysis buffer (50 mM Tris, pH 7.3, 150 mM NaCl, 1% Triton X-100, and 0.1% deoxycholate with protease inhibitors). After immunoprecipitation with homemade rabbit anti-PGRN antibodies [10], the IP products were separated by 16% Tricine SDS-PAGE. Fixation solution (10% methanol and 10% acetic acid) was added, the gels were subsequently saturated with amplification solution (1 M sodium salicylate, 10% glycerol) and the autoradiographs of dried gels were obtained on X-ray film at –80°C.

***In vitro* cleavage of PGRN by cathepsins**

1 µg of recombinant human PGRN and 0.25 µg of recombinant cathepsin B, D, or L, or PBS control were combined and pre-incubated for 0.5 hours on ice. 3x assay buffer (150 mM NaOAc pH 5.3, 12 mM EDTA, 24 mM DTT for cathepsin B and L; 300 mM NaOAc, 0.6M NaCl, pH 3.5 for cathepsin D) was added and brought to 1x by the addition of H_2O to a final volume of 15 µl. The reactions were kept at 37°C for 4 hours (cathepsin B and L) or 16 hours (cathepsin D) and the reaction stopped by the addition

of 2x Laemmli sample buffer. Proteins were separated on a 4-12% Bis-Tris gel and visualized using Western blotting with goat anti-human PGRN antibodies.

Western blot analysis

Samples were separated by 4-12% Bis-Tris PAGE (Invitrogen) and transferred to 0.2 μm nitrocellulose. Western blot analysis was performed using anti-PGRN antibodies as described [10].

Declarations

Abbreviations

FTLD: frontotemporal lobar degeneration; NCL: neuronal ceroid lipofuscinosis; PGRN: progranulin; Cts: cathepsin; MEF: mouse embryonic fibroblast

Ethical Approval and Consent to Participate

All applicable international, national, and/or institutional guidelines for the care and use of animals were followed. The work under animal protocol 2014-0071 is approved by the Institutional Animal Care and Use Committee at Cornell University.

Consent for publication

All authors have given consent for publication.

Competing interests

The authors declare that they have no competing interests.

Funding

This work is supported by NINDS (R01NS088448-01) to F.H.. X.Z. is supported by the Weill Institute Fleming Postdoctoral Fellowship.

Authors' contributions

X.Z. and D.H.P collected all the data. T.F. collected WT, Grn+/- tissue and MEF samples. L.S. purified recombinant PGRN and cathepsin B and helped with the *in vitro* cleavage assays. T.R. provided cathepsin knockout fibroblasts. F.H. supervised the project and wrote the manuscript with X.Z and D.H.P. X.Z., D.H.P, T.R. and F.H. edited the manuscript. All authors read and approved the final manuscript.

2.6 Acknowledgements

We thank Dr. Haiyuan Yu for his kind gift of Cathepsin B and D cDNAs and Mrs. Xiaochun Wu for technical assistance. This work is supported by funding to F.H. from the Weill Institute for Cell and Molecular Biology and NINDS (R01NS088448) and by funding to X. Z. from the Weill Institute Fleming Postdoctoral Fellowship.

Authors' information

X.Z., D.H.P., T.F., L.S. and F.H. are from the Department of Molecular Biology and Genetics, Weill Institute for Cell and Molecular Biology, Cornell University, Ithaca, NY 14853, USA

T.R. is from the Institute of Molecular Medicine and Cell Research, Medical Faculty and BIOSS Centre for Biological Signalling Studies, Albert-Ludwigs-University Freiburg, 79104 Freiburg, Germany

L.S. is also affiliated with the Department of Neurobiology, School of Basic Medical Sciences, Southern Medical University, Guangzhou, China

REFERENCES

1. Ahmed Z, Mackenzie IR, Hutton ML, Dickson DW. Progranulin in frontotemporal lobar degeneration and neuroinflammation. J Neuroinflammation. 2007;4:7. doi:1742-2094-4-7 [pii]10.1186/1742-2094-4-7.

2. Cenik B, Sephton CF, Kutluk Cenik B, Herz J, Yu G. Progranulin: a proteolytically processed protein at the crossroads of inflammation and neurodegeneration. J Biol Chem. 2012;287(39):32298-306. doi:R112.399170 [pii]10.1074/jbc.R112.399170.

3. Bateman A, Bennett HP. The granulin gene family: from cancer to dementia. Bioessays. 2009;31(11):1245-54. doi:10.1002/bies.200900086.

4. Nicholson AM, Gass J, Petrucelli L, Rademakers R. Progranulin axis and recent developments in frontotemporal lobar degeneration. Alzheimers Res Ther. 2012;4(1):4. doi:alzrt102 [pii]10.1186/alzrt102.

5. Neary D, Snowden JS, Gustafson L, Passant U, Stuss D, Black S et al. Frontotemporal lobar degeneration: a consensus on clinical diagnostic criteria. Neurology. 1998;51(6):1546-54.

6. Smith KR, Damiano J, Franceschetti S, Carpenter S, Canafoglia L, Morbin M et al. Strikingly different clinicopathological phenotypes determined by progranulin-mutation dosage. Am J Hum Genet. 2012;90(6):1102-7. doi:10.1016/j.ajhg.2012.04.021S0002-9297(12)00254-6 [pii].

7. Almeida MR, Macario MC, Ramos L, Baldeiras I, Ribeiro MH, Santana I. Portuguese family with the co-occurrence of frontotemporal lobar degeneration and neuronal ceroid lipofuscinosis phenotypes due to progranulin gene mutation. Neurobiol Aging. 2016. doi:S0197-4580(16)00178-0 [pii]10.1016/j.neurobiolaging.2016.02.019.

8. Belcastro V, Siciliano V, Gregoretti F, Mithbaokar P, Dharmalingam G, Berlingieri S et al. Transcriptional gene network inference from a massive dataset elucidates transcriptome organization and gene function. Nucleic Acids Res. 2011;39(20):8677-88. doi:gkr593 [pii]10.1093/nar/gkr593.

9. Hu F, Padukkavidana T, Vaegter CB, Brady OA, Zheng Y, Mackenzie IR et al. Sortilin-mediated endocytosis determines levels of the frontotemporal dementia protein, progranulin. Neuron. 2010;68(4):654-67. doi:S0896-6273(10)00776-2 [pii]10.1016/j.neuron.2010.09.034.

10. Zhou X, Sun L, Bastos de Oliveira F, Qi X, Brown WJ, Smolka MB et al. Prosaposin facilitates sortilin-independent lysosomal trafficking of progranulin.

J Cell Biol. 2015;210(6):991-1002. doi:10.1083/jcb.201502029jcb.201502029 [pii].

11. O'Brien JS, Kishimoto Y. Saposin proteins: structure, function, and role in human lysosomal storage disorders. FASEB J. 1991;5(3):301-8.

12. Qi X, Grabowski GA. Molecular and cell biology of acid beta-glucosidase and prosaposin. Prog Nucleic Acid Res Mol Biol. 2001;66:203-39.

13. Matsuda J, Yoneshige A, Suzuki K. The function of sphingolipids in the nervous system: lessons learnt from mouse models of specific sphingolipid activator protein deficiencies. J Neurochem. 2007;103 Suppl 1:32-8. doi:JNC4709 [pii]10.1111/j.1471-4159.2007.04709.x.

14. Zhu J, Nathan C, Jin W, Sim D, Ashcroft GS, Wahl SM et al. Conversion of proepithelin to epithelins: roles of SLPI and elastase in host defense and wound repair. Cell. 2002;111(6):867-78.

15. Suh HS, Choi N, Tarassishin L, Lee SC. Regulation of progranulin expression in human microglia and proteolysis of progranulin by matrix metalloproteinase-12 (MMP-12). PLoS ONE. 2012;7(4):e35115. doi:10.1371/journal.pone.0035115PONE-D-12-01133 [pii].

16. Zhou X, Sullivan PM, Sun L, Hu F. The interaction between progranulin and prosaposin is mediated by granulins and the linker region between saposin B and C. J Neurochem. 2017. doi:10.1111/jnc.14110.

17. Stoka V, Turk V, Turk B. Lysosomal cathepsins and their regulation in aging and neurodegeneration. Ageing Res Rev. 2016;32:22-37. doi:S1568-1637(16)30067-8 [pii]10.1016/j.arr.2016.04.010.

18. Ketterer S, Gomez-Auli A, Hillebrand LE, Petrera A, Ketscher A, Reinheckel T. Inherited diseases caused by mutations in cathepsin protease genes. FEBS J. 2016;doi: 10.1111/febs.13980. doi:10.1111/febs.13980.

19. Sevenich L, Pennacchio LA, Peters C, Reinheckel T. Human cathepsin L rescues the neurodegeneration and lethality in cathepsin B/L double-deficient mice. Biol Chem. 2006;387(7):885-91. doi:10.1515/BC.2006.112.

20. Lee CW, Stankowski JN, Chew J, Cook CN, Lam YW, Almeida S et al. The lysosomal protein cathepsin L is a progranulin protease. Mol Neurodegener. 2017;12(1):55. doi:10.1186/s13024-017-0196-610.1186/s13024-017-0196-6 [pii].

21. Beel S, Moisse M, Damme M, De Muynck L, Robberecht W, Van Den Bosch L et al. Progranulin functions as a cathepsin D chaperone to stimulate axonal outgrowth in vivo. Hum Mol Genet. 2017. doi:10.1093/hmg/ddx1623768439 [pii].

22. Zhou X, Paushter DH, Feng T, Pardon CM, Mendoza CS, Hu F. Regulation of cathepsin D activity by the FTLD protein progranulin. Acta Neuropathol. 2017. doi:10.1007/s00401-017-1719-510.1007/s00401-017-1719-5 [pii].

23. Vancha AR, Govindaraju S, Parsa KV, Jasti M, Gonzalez-Garcia M, Ballestero RP. Use of polyethyleneimine polymer in cell culture as attachment factor and lipofection enhancer. BMC Biotechnol. 2004;4:23. doi:1472-6750-4-23 [pii]10.1186/1472-6750-4-23.

24. Saftig P, Hetman M, Schmahl W, Weber K, Heine L, Mossmann H et al. Mice deficient for the lysosomal proteinase cathepsin D exhibit progressive atrophy of the intestinal mucosa and profound destruction of lymphoid cells. Embo J. 1995;14(15):3599-608.

25. Halangk W, Lerch MM, Brandt-Nedelev B, Roth W, Ruthenbuerger M, Reinheckel T et al. Role of cathepsin B in intracellular trypsinogen activation and the onset of acute pancreatitis. J Clin Invest. 2000;106(6):773-81. doi:10.1172/JCI9411.

26. Roth W, Deussing J, Botchkarev VA, Pauly-Evers M, Saftig P, Hafner A et al. Cathepsin L deficiency as molecular defect of furless: hyperproliferation of keratinocytes and pertubation of hair follicle cycling. FASEB J. 2000;14(13):2075-86. doi:10.1096/fj.99-0970com14/13/2075 [pii].

27. Saftig P, Hunziker E, Wehmeyer O, Jones S, Boyde A, Rommerskirch W et al. Impaired osteoclastic bone resorption leads to osteopetrosis in cathepsin-K-deficient mice. Proc Natl Acad Sci U S A. 1998;95(23):13453-8.

28. Sevenich L, Schurigt U, Sachse K, Gajda M, Werner F, Muller S et al. Synergistic antitumor effects of combined cathepsin B and cathepsin Z deficiencies on breast cancer progression and metastasis in mice. Proc Natl Acad Sci U S A. 2010;107(6):2497-502. doi:10.1073/pnas.09072401070907240107 [pii].

CHAPTER 3

REGULATION OF CATHEPSIN D ACTIVITY BY THE FTLD PROTEIN, PROGRANULIN

Published as Zhou X, Paushter DH, Feng T, Pardon CM, Mendoza CS, Hu F. Regulation of cathepsin D activity by the FTLD protein progranulin. Acta Neuropathol. 2017 Jul;134(1):151-153. doi: 10.1007/s00401-017-1719-5.

3.1 Main Text

Progranulin (PGRN) protein encoded by the granulin (*GRN*) gene has been recently implicated in several neurodegenerative diseases [2,5]. While haploinsufficiency of PGRN leads to frontotemporal lobar degeneration (FTLD) [2,5], the most prevalent form of early onset dementia after Alzheimer's disease (AD), complete loss of PGRN is known to cause neuronal ceroid lipofuscinosis (NCL) [1,13], a group of lysosomal storage diseases. PGRN is a secreted glycoprotein of 7.5 granulin repeats [2,5]. However, within the cell, PGRN is localized to lysosomes through two independent trafficking pathways [8,17]. Furthermore, *GRN* is transcriptionally co-regulated with a number of essential lysosomal genes by the transcriptional factor TFEB [3]. While all this evidence suggests an essential role of PGRN in regulating lysosomal function, how PGRN does so is still unclear.

Cathepsin D (CTSD) is a lysosomal aspartic-type protease involved in many neurodegenerative diseases [14]. Mutations in the cathepsin D gene (*CTSD*) result in

NCL in humans [9]. Interestingly, mice deficient in CTSD also develop TDP-43 aggregates **(Supplementary Fig. 3.1)** [7], a hallmark of FTLD with *GRN* mutations. FTLD patients with *GRN* mutations exhibit typical pathological features of NCL [7]. These data support that lysosomal dysfunction might serve as a common mechanism for FTLD and NCL and suggest that PGRN and CTSD might function together to regulate lysosomal activities. In support of this hypothesis, granulin motifs are found in cathepsin-like cysteine proteases in plants [11,16]. These lines of evidence led us to postulate that an interaction between PGRN and CTSD may exist.

To test the physical interaction between PGRN and CTSD, FLAG-tagged CTSD was co-transfected with untagged PGRN in HEK293T cells. Cell lysates were immunoprecipitated with anti-FLAG antibodies. PGRN signal is detected in anti-FLAG CTSD immunoprecipitates but not in the controls **(Fig. 3.1a)**, suggesting a physical interaction between PGRN and CTSD. Since CTSD is known to interact with prosaposin (PSAP) [6,10], which we previously showed to bind to PGRN as well [17], it is possible that the PGRN and CTSD interaction might be bridged by endogenous PSAP in HEK293T cells. To rule out this possibility, we compared the interaction between PGRN and CTSD in control N2a cells or N2a cells with PSAP expression depleted using the CRISPR/Cas9 system [17]. PSAP ablation has no effect on PGRN-CTSD binding in the co-immunoprecipitation assay **(Fig. 3.1b)**, indicating that the interaction between PGRN and CTSD is not mediated by PSAP. Co-immunoprecipitation studies between individual granulins and CTSD suggest that multiple granulin motifs interact with CTSD **(Supplementary Fig. 3.2a, 3.2b)**.

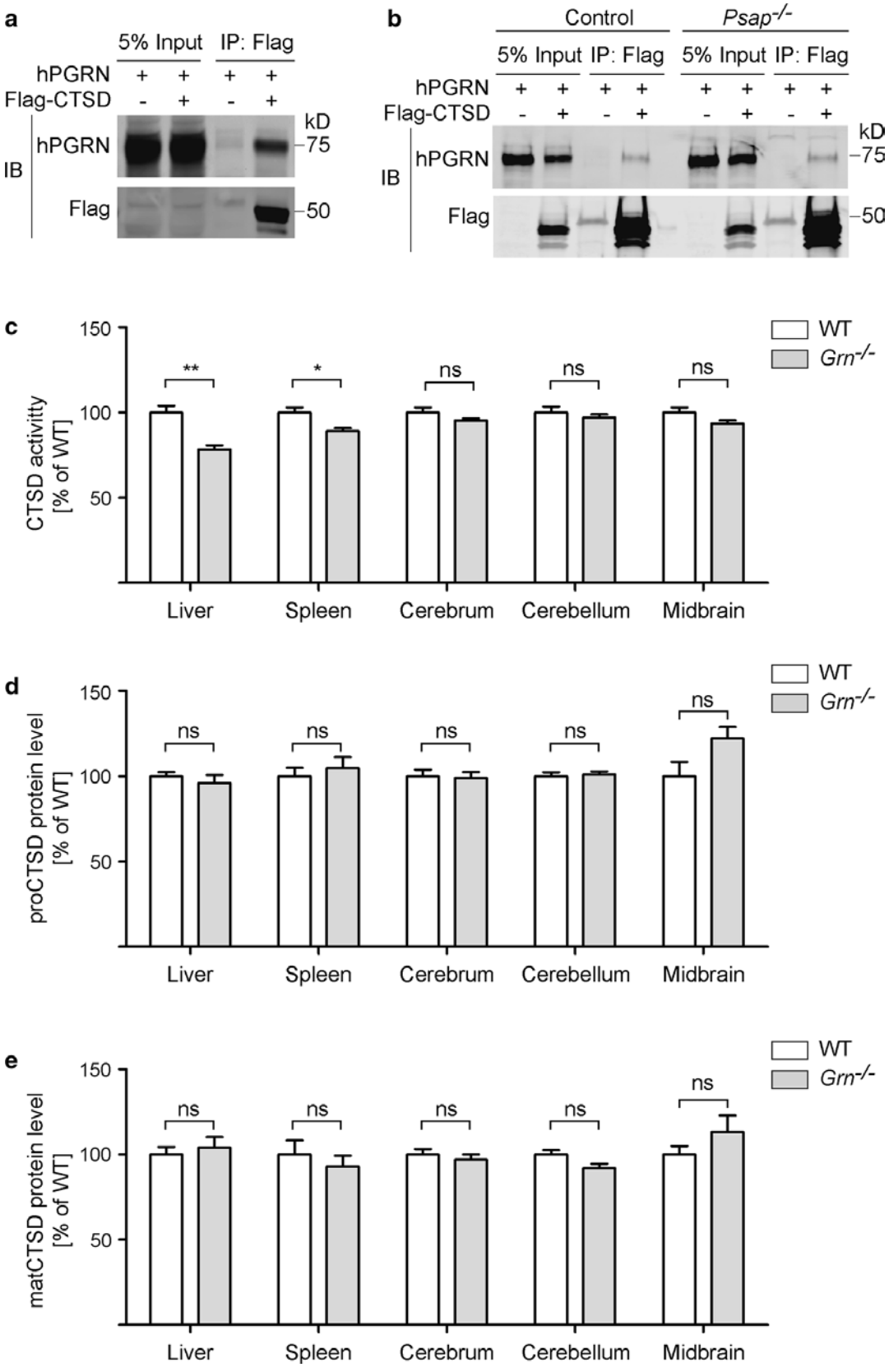
a
5% Input
IP: Flag
hPGRN + + + +
Flag-CTSD - + - +
IB
hPGRN
Flag
kD
75
50
b
Control
Psap-/-
5% Input
IP: Flag
5% Input
IP: Flag
hPGRN + + + + + + + +
Flag-CTSD - + - + - + - +
IB
hPGRN
Flag
kD
75
50
c
CTSD activitty [% of WT]
150
100
50
**
*
ns
ns
ns
WT
Grn-/-
Liver
Spleen
Cerebrum
Cerebellum
Midbrain
d
proCTSD protein level [% of WT]
150
100
50
ns
ns
ns
ns
ns
WT
Grn-/-
Liver
Spleen
Cerebrum
Cerebellum
Midbrain
e
matCTSD protein level [% of WT]
150
100
50
ns
ns
ns
ns
ns
WT
Grn-/-
Liver
Spleen
Cerebrum
Cerebellum
Midbrain

Figure 3.1. PGRN binds to CTSD and regulates its activity. **a)** HEK293T cells transfected with the indicated constructs were lysed and immunoprecipitated with anti-FLAG antibodies. **b)** Control N2a cells or *Psap*$^{-/-}$ N2a cells generated using CRIPSR/Cas9 were transfected with the indicated constructs, lysed and immunoprecipitated with anti-FLAG antibodies. **c)** CTSD activities in tissue lysates of 2-month-old WT or *Grn*$^{-/-}$ mice, as indicated. **d, e**) The levels of both the pro (d) and mature (e) forms of cathepsin D in the tissue lysates of WT or *Grn*$^{-/-}$ mice were quantified and normalized to GAPDH. n=5-6, +/- SEM, *p-value <0.05, **p-value <0.01, ns, not significant, Student's t-test. c-e contributed by X.Z.

With the physical interaction between PGRN and CTSD confirmed, next we wanted to investigate its functional relevance. Since CTSD deficiency results in much more severe lysosomal phenotypes than PGRN deficiency [4], we hypothesized that PGRN might regulate CTSD activities. Therefore, we measured CTSD activities in 2-month-old wild type (WT) and PGRN deficient mice before the appearance of any obvious lysosomal abnormalities or glial activation. Indeed, liver and spleen lysates from PGRN-deficient mice showed significantly lower CTSD activities compared to those from WT mice **(Fig. 3.1c)**, without any changes in CTSD protein levels or maturation status **(Fig. 3.1d, 1e, Supplementary Fig. 3.3)**. Lysates from cerebrum and cerebellum also show a trend of lower CTSD activities in *Grn*$^{-/-}$ mice **(Fig. 3.1c)**. Notably, in *Grn*$^{-/-}$ midbrain, although the protein levels of CTSD are slightly increased, CTSD activities are slightly lower than WT, indicating that the midbrain is one of earliest affected brain regions in *Grn*$^{-/-}$ mice **(Fig. 3.1c-e)**. It should be noted that *Grn*$^{-/-}$ mice do not develop TDP-43 pathology and neurodegeneration as seen in FTLD patients [12]. Thus, it is possible that PGRN more strongly regulates CTSD activity in humans than in mice. Indeed, a recent study demonstrated reduced cathepsin D activity in fibroblasts derived from FTLD patients with heterozygous *GRN* mutations [15].

In summary, we demonstrate that PGRN interacts with the lysosomal protease CTSD and maintains its proper activity *in vivo*. CTSD mediated proteolysis is essential to neuronal cell homeostasis through the degradation of aggregates delivered to lysosomes via autophagy or endocytosis [14]. Therefore, by regulating CTSD activity, PGRN may modulate protein homeostasis. This could potentially explain the TDP-43 aggregation observed in FTLD with *GRN* mutations. Although the mechanism by

which PGRN regulates CTSD activity remains to be determined, our data argue that reduced CTSD activities are a disease mechanism for FTLD with *GRN* mutations.

3.2 Materials and methods

Pharmacological Reagents and Antibodies - The following antibodies were used in this study: mouse anti-FLAG (M2) and anti-FLAG antibody conjugated beads (EZ view) from Sigma, mouse anti-GAPDH from Proteintech Group, goat anti-human PGRN and sheep anti-mouse PGRN from R&D systems, mouse anti-phospho-TDP-43 from Cosmo bio, GFP trap from Chromo-Tek and goat anti-cathepsin D from Santa Cruz. Cathepsin D substrate (MOCAc-GKPILF~FRLK(Dnp)-D-R-NH_2) was from Calbiochem (Cat#219360).

Expression Constructs– Human CTSD cDNA in the pDONR223 vector was obtained from ORFeome Collection (kind gifts from Dr. Haiyuan Yu). FLAG tagged CTSD construct was generated by cloning CTSD (from aa 19-end) into the pSectag2B vector (Invitrogen) using BglII and XhoI with N-terminal 3X FLAG inserted into the SfilI and HindIII sites. Human PGRN expression construct was obtained from Origene as described [1]. GFP tagged granulins were constructed by cloning each individual granulin motifs into pSectag2 vector with N-terminal GFP tag.

Cell Culture, DNA Transfection, and Drug Treatment - HEK293T and mouse N2a were maintained in Dulbecco's Modified Eagle's medium (Cellgro) supplemented with 10% fetal bovine serum (Gibco) and 1% Penicillin–Streptomycin (Invitrogen) in a humidified incubator at 37ºC and 5% CO_2. Cells were transiently transfected with polyethylenimine as described [3]. N2a cells with PSAP ablation were generated using

the CRIPSR/Cas9 system and selected with 2 μg/mL puromycin as described [5].

Brain section staining- Brain sections from p24 WT and *Ctsd*$^{-/-}$ mice [2] (littermates) were stained with mouse anti-phospho-TDP43 409/410 (1:750) and imaged under confocal microscope as described [5].

Immunoprecipitation and Western Blot Analysis - Cells were washed with PBS 40-48 hours post- transfection and cell lysates were collected in the IP buffer (50 mM Tris pH 8.0, 150 mM NaCl, 1% Triton, 0.1% deoxycholate with protease inhibitors) as described [5]. Lysates were immunoprecipitated using either anti-FLAG antibody conjugated beads or GFP-trap beads. To determine the interaction between CTSD and PGRN/granulins in the medium, 2 mL FLAG-CTSD containing conditioned medium was incubated with 2 mL conditioned medium containing GFP, GFP-PGRN, or GFP-tagged granulins for 2 hours before adding GFP-trap beads. Western blot analysis was performed as described [5].

Cathepsin D activity assay - C57/BL6 and *Grn*$^{-/-}$ [4] mice were obtained from the Jackson Laboratory. Tissues from 2-month-old WT and *Grn*$^{-/-}$ mice were lysed in lysis buffer (0.2% (w/v) taurocholate and 0.2% (v/v) Triton X-100 at pH 5.2) at a 1:10 ratio of tissue weight (g) to lysis buffer (mL). Followed by a concentration determination using the Bradford, equal amounts of tissue lysates were incubated at 37°C for 30 minutes in 100 μL assay buffer (50 mM sodium acetate (pH 5.5), 0.1 M NaCl, 1 mM EDTA, and 0.2% (v/v) Triton X-100) in the presence of the fluorogenic substrate. The fluorescence released as a result of cathepsin D proteolytic activity was read at 340 nm (excitation) and 420 nm (emission).

3.3 Acknowledgements

We thank Dr. Paul Saftig and Dr. Jianhua Zhang for *Ctsd*$^{+/-}$ mice, Dr. Haiyuan Yu for his kind gift of Cathepsin D cDNA and Mrs. Xiaochun Wu for technical assistance. This work is supported by funding to F.H. from the Weill Institute for Cell and Molecular Biology and NINDS (R01NS088448) and by funding to X. Z. from the Weill Institute Fleming Postdoctoral Fellowship.

Conflict of interest: The authors declare no competing conflict of interest.

REFERENCES

1. Almeida MR, Macario MC, Ramos L, Baldeiras I, Ribeiro MH, Santana I (2016) Portuguese family with the co-occurrence of frontotemporal lobar degeneration and neuronal ceroid lipofuscinosis phenotypes due to progranulin gene mutation. Neurobiol Aging 41:200 e201-205.

2. Bateman A, Bennett HP (2009) The granulin gene family: from cancer to dementia. Bioessays 31:1245-1254.

3. Belcastro V, Siciliano V, Gregoretti F, Mithbaokar P, Dharmalingam G, Berlingieri S, Iorio F, Oliva G, Polishchuck R, Brunetti-Pierri N, di Bernardo D (2011) Transcriptional gene network inference from a massive dataset elucidates transcriptome organization and gene function. Nucleic Acids Res 39:8677-8688.

4. Carcel-Trullols J, Kovacs AD, Pearce DA (2015) Cell biology of the NCL proteins: What they do and don't do. Biochim Biophys Acta 1852:2242-2255.

5. Cenik B, Sephton CF, Kutluk Cenik B, Herz J, Yu G (2012) Progranulin: a proteolytically processed protein at the crossroads of inflammation and neurodegeneration. J Biol Chem 287:32298-32306.

6. Gopalakrishnan MM, Grosch HW, Locatelli-Hoops S, Werth N, Smolenova E, Nettersheim M, Sandhoff K, Hasilik A (2004) Purified recombinant human prosaposin forms oligomers that bind procathepsin D and affect its autoactivation. Biochem J 383:507-515.

7. Gotzl JK, Mori K, Damme M, Fellerer K, Tahirovic S, Kleinberger G, Janssens J, van der Zee J, Lang CM, Kremmer E, Martin JJ, Engelborghs S, Kretzschmar HA, Arzberger T, Van Broeckhoven C, Haass C, Capell A (2014) Common pathobiochemical hallmarks of progranulin-associated frontotemporal lobar degeneration and neuronal ceroid lipofuscinosis. Acta Neuropathol 127:845-860.

8. Hu F, Padukkavidana T, Vaegter CB, Brady OA, Zheng Y, Mackenzie IR, Feldman HH, Nykjaer A, Strittmatter SM (2010) Sortilin-mediated endocytosis determines levels of the frontotemporal dementia protein, progranulin. Neuron 68:654-667.

9. Ketterer S, Gomez-Auli A, Hillebrand LE, Petrera A, Ketscher A, Reinheckel T (2016) Inherited diseases caused by mutations in cathepsin protease genes. FEBS J doi: 10.1111/febs.13980.

10. Laurent-Matha V, Lucas A, Huttler S, Sandhoff K, Garcia M, Rochefort H (2002) Procathepsin D interacts with prosaposin in cancer cells but its

internalization is not mediated by LDL receptor-related protein. Exp Cell Res 277:210-219.

11. Palfree RG, Bennett HP, Bateman A (2015) The Evolution of the Secreted Regulatory Protein Progranulin. PLoS ONE 10:e0133749.

12. Roberson ED (2012) Mouse models of frontotemporal dementia. Ann Neurol 72:837-849.

13. Smith KR, Damiano J, Franceschetti S, Carpenter S, Canafoglia L, Morbin M, Rossi G, Pareyson D, Mole SE, Staropoli JF, Sims KB, Lewis J, Lin WL, Dickson DW, Dahl HH, Bahlo M, Berkovic SF (2012) Strikingly different clinicopathological phenotypes determined by progranulin-mutation dosage. Am J Hum Genet 90:1102-1107.

14. Vidoni C, Follo C, Savino M, Melone MA, Isidoro C (2016) The Role of Cathepsin D in the Pathogenesis of Human Neurodegenerative Disorders. Med Res Rev 36:845-870.

15. Ward ME, Chen R, Huang HY, Ludwig C, Telpoukhovskaia M, Taubes A, Boudin H, Minami SS, Reichert M, Albrecht P, Gelfand JM, Cruz-Herranz A, Cordano C, Alavi MV, Leslie S, Seeley WW, Miller BL, Bigio E, Mesulam MM, Bogyo MS, Mackenzie IR, Staropoli JF, Cotman SL, Huang EJ, Gan L, Green AJ (2017) Individuals with progranulin haploinsufficiency exhibit features of neuronal ceroid lipofuscinosis. Sci Transl Med 9.

16. Yamada K, Matsushima R, Nishimura M, Hara-Nishimura I (2001) A slow maturation of a cysteine protease with a granulin domain in the vacuoles of senescing Arabidopsis leaves. Plant Physiol 127:1626-1634.

17. Zhou X, Sun L, Bastos de Oliveira F, Qi X, Brown WJ, Smolka MB, Sun Y, Hu F (2015) Prosaposin facilitates sortilin-independent lysosomal trafficking of progranulin. J Cell Biol 210:991-1002.

3.4 Supplementary Data

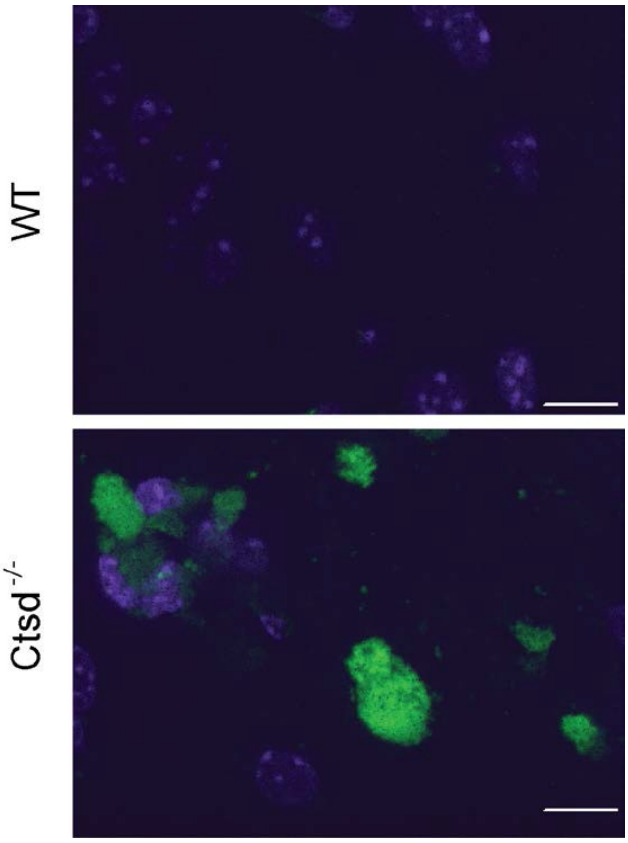

Supplementary Figure 3.1. TDP-43 pathology in *Ctsd*$^{-/-}$ mice. Brain sections from littermate WT and *Ctsd*$^{-/-}$ mice (p24) were stained with mouse anti-phospho-TDP-43 409/410 antibodies (green) and Hoechst (blue, nuclei). Representative images from the thalamus are shown. Scale bar = 10 µm. Contributed by T.F.

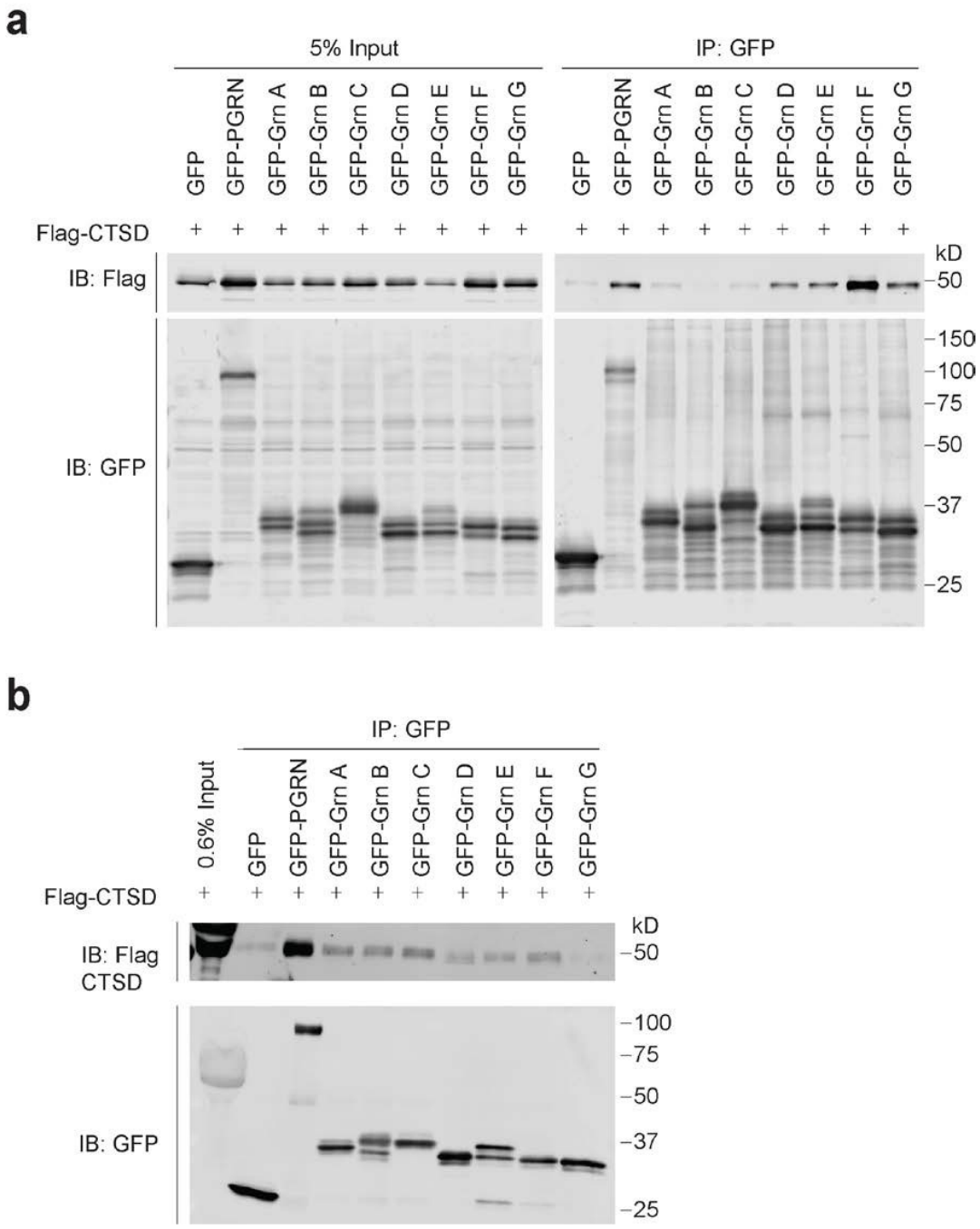

Supplementary Figure 3.2. Interaction between CTSD and granulins. a) HEK293T cells transfected with the indicated constructs were lysed after 2 days and immunoprecipitated with anti-GFP antibodies. **b**) 2 mL conditioned medium containing FLAG-CTSD was incubated with 2 mL conditioned medium containing GFP, GFP-PGRN, or GFP-tagged granulins for 2 hours before adding GFP-trap beads. The beads were washed with IP lysis buffer.

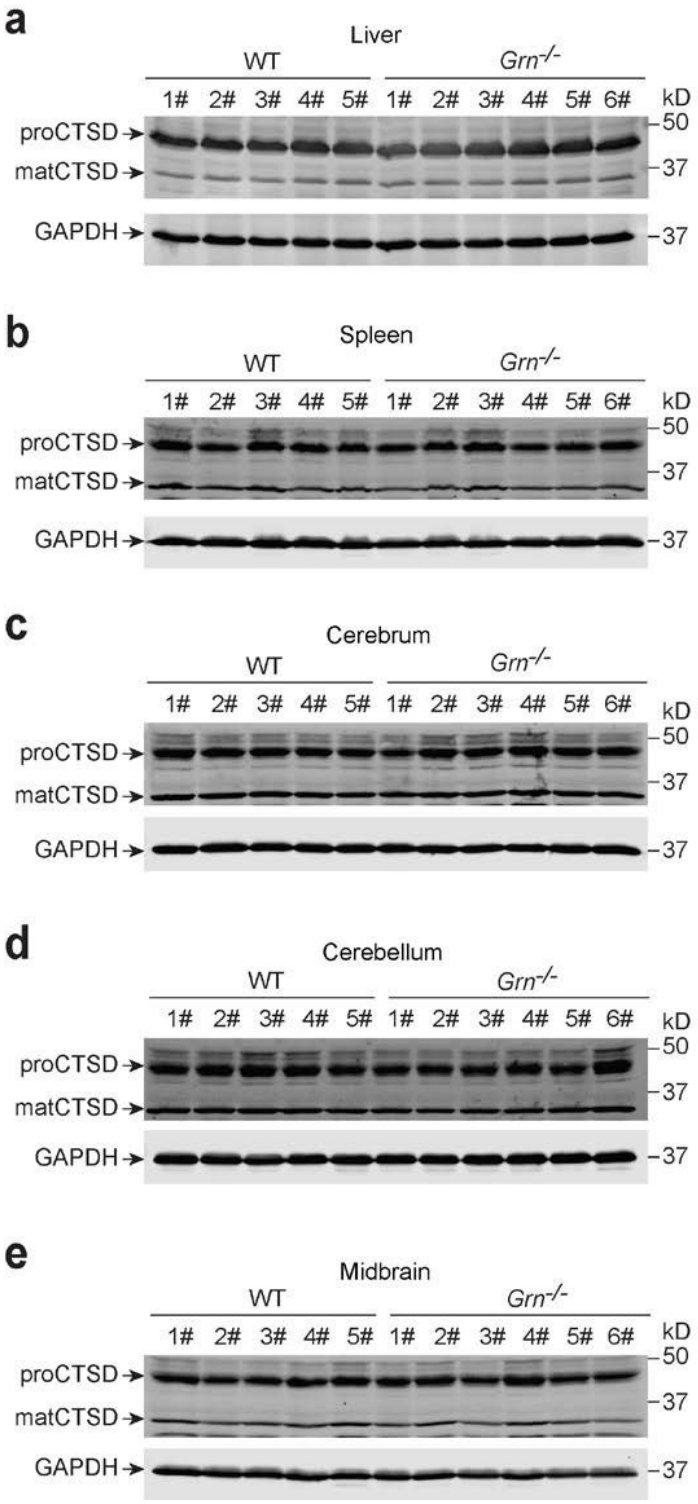

Supplementary Figure 3.3. CTSD protein levels in tissue lysates of WT and *Grn*$^{-/-}$ mice. Tissue lysates from WT or *Grn*$^{-/-}$ mice were blotted with anti-CTSD or anti-GAPDH antibodies, as indicated. Contributed by X.Z.

REFERENCES

1. Hu F, Padukkavidana T, Vaegter CB, Brady OA, Zheng Y, Mackenzie IR, Feldman HH, Nykjaer A, Strittmatter SM (2010) Sortilin-mediated endocytosis determines levels of the frontotemporal dementia protein, progranulin. Neuron 68:654-667.

2. Saftig P, Hetman M, Schmahl W, Weber K, Heine L, Mossmann H, Koster A, Hess B, Evers M, von Figura K, et al. (1995) Mice deficient for the lysosomal proteinase cathepsin D exhibit progressive atrophy of the intestinal mucosa and profound destruction of lymphoid cells. Embo J 14:3599-3608.

3. Vancha AR, Govindaraju S, Parsa KV, Jasti M, Gonzalez-Garcia M, Ballestero RP (2004) Use of polyethyleneimine polymer in cell culture as attachment factor and lipofection enhancer. BMC Biotechnol 4:23.

4. Yin F, Banerjee R, Thomas B, Zhou P, Qian L, Jia T, Ma X, Ma Y, Iadecola C, Beal MF, Nathan C, Ding A (2010) Exaggerated inflammation, impaired host defense, and neuropathology in progranulin-deficient mice. J Exp Med 207:117-128.

5. Zhou X, Sun L, Bastos de Oliveira F, Qi X, Brown WJ, Smolka MB, Sun Y, Hu F (2015) Prosaposin facilitates sortilin-independent lysosomal trafficking of progranulin. J Cell Biol 210:991-1002.

CHAPTER 4

GLUCOCEREBROSIDASE DEFICIENCY RESULTING FROM THE LOSS OF PROGRANULIN

4.1 Abstract

Mutation in the *GRN* gene leading to reduced expression of the protein, PGRN, shows a dose-dependent disease correlation, wherein haploinsufficiency results in frontotemporal lobar degeneration (FTLD) and complete loss results in neuronal ceroid lipofuscinosis (NCL). Although the exact function of PGRN is unknown, it has been increasingly implicated in lysosomal physiology. Recently, it has been found to activate the lysosomal protease, cathepsin D (CTSD), as well as act as a co-chaperone to ensure proper folding and localization of the enzyme, glucocerebrosidase (GBA). In this study, we demonstrate that PGRN deficiency in mice leads to a decrease in GBA activity with no change in total GBA protein levels. While the mechanism of this activity decrease remains indeterminate, this finding is significant as decreased GBA activity is associated with neuronal death. This is further evidence that reduced lysosomal hydrolase activity may be a pathological mechanism in cases of *GRN*-related FTLD and NCL.

4.2 Introduction

Progranulin (PGRN), encoded by the *GRN* gene, is a glycosylated secretory protein that is comprised of seven full, and one half, conserved and highly disulfide-bonded

homologous granulin (Grn) domains connected by short linker regions [1-6]. While the exact function of PGRN remains elusive, it has been found to be involved in numerous normal physiologic and pathologic processes, including regulating inflammation, wound healing, and tumorigenesis, as well as functioning as a growth and neurotrophic factor [7-16]. PGRN is interesting as it has clear, dose-dependent disease associations. Heterozygous mutations, resulting in PGRN haploinsuffiency, are known to cause frontotemporal lobar degeneration (FTLD), a clinically and pathologically heterogeneous neurodegenerative disease that is the second leading cause of early-onset dementia after Alzheimer's disease [17-23]. Homozygous mutations, resulting in complete loss of PGRN, cause a separate disease, neuronal ceroid lipofuscinosis (NCL) [24, 25]. Like FTLD, NCLs are a symptomatically and pathologically diverse family of neurodegenerative diseases [26-28]. However, a unifying feature of NCLs is the classification as lysosomal storage diseases (LSD), presenting with severe lysosomal dysfunction due to disruption of normal lysosomal physiology, such as can occur with mutation of specific lysosomal hydrolases. Although these two diseases are distinct, NCL-related phenotypes have been reported in FTLD patients with *GRN* mutation, suggesting that lysosomal dysfunction might serve as a common mechanism [29-31].

With these findings, it was speculated that PGRN may be involved in lysosomal physiology, and increasing lines of evidence indicate that this is likely the case. In addition to being lysosomally localized, having two independent trafficking pathways to the lysosome [32, 33], and being under transcriptional regulation with the majority of known lysosomal proteins [34], PGRN has recently been shown to be proteolytically processed to produce stable and functional Grn peptides [35-37], and is linked to the

direct or indirect regulation of two lysosomal hydrolases. PGRN deficiency was found to reduce the activity of cathepsin D (CTSD) *in vivo*, and PGRN was shown to stabilize and directly modulate the activity of this protease *in vitro* [31, 38, 39]. In tandem with heat shock protein 70 (HSP70), PGRN is also purported to be a co-chaperone of glucocerebrosidase (GBA) [40, 41], a β-glucosidase that cleaves glucocerebroside into glucose and ceramide [42], and PGRN knockout mice with induced chronic inflammation display Gaucher-like tissue and cellular phenotypes. Paralleling the dose-dependent disease association of *GRN*, GBA haploinsufficiency is a risk factor for Parkinson's disease (PD) [43], while complete loss of GBA results in Gaucher disease (GD), the most common LSD [42, 44]. A study published this past year demonstrated that a pathophysiological cascade ultimately resulting in a reduction in GBA activity was causative in PD [45].

To better understand the lysosomal role of PGRN, we performed a stable isotope labeling by amino acids in cell culture (SILAC)-based proteomic screen for PGRN protein interactors. One of the top hits from this was GBA. Because of the recent indications of lysosomal hydrolase deficiency with PGRN loss and previous reports of an association between PGRN and GBA, we chose to pursue this interaction and assess the *in vivo* physiologic relevance in a mouse model of PGRN deficiency. In this study, we demonstrate that PGRN loss results in a substantial decrease in GBA activity, without any compromise in protein levels.

4.3 Results

In order to better understand the role of PGRN in the lysosome through identification of its protein interactors, SILAC was performed **(Fig. 4.1A, 4.1B)**. Of the high-confidence hits from this experiment, the lysosomal enzyme, GBA, stood out as PGRN has already been shown to directly regulate the activity of one lysosomal hydrolase and has been shown to act as a co-chaperone of GBA. Because of this, we chose to further investigate the relationship between PGRN and GBA.

To verify the physical interaction between PGRN and GBA, FLAG-PGRN and GBA-MycHis were co-transfected in HEK293T cells, then anti-PGRN immunoprecipitation (IP) was performed. GBA-MycHis was observed in the FLAG-PGRN, but not the control sample, indicating a specific binding interaction **(Fig. 4.1C)**. Additionally, PGRN has been shown to be processed into individual granulin (Grn) peptides within the lysosome [35, 36] and two of these peptides, Grn E and Grn F, have been shown to interact with GBA [40, 41]. Because both PGRN and Grn peptides pulled down in the anti-PGRN IP **(Fig. 4.1C)**, it is possible that one or several of these peptides could potentially interact with GBA. To test whether GBA can bind to specific Grn peptides, N-terminal GFP-tagged Grn peptides or PGRN were co-transfected with MycHis-tagged GBA, followed by anti-GFP IP. While there was no obvious binding to Grn E, Grn F did bind GBA, as did Grn A, although less strongly **(Fig. 4.1D)**.

Previous lipidomic analysis has shown defects in lipid metabolism in lysosomes from granulin-deficient humans and mice [46]. Considering this, as well as the well-defined, singular lipid-hydrolyzing function of GBA and the overlap of pathologies between PGRN- and GBA-related diseases, we hypothesized that GBA dysfunction

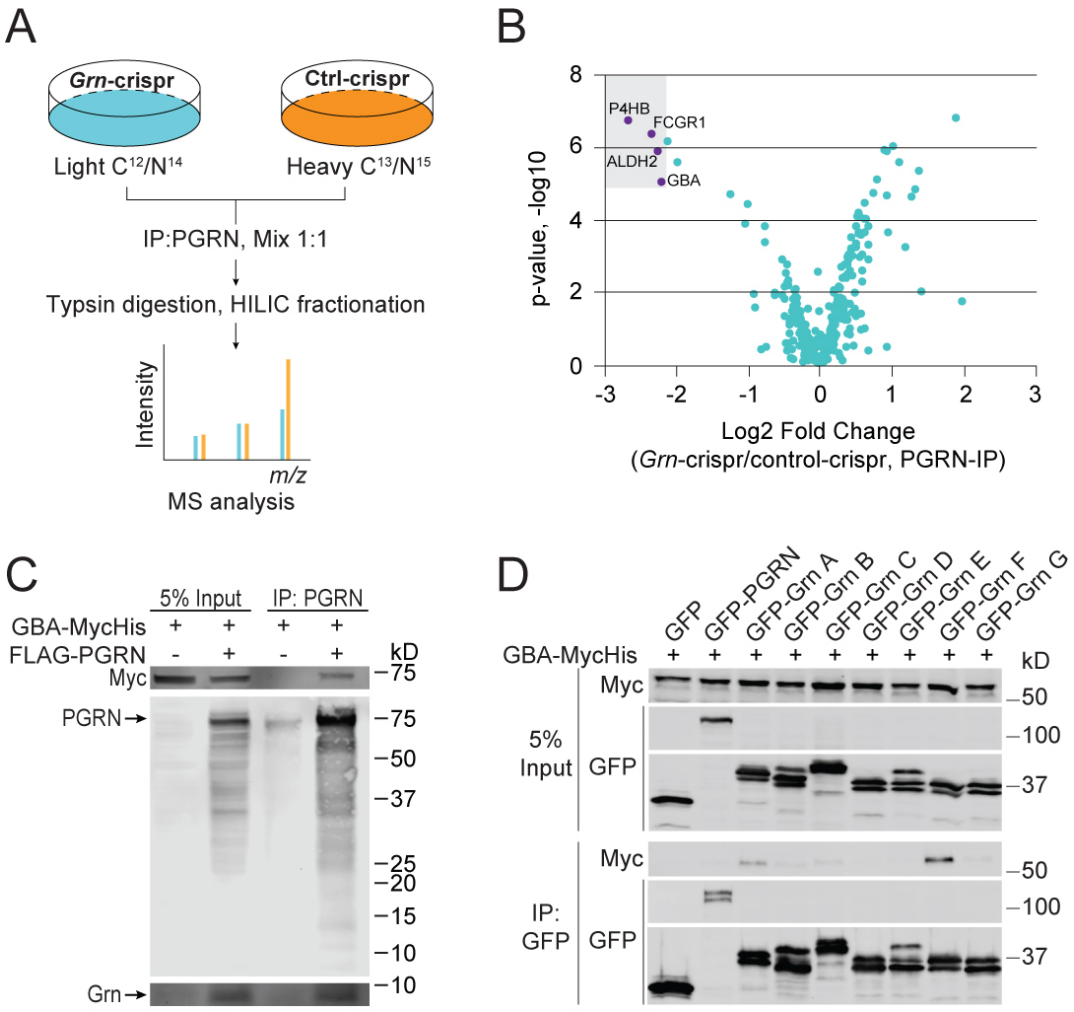

Figure 4.1. Proteomic analysis and co-immunoprecipitations. **A)** Schematic illustration of the SILAC experiment searching for PGRN interactors. **B)** Volcano plot of SILAC hits. Top hits identified in the heavy fraction are highlighted. **C)** Anti-PGRN co-immunoprecipitation of FLAG-PGRN and GBA-MycHis overexpressed in HEK293T cells. **D)** Anti-GFP co-immunoprecipitation of GFP-PGRN or individual GFP-Grn constructs and GBA-MycHis overexpressed in HEK293T cells shows binding primarily to Grn F, with weaker binding to Grn A and other Grn peptides.

may be a mechanism of *GRN*-related FTLD and NCL. We performed an *in* vitro GBA activity assay using a well-established 4-MU fluorogenic substrate [47-49] **(Fig. 4.2)**. GBA activity was measured in tissue lysates from 2-month-old WT and *Grn*$^{-/-}$ mice, before obvious lysosomal phenotypes are observed. Liver and spleen lysates from *Grn*$^{-/-}$ mice showed a significant decrease in GBA activity. While the cerebrum and cerebellum showed a trend toward decreased GBA activity, it was not significant. However, the midbrain, which is the region where we tend to observe the most severe defects in our knockout mouse line, showed a significant decrease in activity.

A follow-up test of GBA activity was performed using a recently developed ultrasensitive fluorescent probe, MDW941, which specifically reacts with only active forms of the enzyme and has been shown to be sensitive enough to detect the activity of recombinant GBA in the attomolar range [50-52]. Using this probe, an even greater disparity between GBA activity in WT and *Grn*$^{-/-}$ tissues was observed **(Fig. 4.3)**. To verify that any changes in activity were not due to alterations in total GBA protein levels, SDS-PAGE and western blot of the tissues lysates were performed, with no significant differences seen between groups **(Fig. 4.3)**.

Once we confirmed GBA deficiency in *Grn*$^{-/-}$ mouse tissues, we wanted to know whether this defect would translate to human cases. Brain lysates from healthy control or FTLD patients with *GRN* mutation were lysed and GBA activity was measured with the 4-MU substrate **(Fig. 4.4)**. FTLD patient brain samples showed a significant decrease in GBA activity of ~28% compared to control samples.

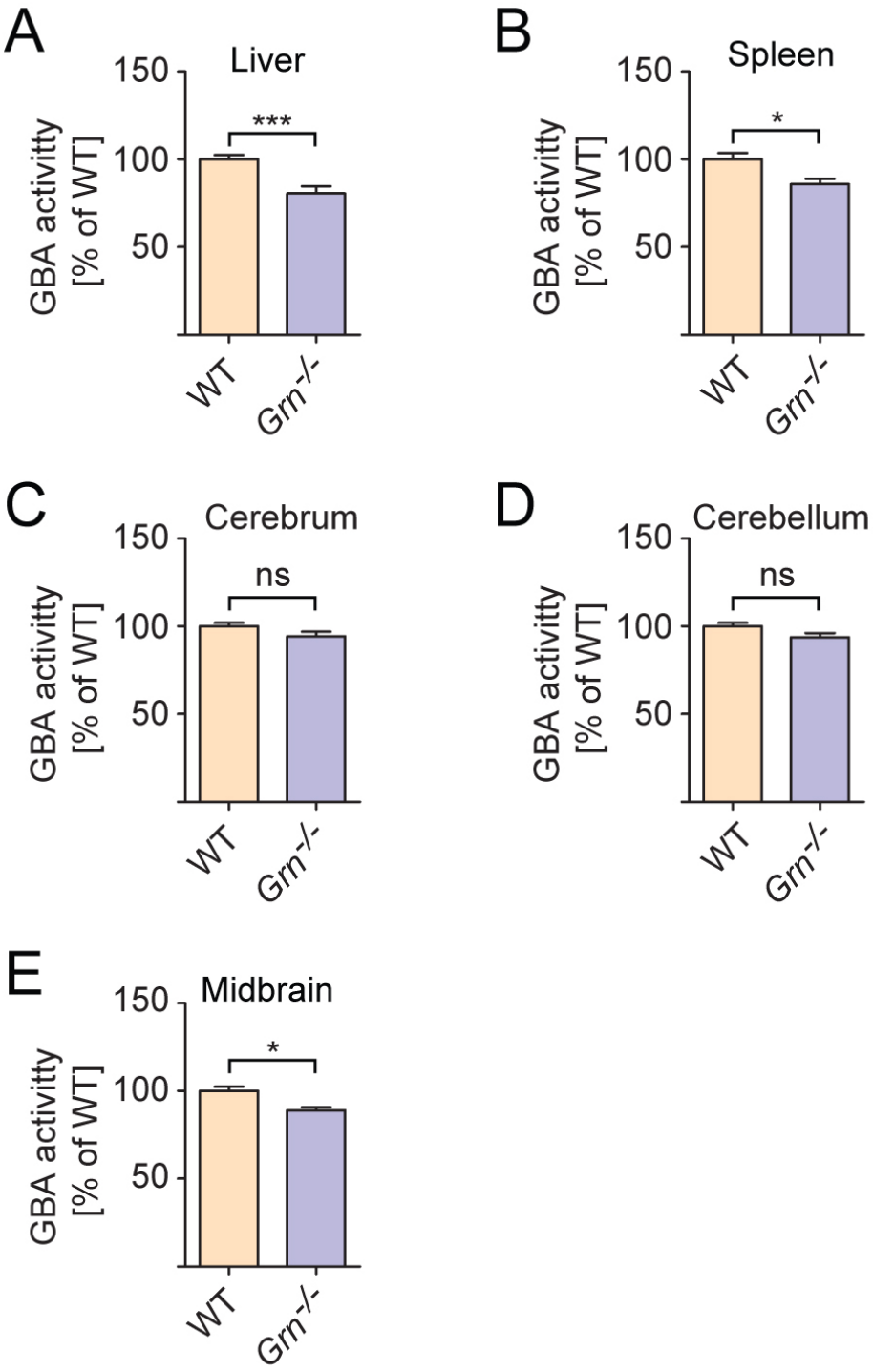

Figure 4.2. PGRN deficiency results in decreased GBA activity in mice. GBA activity was assessed in mouse tissue lysates from 2-month-old WT and *Grn*$^{-/-}$ mice, as indicated. n = 5–6, ±SEM, *p-value <0.05, ***p-value <0.001, ns, not significant, Student's t-test. Contributed by X.Z.

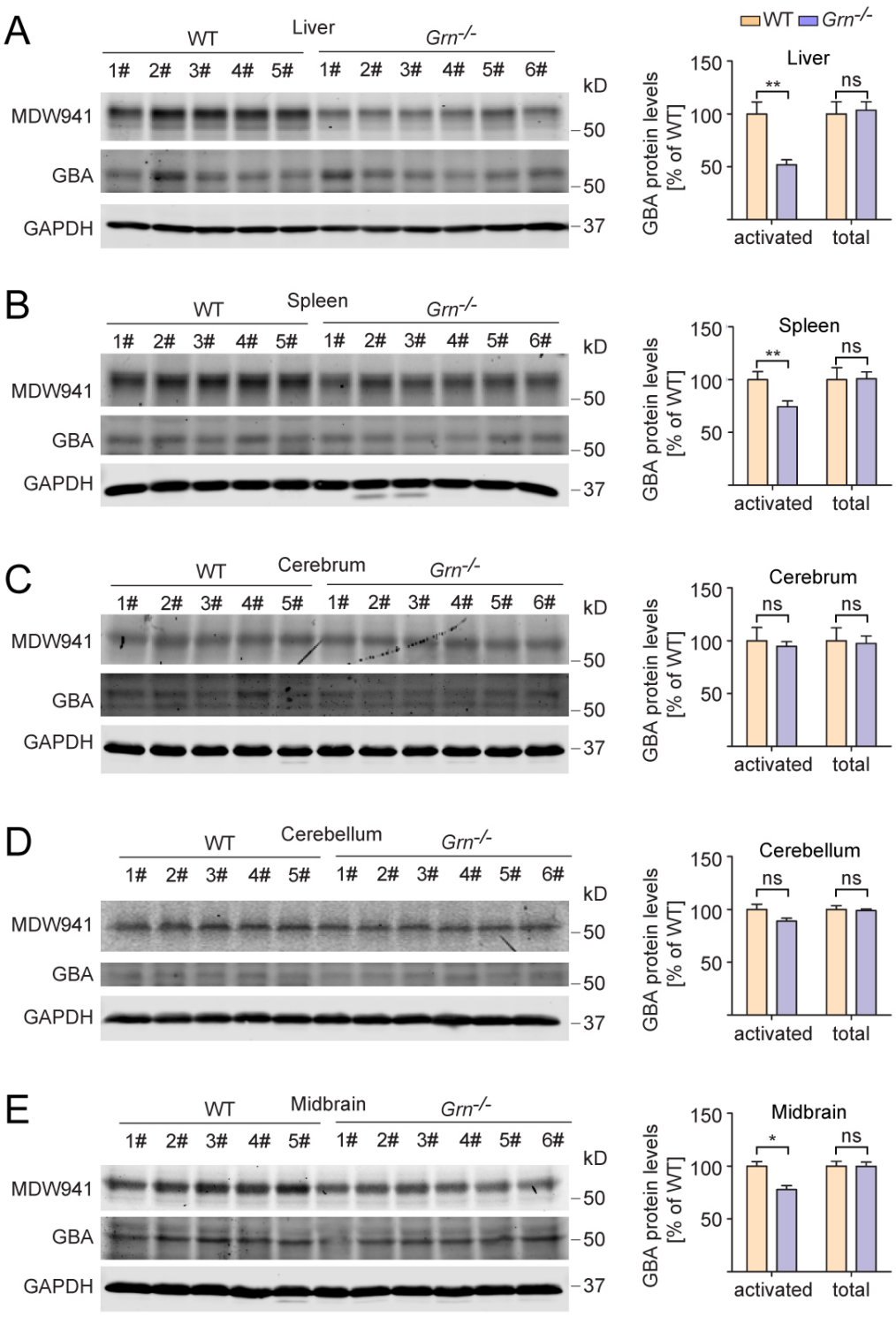

Figure 4.3. GBA protein levels and MDW941 activity. Mouse tissue lysates from 2-month-old WT and *Grn*$^{-/-}$ mice were incubated with the MDW941 GBA activity probe prior to scanning, then western blot was performed to assess total GBA protein levels. n = 5–6, ±SEM, *p-value <0.05, **p-value <0.01, ns, not significant, Student's t-test. Contributed by X.Z.

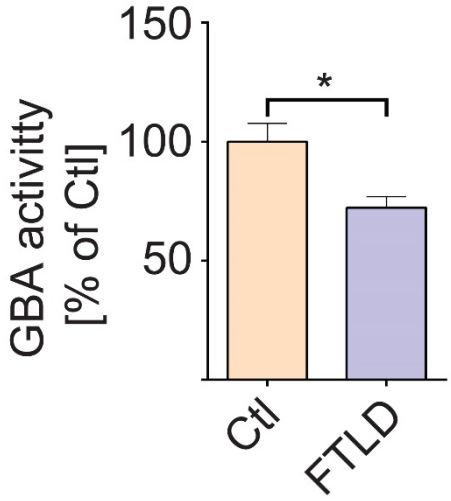

Figure 4.4. GBA activity is reduced in FTLD with *GRN* mutation patient brain compared to healthy control. GBA activity was assessed in human healthy control and FTLD with *GRN* mutation patient brain lysates, as indicated. n = 3, ±SEM, *p-value <0.05, Student's t-test.

With the changes we observed in GBA activity, and because PGRN and one Grn peptide have been shown to directly activate CTSD *in vitro*, we wanted to test whether PGRN, Grn E, or Grn F could directly augment the activity of GBA. We performed a 4-MU activity assay of a pharmaceutical grade recombinant GBA (Cerezyme) with the addition of recombinant His-PGRN, GST-Grn peptides, His-SUMO-saposin C, or GST control. No change in GBA activity was observed with the addition of PGRN-related proteins, indicating that they do not directly modulate GBA activity **(Fig. 4.5)**. We also attempted to recover GBA activity in mouse liver lysates by adding back recombinant PGRN, Grn E, or Grn F, but no change in activity was seen (data not shown).

Because of the known binding and trafficking relationship shared by PGRN and PSAP, and because saposins A and C are known activators of GBA, this raised the possibility that with PGRN loss, the observed decrease in GBA activity could be due to a decrease in PSAP or saposin peptides. Unfortunately, with the available antibodies, we were unable to examine changes in individual saposin peptides, however, we did not observe a significant change in PSAP or total saposins in the tissues where GBA activity was reduced **(Fig. 4.6)**.

4.4 Discussion

In this study, we have confirmed a previously reported association between the FTLD-related protein, PGRN, and the lysosomal enzyme, GBA [40, 41]. We observed binding between GBA and Grn F, but not the previously reported Grn E. This is likely due to differences in the expression constructs used. Our Grn E construct included only residues 519-575 of PGRN, a segment which remains intact after cleavage of the full-

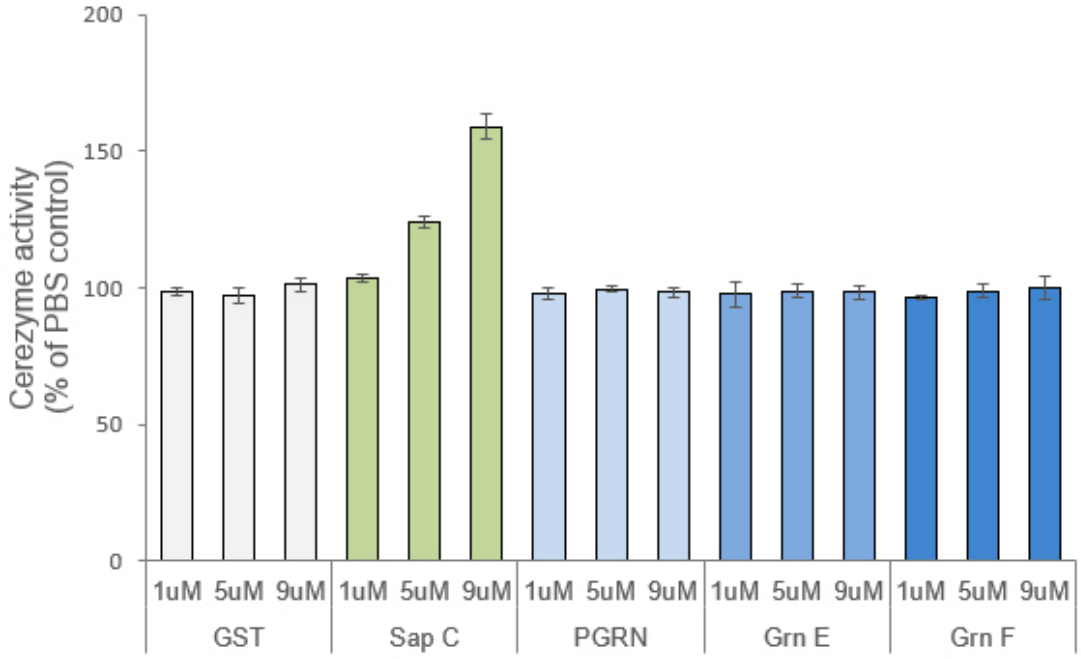

Figure 4.5. Recombinant PGRN, Grn E, or Grn F does not directly increase GBA activity. Activity of recombinant GBA (Cerezyme) was measured with the addition of recombinant PGRN, Grn E, Grn F, or recombinant saposin C as a positive control.

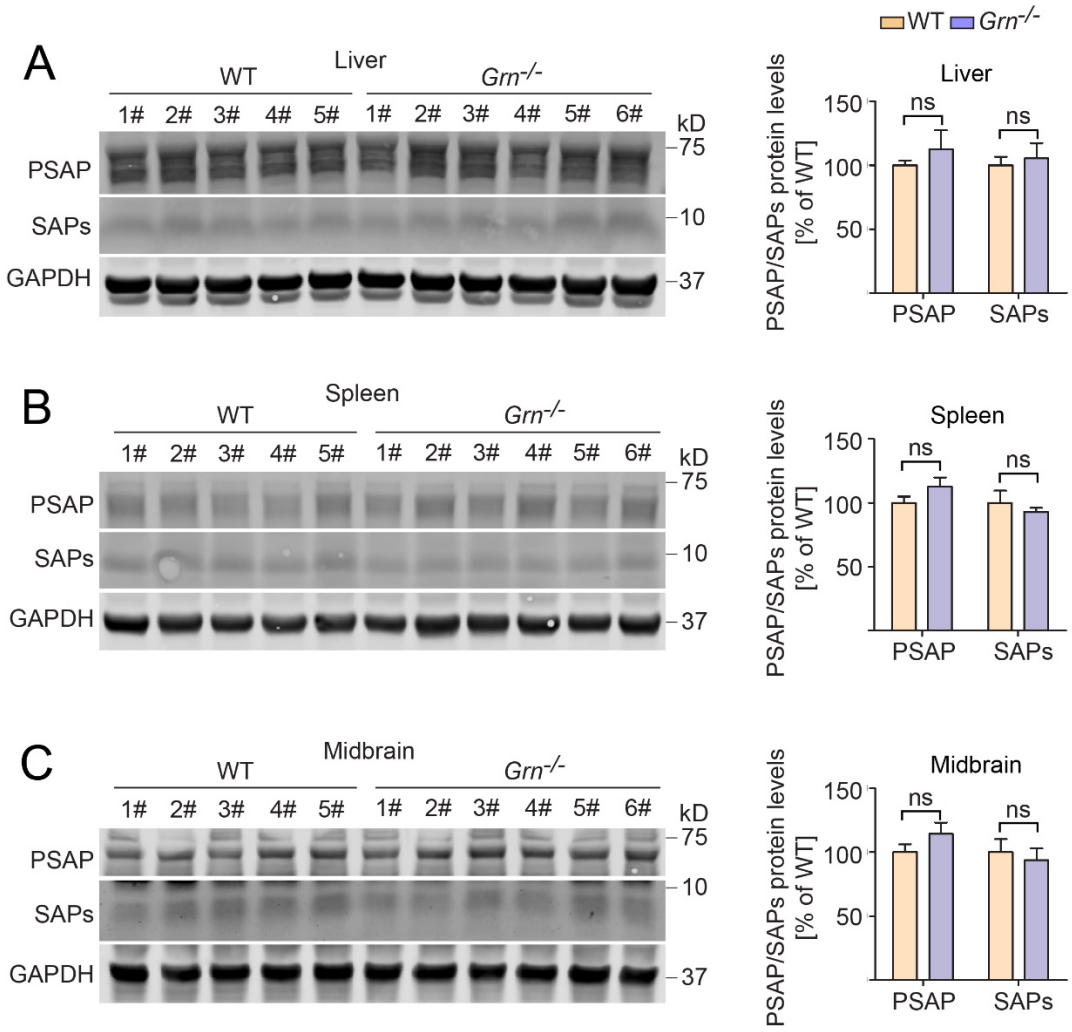

Figure 4.6. PSAP and total saposin protein levels. Mouse tissue lysates from 2-month-old WT and *Grn*$^{-/-}$ mice were assessed for PSAP and total saposin peptide levels, which were normalized to GAPDH. n = 5–6, ±SEM, ns, not significant, Student's t-test. Contributed by X.Z.

length protein by either of two known PGRN proteases, cathepsin L or neutrophil elastase [37]. The truncation construct used in the previous study was much larger, incorporating residues 496-593. This includes the entirety of both linker regions which encompass the Grn domain. It is possible that the folding of the two products differs or that GBA is binding to one or both of these linker regions. Importantly, ours is the first report demonstrating GBA dysfunction in a mouse model of PGRN deficiency and in human FTLD patient brain samples.

The previous studies examining the relationship between PGRN and GBA primarily utilized a chronic inflammation model based on the administration of ovalbumin (OVA) to WT and *Grn*$^{-/-}$ mice over the course of multiple weeks. The authors showed that PGRN interacts with GBA and HSP70 to act as co-chaperones of GBA and its trafficking receptor, lysosome membrane protein 2 (LIMP-2), and in cases of chronic lung inflammation with PGRN loss, LIMP-2 and GBA aggregate in the cytoplasm. Unfortunately, despite many repeated attempts at immunostaining to localize GBA, we were unable to find a single commercial antibody that produced a strong, specific signal for the endogenous protein. In fact, the only antibody that we found to produce a signal above background showed an equally strong lysosomal signal in primary *Gba*$^{-/-}$ mouse embryonic fibroblast (MEF) cells, indicating that the antibody is non-specific, recognizing an antigen other than GBA (data not shown). As such, we were not able to verify the localization of GBA in cells or tissue sections. However, in this instance we believe that it is unlikely that GBA is mislocalized and aggregated, as the study indicating this finding only observed it in the case of severe, chronically-induced inflammation, and in our young PGRN-deficient mice, it is unlikely that such

inflammation exists. The authors also did not observe a defect in GBA activity in the lung tissues of these mice, possibly due to differences in strain or tissue specificity.

The relationship between PGRN and GBA is complicated by a series of interrelated factors. Two peptides derived from PSAP, saposin A and saposin C, are known activators of GBA [48, 53, 54]. We have previously shown that PGRN and PSAP share a lysosomal co-trafficking relationship, wherein PGRN can carry PSAP to the lysosome via the receptor, sortilin, and PSAP can carry PGRN to the lysosome via the cation-independent mannose-6-phosphate receptor (CI-M6PR) or the low-density lipoprotein receptor-related protein 1 (LRP1) [33, 55, 56]. One result of this is that a reduction in total PGRN or PSAP protein levels may disrupt these necessary pathways, reducing lysosomal concentrations of the proteins. Additionally, PGRN has recently been shown to bind and modulate the activity of the lysosomal protease, cathepsin D (CTSD), which is the major contributor to proteolytic PSAP processing. Because of these factors, we have to consider the possibility that PGRN deficiency results in an alteration in PSAP processing and production of saposin peptides. Any reduction in PSAP levels could potentially lower saposin A and C levels as well, thereby reducing GBA activation. We attempted to address this by examining PSAP and total saposin levels in the tissue lysates in which we measured GBA activity. We were able to show that these levels do not change significantly. However, because we do not have antibodies that are specific to saposin A or C for western blot, we cannot rule out the possibility that one or both of these proteins are specifically decreased and saposin B and/or D are specifically increased, although this seems unlikely.

Although we did not see any change in GBA activity with the addition of recombinant PGRN or Grn peptides, this does not entirely rule out the possibility of a direct activation. PGRN and Grn E have been reported to directly activate CTSD *in vitro*, but our attempts to replicate these results have not been successful. This may be due to a number of technical factors, including misfolding of proteins in as a result of the expression system or purification procedures used.

While the exact mechanism of our findings is currently unknown, and more work needs to be performed to sift through the somewhat muddled relationships of the proteins involved, the result is clear: that PGRN deficiency can lead to defects in GBA activity. This is significant, as lysosomal dysfunction is a commonality between NCL and FTLD with *GRN* mutation. It is possible that lysosomal dysfunction due to the decreased activity of multiple lysosomal hydrolases, including GBA and CTSD, is a mechanism of these two diseases.

4.5 Materials and Methods

Primary Antibodies and Reagents

The following antibodies were used in this study: 9E10 mouse anti-myc (homemade), and mouse anti-GAPDH (Proteintech Group), mouse anti-GBA (MilliporeSigma), rabbit anti-GBA (Sigma), rat anti-mouse LAMP1 (BD Biosciences), and sheep anti-mouse PGRN (R&D Systems). Rabbit anti-mouse PSAP and PGRN antibodies were produced as previously described [33], GFP-Trap beads (ChromoTek). 4-Methylumbelliferyl β-D-glucopyranoside (4-MU) GBA substrate (Sigma). The MDW941 probe was a kind gift from Dr. Hermen Overkleeft (Leiden University).

Plasmids

Human GBA cDNA in the pDONR223 vector from the human ORFeome 8.1 collection was a gift from Dr. Haiyuan Yu (Cornell University). GBA was ligated into pcDNA3.1/myc-His A vector (Thermo Fisher Scientific) after digestion with EcoRI and XhoI. Human PGRN in the pCMV-Sport6 vector was obtained as previously described [32]. GFP-PGRN was produced as previously described [33]. GFP-Grn peptides were produced as described [39].

Protein Production and Purification

GST-Grn E, GST-Grn F, and His-SUMO-saposin C proteins were produced from the Origami B(DE3) bacterial strain (MilliporeSigma) with 0.1 mM IPTG induction overnight at 18°C. GST-tagged proteins were purified with glutathione cross-linked beads and eluted with excess glutathione. His-PGRN and His-SUMO-saposin C were purified with cobalt beads from the culture media of HEK293T cells as previously described [33]. All purified proteins were concentrated and transitioned to PBS buffer with Centricon Centrifugal Filter Units (MilliporeSigma).

Human Brain Tissues

Human brain tissues were obtained from the Neurodegenerative Disease Brain Bank at the University of California, San Francisco. Authorization for autopsy was provided by patients' next-of-kin, and procedures were approved by the UCSF Committee on Human Research. Neuropathological diagnoses were made in accordance with consensus diagnostic criteria [57, 58]. Cases were selected based on neuropathological diagnosis and genetic analysis. Freshly frozen blocks were used from subjects with FTLD-TDP, Type A, due to GRN mutations and healthy controls. Healthy control tissue was

obtained from individuals without dementia who had minimal age-related neurodegenerative changes.

Cell Culture

HEK293T were maintained in Dulbecco's Modified Eagle's Medium (Cellgro) supplemented with 10% fetal bovine serum (Gibco) in a humidified incubator at 37ºC with 5% CO_2.

Transfection, Immunoprecipitation, and Western Blot Analysis

Cells were transfected with polyethylenimine as previously described [59]. Cells were lysed in a cold solution containing 150 mM NaCl, 50 mM Tris (pH 8.0), 1% Triton X-100, 0.1% deoxycholic acid, 1X protease inhibitors (Roche). After centrifugation at 14,000 g, for 15 minutes, at 4ºC, supernatants were transferred to clean tubes on ice, to which GFP-Trap beads or rabbit anti-PGRN antibody-conjugated Affi-Gel 15 (Bio-Rad Laboratories) was added, then rocked for 3-4 hours at 4ºC. Samples were centrifuged at 2,500 g for 20 seconds at 4ºC, then washed with 1 mL of a solution containing 150 mM NaCl, 50 mM Tris (pH 8.0), and 1% Triton X-100. This was repeated for a total of 3 washes. After a final centrifugation, all supernatant was aspirated and samples were eluted by the addition of 25 µL of Laemmli Sample Buffer with 5% β-Mercaptoethanol.

Samples were run on a 12% or 8% polyacrylamide gel or a 4-12% Bis-Tris gel (Bio-Rad Laboratories), then transferred to Immobilon-FL polyvinylidene fluoride membranes (Millipore Corporation) or nitrocellulose membranes (Millipore Corporation). Membranes were blocked with either 5% non-fat milk in PBS or Odyssey Blocking Buffer (LI-COR Biosciences) for 1 hour, then washed with tris-buffered saline

with 0.1% Tween-20 (TBST) 3x for 5m, each. Membranes were incubated with primary antibodies diluted in TBST, rocking overnight at 4ºC, then washed as above, incubated with secondary antibodies diluted in TBST for 2 h at room temperature, then washed again. Membranes were scanned using an Odyssey Infrared Imaging System (LI-COR Biosciences). Densitometry was performed with Image Studio (LI-COR Biosciences).

Tissue Preparation for Enzyme Assays and Western Blot

Tissues from 2-month- old WT and *Grn*$^{-/-}$ mice were homogenized on ice with a glass Dounce homogenizer in a cold solution of either 1% (w/v) sodium taurocholate and 1% (v/v) Triton X-100, pH 5.2, for 4-MU activity assays or 0.2% (w/v) sodium taurocholate and 0.1% (v/v) Triton X-100 for MDW941 assays. Protein concentrations were determined via Bradford assay, then standardized.

Mouse Strains

C57/BL6 and *Grn*$^{-/-}$ mice were obtained from The Jackson Laboratory [60].

GBA Activity Assay with 4-MU Substrate

Tissue lysates, prepared as described, were diluted in a cold buffer of 0.1 M citric acid/0.2 M disodium phosphate (pH 5.0), with 2 mg/mL bovine serum albumin added. Ten microliters of each sample were added to 75 µL of cold 10 mM 4-MU substrate in the same buffer and incubated at 37ºC for 30 minutes. Reactions were stopped by the addition of 200 µL of a 0.3 M glycine/0.2 M sodium carbonate (pH 10.7) stop solution. Plates were read at 360 nm excitation/460 nm emission with an Infinite M100 microplate reader (Tecan).

To test for the direct activation of recombinant GBA, a 50 µL reaction mixture containing 1 mg/mL BSA, 0.1 M sodium acetate (pH 4.5), 0.02 U Cerezyme (Sanofi

Genzyme), 0.2 mM 4-MU substrate, 0.1% Triton X-100, and 1, 5, or 9 μM recombinant PGRN, Grn E, Grn F, or saposin C, or an equal volume of PBS was incubated at 37ºC for 30 minutes. Reactions were stopped by the addition of 50 μL of a 0.32 M glycine/0.32 M sodium carbonate (pH 10.4) stop solution. Plates were read at 340 nm excitation/420 nm emission with an Infinite M100 microplate reader (Tecan). Assays were also performed wherein Cerezyme and 1, 5, or 9 μM recombinant PGRN, Grn E, Grn F, or saposin C, or an equal volume of PBS were pre-incubated together on ice for 30 minutes in a volume of 15 μL, after which reactions were brought to the final volume and substrate concentration listed above.

Active GBA Assessment with MDW941 Probe

MDW941 was diluted to 100nM in tissue lysates, which were then incubated at 37ºC for 30 minutes. Reactions were stopped by the addition of an equal volume of 2x Laemmli sample buffer with 10% β-Mercaptoethanol before heating at 95ºC for 5 minutes. An equal amount of each sample (50 μg total protein) was run on a 12% polyacrylamide gel, which was scanned at 532 nm excitation/580 nm emission with a Typhoon Imaging System (GE Healthcare), then western blot and assessment were performed as described above, with all values normalized to GAPDH.

MDW941 Cell Labeling, Immunostaining, and Confocal Microscopy

WT and Grn-/- MEF cells were cultured on glass coverslips overnight. The next day, MDW941 was diluted to 5nM in culture media, then equal volumes were added to each well and the plate was incubated at 37ºC for 2h. Cells were washed 2x with PBS, fixed with 3.7% paraformaldehyde for 15 minutes at room temperature, followed by 3 additional PBS washes. Cells were permeabilized with Odyssey Blocking Buffer LI-

COR Biosciences) + 0.05% saponin for 30 minutes at room temperature. Primary antibodies were diluted in the same buffer and added to coverslips, which were incubated in a humidified chamber overnight at 4ºC. Coverslips were washed 3x with PBS, for 5 minutes each, then secondary antibodies diluted in the same blocking/permeabilization solution were added to the coverslips, which were incubated at room temperature, in the dark, for 2 hours. After 3 additional PBS washes, coverslips were mounted on slides with Fluoromount-G (SouthernBiotech). Images were acquired with a CSU-X series spinning disc confocal microscope (Intelligent Imaging Innovations) with an HQ2 CCD camera (Photometrics) using a 100x objective.

SILAC and Mass Spectrometry

WT and *Grn* CRISPR knockout BV-2 cells were grown a minimum of five generations in DMEM with 10% dialyzed fetal bovine serum (Sigma) supplemented with either heavy (C13, N15 arginine and lysine) amino acids or light (C12, N14 arginine and lysine). Cells were grown to confluency in two 15-cm plates, each, and lysed in 3 mL of a solution containing 150 mM NaCl, 20 mM sodium acetate (pH 5.3), 1% Triton X-100, and protease inhibitors (Roche), then immunoprecipitated as described above using homemade rabbit anti-PGRN antibodies bound to Affi-Gel 15 (Bio-Rad Laboratories). Samples were then mixed and boiled 5 min with 1% DTT followed by alkylation by treating samples with a final concentration of 28 mM iodoacetamide. Proteins were precipitated on ice for 30 min with a mixture of 50% acetone/49.9% ethanol/0.1% acetic acid. Protein was pelleted and washed with this buffer, reprecipitated on ice, and dissolved in 8 M urea/50 mM Tris (pH 8.0) followed by dilution with three volumes of 50 mM Tris (pH 8.0)/150 mM NaCl. Proteins were digested overnight at 37°C with 1

μg of mass spectrometry grade Trypsin (Promega). The resulting peptide samples were cleaned up for mass spectrometry by treatment with 10% formic acid and 10% trifluoroacetic acid and washed twice with 0.1% acetic acid on preequilibrated Sep-Pak C18 cartridges (Waters). Samples were eluted with 80% acetonitrile/0.1% acetic acid into silanized vials (National Scientific) and evaporated using a SpeedVac. Samples were redissolved in H2O with ~1% formic acid and 70% acetonitrile. Peptides were separated using hydrophilic interaction liquid chromatography on an Ultimate 300 LC (Dionex). Each fraction was evaporated with a SpeedVac and resuspended in 0.1% trifluoroacetic acid with 0.1 pM angiotensin internal standard. Samples were run on an LTQ Orbitrap XL mass spectrometer (Thermo Fisher Scientific) and data were analyzed using the SORCERER system (Sage-N Research).

4.6 Acknowledgements

We would like to thank Dr. Hermen Overkleeft for his kind gift of MDW941; Dr. Raquel Lieberman (Georgia Institute of Technology) for her gift of Cerezyme; Dr. Ying Sun (Cincinnati Children's Hospital) for her gifts of *Gba*$^{-/-}$ tissues and MEF cells; Dr. Haiyuan Yu for his gifts of cDNA; and Xiaochun Wu for technical assistance. Human tissue samples were provided by the Neurodegenerative Disease Brain Bank at the University of California, San Francisco, which receives funding support from NIH Grants P01AG019724 and P50AG023501, the Consortium for Frontotemporal Dementia Research and the Tau Consortium. This work is supported by funding to F. Hu from the Weill Institute for Cell and Molecular Biology, the Alzheimer's

Association, the Association of Frontotemporal Dementia, the Muscular Dystrophy Association, and NINDS (R21 NS081357-01 and R01 NS095954).

The authors declare no additional competing financial interests.

List of Abbreviations

CI-M6PR – Cation-independent mannose-6-phosphate receptor
CRISPR – Clustered regularly interspaces short palindromic repeats
CTSD – Cathepsin D
FTLD – Frontotemporal lobar degeneration
GBA – Glucocerebrosidase
Grn – Granulin
HSP70 – Heat shock protein 70
LIMP-2 – lysosome membrane protein 2
LRP1 – Low-density lipoprotein receptor-related protein 1
LSD – Lysosomal storage disease
MEF – Mouse embryonic fibroblasts
PD – Parkinson's disease
PGRN – Progranulin
PSAP – Prosaposin
SILAC – Stable isotope labeling of amino acids in cell culture
TBST – Tris-buffered saline with 0.1% Tween-20

REFERENCES

1. Songsrirote, K., et al., Development and application of mass spectrometric methods for the analysis of progranulin N-glycosylation. J Proteomics, 2010. **73**(8): p. 1479-90.

2. Tolkatchev, D., et al., Structure dissection of human progranulin identifies well-folded granulin/epithelin modules with unique functional activities. Protein Sci, 2008. **17**(4): p. 711-24.

3. Hrabal, R., et al., The hairpin stack fold, a novel protein architecture for a new family of protein growth factors. Nat Struct Biol, 1996. **3**(9): p. 747-52.

4. Tolkatchev, D., et al., Design and solution structure of a well-folded stack of two beta-hairpins based on the amino-terminal fragment of human granulin A. Biochemistry, 2000. **39**(11): p. 2878-86.

5. Vranken, W.F., et al., A 30-residue fragment of the carp granulin-1 protein folds into a stack of two beta-hairpins similar to that found in the native protein. J Pept Res, 1999. **53**(5): p. 590-7.

6. Palfree, R.G., H.P. Bennett, and A. Bateman, The Evolution of the Secreted Regulatory Protein Progranulin. PLoS ONE, 2015. **10**(8): p. e0133749.

7. He, Z. and A. Bateman, Progranulin (granulin-epithelin precursor, PC-cell-derived growth factor, acrogranin) mediates tissue repair and tumorigenesis. J Mol Med, 2003. **81**(10): p. 600-12.

8. Shoyab, M., et al., Epithelins 1 and 2: isolation and characterization of two cysteine-rich growth-modulating proteins. Proc Natl Acad Sci U S A, 1990. **87**(20): p. 7912-6.

9. Plowman, G.D., et al., The epithelin precursor encodes two proteins with opposing activities on epithelial cell growth. J Biol Chem, 1992. **267**(18): p. 13073-8.

10. Daniel, R., et al., Cellular localization of gene expression for progranulin. J Histochem Cytochem, 2000. **48**(7): p. 999-1009.

11. Toh, H., et al., Expression of the growth factor progranulin in endothelial cells influences growth and development of blood vessels: a novel mouse model. PLoS ONE, 2013. **8**(5): p. e64989.

12. He, Z., et al., Progranulin is a mediator of the wound response. Nat Med, 2003. **9**(2): p. 225-9.

13. Jian, J., J. Konopka, and C. Liu, Insights into the role of progranulin in immunity, infection, and inflammation. J Leukoc Biol, 2013. **93**(2): p. 199-208.

14. Toh, H., et al., Structure, function, and mechanism of progranulin; the brain and beyond. J Mol Neurosci, 2011. **45**(3): p. 538-48.

15. Cenik, B., et al., Progranulin: a proteolytically processed protein at the crossroads of inflammation and neurodegeneration. J Biol Chem, 2012. **287**(39): p. 32298-306.

16. Tanaka, Y., et al., Exacerbated inflammatory responses related to activated microglia after traumatic brain injury in progranulin-deficient mice. Neuroscience, 2013. **231**: p. 49-60.

17. Neary, D., et al., Frontotemporal lobar degeneration: a consensus on clinical diagnostic criteria. Neurology, 1998. **51**(6): p. 1546-54.

18. Baker, M., et al., Mutations in progranulin cause tau-negative frontotemporal dementia linked to chromosome 17. Nature, 2006. **442**(7105): p. 916-9.

19. Cruts, M., et al., Null mutations in progranulin cause ubiquitin-positive frontotemporal dementia linked to chromosome 17q21. Nature, 2006. **442**(7105): p. 920-4.

20. Gass, J., et al., Mutations in progranulin are a major cause of ubiquitin-positive frontotemporal lobar degeneration. Hum Mol Genet, 2006. **15**(20): p. 2988-3001.

21. Mackenzie, I.R., et al., The neuropathology of frontotemporal lobar degeneration caused by mutations in the progranulin gene. Brain, 2006. **129**(Pt 11): p. 3081-90.

22. Snowden, J.S., et al., Progranulin gene mutations associated with frontotemporal dementia and progressive non-fluent aphasia. Brain, 2006. **129**(Pt 11): p. 3091-102.

23. Mukherjee, O., et al., HDDD2 is a familial frontotemporal lobar degeneration with ubiquitin-positive, tau-negative inclusions caused by a missense mutation in the signal peptide of progranulin. Ann Neurol, 2006. **60**(3): p. 314-22.

24. Smith, K.R., et al., Strikingly different clinicopathological phenotypes determined by progranulin-mutation dosage. Am J Hum Genet, 2012. **90**(6): p. 1102-7.

25. Almeida, M.R., et al., Portuguese family with the co-occurrence of frontotemporal lobar degeneration and neuronal ceroid lipofuscinosis

phenotypes due to progranulin gene mutation. Neurobiol Aging, 2016. **41**: p. 200 e1-5.

26. Nita, D.A., S.E. Mole, and B.A. Minassian, Neuronal ceroid lipofuscinoses. Epileptic Disord, 2016. **18**(S2): p. 73-88.

27. Mole, S.E. and S.L. Cotman, Genetics of the neuronal ceroid lipofuscinoses (Batten disease). Biochim Biophys Acta, 2015. **1852**(10 Pt B): p. 2237-41.

28. Kohlschutter, A. and A. Schulz, Towards understanding the neuronal ceroid lipofuscinoses. Brain Dev, 2009. **31**(7): p. 499-502.

29. Ward, M.E., et al., Individuals with progranulin haploinsufficiency exhibit features of neuronal ceroid lipofuscinosis. Sci Transl Med, 2017. **9**(385).

30. Gotzl, J.K., et al., Common pathobiochemical hallmarks of progranulin-associated frontotemporal lobar degeneration and neuronal ceroid lipofuscinosis. Acta Neuropathol, 2014. **127**(6): p. 845-60.

31. Valdez, C., et al., Progranulin-mediated deficiency of cathepsin D results in FTD and NCL-like phenotypes in neurons derived from FTD patients. Hum Mol Genet, 2017. **26**(24): p. 4861-4872.

32. Hu, F., et al., Sortilin-mediated endocytosis determines levels of the frontotemporal dementia protein, progranulin. Neuron, 2010. **68**(4): p. 654-67.

33. Zhou, X., et al., Prosaposin facilitates sortilin-independent lysosomal trafficking of progranulin. J Cell Biol, 2015. **210**(6): p. 991-1002.

34. Belcastro, V., et al., Transcriptional gene network inference from a massive dataset elucidates transcriptome organization and gene function. Nucleic Acids Res, 2011. **39**(20): p. 8677-88.

35. Holler, C.J., et al., Intracellular Proteolysis of Progranulin Generates Stable, Lysosomal Granulins that Are Haploinsufficient in Patients with Frontotemporal Dementia Caused by GRN Mutations. Eneuro, 2017. **4**(4).

36. Zhou, X., et al., Lysosomal processing of progranulin. Mol Neurodegener, 2017. **12**(1): p. 62.

37. Lee, C.W., et al., The lysosomal protein cathepsin L is a progranulin protease. Mol Neurodegener, 2017. **12**(1): p. 55.

38. Beel, S., et al., Progranulin functions as a cathepsin D chaperone to stimulate axonal outgrowth in vivo. Hum Mol Genet, 2017.

39. Zhou, X., et al., Regulation of cathepsin D activity by the FTLD protein progranulin. Acta Neuropathol, 2017. **134**(1): p. 151-153.

40. Jian, J., et al., Progranulin Recruits HSP70 to beta-Glucocerebrosidase and Is Therapeutic Against Gaucher Disease. EBioMedicine, 2016. **13**: p. 212-224.

41. Jian, J., et al., Association Between Progranulin and Gaucher Disease. EBioMedicine, 2016. **11**: p. 127-137.

42. Beutler, E., A. Demina, and T. Gelbart, Glucocerebrosidase mutations in Gaucher disease. Mol Med, 1994. **1**(1): p. 82-92.

43. Schapira, A.H., Glucocerebrosidase and Parkinson disease: Recent advances. Mol Cell Neurosci, 2015. **66**(Pt A): p. 37-42.

44. Beutler, E. and G. Grabowski, Guacher disease. The Metabolic Basis of Inherited Disease, ed. C. Scriver, et al. Vol. 7th Ed. 1995, New York: McGraw-Hill.

45. Burbulla, L.F., et al., Dopamine oxidation mediates mitochondrial and lysosomal dysfunction in Parkinson's disease. Science, 2017. **357**(6357): p. 1255-1261.

46. Evers, B.M., et al., Lipidomic and Transcriptomic Basis of Lysosomal Dysfunction in Progranulin Deficiency. Cell Rep, 2017. **20**(11): p. 2565-2574.

47. Osiecki-Newman, K., et al., Human acid beta-glucosidase: use of inhibitors, alternative substrates and amphiphiles to investigate the properties of the normal and Gaucher disease active sites. Biochim Biophys Acta, 1987. **915**(1): p. 87-100.

48. Sun, Y., X. Qi, and G.A. Grabowski, Saposin C is required for normal resistance of acid beta-glucosidase to proteolytic degradation. J Biol Chem, 2003. **278**(34): p. 31918-23.

49. Qi, X., et al., Functional organization of saposin C. Definition of the neurotrophic and acid beta-glucosidase activation regions. J Biol Chem, 1996. **271**(12): p. 6874-80.

50. Witte, M.D., et al., Ultrasensitive in situ visualization of active glucocerebrosidase molecules. Nat Chem Biol, 2010. **6**(12): p. 907-13.

51. Ben Bdira, F., et al., Stabilization of Glucocerebrosidase by Active Site Occupancy. ACS Chem Biol, 2017. **12**(7): p. 1830-1841.

52. Herrera Moro Chao, D., et al., Visualization of Active Glucocerebrosidase in Rodent Brain with High Spatial Resolution following In Situ Labeling with Fluorescent Activity Based Probes. PLoS One, 2015. **10**(9): p. e0138107.

53. Morimoto, S., et al., Saposin A: second cerebrosidase activator protein. Proc Natl Acad Sci U S A, 1989. **86**(9): p. 3389-93.

54. Tamargo, R.J., et al., The role of saposin C in Gaucher disease. Mol Genet Metab, 2012. **106**(3): p. 257-63.

55. Zhou, X., et al., Impaired prosaposin lysosomal trafficking in frontotemporal lobar degeneration due to progranulin mutations. Nat Commun, 2017. **8**: p. 15277.

56. Zhou, X., et al., The interaction between progranulin and prosaposin is mediated by granulins and the linker region between saposin B and C. J Neurochem, 2017.

57. Hyman, B.T., et al., National Institute on Aging-Alzheimer's Association guidelines for the neuropathologic assessment of Alzheimer's disease. Alzheimers Dement, 2012. **8**(1): p. 1-13.

58. Mackenzie, I.R., et al., A harmonized classification system for FTLD-TDP pathology. Acta Neuropathol, 2011. **122**(1): p. 111-3.

59. Vancha, A.R., et al., Use of polyethyleneimine polymer in cell culture as attachment factor and lipofection enhancer. BMC Biotechnol, 2004. **4**: p. 23.

60. Yin, F., et al., Exaggerated inflammation, impaired host defense, and neuropathology in progranulin-deficient mice. J Exp Med, 2010. **207**(1): p. 117-28.

4.7 Supplementary Data

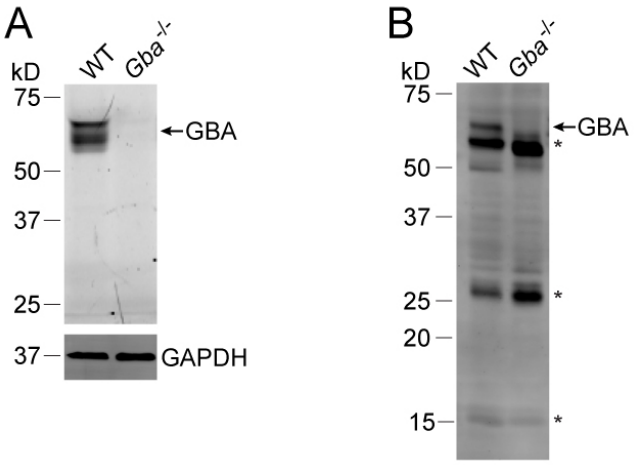

Supplementary Figure 4.1. Specificity of mouse anti-GBA antibody for western blot. A) Primary MEF cells from WT and *Gba*$^{-/-}$ mice. **B)** Lung tissue from WT and *Gba*$^{-/-}$ mice. *indicates non-specific bands.

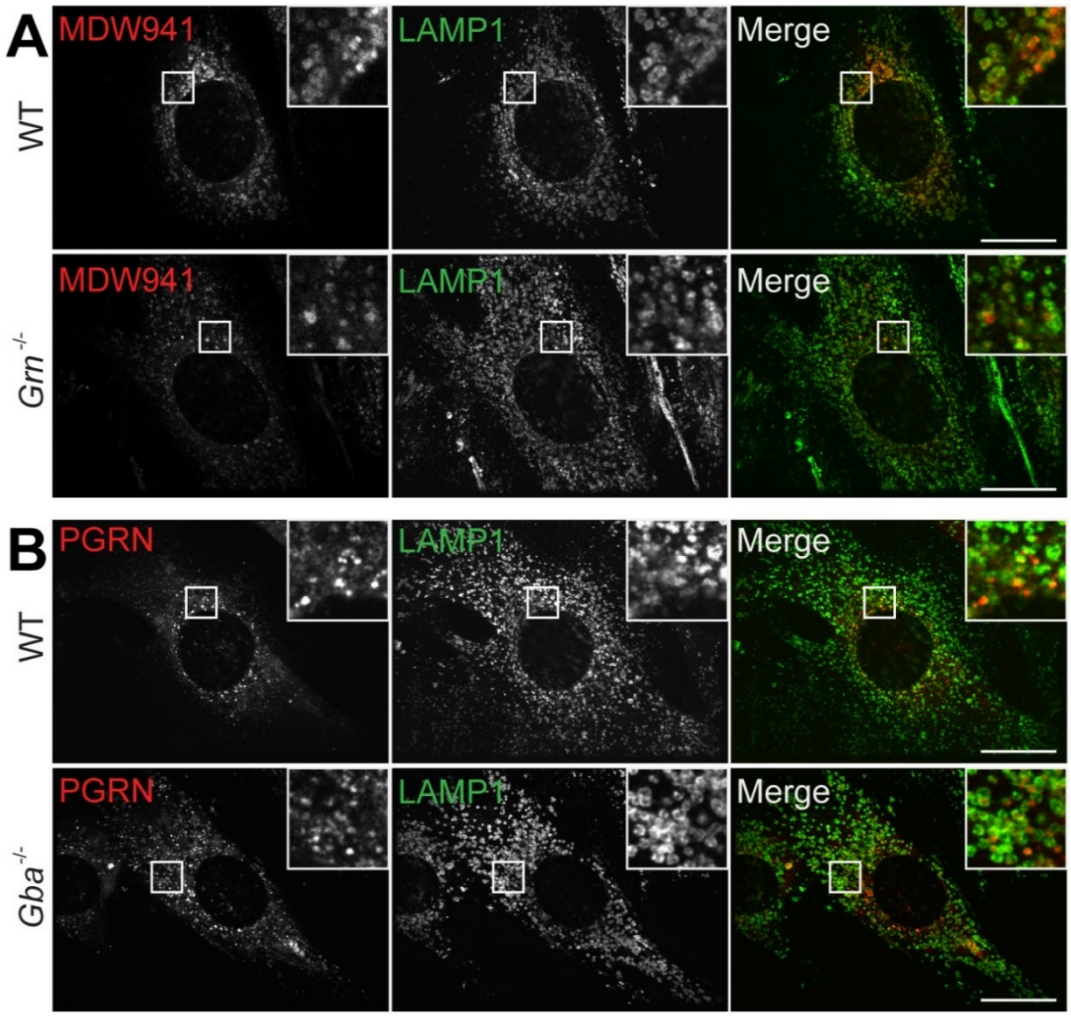

Supplementary Figure 4.2. Decreased MDW941 signal in *Grn*$^{-/-}$ compared to WT MEF cells, and PGRN immunostaining in WT and *Gba*$^{-/-}$ MEF cells. A) WT and *Grn*$^{-/-}$ MEF cells were labeled for 2 hours with MDW941 before fixation and immunostaining. **B)** Immunostaining shows no observable change in PGRN signal in *Gba*$^{-/-}$ MEF cells compared to WT MEF cells. Scale bar = 20 μm.

CHAPTER 5

α-N-ACETYLGALACTOSAMINIDASE ACTIVITY IS REDUCED IN PROGRANULIN-DEFICIENT MICE

5.1 Abstract

We have previously found that two lysosomal enzymes, cathepsin D (CTSD) and glucocerebrosidase (GBA), interact with progranulin (PGRN) and show reduced activity when PGRN is lost. Using stable isotope labeling of amino acids in cell culture (SILAC), we have identified a third lysosomal enzyme, α-N-acetylgalactosaminidase (NAGA), as a putative interactor of PGRN. NAGA hydrolyzes α-N-acetylgalactosaminyl moieties from glycoconjugates, and deficiency of this protein results in the accumulation of undegraded substrates and the lysosomal storage disease (LSD), Schindler disease. The interaction was confirmed by co-immunoprecipitation experiments, which also demonstrated potential binding between multiple granulin peptides and NAGA. We found NAGA protein levels to be upregulated in spleen lysates, but not liver lysates, of *Grn*$^{-/-}$ mice. When compared to total NAGA protein, activity of the enzyme was significantly reduced in both spleen and liver lysates of these mice. Although the mechanism of this activity reduction is currently unclear, this is further evidence that the dysfunction of multiple lysosomal hydrolases may play a role in PGRN-related disease.

5.2 Introduction

To better understand the lysosomal function of PGRN, we completed a stable isotope labeling by amino acids in cell culture (SILAC) screen to identify its protein binding partners. One promising candidate was the lysosomal enzyme, α-N-acetylgalactosaminidase (NAGA). NAGA assists in the degradation of lysosomal cargo by hydrolyzing α-N-acetylgalactosaminyl (GalNac) moieties of glycoconjugates [1-3]. Deficiency of NAGA, generally due to mutation, results in Schindler disease, also known as Kanzaki disease, a lysosomal storage disease (LSD) with neurological sequelae [4-7]. As our lab has identified two additional lysosomal enzymes to which PGRN binds, cathepsin D (CTSD) and glucocerebrosidase (GBA), which show a reduction in activity when PGRN is lost, we hypothesized that a similar reduction in activity may occur with NAGA. We found NAGA protein levels to be upregulated in spleen lysates, but not liver lysates, of *Grn*$^{-/-}$ mice. When normalized to total NAGA protein, activity of the enzyme was significantly reduced in both spleen and liver lysates of these mice. We also found evidence of the accumulation of undegraded NAGA substrates in the brains of *Grn*$^{-/-}$ mice.

5.3 Results

A SILAC screen identified NAGA as a potential interactor of PGRN. To verify binding between PGRN and NAGA, FLAG-PGRN and NAGA-MycHis were co-transfected in HEK293T cells and anti-FLAG IP was performed **(Fig. 5.1A)**. NAGA-MycHis was observed in the FLAG-PGRN sample, but not the control sample, indicating specific binding. To narrow the region of PGRN to which NAGA binds, a series of FLAG-

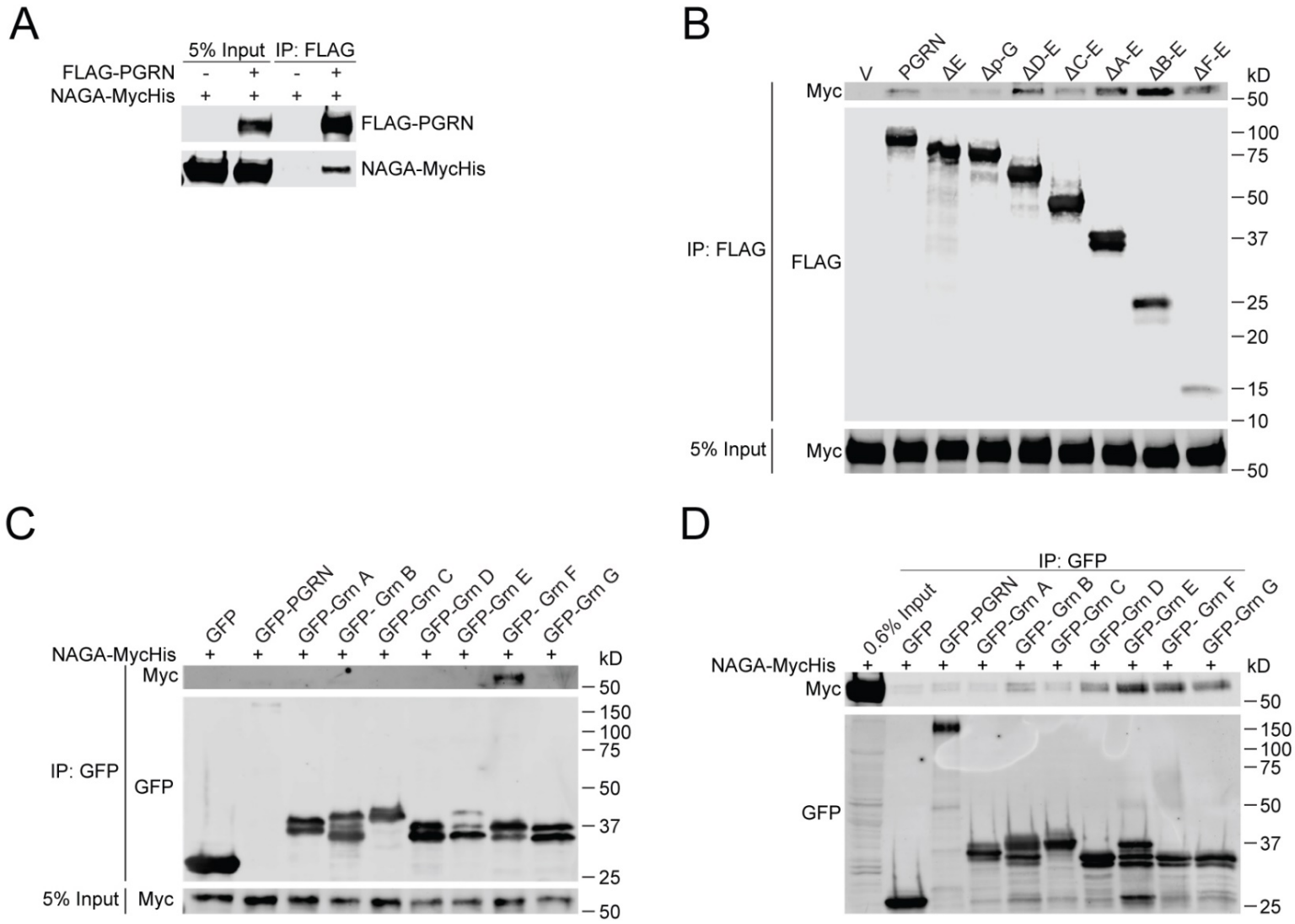
A
5% Input
IP: FLAG
FLAG-PGRN
NAGA-MycHis
FLAG-PGRN
NAGA-MycHis
B
V
PGRN
ΔE
Δp-G
ΔD-E
ΔC-E
ΔA-E
ΔB-E
ΔF-E
kD
Myc
IP: FLAG
FLAG
5% Input
Myc
C
GFP
GFP-PGRN
GFP-Grn A
GFP- Grn B
GFP-Grn C
GFP-Grn D
GFP-Grn E
GFP- Grn F
GFP-Grn G
NAGA-MycHis
kD
Myc
IP: GFP
GFP
5% Input
Myc
D
IP: GFP
0.6% Input
GFP
GFP-PGRN
GFP-Grn A
GFP- Grn B
GFP-Grn C
GFP-Grn D
GFP-Grn E
GFP- Grn F
GFP-Grn G
NAGA-MycHis
kD
Myc
GFP

Figure 5.1. Co-immunoprecipitation experiments. A) FLAG-PGRN was co-transfected with NAGA-MycHis in HEK293T cells and anti-FLAG IP was performed. **B)** FLAG-PGRN truncations were co-transfected with NAGA-MycHis and anti-FLAG IP was performed. **C)** GFP-PGRN or GFP-Grn peptides were co-transfected with NAGA-MycHis and anti-GFP was performed from cell lysate. **D)** GFP-PGRN or GFP-Grn peptides were transfected separately from NAGA-MycHis. Conditioned media containing GFP-PGRN or GFP-Grn peptides were collected and anti-GFP IP was performed. These beads were then added to NAGA-MycHis-overexpressing cell lysate.

PGRN truncations were co-transfected with NAGA-MycHis and anti-FLAG IP was performed **(Fig. 5.1B)**. Surprisingly, this did not identify a specific, isolated region of binding. While binding occurs at variable levels across all truncations, there is a clear trend toward more robust binding as the size of the PGRN fragment decreases. It appears that the p-G fragment is sufficient for binding, but stronger binding is seen when granulin (Grn) F and/or C is present. To further clarify these results and determine whether one or more specific Grn peptides bind NAGA, N-terminal GFP-tagged Grn peptides or PGRN were co-transfected with NAGA-MycHis, followed by anti-GFP IP **(Fig. 5.1C)**. Grn F showed pronounced binding, while the binding between NAGA-MycHis and Grn G was minimal. We repeated this experiment using conditioned media of individual secreted GFP-Grn peptides and NAGA-MycHis lysate **(Fig. 5.1D)**. In this experiment, binding was more promiscuous, with multiple Grn peptides showing binding, and Grn E being the strongest.

As we have detected decreased cathepsin D and glucocerebrosidase activity in the tissues of PGRN-deficient mice, we wanted to test whether NAGA activity is also reduced in these animals. After normalization of total protein levels, the activity of NAGA was assessed in liver and spleen lysates from 2-month-old WT and *Grn*$^{-/-}$ mice using an established enzyme activity assay based on the cleavable substrate, 4-Nitrophenyl N-acetyl-α-D-galactosaminide (pNPα-GalNAc) **(Fig. 5.2A)** [8-10]. Liver lysates from *Grn*$^{-/-}$ mice showed a significant decrease in NAGA activity compared to WT, while spleen lysates, surprisingly, showed an increase in activity, although it was not statistically significant. Because this increase in activity could be due to an upregulation of NAGA expression, we performed SDS-PAGE, western blot, and

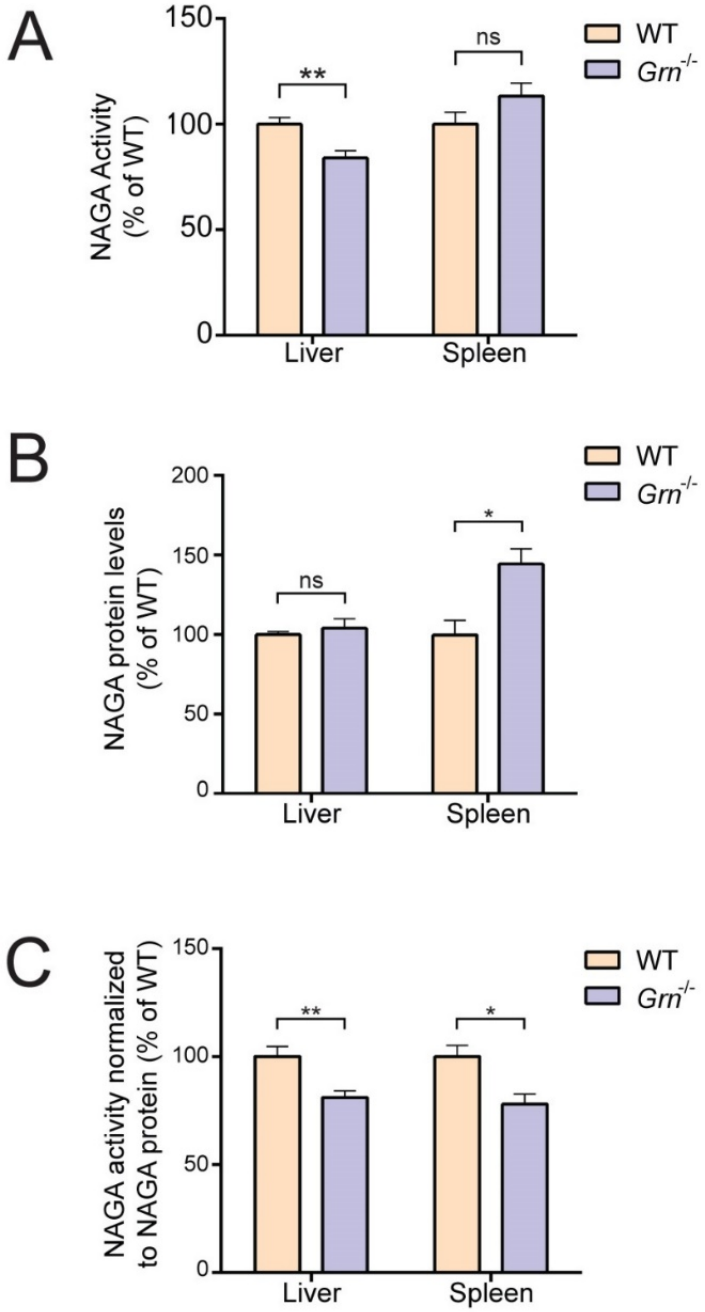

Figure 5.2. NAGA activity and protein levels in 2-month-old WT and *Grn*$^{-/-}$ mouse tissue lysates. **A)** NAGA activity was measured in liver and spleen lysates. **B)** NAGA protein levels were quantified and normalized to GAPDH **C)** NAGA activity was normalized to protein levels. n = 5–6, ± SEM, *p-value < 0.05, **p-value < 0.01, ns, not significant, Student's t-test.

densitometry of the tissue lysates to quantify NAGA protein levels normalized to GAPDH **(Fig. 5.2B, Supplementary Fig. 5.1)**. No significant change was observed in the liver samples, but NAGA levels in *Grn*$^{-/-}$ spleen samples were significantly increased compared to WT. We speculated that the increase in NAGA activity observed in the spleen is likely to be a direct result of the increase in total NAGA protein, and that the NAGA activity per unit of protein was likely still decreased compared to WT. We quantified the ratio of NAGA activity to total NAGA protein in the spleen to determine whether the activity per unit of protein was reduced **(Fig. 5.2C)**. When we normalized activity to protein levels, we found that NAGA was significantly less active in the spleen lysates of *Grn*$^{-/-}$ mice.

In human patients suffering from NAGA deficiency, substrates bearing terminal GalNac moieties are unable to be properly degraded and are found to accumulate in lysosomes. Such inclusions can be histologically visualized via a lectin specific for the terminal residue of interest [9-11]. Because we hypothesized that the enzymatic activity of NAGA would be decreased in *Grn*$^{-/-}$ mice, we expected an accumulation of undegraded NAGA substrates in the tissues of these animals. To test this, brain sections from aged WT and *Grn*$^{-/-}$ mice were immunostained and labeled with rhodamine-tagged soybean agglutinin (SBA), a lectin that preferentially binds terminal GalNac moieties. An increased number of neuronal inclusions was observed in the cortex **(Fig. 5.3A)** and midbrain **(Fig. 5.3B)** of PGRN-deficient mice.

In order to test whether PGRN or Grn F can directly modulate NAGA activity, the activity of recombinant NAGA was assayed with the addition of increasing

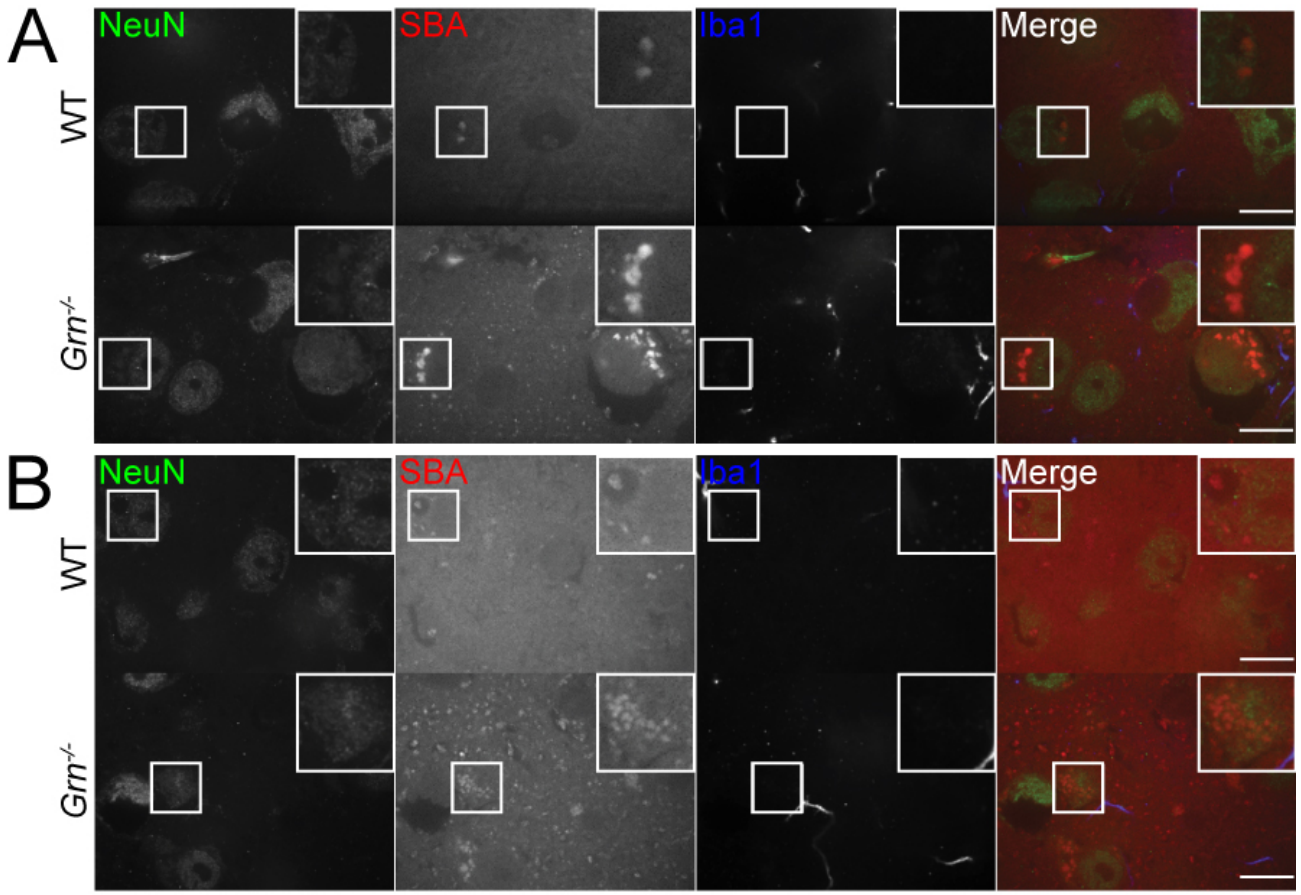

Figure 5.3. Increased terminal GalNac-bearing inclusions in aged *Grn*$^{-/-}$ mouse brain. Brain sections from 20-month-old WT and *Grn*$^{-/-}$ mice were stained with the GalNac-binding lectin, SBA, labeled with rhodamine, as well as with anti-NeuN (neuronal marker) and anti-Iba1 (microglial marker) antibodies. *Grn*$^{-/-}$ mouse brain shows an increase in neuronal inclusions, as seen by the greater number and signal intensity of SBA-positive puncta. **A)** Cortex. **B)** Midbrain. Scale bar = 10 μm.

concentrations of recombinant His-PGRN or GST-Grn F (data not shown). However, no specific change in activity was detected under these conditions.

5.4 Discussion

In this study, we have identified an interaction between PGRN/Grn peptides and the lysosomal hydrolase, NAGA. Furthermore, we have showed that NAGA protein levels are increased in spleen lysates, but not liver lysates, of *Grn*$^{-/-}$ mice and that activity of the enzyme compared to total NAGA protein levels was significantly reduced in both spleen and liver lysates of these mice. These preliminary results are promising, but further tests need to be performed to assess changes in NAGA activity in the brain, which is more relevant to frontotemporal lobar degeneration (FTLD) and neuronal ceroid lipofuscinosis (NCL). However, SBA staining indicates an accumulation of terminal GalNac-bearing products in the midbrain and cortex of *Grn*$^{-/-}$ mice, suggesting a NAGA deficiency in these regions.

Unfortunately, we are currently unable to validate our anti-NAGA antibodies for use in the detection of endogenous murine protein by western blot. Because of this, the reliability of our protein quantifications remains an issue. To address this, we attempted to knock out NAGA in several human- and mouse-derived cell lines using clustered regularly interspaced short palindromic repeats (CRISPR)-mediated genome editing. However, no change in banding pattern was seen on western blot, indicating that either the knockouts were unsuccessful or the antibodies are non-specific (data not shown).

As with CTSD and GBA, we did not see direct activation of NAGA with the addition of recombinant PGRN or Grn F. However, in follow-up binding experiments,

we found NAGA to potentially interact with multiple Grn peptides **(Fig. 5.1D)**. It may be that one of these peptides activates NAGA, rather than Grn F. As such, it may be worth re-examining the activation of recombinant NAGA with other Grn peptides.

Regardless of the mechanism of NAGA deficiency as a result of the loss of PGRN, lysosomal dysfunction due to the decreased activity of multiple lysosomal hydrolases, including NAGA, GBA, and CTSD, is increasingly supported as a potential mechanism of FTLD and NCL.

5.5 Materials and Methods

Primary Antibodies and Reagents

The following antibodies were used in this study: M2 mouse anti-FLAG (Sigma), M2 mouse anti-FLAG-conjugated beads (Sigma), 9E10 mouse anti-myc (homemade), rabbit anti-GFP (homemade), GFP-Trap beads (ChromoTek), mouse anti-NeuN (Millipore Corporation), rabbit anti-Iba1 (Wako Pure Chemical Corporation), and sheep anti-NAGA (R&D Systems). Rabbit anti-PGRN antibodies were produced as previously described [12]. Rhodamine-labeled Soybean Agglutinin (Vector Labs). 4-Nitrophenyl N-acetyl-α-D-galactosaminide (Sigma).

Plasmids

NAGA cDNA was a gift of Dr. Haiyuan Yu (Cornell University). NAGA was cloned into the pcDNA3.1/myc-His A vector. Human PGRN was obtained as previously described [13]. GFP-PGRN was produced as previously described [12]. GFP-Grn peptides were produced as described [14].

Protein Production and Purification

GST and GST-Grn F proteins were produced from the Origami B(DE3) bacterial strain (MilliporeSigma) with 0.1 mM IPTG induction overnight at 18°C and purified with glutathione cross-linked beads and eluted with excess glutathione. His-PGRN was purified with cobalt beads from the culture media of HEK293T cells as previously described [12]. All purified proteins were concentrated and transitioned to PBS buffer with Centricon Centrifugal Filter Units (MilliporeSigma).

Cell Culture

HEK293T, COS-7, and N2a cells were maintained in Dulbecco's Modified Eagle's Medium (Cellgro) supplemented with 10% fetal bovine serum (Gibco) in a humidified incubator at 37ºC with 5% CO_2.

Transfection, Immunoprecipitation, and Western Blot Analysis

Cells were transfected with polyethylenimine as previously described [15]. Cells were lysed in a cold solution containing 150 mM NaCl, 50 mM Tris (pH 8.0), 1% Triton X-100, 0.1% deoxycholic acid, 1X protease inhibitors (Roche). After centrifugation at 14,000 g, for 15 minutes, at 4ºC, supernatants were transferred to clean tubes on ice, to which mouse anti-FLAG antibody-conjugated beads or GFP-Trap beads (ChromoTek) was added, then rocked for 3-4 hours at 4ºC. Samples were centrifuged at 2,500 g for 20 seconds at 4ºC, then washed with 1 mL of a solution containing 150 mM NaCl, 50 mM Tris (pH 8.0), and 1% Triton X-100. This was repeated for a total of 3 washes. After a final centrifugation, all supernatant was aspirated and samples were eluted by the addition of 25 µL of Laemmli Sample Buffer with 5% β-Mercaptoethanol.

Samples were run on a 12% polyacrylamide gel, then transferred to Immobilon-FL polyvinylidene fluoride membranes (Millipore Corporation). Membranes were blocked with either 5% non-fat milk in PBS or Odyssey Blocking Buffer (LI-COR Biosciences) for 1 hour, then washed with tris-buffered saline with 0.1% Tween-20 (TBST) 3x for 5m, each. Membranes were incubated with primary antibodies diluted in TBST, rocking overnight at 4ºC, then washed as above, incubated with secondary antibodies diluted in TBST for 2 h at room temperature, then washed again. Membranes were scanned using an Odyssey Infrared Imaging System (LI-COR Biosciences). Densitometry was performed with Image Studio (LI-COR Biosciences).

Immunostaining, Lectin Staining, and Confocal Microscopy

Cells were cultured on glass coverslips overnight. For transfection experiments, cells were transfected the next morning and proteins were allowed to express for ~2 days before experiments were performed. Cells were washed 2x with PBS, fixed with 3.7% paraformaldehyde for 15 minutes at room temperature, followed by 3 additional PBS washes. Cells were permeabilized with Odyssey Blocking Buffer (LI-COR Biosciences) + 0.05% saponin for 30 minutes at room temperature. Primary antibodies were diluted in the same buffer and added to coverslips, which were incubated in a humidified chamber overnight at 4ºC. Coverslips were washed 3x with PBS, for 5 minutes each, then secondary antibodies diluted in the same blocking/permeabilization solution were added to the coverslips, which were incubated at room temperature, in the dark, for 2 hours. After 3 additional PBS washes, coverslips were mounted on slides with Fluoromount-G (SouthernBiotech). Images were acquired with a CSU-X series

spinning disc confocal microscope (Intelligent Imaging Innovations) with an HQ2 CCD camera (Photometrics) using a 100x objective.

For tissue staining, mice were perfused with PBS, then tissues were collected and incubated in 4% paraformaldehyde, rocking at 4°C for 48 hours. Tissues were washed 3x with PBS the incubated in PBS with 15% (w/v) sucrose rocking at 4°C for 24, followed by a similar incubation in in PBS with 30% (w/v) sucrose. Tissues were embedded in Tissue-Tek O.C.T. Compound (Sakura Finetek) and frozen at -80°C before cryotome sectioning. Immunostaining was performed as with cells, except tissue sections were incubated with 0.1% Sudan Black in 70% EtOH for 20 minutes, rocking at room temperature to inhibit autofluorescence, and blocking and permeabilization were performed with 0.1% saponin in Odyssey Blocking Buffer.

NAGA Enzyme Activity Assays

Tissues were lysed in a cold solution of 20 mM NaOAc, pH 5.3, 150 mM NaCl, and 1% Triton X-100 at a 1:10 ratio of tissue weight (g) to lysis buffer (mL). Protein concentrations were measured via Bradford protein assay and normalized. Reactions were performed in a final reaction mixture of 0.1 M citrate buffer (pH 4.3), 2 mM substrate, 75 μg tissue lysate, in a final volume of 100 μL. Samples were incubated at 37°C for 4 hours. Reactions were stopped by the addition of trichloroacetic acid to a final concentration of 2.9%. Samples were incubated on ice for 15 minutes then centrifuged at 14,000 g and 4°C for 15 minutes. Supernatants were transferred to a 96-well plate, then glycine-carbonate buffer (pH 9.7) and NaOH were added to a final concentration of 0.088 M and 0.13 M, respectively, before measuring absorbance at 410 nm with an Infinite M100 microplate reader (Tecan).

SILAC and Mass Spectrometry

Grn CRISPR knockout T98G cells were grown a minimum of five generations in DMEM with 10% dialyzed fetal bovine serum (Sigma) supplemented with either heavy (C13, N15 arginine and lysine) amino acids or light (C12, N14 arginine and lysine). Cells were grown to confluency in two 15-cm plates, each, and lysed in 3 mL of a solution containing 150 mM NaCl, 20 mM sodium acetate (pH 5.3), 1% Triton X-100, and protease inhibitors (Roche). Lysates were incubated with His-tagged and purified mammalian-expressed PGRN conjugated to Affigel 15 (Bio-Rad Laboratories) as the bait or BSA as control for 4 hours before washing and elution. Samples were then mixed and boiled 5 min with 1% DTT followed by alkylation by treating samples with a final concentration of 28 mM iodoacetamide. Proteins were precipitated on ice for 30 min with a mixture of 50% acetone/49.9% ethanol/0.1% acetic acid. Protein was pelleted and washed with this buffer, reprecipitated on ice, and dissolved in 8 M urea/50 mM Tris (pH 8.0) followed by dilution with three volumes of 50 mM Tris (pH 8.0)/150 mM NaCl. Proteins were digested overnight at 37°C with 1 μg of mass spectrometry grade Trypsin (Promega). The resulting peptide samples were cleaned up for mass spectrometry by treatment with 10% formic acid and 10% trifluoroacetic acid and washed twice with 0.1% acetic acid on preequilibrated Sep-Pak C18 cartridges (Waters). Samples were eluted with 80% acetonitrile/0.1% acetic acid into silanized vials (National Scientific) and evaporated using a SpeedVac. Samples were re-dissolved in H2O with ~1% formic acid and 70% acetonitrile. Peptides were separated using hydrophilic interaction liquid chromatography on an Ultimate 300 LC (Dionex). Each fraction was evaporated with a SpeedVac and resuspended in 0.1% trifluoroacetic acid

with 0.1 pM angiotensin internal standard. Samples were run on an LTQ Orbitrap XL mass spectrometer (Thermo Fisher Scientific) and data were analyzed using the SORCERER system (Sage-N Research).

5.6 Acknowledgements

We would like to thank Dr. Haiyuan Yu for his gifts of cDNA and Xiaochun Wu for technical assistance. This work is supported by funding to F. Hu from the Weill Institute for Cell and Molecular Biology, the Alzheimer's Association, the Association of Frontotemporal Dementia, the Muscular Dystrophy Association, and the NINDS (R21 NS081357-01 and R01 NS095954).

The authors declare no additional competing financial interests.

List of Abbreviations

CRISPR – Clustered regularly interspaces short palindromic repeats
CTSD – Cathepsin D
FTLD – Frontotemporal lobar degeneration
GalNac – α-N-acetylgalactosaminyl/α-N-acetylgalactosaminide
GBA – Glucocerebrosidase
Grn – Granulin
LSD – Lysosomal storage disease
NCL – Neuronal ceroid lipofuscinosis
PGRN – Progranulin
pNPα-GalNAc – 4-Nitrophenyl N-acetyl-α-D-galactosaminide
SILAC – stable isotope labeling of amino acids in cell culture
TBST – Tris-buffered saline with 0.1% Tween-20

REFERENCES

1. Keulemans, J.L., et al., Human alpha-N-acetylgalactosaminidase (alpha-NAGA) deficiency: new mutations and the paradox between genotype and phenotype. J Med Genet, 1996. **33**(6): p. 458-64.

2. Wang, A.M., T. Kanzaki, and R.J. Desnick, The molecular lesion in the alpha-N-acetylgalactosaminidase gene that causes angiokeratoma corporis diffusum with glycopeptiduria. J Clin Invest, 1994. **94**(2): p. 839-45.

3. Ferreira, C.R. and W.A. Gahl, Lysosomal storage diseases. Transl Sci Rare Dis, 2017. **2**(1-2): p. 1-71.

4. van Diggelen, O.P., et al., Lysosomal alpha-N-acetylgalactosaminidase deficiency: a new inherited metabolic disease. Lancet, 1987. **2**(8562): p. 804.

5. Wang, A.M., D. Schindler, and R. Desnick, Schindler disease: the molecular lesion in the alpha-N-acetylgalactosaminidase gene that causes an infantile neuroaxonal dystrophy. J Clin Invest, 1990. **86**(5): p. 1752-6.

6. Desnick, R.J. and A.M. Wang, Schindler disease: an inherited neuroaxonal dystrophy due to alpha-N-acetylgalactosaminidase deficiency. J Inherit Metab Dis, 1990. **13**(4): p. 549-59.

7. Hirabayashi, Y., et al., Isolation and characterization of major urinary amino acid O-glycosides and a dipeptide O-glycoside from a new lysosomal storage disorder (Kanzaki disease). Excessive excretion of serine- and threonine-linked glycan in the patient urine. J Biol Chem, 1990. **265**(3): p. 1693-701.

8. Callahan, J.W., et al., Alpha-N-acetylgalactosaminidase: isolation, properties and distribution of the human enzyme. Biochem Med, 1973. **7**(3): p. 424-31.

9. de Jong, J., et al., alpha-N-acetylgalactosaminidase deficiency with mild clinical manifestations and difficult biochemical diagnosis. J Pediatr, 1994. **125**(3): p. 385-91.

10. van Diggelen, O.P., et al., alpha-N-acetylgalactosaminidase deficiency, a new lysosomal storage disorder. J Inherit Metab Dis, 1988. **11**(4): p. 349-57.

11. Alroy, J., R. De Gasperi, and C.D. Warren, Application of lectin histochemistry and carbohydrate analysis to the characterization of lysosomal storage diseases. Carbohydr Res, 1991. **213**: p. 229-50.

12. Zhou, X., et al., Prosaposin facilitates sortilin-independent lysosomal trafficking of progranulin. J Cell Biol, 2015. **210**(6): p. 991-1002.

13. Hu, F., et al., Sortilin-mediated endocytosis determines levels of the frontotemporal dementia protein, progranulin. Neuron, 2010. **68**(4): p. 654-67.

14. Zhou, X., et al., Regulation of cathepsin D activity by the FTLD protein progranulin. Acta Neuropathol, 2017. **134**(1): p. 151-153.

15. Vancha, A.R., et al., Use of polyethyleneimine polymer in cell culture as attachment factor and lipofection enhancer. BMC Biotechnol, 2004. **4**: p. 23.

5.7 Supplementary Data

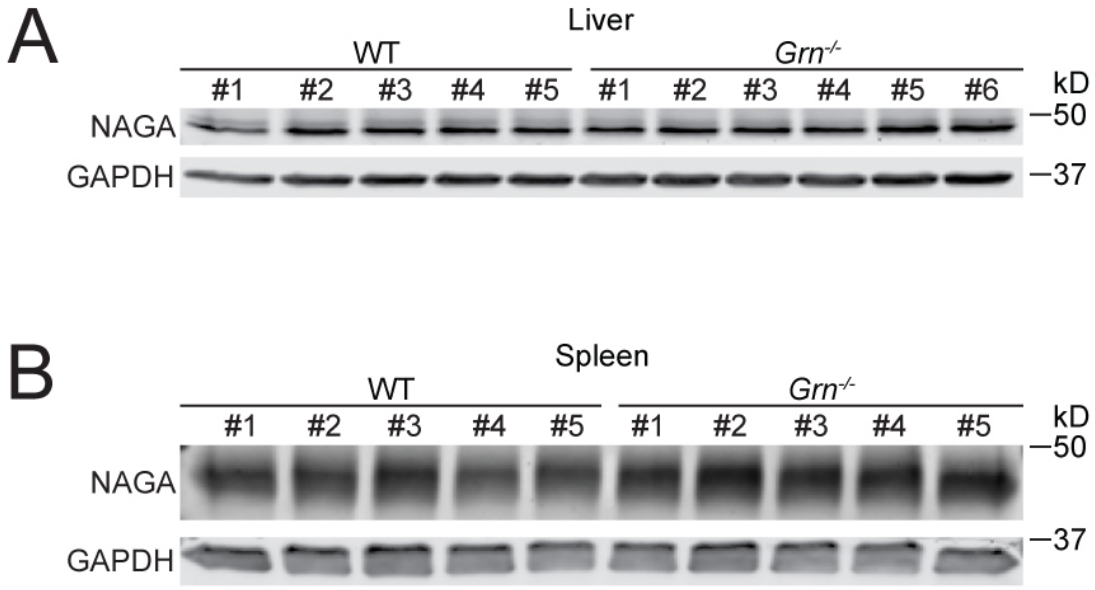

Supplementary Figure 5.1. Western blots of WT and *Grn*$^{-/-}$ mouse liver and spleen lysates. Protein quantified and used to normalize NAGA activity in Fig. 5.2B and Fig. 5.2C, respectively.

CHAPTER 6

A HIGH-THROUGHPUT SCREEN IDENTIFIES CD68 AND NEUROPILIN 2 AS PUTATIVE PROGRANULIN RECEPTORS

6.1 Abstract

Mutation in the *GRN* gene leading to reduced expression of the protein, progranulin (PGRN), shows a dose-dependent disease correlation, wherein haploinsufficiency results in frontotemporal lobar degeneration (FTLD) and complete loss results in neuronal ceroid lipofuscinosis (NCL). While PGRN has been increasingly associated with lysosomal homeostasis, it has also been shown to possess neurotrophic properties. PGRN and the granulin (Grn) peptide, Grn E, are both capable of modulating neuronal survival and neurite outgrowth. However, no PGRN neurotrophic receptor has been discovered. To attempt to identify a neurotrophic receptor of PGRN, we performed a high-throughput enzyme-based cell surface binding screen of >2,800 transmembrane proteins. From this screen and follow-up binding studies, we identified cluster of differentiation 68 (CD68) and neuropilin 2 (NRP2) as putative PGRN and Grn E receptors.

6.2 Introduction

In addition to being involved in lysosomal homeostasis, there is strong evidence that progranulin (PGRN) can function as a neurotrophic factor, promoting neuronal survival and neurite outgrowth [1-9]. It is possible that in cases of PGRN-deficiency, as occurs

with frontotemporal lobar degeneration (FTLD) and neuronal ceroid lipofuscinosis (NCL) with granulin (*GRN*) mutation, neuronal death is not only due to lysosomal dysfunction, but loss of direct neurotrophic signaling. One study found that application of recombinant PGRN or the granulin (Grn) peptide, Grn E, to motor or cortical neurons isolated from rat spinal cords and cultured in serum-free media produced a dose-dependent increase in survival time.[1] This was especially pronounced for the Grn E-treated cells, which showed up to a 100% increase in survival by the end of 6 days in culture. In addition, it was also found that PGRN, and to a lesser extent, Grn E, applied to primary rat cortical or motor neuron cultures, could promote neurite outgrowth. Separately, recombinant PGRN added to the cultured media of the neuron-like PC-12 cell line was able to increase the proliferation of these cells.[9] It has been assumed that there is a cell surface signaling receptor to which PGRN binds that mediates these responses. However, no PGRN neurotrophic receptor has been discovered.

In an attempt to identify this receptor, we performed a high-throughput interactor screen based on a well-established enzymatic assay, which has been used to identify many novel interactions, including the interaction between PGRN and its trafficking receptor, sortilin [10-13]. In this assay, a ligand fused to a heat-resistant alkaline phosphatase (AP) is incubated with COS-7 cells overexpressing an individual transmembrane protein to allow binding to the potential cognate receptor. Excess AP-ligand is washed off, cells are fixed, endogenous AP is heat-inactivated, then a mixture of an AP substrate and oxidant are added. If the AP-ligand remains bound to the overexpressed receptor, the active AP produces a dark, purple-black precipitate that can be visualized by brightfield microscopy.

We acquired a transmembrane protein plasmid library derived from the human ORFeome 8.1 as an extremely kind gift of Dr. Haiyuan Yu (Cornell University). The human genome is predicted to encode 5,521 transmembrane proteins, and the human ORFeome 8.1 that we possess contains 2,815 cDNAs, representing 51% of these proteins [14, 15]. These cDNAs were cloned into the mammalian expression vector pcDNA-DEST47 with a C-terminal GFP tag, enabling visual confirmation of expression and subcellular localization, via the Gateway LR reaction.

From this screen, and through further binding studies, we identified two potential receptors of Grn E, which were then also found to bind PGRN via co-immunoprecipitation (co-IP): cluster of differentiation 68 (CD68) and neuropilin 2 (NRP2). CD68 is a member of the lysosomal-associated membrane protein (LAMP) family and is a poorly characterized scavenger receptor involved in the uptake of oxidized low-density lipoprotein (LDL) and recognition of polyanionic ligands, including exposed phosphatidylserine [16-18]. As CD68 expression is limited to immune cells and is well-established marker of macrophages and reactive microglia [19], it is unlikely to be involved in the neurotrophic functions of PGRN. CD68 has also been found to be highly upregulated in the microglia of PGRN-deficient mice, although it is unclear whether this is an indirect result of transcriptional upregulation of lysosomal genes or enhanced inflammation [20-23].

NRP2 and the highly homologous NRP1 interact with many ligands, including transforming growth factor-β (TGF-β), and vascular endothelial growth factor (VEGF) and semaphorin family members [24-28]. NRP2 has well-defined roles in axon guidance and lymphangiogenesis, as well as more loosely defined roles in endothelial

cell migration and immune regulation. In this study, we describe binding studies and preliminary tests of the function of these relationships.

6.3 Results

AP cell surface binding screen identifies two candidate receptors

Of the >2,800 transmembrane proteins transfected, only ~40% were positive for GFP signal. Transmembrane proteins were tested for binding to AP-PGRN, AP-PGRN + AP-prosaposin (PSAP), or a mixture of the AP-Grn peptides: A, B, D, E, and G (AP-Grn C and AP-Grn F did not express). As PSAP is an exceedingly strong interactor of PGRN and partially mediates its lysosomal trafficking, we posited that the heterodimerization may alter the conformation and binding affinities of PGRN, which spurred its inclusion in the study. From this screen, two positive interactions were identified, both with the peptide, Grn E, but not full-length PGRN: CD68 **(Fig. 6.1)** and NRP2 **(Fig. 6.2)**. Differentially truncated AP-Grn E constructs were tested to localize the region of binding to this peptide. Interaction with CD68 was found to be primarily dependent on the N-terminus of Grn E **(Fig. 6.1D)**. Binding to NRP2 was seen with a variety of constructs, but the strongest interaction occurred when the full N-terminus was present, and the C-terminal residues of the AP-fused protein consisted of a di-arginine **(Fig. 6.2C)**. Consistent with this finding, neuropilin ligands, such as VEGF and semaphorin family members, often contain a C-terminal arginine that mediates receptor binding [28-30].

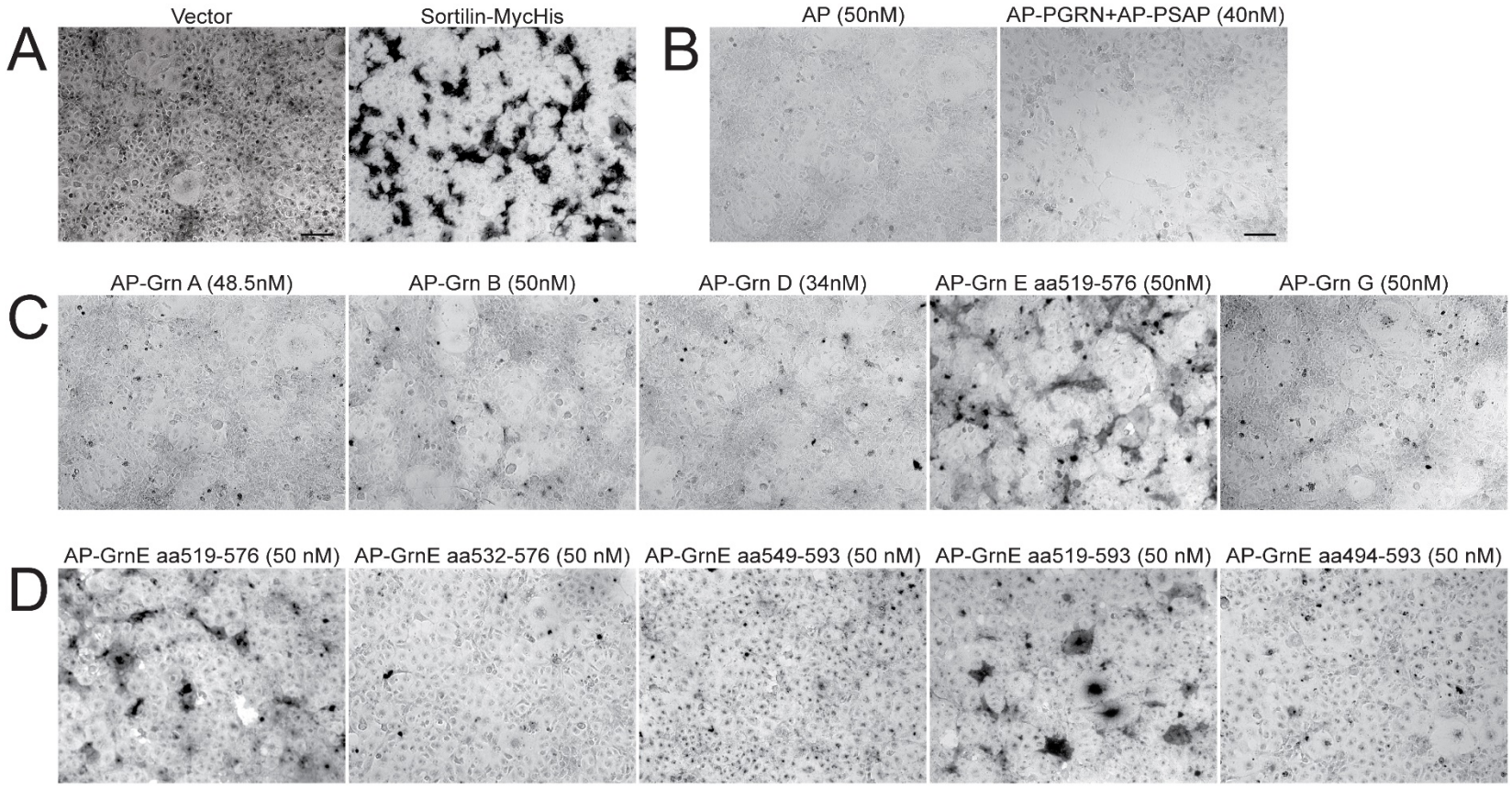

Figure 6.1. CD68 AP cell surface binding assay results. A) Control samples tested with 50nM AP-PGRN demonstrate negative (vector) and positive (sortilin) binding results. **B)** AP negative control and AP-PGRN show no binding to CD68-GFP. **C)** AP-Grn E, but no other Grn peptide, shows binding to CD68-GFP. **D)** Grn E truncations were tested to narrow the region of binding to overexpressed CD68-MycHis.

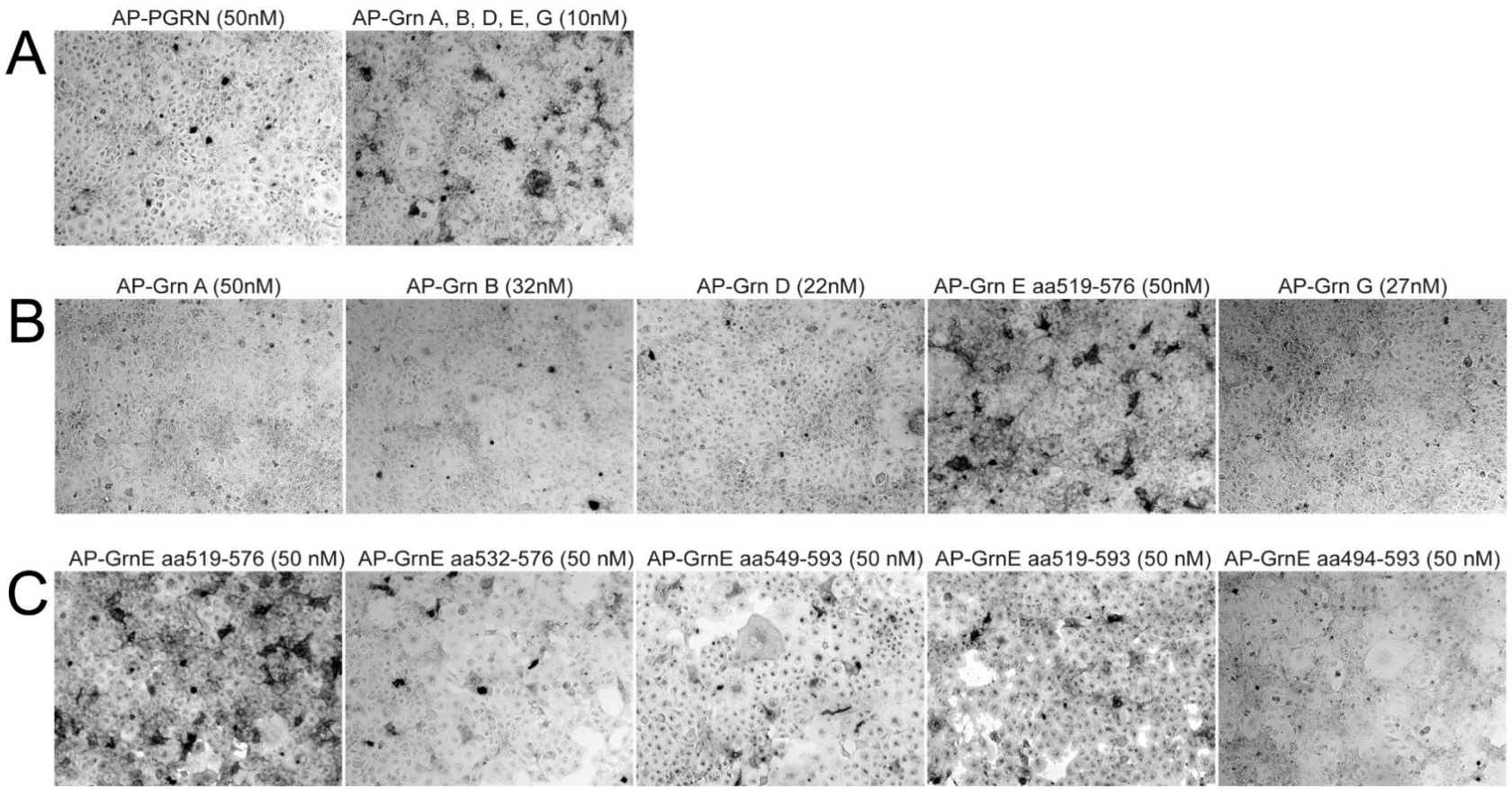

Figure 6.2. NRP2 AP cell surface binding assay results. A) AP-PGRN shows no obvious binding to NRP2-GFP, but binding is observed with a mixture of AP-Grn peptides. **B)** AP-Grn E, but no other Grn peptide, shows binding to NRP2-GFP. **C)** Grn E truncations were tested to narrow the region of binding to overexpressed NRP2-GFP.

Additional PGRN, Grn E, and CD68 binding studies

To further examine binding between PGRN or Grn peptides and CD68, co-IP studies were performed. To test for binding between PGRN and CD68, FLAG-PGRN and CD68-GFP were co-transfected in HEK293T cells, then anti-FLAG IP was performed. Somewhat surprisingly, because no interaction was seen in the AP cell surface binding assay, CD68-GFP was found to weakly pull out with FLAG-PGRN, but not in the control sample **(Fig. 6.3A)**. To verify binding between Grn E and CD68, as well as test for binding to Grn C and Grn F, which were not available for use in the screen, GFP-tagged Grn peptides were co-transfected with CD68-MycHis and anti-GFP IP was performed **(Fig. 6.3B)**. The results of this were clear: binding was strong and specific to Grn E. Interestingly, more intense binding was seen between Grn E and the lowest molecular weight CD68 band, suggesting a preferential binding to a slightly less glycosylated form of the receptor.

To test whether endogenously produced Grn peptides can bind to CD68, FLAG-PGRN was co-transfected with CD68-GFP and anti-GFP IP was performed. These samples were run on a 4-12% Bis-Tris gel for visualization of Grn peptides **(Fig. 6.3C)**. Both PGRN and Grn peptides were seen to co-immunoprecipitate with CD68-GFP. To be entirely sure that the low molecular weight bands observed to co-immunoprecipitate with CD68 in the previous experiment were derived from PGRN, we performed a pull-down assay. CD68-GFP was transfected in HEK293T cells. The next day, recombinant PGRN was proteolytically cleaved overnight with neutrophil elastase, an enzyme previously established to process PGRN to Grn peptides [31]. The cleavage products were mixed with the CD68-GFP-expressing cell lysate and anti-GFP IP was performed

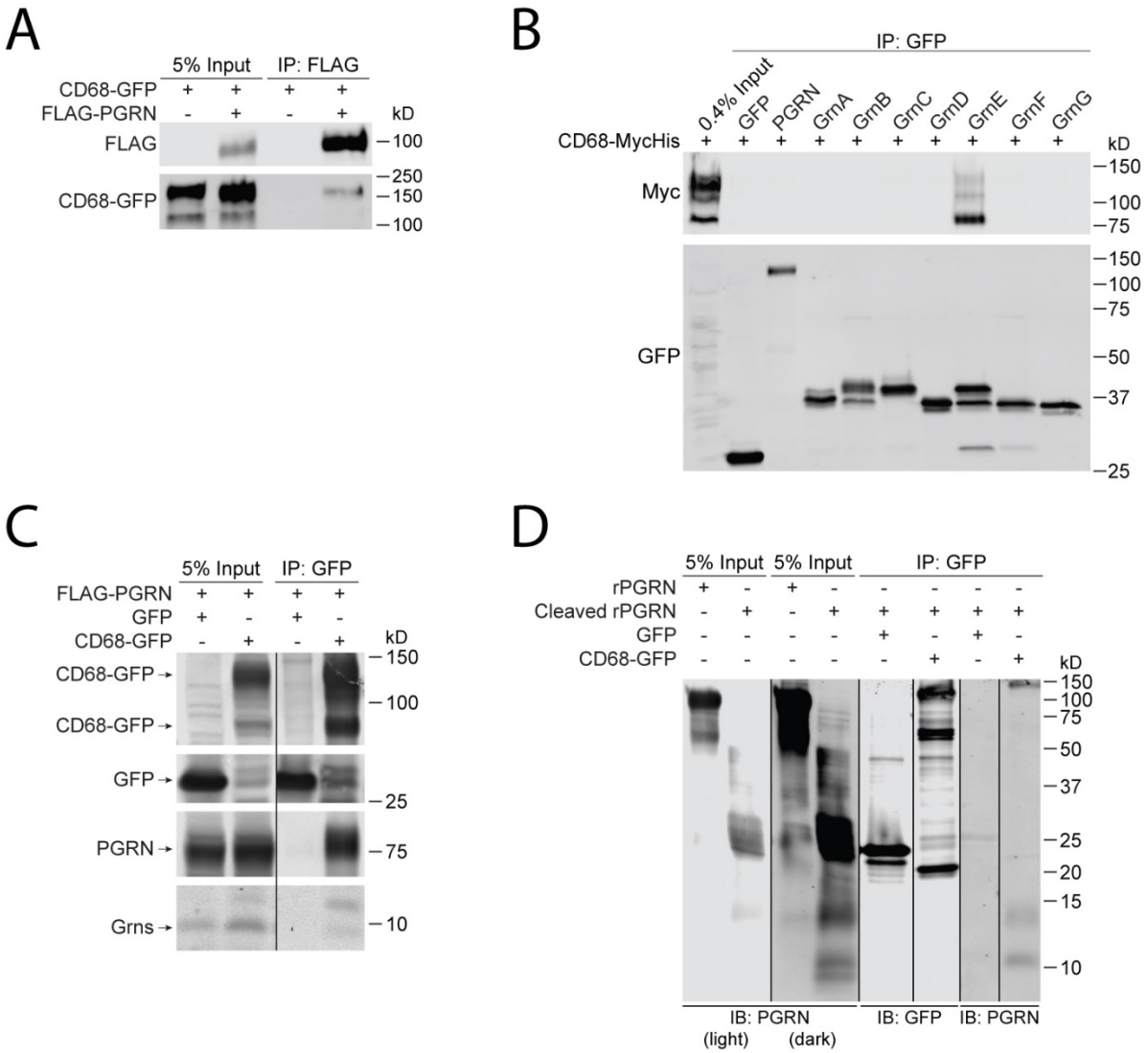
A
5% Input
IP: FLAG
CD68-GFP + + + +
FLAG-PGRN - + - +
kD
FLAG
CD68-GFP
100
250
150
100
B
IP: GFP
0.4% Input
GFP
PGRN
GrnA
GrnB
GrnC
GrnD
GrnE
GrnF
GrnG
CD68-MycHis + + + + + + + + + +
kD
Myc
GFP
150
100
75
150
100
75
50
37
25
C
5% Input
IP: GFP
FLAG-PGRN + + + +
GFP + - + -
CD68-GFP - + - +
kD
CD68-GFP
CD68-GFP
GFP
PGRN
Grns
150
100
25
75
10
D
5% Input
5% Input
IP: GFP
rPGRN + - + - - - - -
Cleaved rPGRN - + - + + + + +
GFP - - - - + - + -
CD68-GFP - - - - - + - +
kD
150
100
75
50
37
25
20
15
10
IB: PGRN
(light)
(dark)
IB: GFP
IB: PGRN

Figure 6.3. PGRN and CD68 binding studies. A) FLAG-PGRN and CD68-GFP were co-transfected and anti-FLAG IP was performed. **B)** GFP-PGRN or GFP-Grn peptides was co-transfected with CD68-MycHis and anti-GFP IP was performed. **C)** CD68-GFP binds full-length PGRN and Grn peptides. FLAG-PGRN and CD68-GFP were co-transfected and anti-GFP IP was performed, then samples were run on a Bis-Tris gel. **D)** CD68-GFP binds to Grn peptides liberated from recombinant PGRN by neutrophil elastase. CD68-GFP was overexpressed and the lysate was combined with recombinant PGRN cleaved by neutrophil elastase, then anti-GFP IP was performed and samples were run on a Bis-Tris gel.

(Fig. 6.3D). Two prominent low molecular weight bands were visible in the CD68-GFP sample. The slightly higher molecular weights indicate that these likely represent Grn dipeptides, tripeptides, or SDS-resistant oligomers.

Based on the Grn AP binding studies, it seemed likely that the interaction between PGRN and CD68 was mediated by the Grn E domain. To test this, FLAG-PGRN or FLAG-PGRN ΔE were co-transfected with CD68-GFP and anti-PGRN IP was performed **(Supplementary Fig. 6.1A)**. CD68 was only observed to bind to full-length PGRN, but not FLAG-PGRN lacking the Grn E domain, indicating that the binding is mediated by Grn E, as expected. Finally, because PGRN is a secreted protein and it is possible that PGRN destined for the extracellular space goes through additional quality control or post-translational processing compared to non-secreted PGRN, we wanted to verify that secreted PGRN can bind to CD68. FLAG-PGRN and CD68-GFP were transfected in separate wells of HEK293T cells. After two days, CD68-GFP cells were lysed and anti-GFP IP was performed. FLAG-PGRN conditioned media were collected and anti-GFP beads, still bound to CD68-GFP, were added to this media **(Supplementary Fig. 6.1B)**. We found that CD68 was able to bind the secreted PGRN.

Additionally, because CD68 is a LAMP family member and shares this domain with the prolific lysosomal membrane proteins, LAMP1, LAMP2, and LAMP3, we wanted to test whether PGRN or Grn E could bind to these. FLAG-PGRN was co-transfected with C-terminally GFP-tagged LAMP proteins and anti-FLAG IP was performed, but no binding was seen (data not shown). The binding of LAMP proteins to Grn E was also tested via the AP binding assay, but no interaction was observed (data not shown).

CD68 is unlikely to be a PGRN lysosomal trafficking receptor

The endocytic receptor, sortilin (SORT1), is a high affinity binding partner of PGRN that is largely responsible for its lysosomal trafficking [13, 32]. Additionally, a second trafficking pathway exists, wherein PGRN binds to the soluble lysosomal protein, PSAP. When PSAP binds to either of its own trafficking receptors, the cation-independent mannose-6-phosphate receptor (CI-M6PR) or the low-density lipoprotein receptor-related protein 1 (LRP1), it carries PGRN along with it to the lysosome [33]. Likewise, PGRN is able to transport PSAP to the lysosome via its own binding to sortilin [34]. Despite PGRN heavily relying on these two trafficking pathways, we have found that in *Psap*$^{-/-}$/*Sort1*$^{-/-}$ mice, PGRN is still delivered successfully to the lysosomes of microglia and hepatocytes, suggesting that at least one additional pathway for PGRN lysosomal trafficking exists **(Supplementary Fig. 6.2)**

Because CD68 is expressed in microglia, one of the two cell types in which PGRN was still observed to be lysosomal, and because of its function as an endocytic receptor, we hypothesized that it may be an unidentified lysosomal trafficking receptor for PGRN. To test this, a PGRN uptake assay was performed. FLAG-PGRN conditioned media were produced by overexpression in HEK293T cells, collected, and applied to HEK293T cells overexpressing CD68-GFP, which were then incubated for 2 hours at 37°C, before fixation and immunostaining. Despite high expression of CD68, no internalization of PGRN was observed, while a sortilin-overexpressing positive control showed high PGRN uptake **(Fig. 6.4a)**.

Additionally, because loss of sortilin, the major known trafficking receptor of PGRN, results in a 5-fold increase in the levels of serum PGRN in mice [13], we wanted

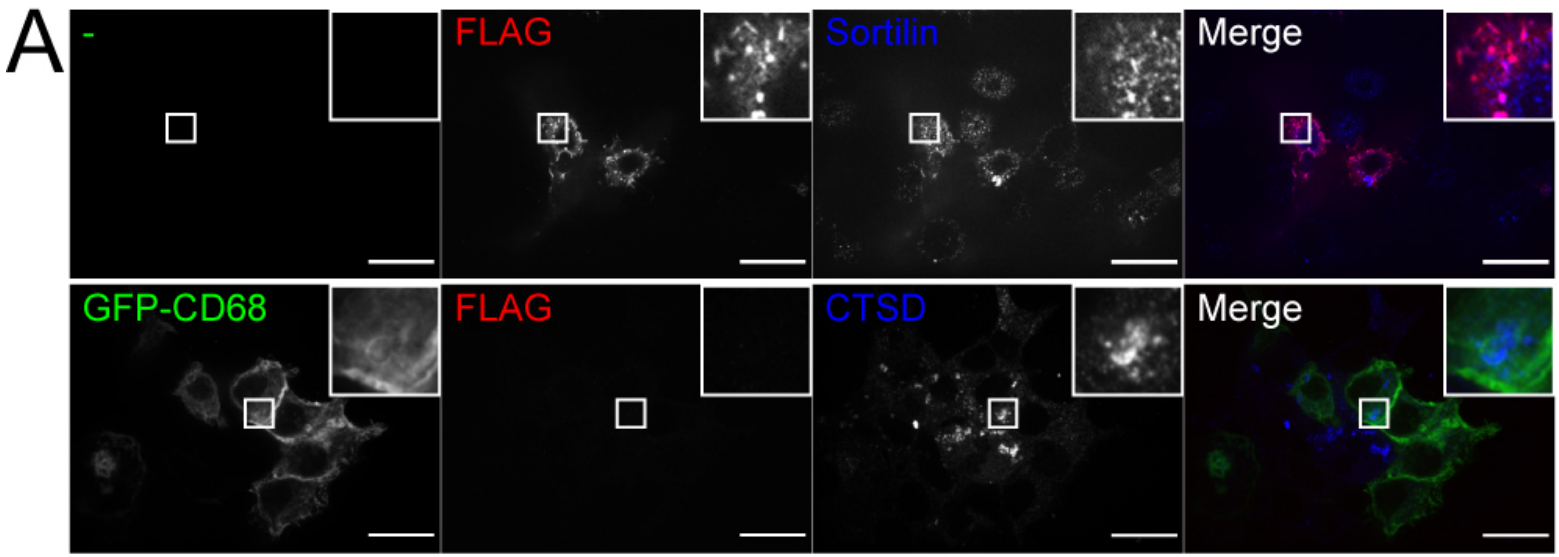
A
-
FLAG
Sortilin
Merge
GFP-CD68
FLAG
CTSD
Merge

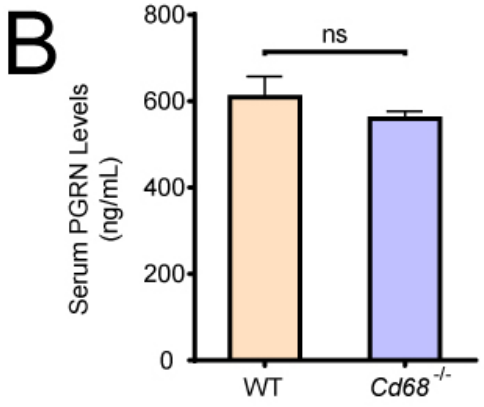
B
Serum PGRN Levels (ng/mL)
800
600
400
200
0
ns
WT
Cd68 -/-

Figure 6.4. CD68 is unlikely to be a PGRN lysosomal trafficking receptor. A) FLAG-PGRN from conditioned media is uptaken by sortilin-overexpressing HEK293T cells (top), as visualized by strong intracellular FLAG signal, but not by CD68-overexpressing cells (bottom). **B)** Serum PGRN levels were measured in sets of approximately 3-month-old littermate WT and *Cd68*$^{-/-}$ mice. Data are presented as ± SEM from four groups of mice, n = 7-8, ns, not significant, Student's t-test. Scale bar = 20 μm.

to test whether any such increase occurs when CD68 is lost. Serum was collected from WT and *Cd68*$^{-/-}$ mice and PGRN ELISA was performed. No significant change in serum PGRN levels was observed, consistent with the lack of PGRN uptake by CD68 seen in the previous assay **(Fig. 6.4b)**.

Additional PGRN, Grn E, and NRP2 binding studies

To test binding between PGRN and NRP2, untagged PGRN and NRP2-GFP were co-transfected and anti-PGRN IP was performed **(Fig. 6.5A)**. Both full-length NRP2-GFP and a lower-molecular weight band, possibly a degradation product, were found to co-IP with PGRN. In a reciprocal binding experiment wherein FLAG-PGRN and NRP2-GFP were co-transfected and anti-GFP IP was performed, FLAG-PGRN was also seen to weakly pull down **(Fig. 6.5**A**)**. As with CD68, we wanted to test whether secreted PGRN could bind to NRP2. FLAG-PGRN and NRP2-GFP were transfected in separate wells of HEK293T cells. After two days, NRP2-GFP cells were lysed and anti-GFP IP was performed. FLAG-PGRN conditioned media were collected and anti-GFP beads, still bound to NRP2-GFP, were added to this media **(Fig. 6.5C)**. NRP2 was able to bind the secreted PGRN with an affinity similar to that of PGRN from cell lysate. In tandem with the CD68-GFP tested previously, binding of NRP2-GFP to elastase-cleaved recombinant PGRN was examined **(Fig. 6.5D)**. NRP2-GFP was transfected in HEK293T cells, then recombinant PGRN was proteolytically cleaved with neutrophil elastase, an enzyme previously established to process PGRN to Grn peptides. The cleavage products were mixed with the NRP2-GFP-expressing cell lysate and anti-GFP IP was performed. The expression of NRP2-GFP was very low, but the same bands that were present in the CD68-GFP sample were also observed to co-immunoprecipitate

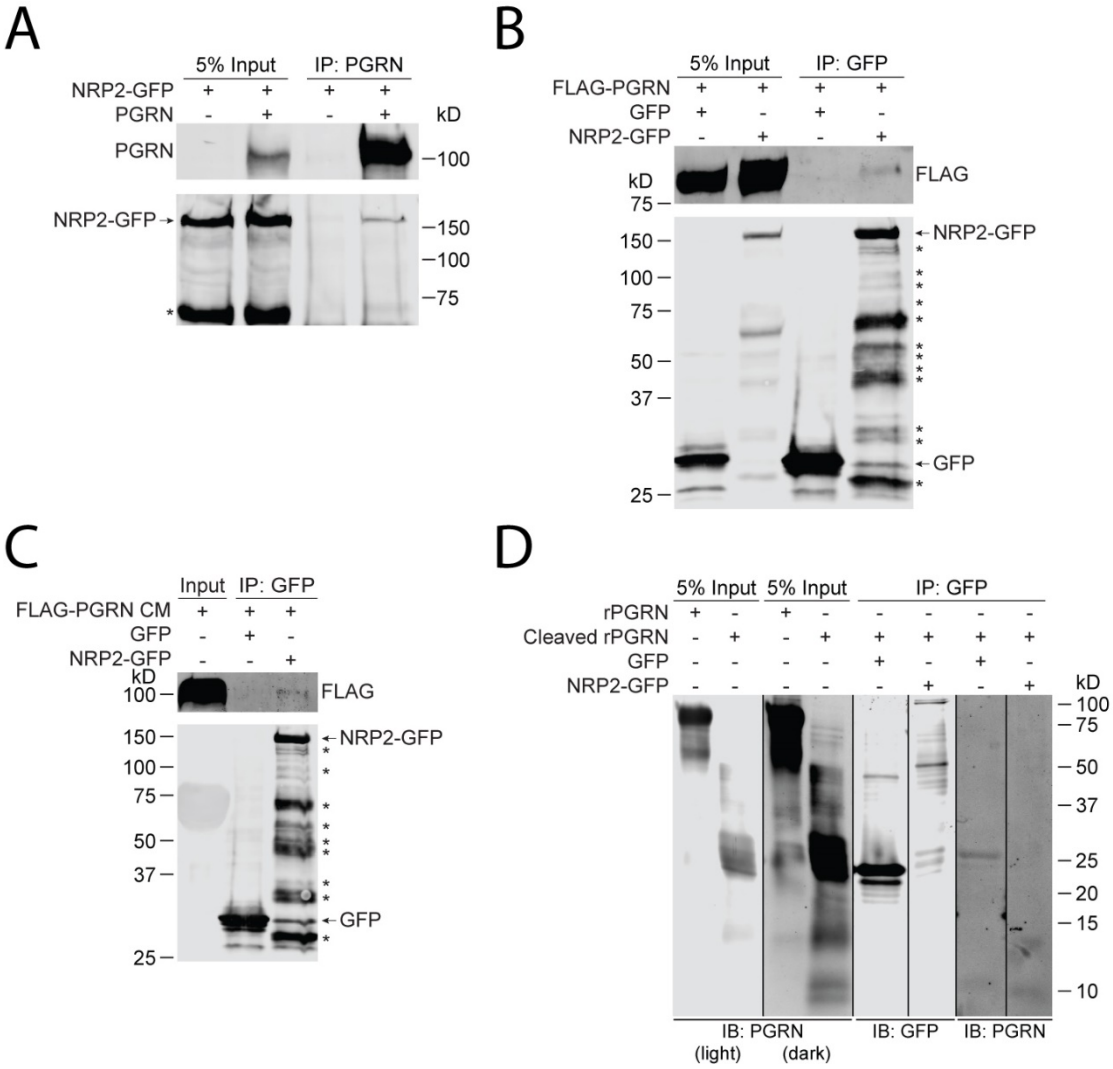
A
5% Input
IP: PGRN
NRP2-GFP + + + +
PGRN - + - +
kD
PGRN
100
NRP2-GFP
150
100
75
*
B
5% Input
IP: GFP
FLAG-PGRN + + + +
GFP + - + -
NRP2-GFP - + - +
kD
75
FLAG
150
100
75
50
37
25
NRP2-GFP
GFP
C
Input
IP: GFP
FLAG-PGRN CM + + +
GFP - + -
NRP2-GFP - - +
kD
100
FLAG
150
100
75
50
37
25
NRP2-GFP
GFP
D
5% Input
5% Input
IP: GFP
rPGRN + - + - - - - -
Cleaved rPGRN - + - + + + + +
GFP - - - - + - + -
NRP2-GFP - - - - - + - +
kD
100
75
50
37
25
20
15
10
IB: PGRN
(light)
(dark)
IB: GFP
IB: PGRN

Figure 6.5. PGRN and NRP2 binding studies. A) Untagged PGRN and NR2-GFP were co-transfected and anti-PGRN IP was performed. **B)** FLAG-PGRN and NRP2-GFP were co-transfected and anti-GFP IP was performed. **C)** NRP2-GFP is able to bind to secreted FLAG-PGRN. FLAG-tagged PGRN and NRP2-GFP were co-transfected in separate wells. Anti-GFP IP was performed from NRP2-GFP cell lysate, then these beads were transferred to FLAG-PGRN conditioned media **D)** NRP2-GFP binds to Grn peptides liberated from recombinant PGRN by neutrophil elastase. NRP2-GFP was overexpressed and the lysate was combined with recombinant PGRN cleaved by neutrophil elastase, then anti-GFP IP was performed and the samples were run on a Bis-Tris gel. *, potential non-specific bands or degradation products of NRP2.

with NRP2, albeit with comparatively lower intensity.

NRP2 is unlikely to be a PGRN neurotrophic receptor

Because we were primarily interested in identifying a neurotrophic receptor of PGRN and NRP2 is known to possess, among other functions, modulation of axon guidance, we wanted to test whether NRP2 could mediate the neurotrophic effects of PGRN. To test this, we used a clustered regularly interspaced short palindromic repeats (CRISPR)-based system with CRISPR-associated protein 9 (Cas9) to produce control and *Nrp2*$^{-/-}$ N2a cell lines **(Fig. 6.6a)**. Cells were then cultured for 5 days in serum-free conditions, with the addition of PBS or 1 μM or 3 μM of recombinant GST, GST-Grn E, or GST-C100 (last 100 amino acids of PGRN). AlamarBlue was then used to assess the viability of the cells **(Fig. 6.6b)**. Recombinant GST had no effect on survivability, but Grn E and C100 showed a dose-dependent increase in viability, with the highest concentration of C100 increasing alamarBlue signal by up to ~300% of the PBS control. Although *Nrp2*$^{-/-}$ cells generally showed slightly decreased survival compared to control cells, the difference was not significant, indicating that this neurotrophic effect is not likely to be mediated by NRP2.

6.4 Discussion

In this study, we describe the completion of a high-throughput AP-based cell surface screen for PGRN receptors. However, there are several limitations to this study. Based on the low percentage of expressing proteins, it is possible that binding between PGRN/Grn peptides and one or more receptors was missed. This low expression could be due to numerous factors, including protein size or the possibility of the GFP tag or

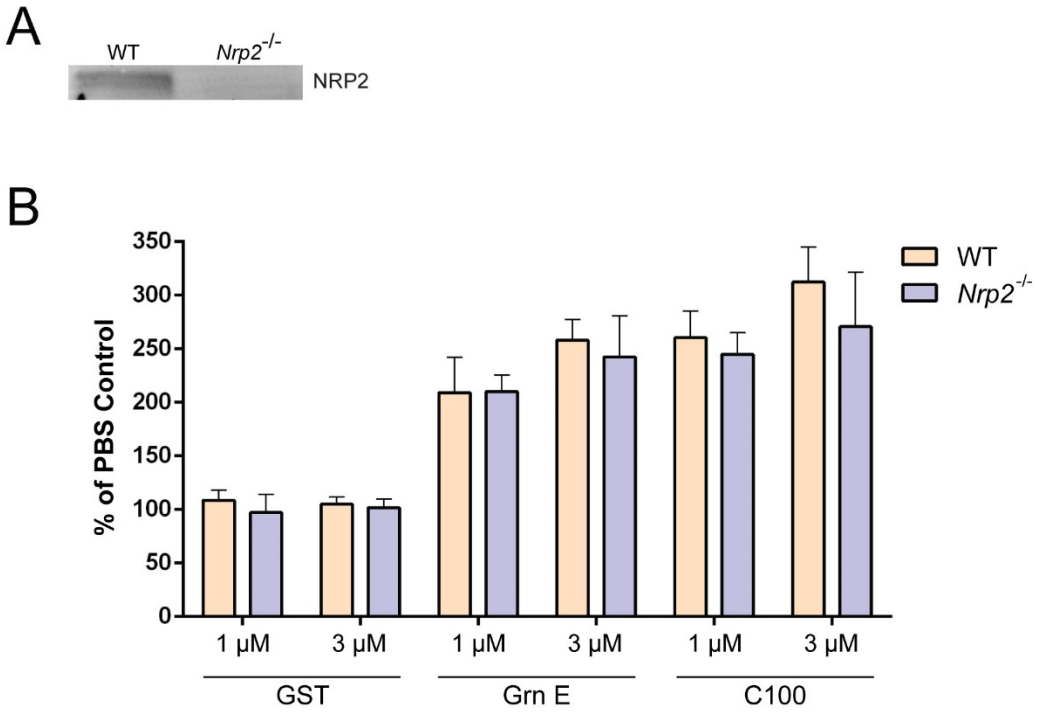

Figure 6.6. Loss of NRP2 does not suppress Grn E neurotrophic function. A) Anti-NRP2 western blot of control and *Nrp2*$^{-/-}$ N2a cell lines. **B)** A survival assay was performed with control or *Nrp2*$^{-/-}$ N2a cells in serum-free conditions for 5 days with the addition of PBS or either 1 µM or 3 µM of recombinant GST, Grn E, or C100. Viability was assessed with alamarBlue reagent. Data are presented as ± SEM from triplicate wells.

recombination sites in the gateway vector interfering with expression or localization. We were also unable to produce AP-tagged Grn C or Grn F, so binding to these two peptides could not be tested. Additional study limitations include the possibility of the AP tag or GFP tag interfering ligand-receptor interactions and only having 51% coverage of predicted transmembrane proteins at study outset.

Despite these limitations, we have identified two putative PGRN and Grn E receptors: CD68 and NRP2. CD68 is a member of the LAMP family of heavily glycosylated endolysosomal proteins of high abundance and unclear function [16]. Although our initial goal was to identify a neurotrophic PGRN receptor, CD68 is unlikely to be a candidate for this role based on its expression being limited to immune cells and its lack of signaling capacity. The significance of this interaction is unclear and complicated by the generally poor characterization of CD68. As such, many potential functions of the relationship exist, but there is little evidence to narrow the focus at the moment. For example, both PGRN [35-40] and CD68 [41-44] expression have been associated with several cancers. It is possible that the interaction between PGRN and CD68 is regulatory in tumor growth and metastasis. Additionally, one study found that increased synaptic pruning by microglia is a mechanism of neuronal death in PGRN-deficient mice [20]. As microglial upregulation of CD68 expression has been reported by multiple groups [20-23], and CD68 recognizes phosphatidylserine [45], a lipid that is involved in recognition of apoptotic cells by phagocytes [46], it is possible that CD68 is also involved in either enhanced synaptic pruning or phagocytosis of unhealthy neurons when PGRN is lost, contributing to neuronal cell death in FTLD and NCL. PGRN has also been found to act as a co-chaperone of the lysosomal hydrolase,

glucocerebrosidase [47]. It is possible that PGRN also acts as a chaperone for CD68, which is very highly glycosylated and has been shown to display altered glycosylation patterns in response to phagocytosis [48]. Using co-IP, we *did* observe stronger binding between GFP-Grn E and a lower molecular weight CD68 band, which likely represents a less glycosylated form of the protein. While we did not observe any uptake of FLAG-PGRN from conditioned media by CD68-GFP-overexpressing cells, it should be noted that there was significant mislocalization of CD68. Although it did show distribution to both lysosomes and the plasma membrane, much of it displayed a pattern suggestive of retention in the endoplasmic reticulum. It is possible that the improperly localized CD68 interfered with the uptake of PGRN. Considering this, it is worth repeating and optimizing the uptake assay to verify our results.

Because PGRN and Grn E bind to the lumenal region of CD68, but not the conserved LAMP domain, it is likely that they associate with the mucin-like domain, a region of high glycosylation. Similar mucin-like domains are found in a number of other lysosomal proteins. It is possible that PGRN and Grn E may interact with one or more of these proteins, which may have better identified functions than CD68, making it easier to identify the significance of the binding.

Compared to CD68, NRP2 is a relatively well-characterized protein. It has a well-defined set of established ligands, including VEGF and semaphorin family members, and has known roles in axon guidance and lymphangiogenesis. Although NRP2 did not appear to mediate the neuron survival-enhancing function of Grn E, we did not specifically test whether it plays a role in Grn E-stimulated neurite outgrowth. It is entirely possible that these two effects are mediated by different receptors. The

Nrp2 CRISPR knockout also may not have been 100% efficient. Any cells still expressing *Nrp2* would skew the results of our survival assay. NRP2 also plays roles in endothelial cell survival and migration [49], tumorigenesis [27, 49], and inflammation [50], which overlap with PGRN function. As previously mentioned, binding to neuropilin receptors is often mediated by a C-terminal arginine on the ligand. We found this to be true for Grn E as well. Although loss of a terminal arginine did not entirely abolish binding, it greatly reduced it. This is a potentially confounding issue, because PGRN is known to be proteolytically processed by multiple enzymes, including neutrophil elastase and matrix metalloproteinases. As different enzymes may have different recognition and cleavage sites and sequences, the physiological relevance of a Grn E construct that specifically terminates with one or two arginine residues is questionable. However, a recent study used liquid chromatography-mass spectrometry (LC-MS) to identify the specific cleavage sites of the newly identified PGRN protease, cathepsin L, and the classical PGRN protease, neutrophil elastase (NE) [51]. They found that not only does one of the Grn E products of NE cleavage terminate in a single arginine, but the only two products of CTSL cleavage both end in arginine, one of which is a di-arginine.

Co-IP studies repeatably showed binding between full-length PGRN and both CD68 and NRP2, although binding was not observed in the AP-based assay. Several possibilities exist as to why this the case, including low expression of CD68 and NRP2 constructs. However, more recent AP-based binding studies between PGRN and CD68 have demonstrated weak binding using this assay, supporting our initial co-IP results.

As these were primarily preliminary studies of binding, it is too early to know what the functions of the interactions between PGRN/Grn E and CD68 and NRP2 may be, but many possibilities exist. Future studies will help expand upon our current findings and resolve the significance of these relationships.

6.5 Materials and Methods

Primary Antibodies and Reagents

The following antibodies were used in this study: M2 mouse anti-FLAG (Sigma), M2 mouse anti-FLAG-conjugated beads (Sigma), 9E10 mouse anti-myc (homemade), rat anti-mouse LAMP1 (BD Biosciences), rabbit anti-GFP (homemade), GFP-Trap beads (ChromoTek), goat anti-human PGRN (R&D Systems), and sheep anti-mouse PGRN (R&D Systems), rabbit anti-sortilin (Thermo Fisher Scientific). Rabbit anti-cathepsin D was a gift from Dr. William Brown (Cornell University). Rabbit anti-PGRN antibodies were produced as previously described [33].

Plasmids

CD68 was cloned into the pEGFP-N2 and p pcDNA3.1/myc-His A vectors. NRP2 was cloned into the pEGFP-N2 vector. Human PGRN in the pCMV-Sport6 vector was obtained as previously described [13]. GFP-PGRN was produced as previously described [33]. GFP-Grn peptides were produced as described [52].

Protein Production and Purification

GST, GST-Grn E, and GST-C100 proteins were produced from Origami B(DE3) bacterial strains (MilliporeSigma) with 0.1 mM IPTG induction overnight at 18°C. Proteins were purified with glutathione cross-linked beads and eluted with excess

glutathione. His-PGRN was purified with cobalt beads from the culture media of HEK293T cells as previously described [33]. All purified proteins were concentrated and transitioned to PBS buffer with Centricon Centrifugal Filter Units (MilliporeSigma).

Transmembrane Library cDNA Cloning

E. coli transformed with transmembrane protein cDNA in gateway donor plasmids (pDONR223) were cultured in 96-well deep-well plates with 1 mL of Terrific Broth (TB) with 50 μg/mL spectinomycin at 37°C, shaking for 18 hours. 96-well plasmid minipreps were performed, concentrations were measured with an Infinite M1000 plate reader (Tecan), and each well was normalized to 100 ng/μL. High-throughput Gateway LR reactions in 96-well-plate format were performed to transfer cDNA from the pDONR223 vector to the pcDNA-DEST47 expression vector. For each LR reaction, 1 μL of the destination vector (100 ng/ μL), 1 μL of donor clone (100 ng/ μL), 2 μL of 5x LR buffer, 2 μL of LR enzyme mixture, and 4 μl of ddH_2O (final volume 10 μL). The expression vector contains a C-terminal GFP fusion tag for easy visualization of expression and localization. 96-well transformations into Top 10 bacteria were performed, then 20 μL of cells were transferred to 1 mL of TB with 100 μg/mL ampicillin and incubating at 37°C, shaking overnight. The next day, glycerol stocks were made and then plasmid minipreps and concentration measurements were performed, as above.

AP Fusion Protein Production

AP-fused proteins were produced by cloning of full-length PGRN, Grn A (PGRN aa 281-337), Grn B (PGRN aa 206-261), Grn D (PGRN aa 441-498), Grn E (PGRN aa

519-576), or Grn G (PGRN 60-115) cDNA into the pAPtag-5 vector (GenHunter). Plasmids were transfected into HEK293T cells and conditioned media collected after 5 days and AP activity was assessed with substrate, p-Nitrophenyl phosphate (Sigma).

Mouse Strains

C57/BL6 and *Cd68*$^{-/-}$ mice were obtained from The Jackson Laboratory [18].

Cell Culture

HEK293T, COS-7, and N2a cells were maintained in Dulbecco's Modified Eagle's Medium (Cellgro) supplemented with 10% fetal bovine serum (Gibco) in a humidified incubator at 37ºC with 5% CO_2.

Transfection, Immunoprecipitation, and Western Blot Analysis

Cells were transfected with polyethylenimine as previously described [53]. Cells were lysed in a cold solution containing 150 mM NaCl, 50 mM Tris (pH 8.0), 1% Triton X-100, 0.1% deoxycholic acid, 1X protease inhibitors (Roche). After centrifugation at 14,000 g, for 15 minutes, at 4ºC, supernatants were transferred to clean tubes on ice, to which mouse anti-FLAG antibody-conjugated beads, GFP-Trap beads (ChromoTek), or rabbit anti-PGRN antibody-conjugated Affi-Gel 15 (Bio-Rad Laboratories) was added, then rocked for 3-4 hours at 4ºC. Samples were centrifuged at 2,500 g for 20 seconds at 4ºC, then washed with 1 mL of a solution containing 150 mM NaCl, 50 mM Tris (pH 8.0), and 1% Triton X-100. This was repeated for a total of 3 washes. After a final centrifugation, all supernatant was aspirated and samples were eluted by the addition of 25 µL of Laemmli Sample Buffer with 5% β-Mercaptoethanol.

Samples were run on a 12% polyacrylamide gel or 4-12% Bis-Tris gel (Bio-Rad Laboratories), then transferred to Immobilon-FL polyvinylidene fluoride membranes

(Millipore Corporation) or nitrocellulose membranes (Millipore Corporation). Membranes were blocked with either 5% non-fat milk in PBS or Odyssey Blocking Buffer (LI-COR Biosciences) for 1 hour, then washed with tris-buffered saline with 0.1% Tween-20 (TBST) 3x for 5m, each. Membranes were incubated with primary antibodies diluted in TBST, rocking overnight at 4ºC, then washed as above, incubated with secondary antibodies diluted in TBST for 2 h at room temperature, then washed again. Membranes were scanned using an Odyssey Infrared Imaging System (LI-COR Biosciences).

Immunostaining and Confocal Microscopy

Cells were cultured on glass coverslips overnight. For transfection experiments, cells were transfected the next morning and proteins were allowed to express for ~2 days before experiments were performed. Cells were washed 2x with PBS, fixed with 3.7% paraformaldehyde for 15 minutes at room temperature, followed by 3 additional PBS washes. Cells were permeabilized with Odyssey Blocking Buffer LI-COR Biosciences) + 0.05% saponin for 30 minutes at room temperature. Primary antibodies were diluted in the same buffer and added to coverslips, which were incubated in a humidified chamber overnight at 4ºC. Coverslips were washed 3x with PBS, for 5 minutes each, then secondary antibodies diluted in the same blocking/permeabilization solution were added to the coverslips, which were incubated at room temperature, in the dark, for 2 hours. After 3 additional PBS washes, coverslips were mounted on slides with Fluoromount-G (SouthernBiotech). Images were acquired with a CSU-X series spinning disc confocal microscope (Intelligent Imaging Innovations) with an HQ2 CCD camera (Photometrics) using a 100x objective.

Alkaline Phosphatase-Based Cell Surface Binding Screen

COS-7 cells were grown overnight in 96-well tissue culture plates (Corning) in triplicate. Each well was transfected with 50-100ng of plasmid DNA for an individual transmembrane protein, sortilin as a positive control for PGRN binding, or pEGFP-C1 vector as a negative control. After two days, the wells were washed 2x with HBH (Hank's Balanced Salt Solution with calcium and magnesium with 20 mM HEPES, pH 6.4, and 0.1% BSA). Binding was tested with AP-PGRN, AP-PGRN + AP-PSAP, or a mixture of AP-Grn peptides in separate plates in parallel. AP fusion protein conditioned media were diluted to working concentrations in HBH, 100 µL was added to each well, and the plate was incubated for 3 hours at room temperature. Following the incubation, wells were washed twice with cold HBH to remove traces of unbound AP-fused ligand, then the cells were fixed with 3.7% formaldehyde at room temperature for 20 minutes. Wells were washed 1x with HBH, then GFP expression was assessed by fluorescence microscopy using the ImageExpress system (Molecular Devices). Wells were then filled with HBH and the plate was sealed tightly with adhesive film (VWR). After an overnight incubation at 65°C to inactivate endogenous alkaline phosphatases, wells were washed 1x with AP buffer (100 mM Tris HCl, pH 9.5, 100 mM NaCl, and 5 mM $MgCl_2$). 100 µL of developing solution composed of AP buffer with 350 µg/mL nitro-blue tetrazolium chloride (NBT) and 175 µg/mL 5-bromo-4-chloro-3'-indolyphosphate p-toluidine salt (BCIP) was added to each well, then the plates were incubated at room temperature for a minimum of 30 minutes or until signal developed. Positive interactions, as indicated by the presence of an insoluble, black-purple precipitate, were visually confirmed by eye using brightfield microscopy.

PGRN Uptake Assay

HEK293T cells were transfected with FLAG-PGRN. Separately, HEK293T cells on glass coverslips were transfected with CD68-GFP or sortilin-MycHis. Two days after transfection, FLAG-PGRN conditioned media were collected, diluted 1:1 with HBH, and 1 mL was added to CD68-GFP or sortilin-MycHis coverslips. Cells were incubated for 2 hours at 37°C, then washed twice with PBS, fixed, and immunostained as described above.

ELISA

Serum samples were collected from four groups of ~3-month-old, littermate WT from *Cd68*$^{-/-}$ mice and analyzed using a mouse PGRN ELISA kit (R&D Systems) according to the manufacturer's instructions.

CRISPR-mediated genome editing

To generate CRISPR constructs, two oligonucleotides with the sequences listed at the end of this section were annealed and ligated to pLenti-CRISPRv2 (Addgene) digested with BsmB1. Lentivirus-containing conditioned media were generated by transfecting lentiviral vectors together with pMD2.G and psPAX2 plasmids in HEK293T cells. Media were collected 3-5 days after transfection.

For CRISPR/Cas9-mediated genome editing, N2a cells were infected with lentiviruses containing pLenti-CRISPRv2 harboring guide RNA sequences targeted to mouse NRP2. Cells were selected with 1 μg/ml puromycin and assayed 1 week after selection. The efficiency of gene knockout was confirmed by western blot analysis.

1) 5′- CACCGTGGTGGGAGGGATAGTCCTG -3'
2) 5- AAACCAGGACTATCCCTCCCACCAC -3'

Cell Survival Assay

WT and *Nrp2*$^{-/-}$ N2a cells were passaged into a 96-well tissue culture plate (Corning) at ~20% confluency. The next day, cells were washed once with warm DMEM to remove serum, then 100 μL of DMEM containing either 1 or 3 μM of recombinant GST, GST-Grn E, GST-C100, or an equal volume of PBS (control) was added to each well in triplicate. Cells were incubated in serum-free conditions for 5 days. AlamarBlue (Thermo Fisher Scientific) was diluted 1:10 to working concentration in warm DMEM, and 100 μL was added to each well after aspiration of old media. The plate was incubated for 4 hours at 37°C and then read at 570 nm excitation/585 nm emission with an Infinite M100 microplate reader (Tecan).

6.6 Acknowledgements

We would like to thank Dr. Haiyuan Yu for his extremely kind gift of transmembrane protein cDNAs and Xiaochun Wu for technical assistance. This work is supported by funding to F. Hu from the Weill Institute for Cell and Molecular Biology, the Alzheimer's Association, the Association of Frontotemporal Dementia, the Muscular Dystrophy Association, and NINDS (R21 NS081357-01 and R01NS095954).

The authors declare no additional competing financial interests.

List of Abbreviations

AP – Alkaline phosphatase
Cas9 – CRISPR-associated protein 9
CD68 – Cluster of differentiation 68
CI-M6PR – Cation-independent mannose-6-phosphate receptor
Co-IP – Co-immunoprecipitation
CRISPR – clustered regularly interspaces short palindromic repeats
FTLD – Frontotemporal lobar degeneration
Grn - Granulin
LAMP – Lysosome-associated membrane protein
LC-MS – Liquid chromatography-mass spectrometer
LDL – Low-density lipoprotein
LRP1 – Low-density lipoprotein receptor-related protein 1
NE – Neutrophil elastase
NRP2 – Neuropilin 2
PGRN – Progranulin
PSAP – Prosaposin
SORT1 – sortilin
TBST – Tris-buffered saline with 0.1% Tween-20
TGF-β – Transforming growth factor-β
VEGF – Vascular endothelial growth factor

REFERENCES

1. Van Damme, P., et al., Progranulin functions as a neurotrophic factor to regulate neurite outgrowth and enhance neuronal survival. J Cell Biol, 2008. **181**(1): p. 37-41.

2. Ryan, C.L., et al., Progranulin is expressed within motor neurons and promotes neuronal cell survival. BMC Neurosci, 2009. **10**: p. 130.

3. Chitramuthu, B.P., et al., Progranulin modulates zebrafish motoneuron development in vivo and rescues truncation defects associated with knockdown of Survival motor neuron 1. Mol Neurodegener, 2010. **5**: p. 41.

4. Gao, X., et al., Progranulin promotes neurite outgrowth and neuronal differentiation by regulating GSK-3beta. Protein Cell, 2010. **1**(6): p. 552-62.

5. Wang, J., et al., Pathogenic cysteine mutations affect progranulin function and production of mature granulins. J Neurochem, 2010. **112**(5): p. 1305-15.

6. Laird, A.S., et al., Progranulin is neurotrophic in vivo and protects against a mutant TDP-43 induced axonopathy. PLoS ONE, 2010. **5**(10): p. e13368.

7. Gass, J., et al., Progranulin regulates neuronal outgrowth independent of sortilin. Mol Neurodegener, 2012. **7**: p. 33.

8. De Muynck, L., et al., The neurotrophic properties of progranulin depend on the granulin E domain but do not require sortilin binding. Neurobiol Aging, 2013. **34**(11): p. 2541-7.

9. Daniel, R., et al., Cellular localization of gene expression for progranulin. J Histochem Cytochem, 2000. **48**(7): p. 999-1009.

10. Flanagan, J.G. and H.J. Cheng, Alkaline phosphatase fusion proteins for molecular characterization and cloning of receptors and their ligands. Methods Enzymol, 2000. **327**: p. 198-210.

11. Flanagan, J.G., et al., Alkaline phosphatase fusions of ligands or receptors as in situ probes for staining of cells, tissues, and embryos. Methods Enzymol, 2000. **327**: p. 19-35.

12. Fournier, A.E., T. GrandPre, and S.M. Strittmatter, Identification of a receptor mediating Nogo-66 inhibition of axonal regeneration. Nature, 2001. **409**(6818): p. 341-6.

13. Hu, F., et al., Sortilin-mediated endocytosis determines levels of the frontotemporal dementia protein, progranulin. Neuron, 2010. **68**(4): p. 654-67.

14. Fagerberg, L., et al., Prediction of the human membrane proteome. Proteomics, 2010. **10**(6): p. 1141-9.

15. Rual, J.F., D.E. Hill, and M. Vidal, ORFeome projects: gateway between genomics and omics. Curr Opin Chem Biol, 2004. **8**(1): p. 20-5.

16. Kurushima, H., et al., Surface expression and rapid internalization of macrosialin (mouse CD68) on elicited mouse peritoneal macrophages. J Leukoc Biol, 2000. **67**(1): p. 104-8.

17. Ramprasad, M.P., et al., Cell surface expression of mouse macrosialin and human CD68 and their role as macrophage receptors for oxidized low density lipoprotein. Proc Natl Acad Sci U S A, 1996. **93**(25): p. 14833-8.

18. Song, L., C. Lee, and C. Schindler, Deletion of the murine scavenger receptor CD68. J Lipid Res, 2011. **52**(8): p. 1542-50.

19. Holness, C.L. and D.L. Simmons, Molecular cloning of CD68, a human macrophage marker related to lysosomal glycoproteins. Blood, 1993. **81**(6): p. 1607-13.

20. Lui, H., et al., Progranulin Deficiency Promotes Circuit-Specific Synaptic Pruning by Microglia via Complement Activation. Cell, 2016.

21. Tanaka, Y., et al., Possible involvement of lysosomal dysfunction in pathological changes of the brain in aged progranulin-deficient mice. Acta Neuropathol Commun, 2014. **2**: p. 78.

22. Takahashi, H., et al., Opposing effects of progranulin deficiency on amyloid and tau pathologies via microglial TYROBP network. Acta Neuropathol, 2017. **133**(5): p. 785-807.

23. Klein, Z.A., et al., Loss of TMEM106B Ameliorates Lysosomal and Frontotemporal Dementia-Related Phenotypes in Progranulin-Deficient Mice. Neuron, 2017. **95**(2): p. 281-296 e6.

24. He, Z. and M. Tessier-Lavigne, Neuropilin is a receptor for the axonal chemorepellent Semaphorin III. Cell, 1997. **90**(4): p. 739-51.

25. Kolodkin, A.L., et al., Neuropilin is a semaphorin III receptor. Cell, 1997. **90**(4): p. 753-62.

26. Wittmann, P., et al., Neuropilin-2 induced by transforming growth factor-beta augments migration of hepatocellular carcinoma cells. BMC Cancer, 2015. **15**: p. 909.

27. Coma, S., A. Shimizu, and M. Klagsbrun, Hypoxia induces tumor and endothelial cell migration in a semaphorin 3F- and VEGF-dependent manner via transcriptional repression of their common receptor neuropilin 2. Cell Adh Migr, 2011. **5**(3): p. 266-75.

28. Parker, M.W., et al., Structural basis for VEGF-C binding to neuropilin-2 and sequestration by a soluble splice form. Structure, 2015. **23**(4): p. 677-87.

29. Parker, M.W., A.D. Linkugel, and C.W. Vander Kooi, Effect of C-terminal sequence on competitive semaphorin binding to neuropilin-1. J Mol Biol, 2013. **425**(22): p. 4405-14.

30. Guo, H.F. and C.W. Vander Kooi, Neuropilin Functions as an Essential Cell Surface Receptor. J Biol Chem, 2015. **290**(49): p. 29120-6.

31. Zhu, J., et al., Conversion of proepithelin to epithelins: roles of SLPI and elastase in host defense and wound repair. Cell, 2002. **111**(6): p. 867-78.

32. Zheng, Y., et al., C-terminus of progranulin interacts with the beta-propeller region of sortilin to regulate progranulin trafficking. PLoS ONE, 2011. **6**(6): p. e21023.

33. Zhou, X., et al., Prosaposin facilitates sortilin-independent lysosomal trafficking of progranulin. J Cell Biol, 2015. **210**(6): p. 991-1002.

34. Zhou, X., et al., Impaired prosaposin lysosomal trafficking in frontotemporal lobar degeneration due to progranulin mutations. Nat Commun, 2017. **8**: p. 15277.

35. Abrhale, T., et al., GP88 (PC-Cell Derived Growth Factor, progranulin) stimulates proliferation and confers letrozole resistance to aromatase overexpressing breast cancer cells. BMC Cancer, 2011. **11**: p. 231.

36. Edelman, M.J., et al., GP88 (progranulin): a novel tissue and circulating biomarker for non-small cell lung carcinoma. Hum Pathol, 2014. **45**(9): p. 1893-9.

37. Kim, W.E. and G. Serrero, PC cell-derived growth factor stimulates proliferation and confers Trastuzumab resistance to Her-2-overexpressing breast cancer cells. Clin Cancer Res, 2006. **12**(14 Pt 1): p. 4192-9.

38. Tangkeangsirisin, W. and G. Serrero, PC cell-derived growth factor (PCDGF/GP88, progranulin) stimulates migration, invasiveness and VEGF expression in breast cancer cells. Carcinogenesis, 2004. **25**(9): p. 1587-92.

39. Wang, W., J. Hayashi, and G. Serrero, PC cell-derived growth factor confers resistance to dexamethasone and promotes tumorigenesis in human multiple myeloma. Clin Cancer Res, 2006. **12**(1): p. 49-56.

40. Yamamoto, Y., et al., Association between increased serum GP88 (progranulin) concentrations and prognosis in patients with malignant lymphomas. Clin Chim Acta, 2017. **473**: p. 139-146.

41. Leek, R.D., et al., Association of macrophage infiltration with angiogenesis and prognosis in invasive breast carcinoma. Cancer Res, 1996. **56**(20): p. 4625-9.

42. Mahmoud, S.M., et al., Tumour-infiltrating macrophages and clinical outcome in breast cancer. J Clin Pathol, 2012. **65**(2): p. 159-63.

43. Jezequel, P., et al., Validation of tumor-associated macrophage ferritin light chain as a prognostic biomarker in node-negative breast cancer tumors: A multicentric 2004 national PHRC study. Int J Cancer, 2012. **131**(2): p. 426-37.

44. Nabeshima, A., et al., Tumour-associated macrophages correlate with poor prognosis in myxoid liposarcoma and promote cell motility and invasion via the HB-EGF-EGFR-PI3K/Akt pathways. Br J Cancer, 2015. **112**(3): p. 547-55.

45. Ramprasad, M.P., et al., The 94- to 97-kDa mouse macrophage membrane protein that recognizes oxidized low density lipoprotein and phosphatidylserine-rich liposomes is identical to macrosialin, the mouse homologue of human CD68. Proc Natl Acad Sci U S A, 1995. **92**(21): p. 9580-4.

46. Fadok, V.A., et al., The role of phosphatidylserine in recognition of apoptotic cells by phagocytes. Cell Death Differ, 1998. **5**(7): p. 551-62.

47. Jian, J., et al., Progranulin Recruits HSP70 to beta-Glucocerebrosidase and Is Therapeutic Against Gaucher Disease. EBioMedicine, 2016. **13**: p. 212-224.

48. da Silva, R.P. and S. Gordon, Phagocytosis stimulates alternative glycosylation of macrosialin (mouse CD68), a macrophage-specific endosomal protein. Biochem J, 1999. **338 (Pt 3)**: p. 687-94.

49. Favier, B., et al., Neuropilin-2 interacts with VEGFR-2 and VEGFR-3 and promotes human endothelial cell survival and migration. Blood, 2006. **108**(4): p. 1243-50.

50. Schellenburg, S., et al., Role of neuropilin-2 in the immune system. Mol Immunol, 2017. **90**: p. 239-244.

51. Lee, C.W., et al., The lysosomal protein cathepsin L is a progranulin protease. Mol Neurodegener, 2017. **12**(1): p. 55.

52. Zhou, X., et al., Regulation of cathepsin D activity by the FTLD protein progranulin. Acta Neuropathol, 2017. **134**(1): p. 151-153.

53. Vancha, A.R., et al., Use of polyethyleneimine polymer in cell culture as attachment factor and lipofection enhancer. BMC Biotechnol, 2004. **4**: p. 23.

6.7 Supplementary Data

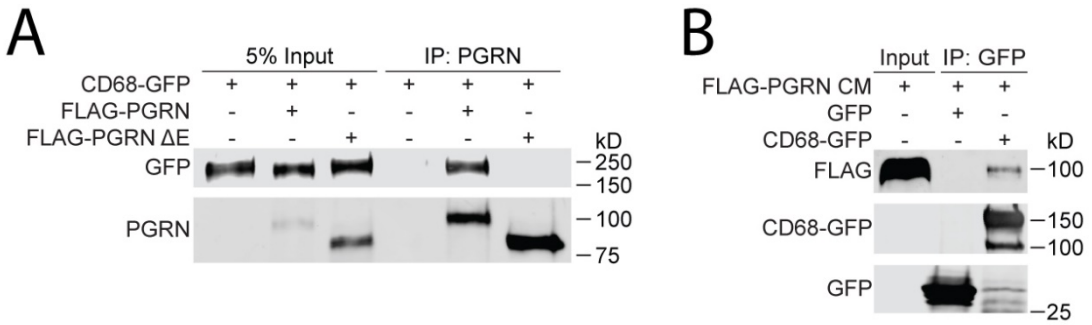

Supplementary Figure 6.1. Additional PGRN and CD68 co-IPs. A) Binding between PGRN and CD68 is dependent upon the Grn E domain. FLAG-tagged PGRN or PGRN ΔE was co-transfected with CD68-GFP and anti-PGRN IP was performed. **B)** CD68-GFP is able to bind to secreted FLAG-PGRN. FLAG-tagged PGRN and CD68-GFP were co-transfected in separate wells. Anti-GFP IP was performed from CD68-GFP cell lysate, then these beads were transferred to FLAG-PGRN conditioned media.

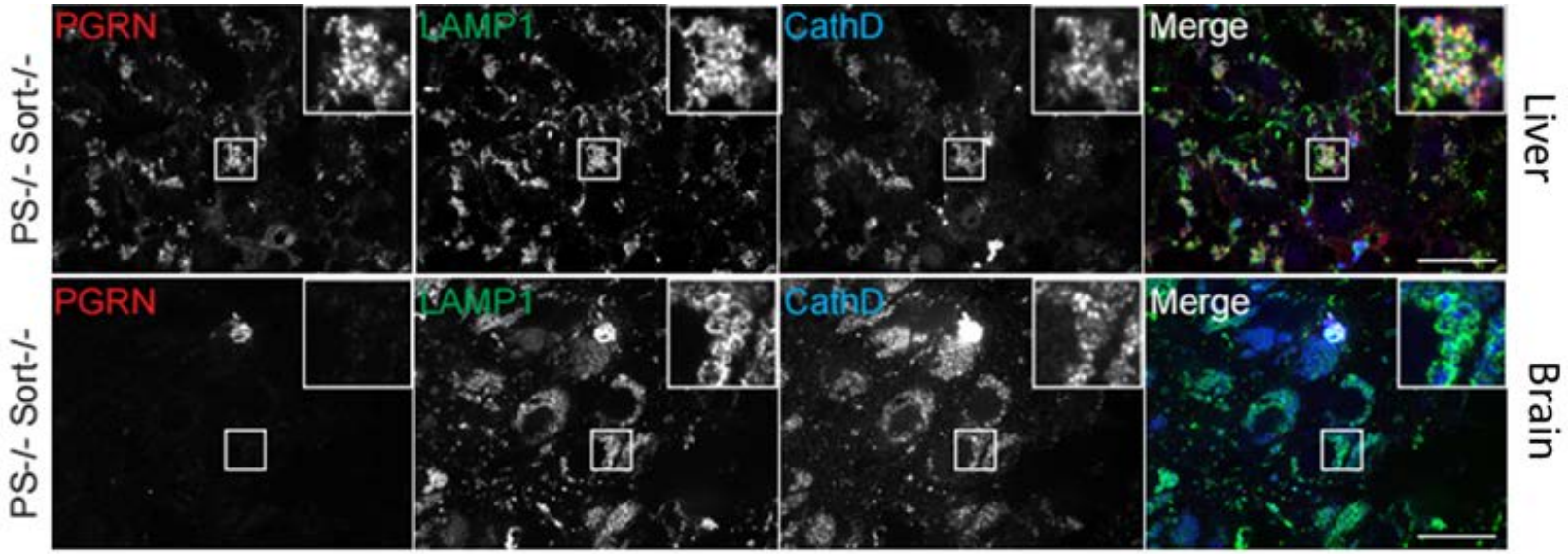

Supplementary Figure 6.2. PGRN localization in *Psap*$^{-/-}$/*Sort*$^{-/-}$ mouse tissue sections. PGRN retains lysosomal localization in microglia and hepatocytes despite loss of both known trafficking pathways. Scale bar = 20 μm. Contributed by X.Z.

CHAPTER 7

TMEM106B IS A POTENTIAL REGULATOR OF CELLULAR PI(3,5)P_2 LEVELS

7.1 Abstract

Mutation in the granulin (*GRN)* gene resulting in haploinsufficiency of the protein, progranulin (PGRN), is a leading cause of familial frontotemporal lobar degeneration (FTLD). Variants of *TMEM106B* have been associated with an increased risk of developing FTLD, especially in cases of *GRN* mutation (FTLD-GRN). While the exact function of TMEM106B is still unknown, overexpression of the protein in mammalian cells is associated with cytotoxicity and lysosomal defects, including lysosomal enlargement, poor acidification, and reduced degradative capacity. We noted a marked overlap in cytotoxicity and vacuole and lysosomal phenotype in yeast and mammalian cells that have had TMEM106B overexpressed and cells that are mutated in the PI kinase Fab1, which is responsible for the synthesis of the primary late endosomal/lysosomal phosphoinositide, PI(3,5)P_2. Because of this, we hypothesized that TMEM106B may regulate PI(3,5)P_2 levels, and that the lysosomal phenotypes associated with its overexpression may be due to a reduction in cellular pools of the phosphoinositide. In this study, we show that the established lysosomal enlargement phenotype associated with mammalian TMEM106B overexpression translates to a yeast model. Furthermore, lysosomal enlargement induced by TMEM106B overexpression can be suppressed by overexpression of hyperactive Fab1 mutants or components of the Fab1 complex. Consistent with these findings in yeast, PIP analysis demonstrates a

significant reduction in $PI(3,5)P_2$ with stable TMEM106B overexpression in mammalian cells.

7.2 Introduction

Frontotemporal lobar degeneration (FTLD) is a devastating, clinically heterogeneous neurodegenerative disease that results in the progressive atrophy of the frontal and temporal lobes of the brain [1]. Most often presenting with drastic alterations in behavior and personality, including social disinhibition as well as gradual decline in language capabilities, FTLD is the second leading cause of early-onset dementia only after Alzheimer's disease [1, 2]. Although its exact mechanism is unknown, several genetic mutations have been linked to the disease. One of the major causes of familial FTLD is haploinsufficiency of the protein, progranulin (PGRN), resulting from mutation in the granulin (*GRN*) gene [3-8]. PGRN haploinsufficiency is associated with a subtype of FTLD wherein the patients develop aggregates of ubiquitinated TAR DNA-binding protein 43 (TDP-43) (FTLD-TDP) [9]. PGRN is a highly glycosylated, 593 amino acid protein that has been implicated in numerous processes, ranging from regulation of inflammation to wound healing and tumorigenesis. While its exact function is unknown, PGRN has been found to be not only be secreted, but also lysosomally localized. Continuing evidence points to a lysosomal role of PGRN, as in addition to contributing to FLTD, homozygous loss-of-function *GRN* mutations result in the lysosomal storage disease (LSD), neuronal ceroid lipofuscinosis (NCL).

In 2010, a genome-wide association study to detect gene loci imparting susceptibility to FTLD-TDP identified a then uncharacterized transmembrane protein,

TMEM106B, which showed risk vulnerability specific to *GRN* mutation carriers [10]. There are some indications that the pathologic connection to TMEM106B is related to increased levels of the protein. Single nucleotide polymorphisms associated with FTLD risk are also associated with increased expression of TMEM106B, rather than alterations in the amino acid sequence of the protein [10, 11], and elevated levels of TMEM106B have been found in the post-mortem brains of FTLD-TDP patients [11]. Likewise, a coding variant, p.T185S, in linkage disequilibrium with a protective minor allele of the gene produces significantly lower protein levels [12-14].

While the function of the protein and its association with FTLD is still undetermined, early characterization found it to be a glycosylated, type II transmembrane protein primarily localized to the endolysosomal system [11, 15, 16]. With the association between elevated TMEM106B levels and disease, significant time has gone into examining the effects of TMEM106B overexpression. The most obvious phenotype associated with its overexpression is drastic lysosomal enlargement, which has been observed in multiple cell lines [11, 15, 17, 18]. Overexpression also results in a decreased capacity to degrade endocytic cargo [15], which could be due to inhibition of lysosomal acidification [11]. TMEM106B has been found to interact with several proteins, including microtubule-associated protein 6 (MAP6), charged multivesicular body protein 2B (CHMP2B), and the vacuolar H^+-ATPase (V-ATPase) AP1 subunit [19-21], but its exact function remains unclear.

TMEM106B is highly conserved among vertebrates and has two paralogs, TMEM106A and TMEM106C, which share approximately 50% amino acid identity [22]. Very little is known about these two proteins, and despite the homology, neither

has been linked to neurodegeneration. TMEM106A has a reported association with cancer suppression and macrophage activation [23, 24], and TMEM106C is a candidate for the arthrogryposis multiplex congenita, but little else is known about it [25].

With the disease relevance and the severity and high replicability of the TMEM106B overexpression lysosomal phenotype, we became interested in further exploring its mechanism. Following expression studies in the budding yeast, *Saccharomyces cerevisiae*, we noted a striking similarity between the phenotypes we observed with TMEM106B and those of another published yeast model, *fab1*Δ. These yeast, which lack the protein, Fab1, show severe cytotoxicity and grossly enlarged, minimally lobulated vacuoles. Because of these similarities, we questioned whether a shared pathway between TMEM106B and Fab1 could explain the comparable phenotypes.

Fab1 is a phosphatidylinositol-3-phosphate 5-kinase involved in phosphoinositide (PI) synthesis, wherein it mediates the production of phosphatidylinositol 3,5-bisphosphate ($PI(3,5)P_2$) from phosphatidylinositol-3-phosphate (PI3P). It has a mammalian homolog, FYVE finger-containing phosphoinositide kinase (PIKfyve). $PI(3,5)P_2$, with all known cellular pools being produced by Fab1/PIKfyve, is the major phosphoinositide species present on both the yeast vacuole and the mammalian lysosome, where it is involved in recruitment of organelle- and process-dependent proteins and cell signaling [26-28].

However, despite its ability to bind directly to PI3P, Fab1 requires complexation with a set of proteins for activation and optimal function. This complex is brought together by the scaffolding protein, Vac14 (mammalian homolog also known as

associated regulator of PIKfyve (ArPIKfyve)). The $PI(3,5)P_2$ 5-phosphatase, Fig4, opposes the effects of Fab1 by removing the 5-phosphate from $PI(3,5)P_2$ to convert it back to PI3P. Despite playing a role directly opposite that of Fab1, Fig4 is an essential component of the complex and is required for full Fab1 activity in both yeast and mammalian cells. In yeast, the protein, Vac7, acts as a specific activator of Fab1. In mammalian cells there is no known Vac7 homolog, and Vac14 and Fig4 appear sufficient to induce PIKfyve activation. An additional protein, Atg18, also appears to be a member of the complex in yeast. Atg18 likely functions as a direct inhibitor of Fab1p, as loss of Atg18 causes a robust increase in $PI(3,5)P_2$ production [29]. Four homologs of Atg18, WIPI1-4 are found in mammalian cells, but have not been shown to be involved in the PIKfyve complex. The seemingly paradoxical inclusion of the oppositional proteins, Fig4 and Atg18, in the Fab1 complex implies a tight regulation of its function and $PI(3,5)P_2$ levels, and that quick adjustments in these phosphoinositide levels may be vital. Indeed, $PI(3,5)P_2$ levels have been shown to quickly respond to stress. In yeast, hyperosmotic shock induces a rapid upregulation of PI(3,5P)2, by as much as 20-fold within 5 minutes [30].

Vac7, Vac14, and Fig4 are so essential for proper Fab1/PIKfyve function that loss of any one component significantly reduces total $PI(3,5)P_2$, with Fig4 mutation reported to result in a 3-fold decrease [31]. In mammals, PIKfyve is essential and deletion of the gene in mice is lethal before embryonic implantation [32]. Vac14 and Fig4 mutations are both associated with neurodegeneration in mammals. Fig4 mutations have been found to cause Charcot-Marie-Tooth Disease type 4 J, Yunis-Varón syndrome, and familial epilepsy with polymicrogyria in humans, while

disruption of Fig4 protein in mice produced the pale tremor mouse, characterized by neurodegeneration, tremor, and abnormal gait [31, 33, 34]. Vac14 mutation has been associated with a pediatric-onset neurological disease [35]. Deficiency of either Vac14 or Fig4, or expression of a dominant-negative PIKfyve mutant also results in large cytoplasmic vacuoles positive for endolysosomal markers [31, 36, 37].

Because of the cellular phenotypes common to TMEM106B overexpression and Fab1 loss, and the association of both proteins with neurodegeneration, we hypothesize that TMEM106B controls lysosomal and vacuolar morphology by regulating $PI(3,5)P_2$ levels, possibly through direct modulation of the Fab1 pathway.

7.3 Results

TMEM106B overexpression causes vacuole enlargement and cytotoxicity in yeast

TMEM106B has previously been demonstrated to show severe toxicity in yeast, although the mechanism was indeterminate [38]. We were interested in further characterizing phenotypes associated with ectopic TMEM106B expression, and because TMEM106B causes severe defects in lysosomal morphology, with the most pronounced effect being enlargement of lysosomes, we were particularly interested in testing whether this phenotype would translate to a yeast system, where these genes and products are not natively present. Because of the shared homology of TMEM106A, B, and C, and their lack of well-defined functions, we chose to perform initial tests of all three.

We found that when overexpressed in yeast, all three TMEM106 proteins localize to the vacuole membrane, as confirmed by co-localization with the vacuole-

specific dye, FM4-64 **(Fig. 7.1A)** [39]. This is interesting because although TMEM106A and B show lysosomal localization in mammalian cells, TMEM106C has previously been observed to reside in the endoplasmic reticulum when overexpressed [40]. GFP-TMEM106A and B caused significant vacuolar enlargement compared to control or GFP-TMEM106C-expressing yeast, paralleling the lysosomal phenotypes observed when overexpressed in mammalian cells **(Fig. 7.1A)**.

With previous reports of cytotoxicity in both yeast and mammalian cells when overexpressed, we wanted to see if TMEM106B would cause observable growth defects. We were able to replicate the published results in a growth retardation assay with overexpression of GFP-TMEM106B. In fact, transient overexpression of GFP-TMEM106B proved to be exceedingly toxic, likely due to high expression levels, so we opted to produce stable GFP-TMEM106A, B, and C yeast lines and use these for all following experiments **(Fig. 7.1B)**. Whereas GFP-TMEM106B-expressing yeast showed a severe growth deficit and temperature sensitivity at 37°C, GFP-TMEM106A had minimal effect, and TMEM106C did not interfere with growth in any observable manner.

Hyperactive Fab1 mutants suppress vacuole enlargement and cytotoxicity

Because of the phenotypic overlap between TMEM106B overexpression and loss of function of the Fab1 complex, we wanted to investigate the possibility that TMEM106B-induced vacuole enlargement and cytotoxicity may be due to a decrease in $PI(3,5)P_2$. We postulated that, if this proved to be the case, then correcting the phosphoinositide deficit should result in suppression of these phenotypes. To test this, we utilized previously identified hyperactive Fab1 point mutants that allow for the

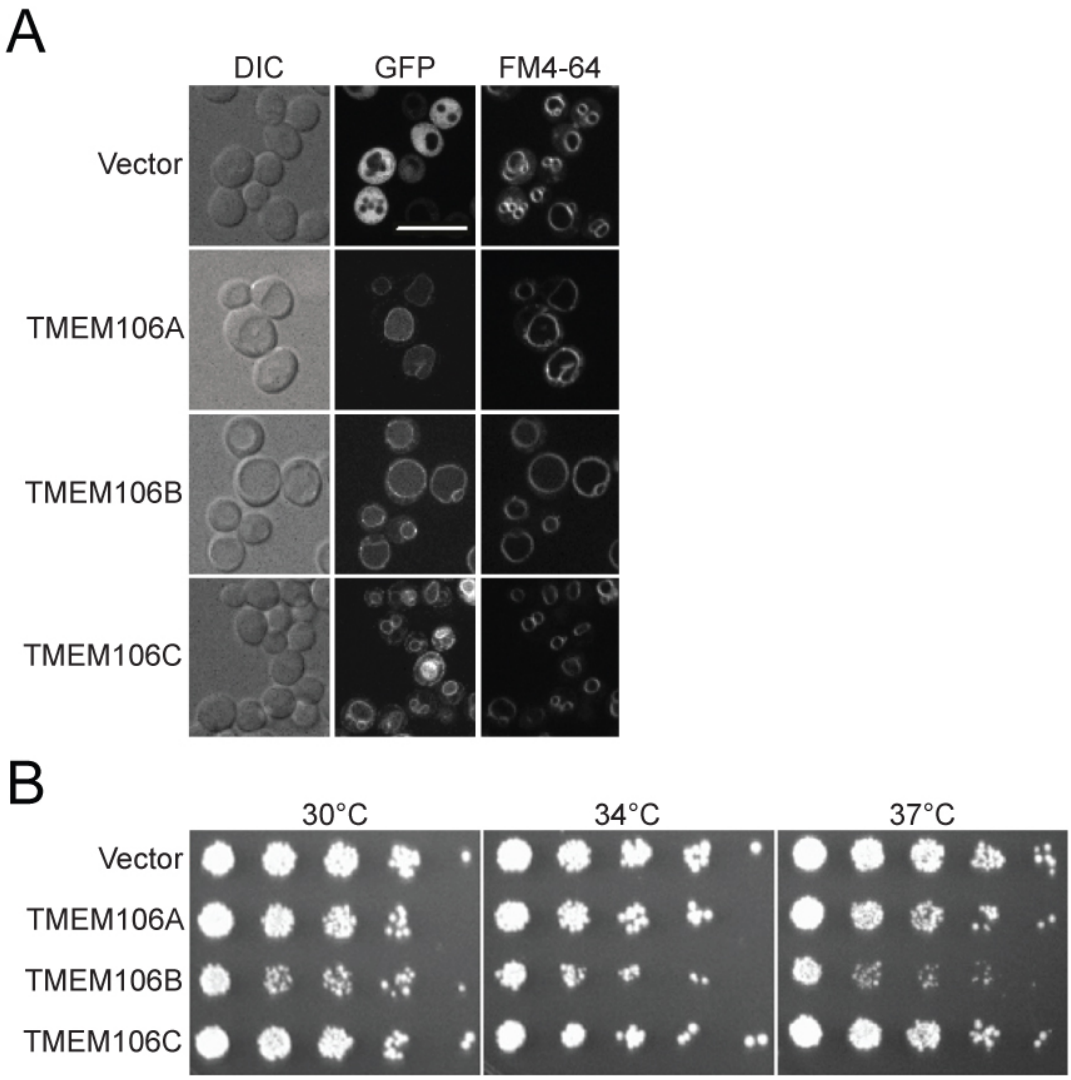

Figure 7.1. GFP-TMEM106 protein localization, vacuole enlargement, and cytotoxicity in yeast. GFP-TMEM106A, B, or C was overexpressed in wildtype yeast. **A)** When transiently overexpressed, each of the three proteins localizes to the limiting membrane of the vacuole, as assessed by colocalization with the marker, FM4-64. Both TMEM106A and TMEM106B overexpression cause severe vacuole enlargement and a decrease in the presence of lobes compared to GFP vector control, while TMEM106C does not drastically alter vacuole morphology. **B)** TMEM106B stable overexpression results in cytotoxicity as assessed by a yeast growth retardation assay. TMEM106A only shows a slight growth defect. TMEM106C does not inhibit growth. Scale bar = 10 μm.

synthesis of $PI(3,5)P_2$ in the absence of Vac7 or Vac14 and at supraphysiological levels [41, 42].

When we overexpressed WT Fab1 or hyperactive Fab1 mutants in GFP-TMEM106A or GFP-TMEM106B integrated yeast strains, we found that, while WT Fab1 overexpression only had a mild effect, if any, on vacuole enlargement, hyperactive Fab1 mutants drastically decreased vacuole size in yeast strains stably expressing either GFP-TMEM106A **(Fig. 7.2)** or GFP-TMEM106B **(Fig. 7.3)**. Likewise, the hyperactive Fab1 mutants decreased cytotoxicity in the GFP-TMEM106B line **(Fig. 7.4)**. The constructs had little effect in GFP-TMEM106A, which did not display a growth defect to begin with **(Supplementary Fig. 7.1A)**. We also expressed the other components of the Fab1 complex in the GPF-TMEM106B-expressing strain to see if they could alter the growth defect **(Supplementary Fig. 7.1B)**. Overexpression of Vac7 or Vac14 greatly rescued the growth defect, while Fig4 overexpression exacerbates TMEM106B-induced toxicity, which is consistent with the function of Fig4 being the conversion of $PI(3,5)P_2$ to PI3P, thus reducing the $PI(3,5)P_2$ levels.

TMEM106B overexpression reduces $PI(3,5)P_2$ levels in HEK293T cells

Because elevated Fab1 activity suppressed the vacuole enlargement and growth defect induced by TMEM106B overexpression, next we directly tested whether $PI(3,5)P_2$ levels are reduced by TMEM106B overexpression. For this purpose, we created HEK293T cells stably expressing GFP-TMEM106B using a lentiviral delivery system.

In a preliminary experiment, control or GFP-TMEM106B stable HEK293T cells were then metabolically labeled with myo-[2-^{3}H]-inositol in collaboration with the laboratory of Dr. Lois Weisman at the University of Michigan. Following perchloric

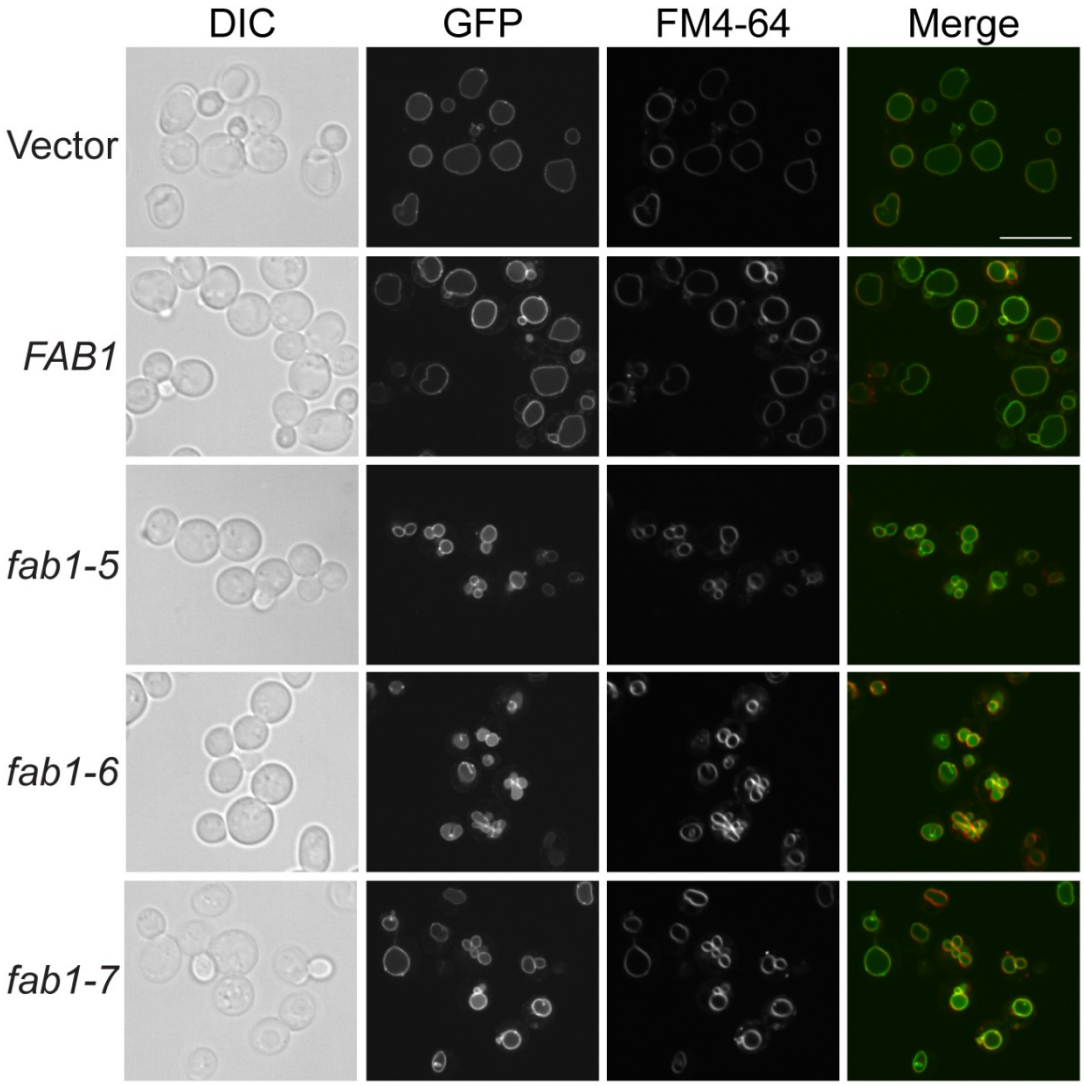

Figure 7.2. Suppression of GFP-TMEM106A-induced vacuole enlargement by hyperactive Fab1 mutants. Stable GFP-TMEM106A integrants produce the same vacuole enlargement phenotype as with transient overexpression. This enlargement can be suppressed by overexpression of hyperactive Fab1 mutants, which produce supraphysiological levels of $PI(3,5)P_2$. Scale bar = 10 μm.

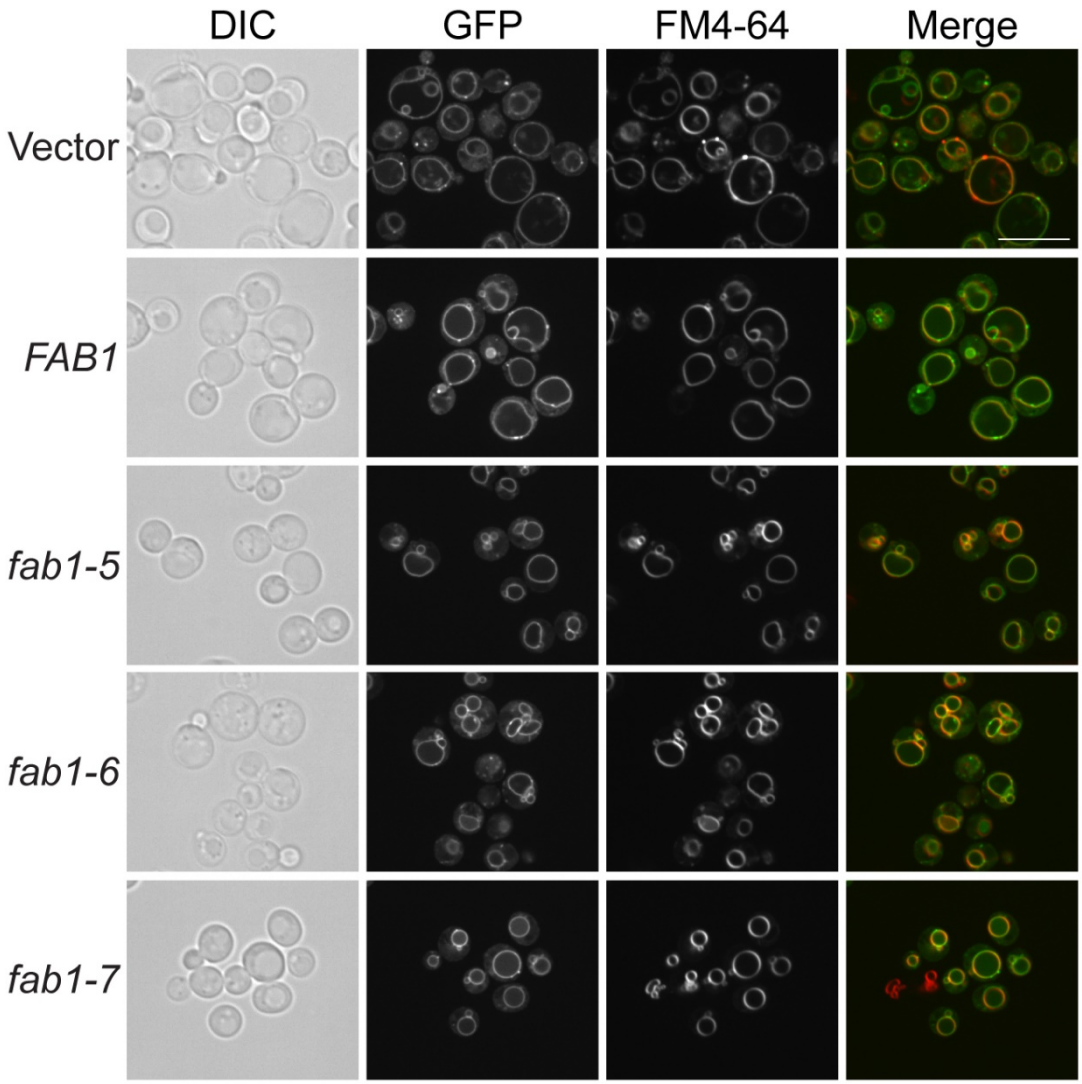

Figure 7.3. Suppression of GFP-TMEM106B-induced vacuole enlargement by hyperactive Fab1 mutants. Stable GFP-TMEM106B integrants produce the same vacuole enlargement phenotype as with transient overexpression. This enlargement can be suppressed by overexpression of hyperactive Fab1 mutants, which produce supraphysiological levels of $PI(3,5)P_2$. Scale bar = 10 μm.

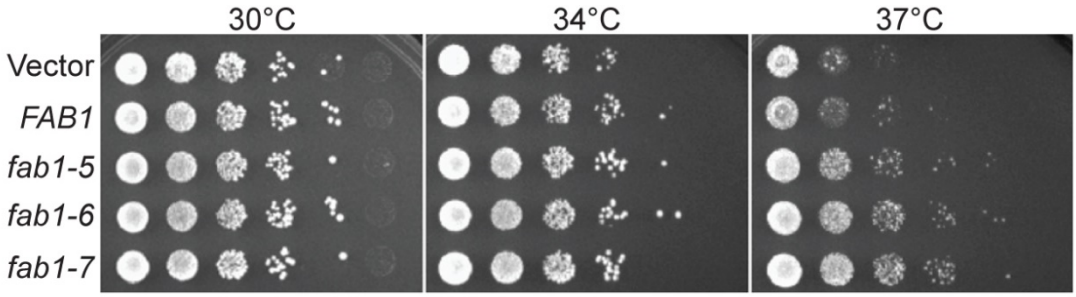

Figure 7.4. Suppression of GFP-TMEM106B cytotoxicity by hyperactive Fab1 mutants. Stable GFP-TMEM106B integrants produce the same growth retardation and temperature sensitivity as with transient overexpression, which can be suppressed by overexpression of hyperactive Fab1 mutants, which produce supraphysiological levels of $PI(3,5)P_2$.

acid precipitation and deacylation, high-performance liquid chromatography (HPLC) was used to separate glycerol-inositol phosphates. Consistent with our hypothesis, $PI(3,5)P_2$ was reduced by 42% in the stable GFP-TMEM106B cell line compared to the control cell line **(Fig. 7.5)**. Smaller changes were also seen in PI5P, $PI(3,4)P_2$, and $PI(3,4,5)P_3$. We also analyzed PIP levels in primary fibroblasts derived from TMEM106B knockout mice. However, these did not show any consistent changes in $PI(3,5)P_2$ levels (data not shown), indicating that loss of TMEM106B does not affect $PI(3,5)P_2$ metabolism.

TMEM106B interacts with Vac14 when overexpressed

Because $PI(3,5)P_2$ is only known to be synthesized from PI3P via PIKfyve kinase activity, the most likely mechanism for TMEM106B overexpression-induced $PI(3,5)P_2$ reduction would be that TMEM106B binds to one or more proteins in the PIKfyve complex, possibly sequestering them and disrupting stoichiometry. To test this, we performed co-immunoprecipitation (co-IP) of overexpressed TMEM106B and individual PIKfyve complex components. No binding was seen between TMEM106B and PIKfyve, Fig4, or WIPI-1 (data not shown). However, GFP-Vac14 co-immunoprecipitated with FLAG-TMEM106B when both proteins were overexpressed in HEK293T cells and anti-FLAG IP was performed **(Fig. 7.6A)**. Surprisingly, Vac14 showed binding to all three TMEM106 proteins, possibly indicating common regulation or an artifact of the experiment. Binding was seen in a second experiment using overexpressed FLAG-TMEM106B and Vac14-MycHis, with anti-FLAG or the reciprocal anti-myc condition **(Fig. 7.6B)**. Although binding was observed when IP of

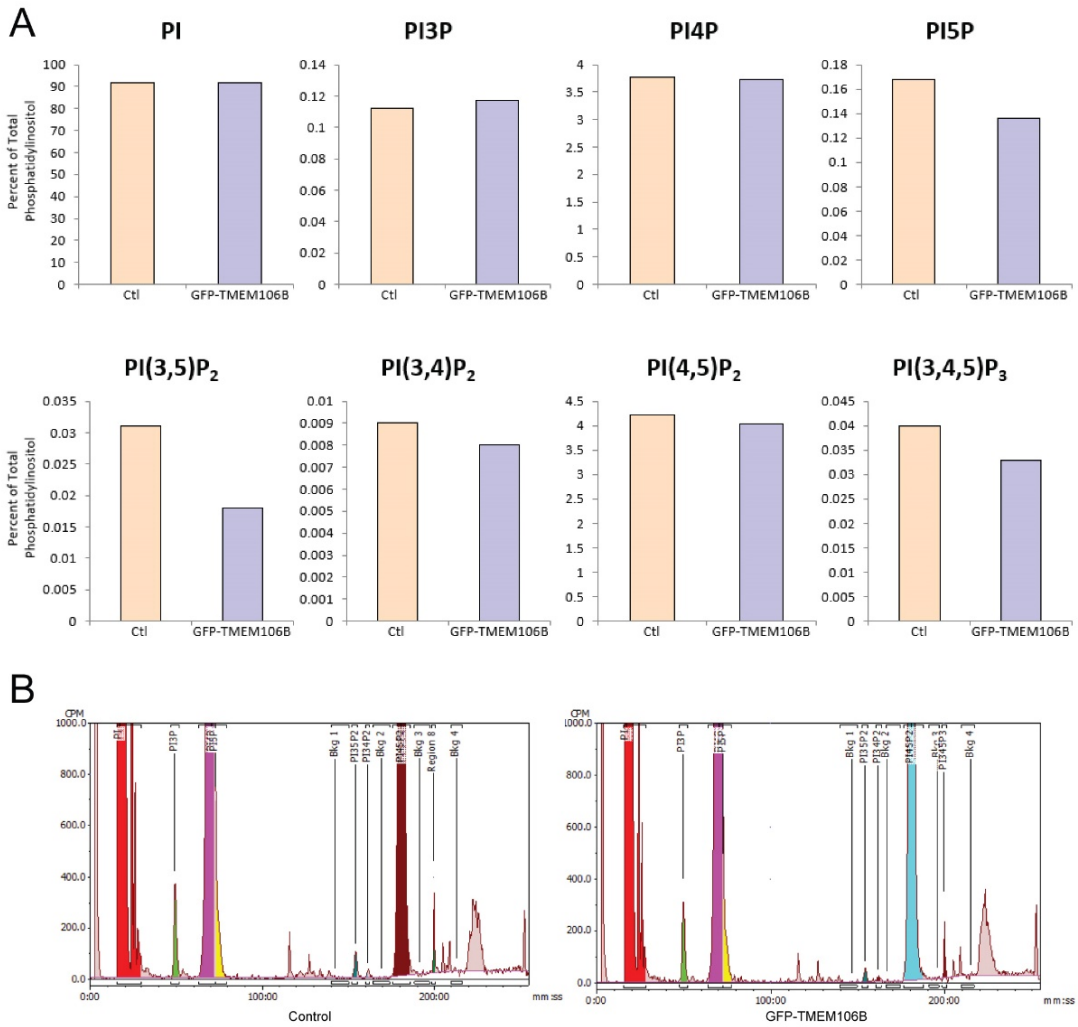

Figure 7.5. Preliminary phosphoinositide analysis of HEK293T control or GFP-TMEM106B stable cell lines. **A)** Quantification of phosphoinositides, with each represented as % of total PI. **B)** HPLC peaks of samples quantified in A. Error bars are not included, as samples have only been analyzed once at the time of writing.

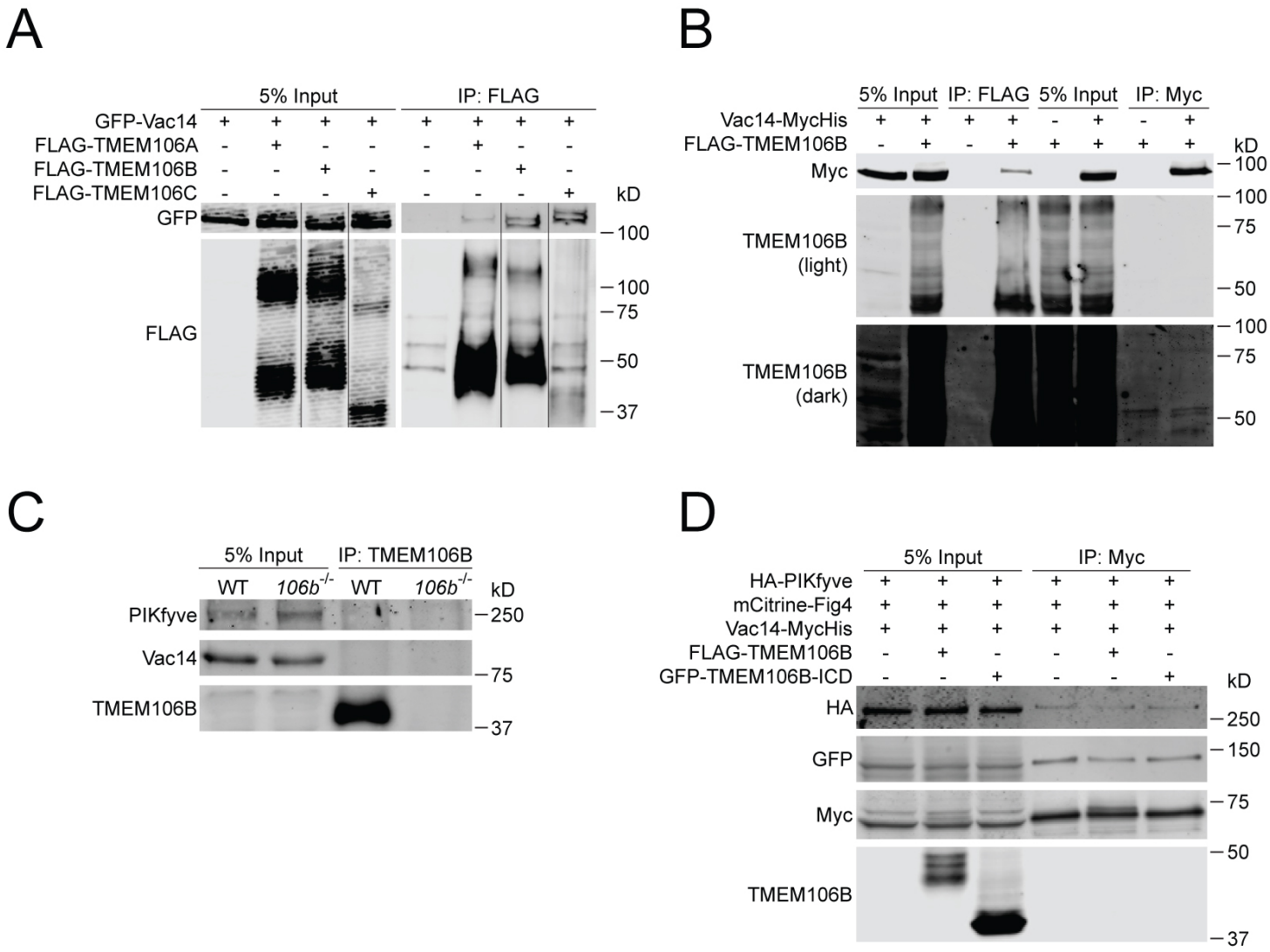
A
5% Input
IP: FLAG
GFP-Vac14
FLAG-TMEM106A
FLAG-TMEM106B
FLAG-TMEM106C
GFP
FLAG
kD
100
100
75
50
37
B
5% Input
IP: FLAG
5% Input
IP: Myc
Vac14-MycHis
FLAG-TMEM106B
Myc
TMEM106B (light)
TMEM106B (dark)
kD
100
100
75
50
100
75
50
C
5% Input
IP: TMEM106B
WT
106b-/-
WT
106b-/-
kD
PIKfyve
Vac14
TMEM106B
250
75
37
D
5% Input
IP: Myc
HA-PIKfyve
mCitrine-Fig4
Vac14-MycHis
FLAG-TMEM106B
GFP-TMEM106B-ICD
kD
HA
GFP
Myc
TMEM106B
250
150
75
50
37

Figure 7.6. TMEM106B binding experiments. A) FLAG-TMEM106 proteins were co-transfected with GFP-Vac14 and then anti-FLAG IP was performed. **B)** FLAG-TMEM106B was co-transfected with Vac14-MycHis and anti-FLAG or anti-myc IP was performed, as indicated. **C)** Anti-TMEM106B IP was performed from WT and *Tmem106b*$^{-/-}$ brain lysates to test for endogenous binding to Vac14 or PIKfyve. **D)** FLAG-TMEM106B or GFP-TMEM106B-ICD was co-transfected with HA-PIKfyve, Vac14-MycHis, and mCitrine-Fig4, then anti-myc IP was performed.

Vac14-MycHis was performed, it was very weak compared to when IP of FLAG-TMEM106B was performed.

To assess binding between TMEM106B and Vac14 at an endogenous level, WT and *Tmem106b*$^{-/-}$ (341bpΔ) mouse brains were lysed and anti-TMEM106B IP was performed **(Fig. 7.6C)**. Although TMEM106B was successfully precipitated in the WT sample, no Vac14 protein was detected in the IP products, indicating that the proteins do not bind at endogenous levels under the conditions of the IP and western blot analysis. However, this does not rule out the possibility that in cases where TMEM106B levels are increased, as may be the case in FTLD-GRN, that an interaction with Vac14 is induced.

With binding between overexpressed TMEM106B and the scaffolding protein, Vac14, one possible mechanism of PI(3,5)P_2 synthesis inhibition could be that TMEM106B binds to Vac14, interfering with its interaction with Fig4 and PIKfyve. To test this, FLAG-TMEM106B or a GFP-tagged construct of its derivative intracellular domain (ICD) were co-transfected with HA-PIKfyve, mCitrine-Fig4, and Vac14-MycHis and anti-myc IP was performed **(Fig. 7.6D)**. If TMEM106B or the ICD were to prevent complex formation, we would expect to see a decrease in the amount of PIKfyve or Fig4 that would co-IP. However, this does not seem to substantially change, indicating that this is unlikely to be the mechanism. In fact, no TMEM106B or ICD was seen to bind to Vac14 in these conditions.

PIKfyve complex protein levels do not change with TMEM106B overexpression

Another potential way that TMEM106B could disrupt PI(3,5)P_2 synthesis is by alteration of the total cellular levels of the different PIKfyve complex components,

possibly via ESCRT-related degradation, as TMEM106B has been associated with the FTLD-related protein, CHMP2B, a subunit of the ESCRT-III complex [20]. However, when HEK293T stable control of GFP-TMEM106B cell lysates were analyzed by western blot, no obvious change in PIKfyve, Vac14, or Fig4 was observed when normalized to GAPDH **(Fig. 7.7A)**. An initial examination of protein levels in yeast strains with endogenously HA-tagged Fab1, Vac14, Fig4, or Vac7 did show a decrease in Vac14 and Fig4 levels (data not shown). However, this needs to be repeated to verify these results. Densitometry of western blots of primary cortical neuron and MEF cultures suggests a trend toward increased Vac14 protein levels with loss of *Tmem106b*, however there is great variability between samples, and *Tmem106b*$^{-/-}$ brain lysates showed no change **(Fig. 7.7B-F)**. PIKfyve signal in these samples was generally too weak to accurately quantify and specific Fig4 signal was not seen.

7.4 Discussion

In this study, we have demonstrated that the FTLD-GRN risk factor, TMEM106B, is a potential regulator of cellular $PI(3,5)P_2$ levels. Interestingly, we found that overexpression of TMEM106B in mammalian cells reduced $PI(3,5)P_2$ levels to an extent that is nearly comparable to that which is seen with loss of the PIKfyve complex protein, Vac14 (42% and 57%, respectively) [36]. We also saw a decrease in PI5P, which is likely due to decreased synthesis directly resulting from a reduced pool of the precursor, $PI(3,5)P_2$. In yeast, overexpression of TMEM106B causes cytotoxicity and a vacuole enlargement phenotype that parallels those seen in mammalian cells. Both the cytotoxicity and the enlargement can be suppressed by the overexpression of the

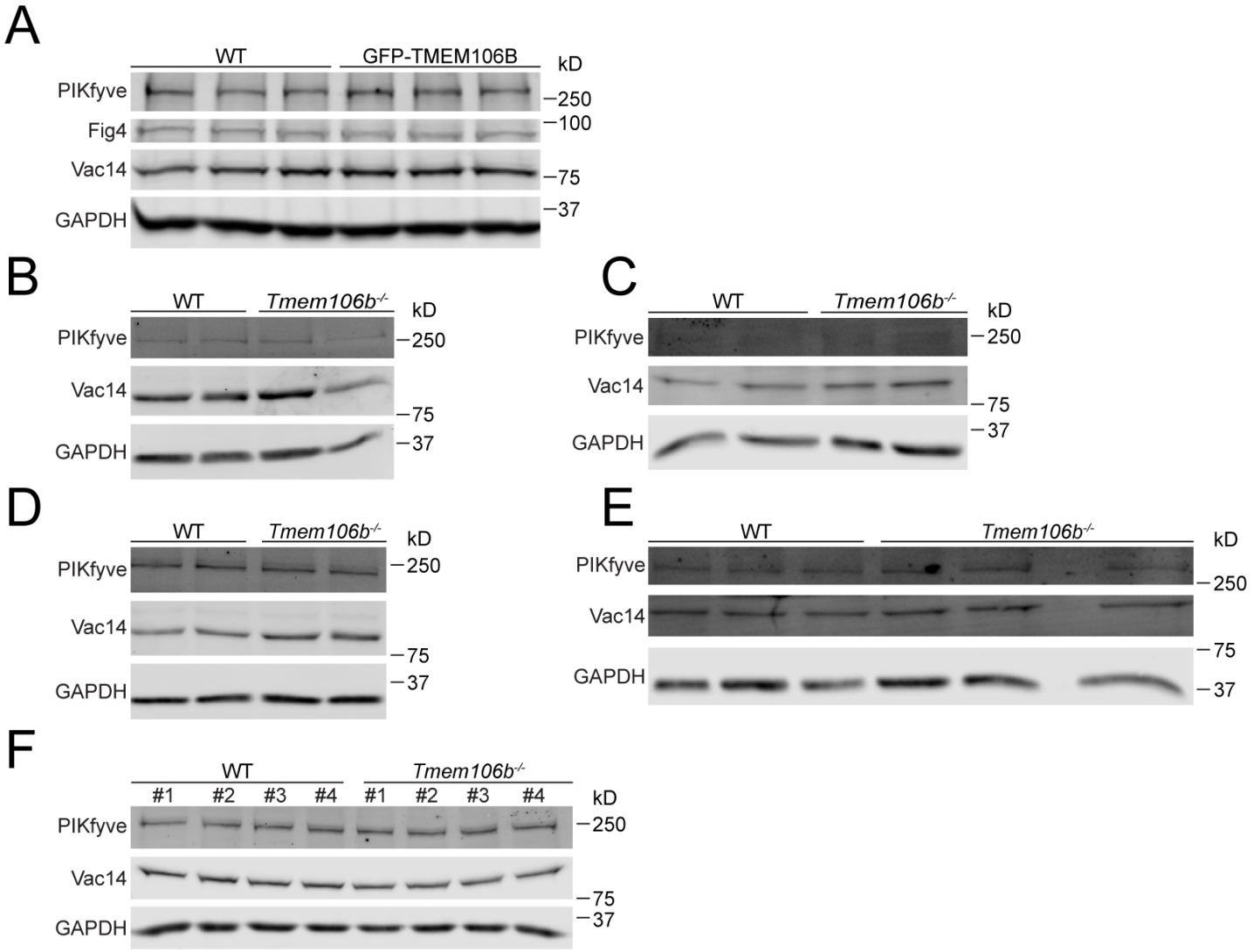
A
WT
GFP-TMEM106B
kD
PIKfyve
Fig4
Vac14
GAPDH
250
100
75
37
B
WT
Tmem106b-/-
kD
PIKfyve
Vac14
GAPDH
250
75
37
C
WT
Tmem106b-/-
kD
PIKfyve
Vac14
GAPDH
250
75
37
D
WT
Tmem106b-/-
kD
PIKfyve
Vac14
GAPDH
250
75
37
E
WT
Tmem106b-/-
kD
PIKfyve
Vac14
GAPDH
250
75
37
F
WT
Tmem106b-/-
#1
#2
#3
#4
#1
#2
#3
#4
kD
PIKfyve
Vac14
GAPDH
250
75
37

Figure 7.7. PIKfyve complex protein levels with TMEM106B overexpression and with *Tmem106b* knockout. **A)** Western blot showing PIKfyve, Fig4, Vac14, and GAPDH protein levels in control and GFP-TMEM106B stable HEK293T cell lines. **B)** Primary cortical neurons cultured in duplicate from a pair of 341bpΔ *Tmem106b*$^{-/-}$ mice – DIV14. **C)** Primary MEF cells cultured from the same mice as in B). **D)** Primary cortical neurons cultured in duplicate from a second pair of 341bpΔ *Tmem106b*$^{-/-}$ mice – DIV5. **E)** Primary MEF cells cultured from the same mice as in D). **F)** Whole brain lysates from 7bpΔ *Tmem106b*$^{-/-}$ mice.

Fab1 complex components, Vac14 or Vac7, or by hyperactive Fab1 mutants, strongly suggesting that the observed phenotypes are due to decreased $PI(3,5)P_2$ levels.

While we have successfully shown that TMEM106B overexpression results in decreased $PI(3,5)P_2$ levels, the exact mechanism and whether the effect is direct or indirect remains unclear. We have identified a possible interaction between TMEM106B and the PIKfyve complex scaffolding protein, Vac14. However, the binding is not particularly strong, it was not seen at an endogenous level, and the functional significance of the relationship is indeterminate at this time. It should be noted that we also observed binding between Vac14 and TMEM106A and TMEM106C. While this could be a functional finding – it is possible that the TMEM106 proteins are co-regulatory – it is also possible that this is an indication that the binding is non-specific and an artifact of overexpression and removal of these proteins from their native membranes.

It is also currently unclear why TMEM106A overexpression in yeast produces a similar vacuole enlargement phenotype, but differs in its cytotoxicity. Phosphoinositide analysis in TMEM106A-overexpressing cells could lend some insight into this phenomenon. It is possible that TMEM106A also reduces $PI(3,5)P_2$ levels, but not to such an extreme degree as TMEM106B where it interferes with cell growth. It is also possible that the mechanism differs and TMEM106A is altering $PI(3,5)P_2$ levels indirectly, possibly by acting either upstream of the Fab1 complex on PI3P synthesis, or downstream on PI5P synthesis, both of which would potentially affect $PI(3,5)P_2$.

In mammalian cells, it is possible that the TMEM106 proteins share similar interactions and functions, but their expression patterns and effects are cell-type-

specific. TMEM106B may be more highly expressed in neurons or other cells of the central nervous system. Similarly, it is possible that the three TMEM106 proteins regulate one another. In cell lysates, TMEM106B can be found as both a monomer and SDS-resistant dimer [15]. It is possible that the TMEM106 proteins form heterodimers that may be under the regulation of different factors. The stoichiometry of these proteins could shift the dimerization and lead to the observed phenotypes.

We also found that *Tmem106B*$^{-/-}$ MEFs do not show any significant changes in PI(3,5)P_2 levels, indicating that TMEM106B is not a critical regulator of PI(3,5)P_2 metabolism at endogenous levels. This suggests that regulation of the phosphoinositide by increased TMEM106B levels, as occurs with disease state or overexpression, may signify a toxic gain-of-function. This will surely be further elucidated when the mechanism is determined, of which there are a myriad of unexplored possibilities. One such possibility is steric hindrance at the lysosome membrane, preventing the PIKfyve complex from interacting with PI3P, without TMEM106B directly binding any complex components. Likewise, TMEM106B could itself be a PI3P binding protein, displacing PIKfyve and preventing phosphorylation. Although TMEM106B does not seem to significantly alter PIKfyve complex protein levels, it could affect the localization of one or more complex components. Future immunostaining studies of the endogenous proteins would be beneficial.

A second question we must consider is what role TMEM106B-induced PI(3,5)P_2 reduction plays in FTLD risk. It is unclear at this time whether the effects we observed play a role in the development of FTLD with *GRN* mutations. However, reduced PI(3,5)P_2 levels due to mutation of PIKfyve complex components are associated with

various neurodegenerative diseases, so it is not unlikely. One important consideration is that TMEM106B has been shown to regulate PGRN levels, with one study indicating that increased TMEM106B expression interferes with the lysosomal processing of PGRN to its functional derivative granulin peptides [43]. This could be due to decreased lysosomal acidification associated with TMEM106B overexpression [11, 21]. Defective vacuolar acidification is a known outcome of $PI(3,5)P_2$ deficiency [44-46]. It is possible that reduced $PI(3,5)P_2$ levels due to increased TMEM106B expression result in decreased PGRN processing and a reduction in already low granulin peptide concentrations. The consequences of decreased $PI(3,5)P_2$ levels may also be more broad, as the phosphoinositide regulates many lysosomal processes, including membrane trafficking, fusion, and calcium efflux [26-28] . PIKfyve has also been shown to protect against glutamate excitotoxicity by internalization of voltage-gated Ca^{2+} channels [47].

Finally, a new TMEM106B disease association was very recently identified, wherein *de novo* D252N mutation causes hypomyelinating leukodystrophy, a condition that results in defective growth or maintenance of myelin in the central nervous system (CNS) [48, 49]. The mechanism is unidentified, and it is currently unknown whether there is a connection between this mutation, TMEM106B function, and FTLD. However, it is possible that this is could be related to the findings explored in our study, as $PI(3,5)P_2$ has been linked to regulation of the differentiation of oligodendrocytes, the cells responsible for producing myelin in the CNS [50].

In this study, we have identified a potentially novel role for TMEM106B in regulating cellular PI(3,5)P_2 levels. However, significant work still needs to be done to truly understand the significance and underpinnings of this finding.

7.5 Materials and Methods

Primary Antibodies and Reagents

The following antibodies were used in this study: M2 mouse anti-FLAG (Sigma), M2 mouse anti-FLAG-conjugated beads (Sigma), 9E10 mouse anti-myc (homemade), Myc-Trap beads (ChromoTek), mouse anti-GAPDH (Proteintech Group), mouse anti-PIKfyve (University of Iowa Developmental Studies Hybridoma Bank, and mouse anti-Fig4 (University of California, Davis NeuroMab). Rabbit anti-Vac14 was a gift from Dr. Lois Weisman (University of Michigan) [51]. Rabbit anti-TMEM106B antibodies were generated as previously described [15].

Plasmids

TMEM106A, TMEM106B, and TMEM106C mammalian expression constructs were obtained or produced as previously described [15, 40]. Human Vac14 cDNA was a gift from Dr. Yuxin Mao, and GFP-Vac14 was produced by cloning Vac14 into the pEGFP-C1 vector and Vac14-MycHis by cloning Vac14 into the pcDNA3.1/myc-His A vector. Fig4 in the pmCitrine vector and PIKfyve in the pCMV-HA vector were gifts from Dr. Lois Weisman (University of Michigan).

Mammalian Cell Culture

HEK293T cells were maintained in Dulbecco's Modified Eagle's Medium (Cellgro) supplemented with 10% fetal bovine serum (Gibco) in a humidified incubator at 37ºC

with 5% CO_2. Primary mouse fibroblasts were isolated from newborn WT and *Tmem106b*$^{-/-}$ mouse pups and grown in Dulbecco's Modified Eagle's Medium supplemented with 10% fetal bovine serum and 1% penicillin–streptomycin (Invitrogen) in a humidified incubator at 37°C and 5% CO2. Primary cortical neurons were isolated from P0–P1 pups and cultured as previously described [52]. For protein level analysis, cultured cells were collected directly in Laemmli Sample Buffer with 5% β-Mercaptoethanol.

Lentivirus Generation and Mammalian Cell Infection

Lentiviruses were generated by co-transfection of lentiviral vectors with pMD2.G and psPAX2 plasmids in HEK293T cells. Lentivirus conditioned media were collected 3 days after transfection. HEK293T were infected with the conditioned media of control or GFP-TMEM106B lentivirus. After 24 hours, conditioned media was replaced with fresh culture media. Two days after infection, fresh media with 2 μg/mL puromycin was added to select for infected cells.

Yeast Transformation and Stable Line Generation

Stable integrated TMEM106A, TMEM106B, and TMEM106C yeast lines were produced by lithium acetate/single-stranded carrier DNA/polyethylene glycol transformation and homologous recombination of AgeI-linearized pRS305 vector containing the appropriate cDNA insert [53, 54].

Tissue Preparation for IP, Gel Electrophoresis and Western Blot

For analysis of protein levels, tissues from 3-month-old WT and 7bpΔ *Tmem106b*$^{-/-}$ mice were homogenized on ice with a glass Dounce homogenizer in cold RIPA buffer containing 150 mM NaCl, 50 mM Tris (pH 7.3), 1% Triton, 1% SDS, 0.5% DOC, 1

mM EDTA, and 1X protease inhibitors (Roche). Protein concentrations were determined via Bradford assay, then standardized. For immunoprecipitation, brains from WT and 341bpΔ *Tmem106b*$^{-/-}$ mice were lysed in a cold solution containing 150 mM NaCl, 50 mM Tris (pH 8.0), 1% Triton X-100, 0.1% deoxycholic acid, 1X protease inhibitors.

Mouse Strains

C57/BL6 were obtained from The Jackson Laboratory. *Tmem106b*$^{-/-}$ mice were produced by CRISPR-Cas9-mediated genome editing using the guide RNA 5' ACCCTATGGGATATATTTAC-3' and 5'-AGTGAAGTGCACAACGAAGA-3' (services provided by the Cornell Stem Cell and Transgenic Core Facility).

Transfection, IP, Gel Electrophoresis, and Western Blot Analysis

Cells were transfected with polyethylenimine as previously described [55]. Cells were lysed in a cold solution containing 150 mM NaCl, 50 mM Tris (pH 8.0), 1% Triton X-100, 0.1% deoxycholic acid, 1X protease inhibitors. After centrifugation at 14,000 g, for 15 minutes, at 4ºC, supernatants were transferred to clean tubes on ice, to which the appropriate antibody-conjugated beads were added, then rocked for 3-4 hours at 4ºC. Samples were centrifuged at 2,500 g for 20 seconds at 4ºC, then washed with 1 mL of a solution containing 150 mM NaCl, 50 mM Tris (pH 8.0), and 1% Triton X-100. This was repeated for a total of 3 washes. After a final centrifugation, all supernatant was aspirated and samples were eluted by the addition of 25 µL of Laemmli Sample Buffer with 5% β-Mercaptoethanol.

Samples were run on a 12% or 8% polyacrylamide gel, then transferred to Immobilon-FL polyvinylidene fluoride membranes (Millipore Corporation).

Membranes were blocked with either 5% non-fat milk in PBS or Odyssey Blocking Buffer (LI-COR Biosciences) for 1 hour, then washed with tris-buffered saline with 0.1% Tween-20 (TBST) 3x for 5m, each. Membranes were incubated with primary antibodies diluted in TBST, rocking overnight at 4ºC, then washed as above, incubated with secondary antibodies diluted in TBST for 2 h at room temperature, then washed again. Membranes were scanned using an Odyssey Infrared Imaging System (LI-COR Biosciences). Densitometry was performed with Image Studio (LI-COR Biosciences).

Mammalian Cell Immunostaining and Confocal Microscopy

Cells were cultured on glass coverslips overnight before transfection. Two days after transfection, cells were washed 2x with PBS, fixed with 3.7% paraformaldehyde for 15 minutes at room temperature, followed by 3 additional PBS washes. Cells were permeabilized with Odyssey Blocking Buffer LI-COR Biosciences) + 0.05% saponin for 30 minutes at room temperature. Primary antibodies were diluted in the same buffer and added to coverslips, which were incubated in a humidified chamber overnight at 4ºC. Coverslips were washed 3x with PBS, for 5 minutes each, then secondary antibodies diluted in the same blocking/permeabilization solution were added to the coverslips, which were incubated at room temperature, in the dark, for 2 hours. Coverslips were washed 3 more times with PBS, then Hoescht stain, diluted 1:2,000 in block/permeabilization solution, was added and allowed to incubate for 10 minutes at room temperature in the dark. After 3 additional PBS washes, coverslips were mounted on slides with Fluoromount-G (SouthernBiotech). Images were acquired with a CSU-X series spinning disc confocal microscope (Intelligent Imaging Innovations) with an HQ2 CCD camera (Photometrics) using a 100x objective.

Yeast Culture, FM4-64 labeling, and Imaging

Yeast were grown in Yeast extract-peptone-dextrose (YPD) medium (Sigma) or yeast nitrogen base (YNB) medium (Sigma). For vacuole labeling with FM4-64, yeast strains were cultured overnight in a 30ºC shaking incubator in YNB with appropriate auxotrophic selection. Optical density was measured with a Genesys 20 spectrophotometer (Thermo Fisher Scientific), then yeast were diluted to 0.2 OD and allowed to go through two doublings to reach log-phase growth. Samples were centrifuged at 5,000 g for 5 minutes at room temperature, the supernatant was aspirated, and the pellet resuspended in 50 µL YPD with 32 µM FM4-64. Cells were incubated 20 minutes at room temperature, then 1 mL YPD was added before another centrifugation. Pellets were resuspended in 5 mL YPD and incubated for 60 minutes in a 30ºC shaking incubator. Samples were centrifuged, supernatant aspirated, and the pellet resuspended in 20-50 µL of YNB. Samples were wet mounted on slides and imaged with a CSU-X series spinning disc confocal microscope (Intelligent Imaging Innovations) with an HQ2 CCD camera (Photometrics) using a 100x objective.

Yeast Growth Retardation Assay

Stable pRS305, GDP-GFP-TMEM106B, or GDP-GFP-TMEM106A yeast lines were transformed with individual *fab1* complex component cDNA. After overnight culture in selective YNB, yeast were diluted into secondary culture and allowed to reach OD of approximately 1. The transformants were then serially diluted and spotted onto appropriate dropout SC Agar plates with a sterilized 96 pin multi-blot replicator, and

incubated at 30°C, 34°C, or 37°C, then imaged using a Molecular Imager® Gel Doc™ XR System (Bio-Rad) equipped with a CCD camera.

Phosphoinositide Labeling and Quantification

Labeling and quantification were performed as previously described [36].

7.6 Acknowledgements

We would like to thank the lab of Dr. Lois Weisman for performing all PIP analyses and providing plasmids; Dr. Scott Emr and Dr. Matthew Baile for providing yeast strains, plasmids, technical advice, and scientific input; Dr. Haiyuan Yu for his gifts of cDNA; and Xiaochun Wu for technical assistance. This work is supported by funding to F. Hu from NINDS (R01NS088448).

The authors declare no additional competing financial interests.

List of Abbreviations

ArPIKfyve – Associated regulator of PIKfyve
CHMP2B – Charged multivesicular body protein 2B
Co-IP – Co-immunoprecipitation
FTLD – Frontotemporal lobar degeneration
FTLD-TDP – FTLD with TAR DNA-binding protein 43-positive inclusions GRN
HPLC – High-performance liquid chromatography
ICD – Intracellular domain
MAP6 – Microtubule-associated protein 6
PGRN – Progranulin
PI – Phosphoinositide
PI3P – Phosphatidylinositol 3-phosphate
$PI(3,5)P_2$ – phosphatidylinositol 3,5-bisphosphate
PIKfyve – FYVE finger-containing phosphoinositide kinase
TBST – Tris-buffered saline with 0.1% Tween-20
TDP-43 – TAR DNA-binding protein 43
V-ATPase – Vacuolar-type H^+-ATPase

REFERENCES

1. Neary, D., et al., Frontotemporal lobar degeneration: a consensus on clinical diagnostic criteria. Neurology, 1998. **51**(6): p. 1546-54.

2. Ratnavalli, E., et al., The prevalence of frontotemporal dementia. Neurology, 2002. **58**(11): p. 1615-21.

3. Baker, M., et al., Mutations in progranulin cause tau-negative fsrontotemporal dementia linked to chromosome 17. Nature, 2006. **442**(7105): p. 916-9.

4. Cruts, M., et al., Null mutations in progranulin cause ubiquitin-positive frontotemporal dementia linked to chromosome 17q21. Nature, 2006. **442**(7105): p. 920-4.

5. Gass, J., et al., Mutations in progranulin are a major cause of ubiquitin-positive frontotemporal lobar degeneration. Hum Mol Genet, 2006. **15**(20): p. 2988-3001.

6. Mackenzie, I.R., et al., The neuropathology of frontotemporal lobar degeneration caused by mutations in the progranulin gene. Brain, 2006. **129**(Pt 11): p. 3081-90.

7. Snowden, J.S., et al., Progranulin gene mutations associated with frontotemporal dementia and progressive non-fluent aphasia. Brain, 2006. **129**(Pt 11): p. 3091-102.

8. Mukherjee, O., et al., HDDD2 is a familial frontotemporal lobar degeneration with ubiquitin-positive, tau-negative inclusions caused by a missense mutation in the signal peptide of progranulin. Ann Neurol, 2006. **60**(3): p. 314-22.

9. Mackenzie, I.R. and M. Neumann, Molecular neuropathology of frontotemporal dementia: insights into disease mechanisms from postmortem studies. J Neurochem, 2016. **138 Suppl 1**: p. 54-70.

10. Van Deerlin, V.M., et al., Common variants at 7p21 are associated with frontotemporal lobar degeneration with TDP-43 inclusions. Nat Genet, 2010. **42**(3): p. 234-9.

11. Chen-Plotkin, A.S., et al., TMEM106B, the Risk Gene for Frontotemporal Dementia, Is Regulated by the microRNA-132/212 Cluster and Affects Progranulin Pathways. J Neurosci, 2012. **32**(33): p. 11213-27.

12. Nicholson, A.M., et al., TMEM106B p.T185S regulates TMEM106B protein levels: implications for frontotemporal dementia. J Neurochem, 2013. **126**(6): p. 781-91.

13. Finch, N., et al., TMEM106B regulates progranulin levels and the penetrance of FTLD in GRN mutation carriers. Neurology, 2011. **76**(5): p. 467-74.

14. Vass, R., et al., Risk genotypes at TMEM106B are associated with cognitive impairment in amyotrophic lateral sclerosis. Acta Neuropathol, 2011. **121**(3): p. 373-80.

15. Brady, O.A., et al., The frontotemporal lobar degeneration risk factor, TMEM106B, regulates lysosomal morphology and function. Hum Mol Genet, 2013. **22**(4): p. 685-95.

16. Lang, C.M., et al., Membrane orientation and subcellular localization of transmembrane protein 106B (TMEM106B), a major risk factor for frontotemporal lobar degeneration. J Biol Chem, 2012. **287**(23): p. 19355-65.

17. Stagi, M., et al., Lysosome size, motility and stress response regulated by fronto-temporal dementia modifier TMEM106B. Mol Cell Neurosci, 2014. **61**: p. 226-40.

18. Busch, J.I., et al., Increased expression of the frontotemporal dementia risk factor TMEM106B causes C9orf72-dependent alterations in lysosomes. Hum Mol Genet, 2016. **25**(13): p. 2681-2697.

19. Schwenk, B.M., et al., The FTLD risk factor TMEM106B and MAP6 control dendritic trafficking of lysosomes. Embo J, 2013.

20. Jun, M.H., et al., TMEM106B, a frontotemporal lobar dementia (FTLD) modifier, associates with FTD-3-linked CHMP2B, a complex of ESCRT-III. Mol Brain, 2015. **8**: p. 85.

21. Klein, Z.A., et al., Loss of TMEM106B Ameliorates Lysosomal and Frontotemporal Dementia-Related Phenotypes in Progranulin-Deficient Mice. Neuron, 2017. **95**(2): p. 281-296 e6.

22. Satoh, J., et al., TMEM106B expression is reduced in Alzheimer's disease brains. Alzheimers Res Ther, 2014. **6**(2): p. 17.

23. Wu, C., et al., TMEM106a is a Novel Tumor Suppressor in Human Renal Cancer. Kidney Blood Press Res, 2017. **42**(5): p. 853-864.

24. Dai, H., et al., Transmembrane protein 106a activates mouse peritoneal macrophages via the MAPK and NF-kappaB signaling pathways. Sci Rep, 2015. **5**: p. 12461.

25. Genini, S., et al., Radiation hybrid mapping of 18 positional and physiological candidate genes for arthrogryposis multiplex congenita on porcine chromosome 5. Anim Genet, 2006. **37**(3): p. 239-44.

26. Sbrissa, D., et al., Core protein machinery for mammalian phosphatidylinositol 3,5-bisphosphate synthesis and turnover that regulates the progression of endosomal transport. Novel Sac phosphatase joins the ArPIKfyve-PIKfyve complex. J Biol Chem, 2007. **282**(33): p. 23878-91.

27. Ikonomov, O.C., D. Sbrissa, and A. Shisheva, Localized PtdIns 3,5-P2 synthesis to regulate early endosome dynamics and fusion. Am J Physiol Cell Physiol, 2006. **291**(2): p. C393-404.

28. Dong, X.P., et al., PI(3,5)P(2) controls membrane trafficking by direct activation of mucolipin Ca(2+) release channels in the endolysosome. Nat Commun, 2010. **1**: p. 38.

29. Efe, J.A., R.J. Botelho, and S.D. Emr, Atg18 regulates organelle morphology and Fab1 kinase activity independent of its membrane recruitment by phosphatidylinositol 3,5-bisphosphate. Mol Biol Cell, 2007. **18**(11): p. 4232-44.

30. Duex, J.E., et al., Phosphoinositide 5-phosphatase Fig 4p is required for both acute rise and subsequent fall in stress-induced phosphatidylinositol 3,5-bisphosphate levels. Eukaryot Cell, 2006. **5**(4): p. 723-31.

31. Chow, C.Y., et al., Mutation of FIG4 causes neurodegeneration in the pale tremor mouse and patients with CMT4J. Nature, 2007. **448**(7149): p. 68-72.

32. Ikonomov, O.C., et al., The phosphoinositide kinase PIKfyve is vital in early embryonic development: preimplantation lethality of PIKfyve-/- embryos but normality of PIKfyve+/- mice. J Biol Chem, 2011. **286**(15): p. 13404-13.

33. Baulac, S., et al., Role of the phosphoinositide phosphatase FIG4 gene in familial epilepsy with polymicrogyria. Neurology, 2014. **82**(12): p. 1068-75.

34. Campeau, P.M., et al., Yunis-Varon syndrome is caused by mutations in FIG4, encoding a phosphoinositide phosphatase. Am J Hum Genet, 2013. **92**(5): p. 781-91.

35. Lenk, G.M., et al., Biallelic Mutations of VAC14 in Pediatric-Onset Neurological Disease. Am J Hum Genet, 2016. **99**(1): p. 188-94.

36. Zhang, Y., et al., Loss of Vac14, a regulator of the signaling lipid phosphatidylinositol 3,5-bisphosphate, results in neurodegeneration in mice. Proc Natl Acad Sci U S A, 2007. **104**(44): p. 17518-23.

37. Ikonomov, O.C., et al., Functional dissection of lipid and protein kinase signals of PIKfyve reveals the role of PtdIns 3,5-P2 production for endomembrane integrity. J Biol Chem, 2002. **277**(11): p. 9206-11.

38. Suzuki, H. and M. Matsuoka, The Lysosomal Trafficking Transmembrane Protein 106B Is Linked to Cell Death. J Biol Chem, 2016. **291**(41): p. 21448-21460.

39. Vida, T.A. and S.D. Emr, A new vital stain for visualizing vacuolar membrane dynamics and endocytosis in yeast. J Cell Biol, 1995. **128**(5): p. 779-92.

40. Brady, O.A., X. Zhou, and F. Hu, Regulated intramembrane proteolysis of the frontotemporal lobar degeneration risk factor, TMEM106B, by signal peptide peptidase-like 2a (SPPL2a). J Biol Chem, 2014. **289**(28): p. 19670-80.

41. Gary, J.D., et al., Regulation of Fab1 phosphatidylinositol 3-phosphate 5-kinase pathway by Vac7 protein and Fig4, a polyphosphoinositide phosphatase family member. Mol Biol Cell, 2002. **13**(4): p. 1238-51.

42. Duex, J.E., F. Tang, and L.S. Weisman, The Vac14p-Fig4p complex acts independently of Vac7p and couples PI3,5P2 synthesis and turnover. J Cell Biol, 2006. **172**(5): p. 693-704.

43. Holler, C.J., et al., Intracellular Proteolysis of Progranulin Generates Stable, Lysosomal Granulins that Are Haploinsufficient in Patients with Frontotemporal Dementia Caused by GRN Mutations. Eneuro, 2017. **4**(4).

44. Dove, S.K., et al., Vac14 controls PtdIns(3,5)P(2) synthesis and Fab1-dependent protein trafficking to the multivesicular body. Curr Biol, 2002. **12**(11): p. 885-93.

45. Gary, J.D., et al., Fab1p is essential for PtdIns(3)P 5-kinase activity and the maintenance of vacuolar size and membrane homeostasis. J Cell Biol, 1998. **143**(1): p. 65-79.

46. Bonangelino, C.J., N.L. Catlett, and L.S. Weisman, Vac7p, a novel vacuolar protein, is required for normal vacuole inheritance and morphology. Mol Cell Biol, 1997. **17**(12): p. 6847-58.

47. Tsuruta, F., et al., PIKfyve regulates CaV1.2 degradation and prevents excitotoxic cell death. J Cell Biol, 2009. **187**(2): p. 279-94.

48. Simons, C., et al., A recurrent de novo mutation in TMEM106B causes hypomyelinating leukodystrophy. Brain, 2017. **140**(12): p. 3105-3111.

49. Yan, H., et al., The recurrent mutation in TMEM106B also causes hypomyelinating leukodystrophy in China and is a CpG hot spot. Brain, 2018.

50. Mironova, Y.A., et al., PI(3,5)P2 biosynthesis regulates oligodendrocyte differentiation by intrinsic and extrinsic mechanisms. Elife, 2016. **5**.

51. Zhang, Y., et al., Modulation of synaptic function by VAC14, a protein that regulates the phosphoinositides PI(3,5)P(2) and PI(5)P. EMBO J, 2012. **31**(16): p. 3442-56.

52. Zhou, X., et al., Prosaposin facilitates sortilin-independent lysosomal trafficking of progranulin. J Cell Biol, 2015. **210**(6): p. 991-1002.

53. Gietz, R.D. and R.A. Woods, Transformation of yeast by lithium acetate/single-stranded carrier DNA/polyethylene glycol method. Methods Enzymol, 2002. **350**: p. 87-96.

54. Longtine, M.S., et al., Additional modules for versatile and economical PCR-based gene deletion and modification in Saccharomyces cerevisiae. Yeast, 1998. **14**(10): p. 953-61.

55. Vancha, A.R., et al., Use of polyethyleneimine polymer in cell culture as attachment factor and lipofection enhancer. BMC Biotechnol, 2004. **4**: p. 23.

7.7 Supplementary Data

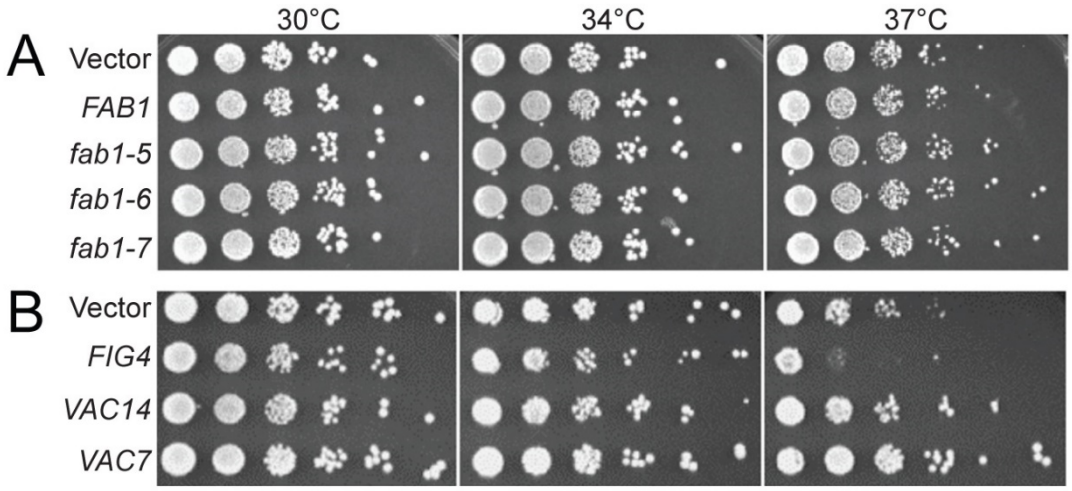

Supplementary Figure 7.1. Suppression of cytotoxicity in GFP-TMEM106A or GFP-TMEM106B stable yeast lines. A) Fab1 or hyperactive Fab1 mutants were overexpressed in GFP-TMEM106A stable yeast. **B)** Fab1 complex component Vac7, Vac14, or Fig4 was overexpressed in GFP-TMEM106B stable yeast.

CHAPTER 8

PERSPECTIVES AND FUTURE DIRECTIONS

The clinical importance of progranulin (PGRN) became evident in 2006, when heterozygous mutations in the *GRN* gene, resulting in haploinsuffiency, were found to cause frontotemporal lobar degeneration (FTLD) [1-6]. FTLD is a clinically heterogeneous, incurable neurodegenerative disease most often presenting with drastic alterations in behavior and personality, including social disinhibition and gradual decline in language capabilities [7]. Although the exact mechanism is unknown, the disease is characterized by progressive atrophy of the frontal and temporal lobes of the brain. FTLD is the second leading cause of early-onset dementia after Alzheimer's disease (AD), and is the third most common cause of cortical dementia [7, 8].

Perhaps the most important finding leading to a hypothetical lysosomal function of PGRN was the 2012 discovery of a pair of siblings with adult-onset neuronal ceroid lipofuscinosis (NCL), with exome sequencing pointing to a homozygous variant in *GRN* resulting in a premature stop [9]. Since then, great strides have been made in elucidating this role – PGRN has been found to be lysosomally localized and trafficked by two independent pathways, it has been shown to be under regulation of the transcription factor regulating most of the known lysosomal proteins, and it has been shown to regulate levels of the lysosomal protein, prosaposin (PSAP), among others [10-17]. The majority of the work presented here seeks to further advance our understanding of the lysosomal function of PGRN and its relationship to neurodegeneration.

In chapter 1, we provide strong evidence that PGRN, which has been shown to be proteolytically cleaved into individual granulin (Grn) peptides by extracellular proteases, is similarly processed in the lysosome [18-20] At nearly the same time that we published on the lysosomal processing of PGRN, similar results were reported by another group, supporting our data [21]. Likewise, we showed that the lysosomal protease, cathepsin L (CTSL), is able to efficiently cleave PGRN, which was also supported by a second group's publication [22]. These findings are significant, as by now it is widely accepted that PGRN plays a role in lysosomal homeostasis, and the discovery of stable Grn peptides hints at the possibility that they may be functional units inside the lysosome. One intriguing possibility is that the development of PGRN-related disease is not due the loss of PGRN so much as it is due to the loss of Grn peptides, which ties into the following few sections.

In chapters 3-5, we identify three lysosomal enzymes, cathepsin D (CTSD), glucocerebrosidase (GBA), and α-N-acetylgalactosaminidase (NAGA), which show variable binding to PGRN and Grn peptides [23]. Importantly, all three enzymes show decreased activity in tissue lysates derived from PGRN-deficient mice, with only NAGA showing a corresponding upregulation in protein levels. While we currently have been unable to demonstrate a clear mechanism for these activity changes, the binding implies a potential direct regulatory role. Indeed, two studies published at approximately the same time showed a mild, but specific, increase in CTSD activity with the addition of recombinant PGRN or Grn E [24, 25]. Similarly, the addition of recombinant PGRN increased the activity of CTSD activity in *Grn*$^{-/-}$ mouse brain lysates. Despite repeated attempts, we were unable to obtain similar results, which may

be due to quality of the recombinant proteins being tested. As we could not demonstrate this effect with CTSD, it is possible that we are missing a similar activity modulation with both GBA and NAGA.

In chapter 6, we describe the completion of a high-throughput screen to identify the receptor responsible for mediating the neurotrophic effects of PGRN and Grn E. While it is unlikely that we discovered a *neurotrophic* receptor from this intensive screen, we were able to identify two potential PGRN/Grn E receptors, cluster of differentiation 68 (CD68) and neuropilin 2 (NRP2), although the functional significance of these new relationships remains to be seen.

Despite substantial progress on elucidating the lysosomal role of PGRN and its association with neurodegeneration, the exact function of the protein is still unclear. Considering the strong binding between PGRN and PSAP, their reciprocal lysosomal trafficking, their shared interactors (CTSD and GBA), and the reduction in neuronal saposin peptides and lysosomal lipidomic changes that occur with PGRN loss, it seems very likely that at least one function of PGRN is to regulate PSAP. This role may be as simple as the previously reported regulation of trafficking, however additional possibilities exist. With the shared interaction between PGRN, PSAP, and CTSD, one prospect is that PGRN regulates the ability of PSAP and CTSD to interact and, more specifically, that it helps moderate the cleavage of PSAP into saposin peptides. It is possible that PSAP cleavage is a situation-dependent process that may require activation or inhibition under specific circumstances. The reduction in GBA activity that we have detected with PGRN deficiency could also be explained by changes in PSAP processing. Decreased saposin A or saposin C peptides would result in a direct decrease in GBA

activity. Additionally, if PGRN were to alter the binding of CTSD to PSAP, it could affect the specific amino acid sequences at which CTSD cleaves in the linker regions of PSAP, potentially resulting in altered saposin peptides, shortened or elongated at the N-terminus, C-terminus, or both. Any modification in the sequence of the canonical saposin fragments could potentially disrupt their ability to interact with GBA or lipids.

As three distinct lysosomal hydrolases have been identified to which PGRN and/or Grn peptides bind and which show activity reduction when PGRN is lost, its function may be to directly regulate enzyme activity. While we have been unable to show a direct augmentation of enzyme activity by PGRN or Grn peptides, two studies have shown an increase in CTSD activity with the addition of PGRN or Grn E [24, 25]. If this finding is correct, perhaps PGRN/Grn peptides also regulate the activity of NAGA, GBA, and possibly other hydrolases. One of these two studies also showed that PGRN can stabilize CTSD *in vitro* [24]. It is possible that the observed increase in CTSD activity with the addition of PGRN or Grn E was not entirely due to a direct activation, but by a reduction in CTSD degradation, resulting in an increase in functional CTSD that persisted throughout the activity assays. Likewise, whether PGRN physiochemically stabilizes CTSD, thereby preventing its degradation, or whether PGRN prevents CTSD from catalyzing its own proteolysis was not entirely clear, despite the use of pepstatin A as a control. It is possible that PGRN, in part, functions to either increase the chemical stability of lysosomal enzymes or that it helps to protect such enzymes from degradation in the lysosome. This potential protective role could extend beyond enzymes to other lysosomal proteins with which PGRN or Grn peptides interact, such as CD68. There is also evidence that certain cathepsins, including CTSD,

can mediate apoptosis [26-29]. As PGRN and Grn E are involved in survival and growth signaling [30-32], one possibility is that they help regulate CTSD-mediated apoptosis, where loss of PGRN shifts the cell toward an apoptotic state.

More speculatively, considering the shared binding between PGRN/Grn peptides and several lysosomal enzymes, it is worth considering the possibility that PGRN assists in the complexation of hydrolases into functional units, potentially increasing their stability or activity, or allowing them to more efficiently sequentially hydrolyze substrates – essentially organizing the lysosomal lumen. Indeed, there is a known example where lysosomal hydrolases are brought together to form a functional complex. A heterotrimer of α-N-acetyl neuraminidase, β-galactosidase, and the protective protein/cathepsin A (PPCA) forms in the lysosome, and this complexation is necessary for the proper localization and full activation of neuraminidase [33]. One especially interesting finding is that cathepsin L (CTSL) appears to be more efficient at producing Grn dipeptides than individual Grn peptides based on *in vitro* reactions. This leads to the question of whether these dipeptides may be functional. One possibility is that each Grn domain of a dipeptide is able to bind to a different hydrolase, helping to recruit them to a more stable, active, or efficient complex.

In the final chapter, we transition from PGRN to the related protein and FTLD risk factor, TMEM106B. Although TMEM106B has been shown to regulate lysosomal morphology and TMEM106B overexpression is associated with decreased degradative capacity, its exact function remains unclear [34-38]. Based on phenotypes, including enlarged lysosomes, reduced lysosomal acidification, and cytotoxicity shared between TMEM106B overexpression and reduced cellular $PI(3,5)P_2$ pools, we hypothesized that

TMEM106B may act in this phosphoinositide pathway to regulate $PI(3,5)P_2$ levels. Yeast studies utilizing hyperactive mutants of Fab1, the kinase primarily responsible for $PI(3,5)P_2$ synthesis, demonstrate that they can successfully suppress the phenotypes associated with TMEM106B expression. We also identify a potential interaction between TMEM106B and the Fab1 complex component, Vac14, but additional tests of the relationship and its function are required. In support of our hypothesis, preliminary phosphoinositide analysis in mammalian cells shows that overexpression of GFP-TMEM106B reduces $PI(3,5)P_2$ by over 40%. However, the mechanism of this finding remains to be determined, and it is possible that the effect is indirect.

List of Abbreviations

CD68 – Cluster of differentiation 68
CTSL – Cathepsin L
CTSD – Cathepsin D
FTLD – Frontotemporal lobar degeneration
GBA – Glucocerebrosidase
Grn – Granulin
NAGA – α-N-acetylgalactosaminidase
NCL – Neuronal ceroid lipofuscinosis
NRP2 – Neuropilin 2
PGRN – Progranulin
PPCA – Protective protein/cathepsin A
PSAP – Prosaposin

REFERENCES

1. Baker, M., et al., Mutations in progranulin cause tau-negative frontotemporal dementia linked to chromosome 17. Nature, 2006. **442**(7105): p. 916-9.

2. Cruts, M., et al., Null mutations in progranulin cause ubiquitin-positive frontotemporal dementia linked to chromosome 17q21. Nature, 2006. **442**(7105): p. 920-4.

3. Gass, J., et al., Mutations in progranulin are a major cause of ubiquitin-positive frontotemporal lobar degeneration. Hum Mol Genet, 2006. **15**(20): p. 2988-3001.

4. Mackenzie, I.R., et al., The neuropathology of frontotemporal lobar degeneration caused by mutations in the progranulin gene. Brain, 2006. **129**(Pt 11): p. 3081-90.

5. Snowden, J.S., et al., Progranulin gene mutations associated with frontotemporal dementia and progressive non-fluent aphasia. Brain, 2006. **129**(Pt 11): p. 3091-102.

6. Mukherjee, O., et al., HDDD2 is a familial frontotemporal lobar degeneration with ubiquitin-positive, tau-negative inclusions caused by a missense mutation in the signal peptide of progranulin. Ann Neurol, 2006. **60**(3): p. 314-22.

7. Neary, D., et al., Frontotemporal lobar degeneration: a consensus on clinical diagnostic criteria. Neurology, 1998. **51**(6): p. 1546-54.

8. Ratnavalli, E., et al., The prevalence of frontotemporal dementia. Neurology, 2002. **58**(11): p. 1615-21.

9. Smith, K.R., et al., Strikingly different clinicopathological phenotypes determined by progranulin-mutation dosage. Am J Hum Genet, 2012. **90**(6): p. 1102-7.

10. Takahashi, H., et al., Opposing effects of progranulin deficiency on amyloid and tau pathologies via microglial TYROBP network. Acta Neuropathol, 2017. **133**(5): p. 785-807.

11. Zheng, Y., et al., C-terminus of progranulin interacts with the beta-propeller region of sortilin to regulate progranulin trafficking. PLoS ONE, 2011. **6**(6): p. e21023.

12. Hu, F., et al., Sortilin-mediated endocytosis determines levels of the frontotemporal dementia protein, progranulin. Neuron, 2010. **68**(4): p. 654-67.

13. Sardiello, M., et al., A gene network regulating lysosomal biogenesis and function. Science, 2009. **325**(5939): p. 473-7.

14. Belcastro, V., et al., Transcriptional gene network inference from a massive dataset elucidates transcriptome organization and gene function. Nucleic Acids Res, 2011. **39**(20): p. 8677-88.

15. Zhou, X., et al., Impaired prosaposin lysosomal trafficking in frontotemporal lobar degeneration due to progranulin mutations. Nat Commun, 2017. **8**: p. 15277.

16. Zhou, X., et al., The interaction between progranulin and prosaposin is mediated by granulins and the linker region between saposin B and C. J Neurochem, 2017.

17. Zhou, X., et al., Prosaposin facilitates sortilin-independent lysosomal trafficking of progranulin. J Cell Biol, 2015. **210**(6): p. 991-1002.

18. Zhu, J., et al., Conversion of proepithelin to epithelins: roles of SLPI and elastase in host defense and wound repair. Cell, 2002. **111**(6): p. 867-78.

19. Suh, H.S., et al., Regulation of progranulin expression in human microglia and proteolysis of progranulin by matrix metalloproteinase-12 (MMP-12). PLoS ONE, 2012. **7**(4): p. e35115.

20. Zhou, X., et al., Lysosomal processing of progranulin. Mol Neurodegener, 2017. **12**(1): p. 62.

21. Holler, C.J., et al., Intracellular Proteolysis of Progranulin Generates Stable, Lysosomal Granulins that Are Haploinsufficient in Patients with Frontotemporal Dementia Caused by GRN Mutations. Eneuro, 2017. **4**(4).

22. Lee, C.W., et al., The lysosomal protein cathepsin L is a progranulin protease. Mol Neurodegener, 2017. **12**(1): p. 55.

23. Zhou, X., et al., Regulation of cathepsin D activity by the FTLD protein progranulin. Acta Neuropathol, 2017. **134**(1): p. 151-153.

24. Beel, S., et al., Progranulin functions as a cathepsin D chaperone to stimulate axonal outgrowth in vivo. Hum Mol Genet, 2017.

25. Valdez, C., et al., Progranulin-mediated deficiency of cathepsin D results in FTD and NCL-like phenotypes in neurons derived from FTD patients. Hum Mol Genet, 2017. **26**(24): p. 4861-4872.

26. Leist, M. and M. Jaattela, Triggering of apoptosis by cathepsins. Cell Death Differ, 2001. **8**(4): p. 324-6.

27. Chwieralski, C.E., T. Welte, and F. Buhling, Cathepsin-regulated apoptosis. Apoptosis, 2006. **11**(2): p. 143-9.

28. Kagedal, K., U. Johansson, and K. Ollinger, The lysosomal protease cathepsin D mediates apoptosis induced by oxidative stress. FASEB J, 2001. **15**(9): p. 1592-4.

29. Johansson, A.C., et al., Cathepsin D mediates cytochrome c release and caspase activation in human fibroblast apoptosis induced by staurosporine. Cell Death Differ, 2003. **10**(11): p. 1253-9.

30. Ryan, C.L., et al., Progranulin is expressed within motor neurons and promotes neuronal cell survival. BMC Neurosci, 2009. **10**: p. 130.

31. Van Kampen, J.M., D. Baranowski, and D.G. Kay, Progranulin gene delivery protects dopaminergic neurons in a mouse model of Parkinson's disease. PLoS ONE, 2014. **9**(5): p. e97032.

32. Van Damme, P., et al., Progranulin functions as a neurotrophic factor to regulate neurite outgrowth and enhance neuronal survival. J Cell Biol, 2008. **181**(1): p. 37-41.

33. Bonten, E.J. and A. d'Azzo, Lysosomal neuraminidase. Catalytic activation in insect cells is controlled by the protective protein/cathepsin A. J Biol Chem, 2000. **275**(48): p. 37657-63.

34. Zhou, X., et al., Elevated TMEM106B levels exaggerate lipofuscin accumulation and lysosomal dysfunction in aged mice with progranulin deficiency. Acta Neuropathol Commun, 2017. **5**(1): p. 9.

35. Brady, O.A., et al., The frontotemporal lobar degeneration risk factor, TMEM106B, regulates lysosomal morphology and function. Hum Mol Genet, 2013. **22**(4): p. 685-95.

36. Brady, O.A., X. Zhou, and F. Hu, Regulated intramembrane proteolysis of the frontotemporal lobar degeneration risk factor, TMEM106B, by signal peptide peptidase-like 2a (SPPL2a). J Biol Chem, 2014. **289**(28): p. 19670-80.

37. Klein, Z.A., et al., Loss of TMEM106B Ameliorates Lysosomal and Frontotemporal Dementia-Related Phenotypes in Progranulin-Deficient Mice. Neuron, 2017. **95**(2): p. 281-296 e6.

38. Chen-Plotkin, A.S., et al., TMEM106B, the Risk Gene for Frontotemporal Dementia, Is Regulated by the microRNA-132/212 Cluster and Affects Progranulin Pathways. J Neurosci, 2012. **32**(33): p. 11213-27.